THE THERAPEUTIC POTENTIAL OF TARGETING HYALURONIC ACID TO PREVENT PERITONEAL METASTATIC DISSEMINATION IN COLORECTAL CANCER

FARIS SOLIMAN

0501141

Cardiff-China Medical Research Collaborative

Cardiff University School of Medicine

2021

Thesis submitted to Cardiff University for the application of degree of Doctor of Medicine (M.D.)

The therapeutic potential of targeting hyaluronic acid to prevent peritoneal metastatic dissemination in colorectal cancer.

Student:	**Mr Faris Soliman**
Student Number:	**0501141**
Supervisors:	**Miss R Hargest**
	Dr L Ye

Cardiff-China Medical Research Collaborative

Henry Wellcome Building

Cardiff University School of Medicine

Heath Park

Cardiff

Wales

UK

Acknowledgements

I am eternally grateful to **Miss Rachel Hargest** who has provided limitless advice, guidance, and care over the years, not only towards this thesis but also more importantly for being a committed mentor and friend throughout my surgical career and training.

I am greatly indebted to **Dr Lin Ye** for his hours of time and patience guiding me though laboratory experimentation. I wish to thank **Professor Wen Jiang** for facilitating and allowing me to carry out my research project under the secure umbrella of his supportive laboratory alongside his team. Thanks again to all the Cardiff China Medical Research Collaborative (CCMRC) staff and students for their support, advice, help and friendship. **Dr Andrew Sanders**, **Miss Catherine Zabkiewiecz, Mrs Fiona Ruge**, **Dr Tracey Martin, Dr Jane Lane, Dr Ben Lanning, Mrs Juliet Davies, and Ms Hayley Spavin** to name but a few.

I also wish to acknowledge and pass on my heartfelt thanks to **Mr John Pollitt**, past programme director for General Surgery in Wales, as well as both the **Wales Postgraduate Deanery** and the **Specialist Training Committee**, for allowing me to take the necessary time out of programme for research.

Most importantly I wish to thank my wife, **Natalie**, for her endless encouragement and love, and for supporting me throughout my surgical training. Secondly, I am completely indebted to my parents, **Mohamed** and **Janet Soliman** for their unwavering support and dedication, and for instilling in me the most important values and principles which have guided me throughout my life. I am eternally grateful to all of you

Finally, I wish to dedicate my thesis to my late father **Dr Mohamed Eid Soliman,** who sadly and unexpectedly passed away in January 2021 and did not get to see this thesis to completion. He gave me the love for Medicine and Surgery. A true gentleman and an exemplary surgeon.

Curse, bless me now with your fierce tears, I pray.
Do not go gentle into that good night
Rage, rage against the dying of the light.
Dylan Thomas. 1947.

Publications and presentations undertaken during the period of research

Published Papers

Soliman F, Ye L, Jiang W, Hargest R. 2021. Targeting Hyaluronic Acid and Peritoneal Dissemination in Colorectal Cancer. Clinical Colorectal Cancer. https:///doi.org/10.1016/j/clcc.2021/11/008. Impact factor 4.481. (Appendix 4.1)

Published abstracts

Soliman F, Ye L, Jiang W, Hargest R. 2021. Hyaluronic Acid Dependent Adhesion in Colorectal Cancer Peritoneal Metastases. British Journal of Surgery. 108(S1): i7-i48. doi.org/10.1093/bjs/znab117.017. (Appendix 4.2)

Soliman F, Ye L, Jiang W, Hargest R. 2021. Peritoneal Metastasis in Colorectal Cancer: hyaluronic acid dependent adhesion. European Journal of Surgical Oncology. 47(1): e6. doi.org/10/1016/j.ejso/2020/11/028. (Appendix 4.3)

Oral presentations

Soliman F, Ye L, Jiang W, Hargest R. 2020. Peritoneal Metastases in Colorectal Cancer: hyaluronic acid dependent adhesion. BASO Annual Scientific Meeting, BASO-ACS proffered papers.

Soliman F, Ye L, Jiang W, Hargest R. 2020. Hyaluronic Acid (HA) Dependent Adhesion in Colorectal Cancer Peritoneal Metastasis. SARS 2020 Patey Prize presentation

Soliman F, Ye L, Jiang W, Hargest R. 2019. Peritoneal Metastases in Colorectal Cancer *in vitro* and *in vivo*: targeting hyaluronic acid dependent adhesion. Royal Society of Medicine Coloproctology section: John of Arderne prize presentation.

Soliman F, Ye L, Jiang W, Hargest R. 2019. Hyaluronic Acid dependent adhesion of peritoneal metastases in colorectal cancer. Cardiff University Department of Cancer and Genetics presentation day.

Soliman F, Ye L, Jiang W, Hargest R. 2019. HA-dependent adhesion of peritoneal metastasis in colorectal cancer. Royal Society of Medicine Surgery section. MIA prize presentation. **Winner**

Abbreviations

Ab - Antibody

AC – Adenocarcinoma

Apaf 1 - Apoptotic protease-activating factor 1

APC – Adenomatous polyposis coli

APS – Ammonium persulphate

ATCC - American Type Culture Collection

Bad - Bcl-2 associated agonist of cell death

Bax - Bcl-2 associated X protein

Bcl-2 - B-cell lymphoma 2 protein

BDIX – Berlin Druckrey IX rat

BID – BH3 Interacting Domain

Bik - Bcl-2 Interacting killer protein

Bim - Bcl-2 like protein 11

Bmf - Bcl-2 Modifying factor protein

BMPR1a – Bone Morphogenic Protein Receptor Type 1a

BRAF – B-Raf Proto-oncogene

CA125 – Cancer antigen 125

Casp-3 - Caspase 3

Casp-6 - Caspase 6

Casp-7 - Caspase 7

Casp-8 - Caspase 8

Casp-9 - Caspase 9

CCK8 – Cell counting kit 8

CEACAM1 – Carcinoembryonic antigen 1

CD1 - Cluster Differentiation- 1

CD44 – Cluster Differentiation 44

CDC – Centre for Disease Control & Prevention

CDH1 – Cadherin-1

CIMP – Cytosine-phosphate-guanosine (CpG) island methylator phenotype

CIN – Chromosomal instability

CK – Cytokeratin

cm - Centimetre

c-MET – Met Proto-oncogene

CO_2 – Carbon dioxide

CpG – Cytosine-phosphate-guanosine

CRC – Colorectal Cancer

CRS – Cytoreductive surgery

Cyr61 – Cystine rich protein 61

Cyt c - Cytochrome c protein

DAPI – 4',6-diamidino-2-phenylindole fluorescent stain

DCC – Deleted in Colorectal Cancer

DEPC – Diethyl pyrocarbonate

DFS – Disease free survival

DMEM - Dulbecco's modified eagle medium

DNA – Deoxyribonucleic acid

ECACC -European Collection of Authenticated Cell Cultures

ECM – Extracellular matrix

EDTA - Ethylenediaminetetraacetic acid

EGFR – Epidermal growth factor receptor

Ep-CAM/EpCAM – Epithelial cellular adhesion molecule

ERK – Extracellular signal-regulated kinase

FAP – Familial adenomatous polyposis

Fas - Fas receptor (also known as apoptosis antigen 1 or CD95)

FCS – Foetal calf serum

FITC – fluorescein isothiocyanate

g - Gram/s

GAG -Glycosaminoglycan

GAPDH – Glyceraldehyde-3-phosphate dehydrogenase housekeeping gene

GEM- Genetically engineered model

GEO – Gene expression omnibus

HA – Hyaluronic acid or Hyaluronan

HAi - Hyaluronic acid Inhibitor

HGF – Hepatocyte Growth Factor

HGFR – Hepatocyte Growth Factor Receptor

HIF-1 – Hypoxia Inducible Factor -1

HIPEC – Heated intraperitoneal chemotherapy

HNPCC- Hereditary non-polyposis colorectal cancer

Homolog – a gene related to a second gene by descent from a common ancestral DNA sequence

Hrk - Harakiri protein

Hrs – Hours

HRT-18 – Human colon carcinoma cell line HRT-18 (Also known as HCT-8)

HT115 - Human colon carcinoma cell line HT115

ICAM-1 – Intracellular adhesion molecule-1

IGF – Insulin-like Growth Factor

IL – Interleukin

ILβ - Interleukin- Beta

Inc – Incorporated

IP - Intra-peritoneal

JP – Juvenile polyposis

kDa – Kilodalton

KLK - Kallikrein-related peptidases

KRAS – Kirsten rat Sarcoma virus gene

K-ras – Kirsten rat sarcoma protein

L1CAM – L1 cell adhesion molecule

LP9 – Human mesothelial cell line

LS – Lynch Syndrome

µg – Microgram

µl - Microlitre

mAb- Monoclonal antibodies

MAP – MUTYH-associated polyposis

MAPK or MEK – Mitogen-Activated Protein Kinase

MC – Mucinous adenocarcinoma

mCRC – Metastatic Colorectal Cancer

MDR1 – Multidrug resistance -1

Mins - Minutes

MLH – MutL homologue

mm – Millimetre

MMPs – Matrix metallopeptidases

MSH- MutS homologue

MSI – Microsatellite instability

MUC1 – Mucin Core peptide -1

MUC16 – Mucin Core peptide 16

MUTYH – MUTY DNA glycosylase homologue

Nm – Nanometre

Noxa - Phorbol-12-myristate-13-acetate-induced protein 1

OS – Overall survival

PI3K-AKT – Phosphatidylinositol 3-Kinase (PI3)- Protein kinase B (AKT) signalling pathway

P53 – Tumour protein 53 (protein)

PBS- - Phosphate buffered saline

PCR – Polymerase chain reaction

PDX – patient derived xenografts

P-gp – P glycoprotein

PIPAC – Pressurised intraperitoneal aerosol chemotherapy

PJS – Peutz-Jeghers Syndrome

PM – Peritoneal Metastases

PMS2 – Postmeiotic Segregation Increased 2

PPL – Procedure project licence

Procasp-8 - Procaspase 8

Procasp-9 - Procaspase 9

Puma - P53 upregulated modulator of apoptosis

Raf – Rapidly accelerated fibrosarcoma protein

rcf – Relative centrifugal force (g-force)

RHAMM – Receptor for hyaluronan mediated motility

RNA – Ribonucleic acid

rpm – Revolutions per minute

RT – Reverse transcription

SCID – severe combined immunodeficiency disease

SD – Standard deviation

SDS-PAGE – Sodium dodecyl sulphate polyacrylamide gel electrophoresis

SF – Scatter factor

SMAD – (Small) Mothers against decapentaplegic (SMAD protein family- also abbreviated to MAD)

Src – Sarcoma viral oncogene homologue

SRCC – Signet ring cell carcinoma

SPS – Serrated polyposis syndrome

SPSS – Statistical package for the social sciences

STK-11 – Serine Threonine Kinase 11

TBE – Tris borate EDTA

t-Bid - Truncated BH3 interacting domain

TBS – Tris buffered saline

TBST – Tris Buffered Saline with Tween

TGF--β - Transforming Growth Factor- Beta

TLM – Trans-lymphatic metastasis

TMM – Trans-mesothelial metastasis

TNF-α, - Tumour necrosis factor – alpha

TNFR 1 - Tumour necrosis factor receptor 1

TNM – Tumour Node Metastases (classification system)

TP53 – Tumour Protein-53 (gene)

Tris – Tris(hydroxymethyl)aminomethane

TRITC – Tetramethylrhodamine

TWIST1 – TWIST-1 homologue

US – United States

USA – United States of America

UK – United Kingdom

VCAM1 – Vascular cell adhesion molecule-1

VEGF – Vascular endothelial growth factor

WNT- Wingless-related integration site

∞ - Infinite hold setting on thermocycler

Abstract

Background

Peritoneal Metastasis (PM) in Colorectal Cancer (CRC) undoubtedly remains a challenge to treat and often portends a poor prognosis for patients. Hyaluronic acid (HA) is found throughout the body and is particularly found in abundance coating the mesothelial cells of the peritoneum. Interaction of HA with HA-dependent adhesion molecules can facilitate cell adhesion to the peritoneum. HA may play a role in spread of PM in CRC in association with known HA-receptor molecules CD44, RHAMM and ICAM-1.

Methods

Expression of HA-dependent and HA-independent adhesion molecules was examined in CRC using tissue microarray datasets and matched to clinicopathological data. *In vitro* peritoneal modelling tested CRC cellular adhesion when treated with either a small peptide competitive binding HA-inhibitor (HAi) or excess exogenous HA. Further *in vitro* testing assessed CRC ability to aggregate and survive when in suspension, evaluating the ability of cells both to survive and to aggregate at fixed time points.

An *in vivo* Xenograft peritoneal model was used, using three groups of CD1 nude mice injected with CRC cells both intraperitoneally (IP) and subcutaneously to monitor tumour growth. Treatment groups received either a further IP injection of HAi or HA continuously for 5 days for the first week of treatment and biweekly for the remaining three weeks and compared to a control. (PPL: PE9445FC2).

Results

Tissue microarray data demonstrated a significant increase in RNA expression of the three HA-dependent adhesion molecules CD44 (p=<0.0001), RHAMM (p=0.0004) and ICAM-1 (p=<0.0001) in CRC. Whereas, in non-HA-dependent adhesion molecules showed either significant downregulation or no expression difference.

In vitro adhesion assays saw significantly reduced cellular adhesion of HT115, HRT-18 and Caco-2 cell lines when treated with either HAi or excess exogenous HA in peritoneal mimicking plate coated models.

Free-floating CRC cells in suspension demonstrated, firstly, significantly decreased viability at 24-hours when compared to controls (HAi p=0.0040, HA312ug/ml p= 0.0039 and HA624ug/ml p= 0.0019). Secondly, treatment groups exhibited reduced aggregation when compared to controls (HAi p=0.0015, HA312ug/ml p=0.0027 and HA624ug/ml p=0.0017).

In vivo experimentation demonstrated no difference in weight or subcutaneous tumour size growth between groups. However, a significant reduction in the number of PM was seen for both treatment groups, compared to controls (HAi p=0.0094, HA p=0.0009). Interestingly, there was no significant difference in average peritoneal tumour nodule size between the groups compared to controls (HAi p=0.7976, HA p=0.4536).

Conclusions

Expression of HA-dependent adhesion molecules is increased in CRC. Targeting HA-dependent adhesion potentially affects CRC cells' ability to survive in the peritoneal environment and may have a potential therapeutic use in treatment or prevention of PM in CRC. Further *in vitro* and *in vivo* modelling is needed.

Table of Contents

General Introduction

Chapter 1

1.1 Colorectal Cancer and Peritoneal Metastases

Colorectal cancer (CRC) is the third most common cancer across the world (Torre, Bray, Siegel *et al.*, 2015)**.** However, metastatic disease remains a challenging barrier to improvement of both survival rates and quality of life**.** It is reported that patients diagnosed with metastatic synchronous or metachronous adenocarcinoma of the colon have an overall 5-year survival rate of 24% and 34%, respectively (Suthananthan, Bhandari, & Platell, 2017)**.** Metastases in CRC often lead to palliative outcomes for these patients.

The treatment of peritoneal metastases (PM) has remained challenging in these cohorts of patients. Even those patients with stage IV CRC with PM of whom are considered 'treated' following an R0 resection (Hermanek & Wittekind, 1994) have a reported recurrence rate of 79.1% and a 5-year overall survival rate of 36.2% (Sato, Kotake, Sugihara *et al.*, 2016).

The eighth edition of the Tumour-Node-Metastasis classification in relation to colorectal, anal and appendiceal cancer has updated the subclassifications of the metastatic organ involvement definitions. Previously the seventh edition classified M1a as single organ involvement without peritoneal metastases and M1b included multiorgan with or without peritoneal metastases. The eighth edition separates the metastatic classification into M1a, M1b and M1c, where M1c includes metastatic disease to the peritoneum, with or without involvement of another organ (Shida, Kanemitsu, Hamaguchi *et al.*, 2019)

Further subclassification of PM is very important in view of peritoneal disease being a negative prognostic indicator in patients with metastatic colorectal cancer. Patients with

isolated non-peritoneal sites (including liver and lung) had significantly better overall survival when given systemic therapy than patients with isolated peritoneal metastatic CRC (mCRC) (Franko, Shi, Meyers *et al.*, 2016). Sugarbaker (1995) advocated that certain PM in GI malignancies could be considered as local dissemination or spread rather than a systemic process, and a different approach to treatment should be considered (Sugarbaker, 1995).

The development of the technique of Cytoreductive Surgery (CRS) and Hyperthermic Intraperitoneal Chemotherapy (HIPEC) has looked to treat selected groups of these patients (Sugarbaker, 2005a, 2005b)**.** This treatment entails major resectional surgery with chemotherapeutic agents placed within the peritoneal cavity.

Often, the drugs used in HIPEC are generic chemotherapeutic regimens and not necessarily tailored to the specific cancer being treated (Lemoine, Sugarbaker, & Van der Speeten, 2017)**.** Understanding molecular pathways of carcinogenesis in CRC and metastatic spread is slowly paving the way to personalised treatment regimens.

1.2. Epidemiology of Colorectal Cancer

1.2.1. Incidence

The incidence of CRC around the world varies quite markedly. There are a multitude of possible reasons behind this. Epigenetics and environmental factors undoubtedly play a large role. The populations of Australia/New Zealand, Europe and North America carry the highest estimated incidence of CRC around the world, Figure 1.1 (Globocan.iarc.fr., 2012).

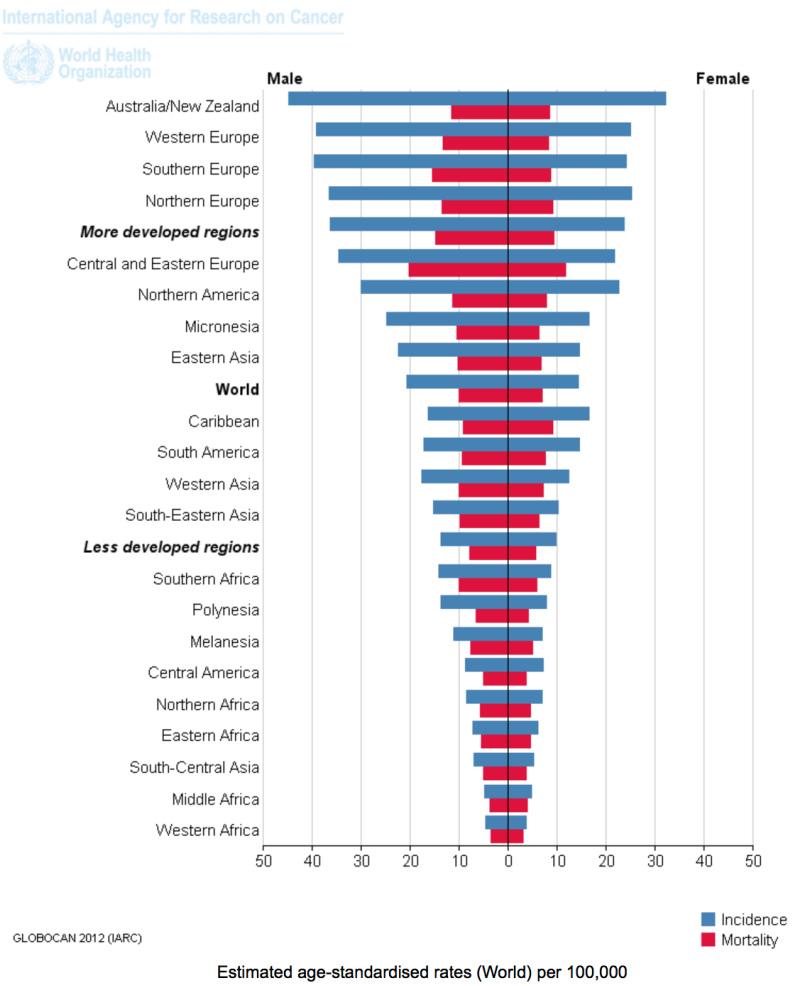

Figure 1.1. Globocan.iarc.fr. (2012). *Fact Sheets by Cancer*. [online] Available at: http://globocan.iarc.fr/Pages/fact_sheets_cancer.aspx [Accessed 21 Aug. 2017].

In the United States (US) mortality due to colorectal cancer has been shown to be steadily decreasing**.** However, this trend has not been reflected worldwide, with developing nations seeing a steady annual increase in both incidence and mortality (Marley & Nan, 2016). The US Centre for Disease Control and Prevention's (CDC) National program of cancer registries estimated that there would be 135,430 new CRC cases (52.7% male and 47.3% female) over the course of 2017 in the US. It also estimated 50,260 (54% male and 46% female) CRC related deaths in that time period (R. L. Siegel, Miller, Fedewa *et al.*, 2017). The age-

standardised annual incidence rate of CRC recorded for 2009-13 was 40.7 per 100 000 of the population with a death rate over 2010-14 of 14.8 per 100 000. In the United Kingdom (UK) in 2014 there were 41 265 new cases of CRC and 15 903 deaths from CRC (CancerResearchUK, 2014).

1.2.2. Age

In Europe and the US only 2-8% of CRC occurs in people under the age of 40. However, in countries such as Egypt and the Philippines, 38% and 17% of CRC is seen in patients under 40 years, respectively (Abou-Zeid, Khafagy, Marzouk *et al.*, 2002; Kaw, Punzalan, Crisostomo *et al.*, 2002)**.** In the UK, incidence rates for bowel cancer are highest in people aged 85-89 and 44% are diagnosed in people aged 75years and over, with rates increasing significantly from age 50-54 (Figure 1.2) (CancerResearchUK, 2014).

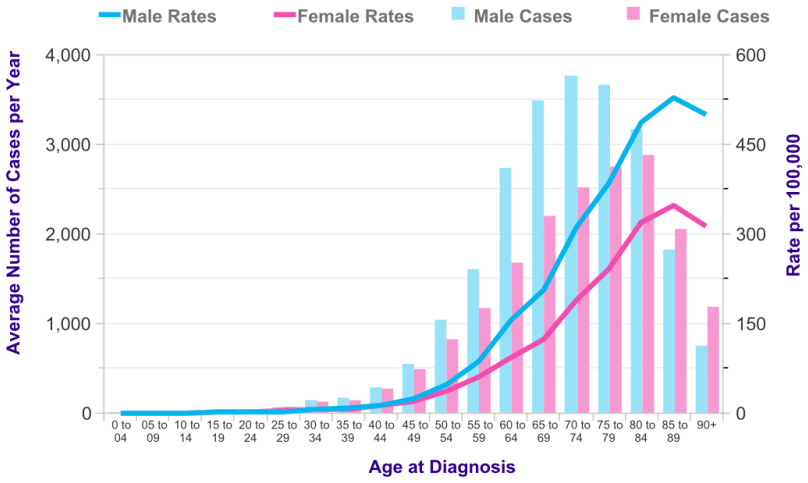

Figure 1.2: Source: cruk.org/cancerstats. Taken from Cancer Research UK, 2014 http://www.cancerresearchuk.org/sites/default/files/cstream-node/cases_crude_bowel_I14.pdf. Accessed August 2017.

1.2.3. Inherited genetic susceptibility

The majority of CRC patients (approximately seventy percent) do not have a familial cause or a genetic predisposition toward developing CRC. Only approximately thirty percent of CRC having a possible hereditary link. There are a group of patients thought to have a more intricate underlying polygenetic underlying cause, where a clear genetic pathway is not fully known. Although this subgroup of patients does have a higher risk of CRC than the general population, the risk is lower than the established inherited syndromes. Between 5-10% of CRC patients arise as a result of one of the well-established Mendelian inherited disorders (Bogaert & Prenen, 2014; Brosens, Offerhaus, & Giardiello, 2015; Lynch & Shaw, 2013). These include, but are not limited to:

1.2.3.1. Hereditary non-polyposis colorectal cancer

Hereditary non-polyposis colorectal cancer (HNPCC) is an autosomal dominant syndrome, also known as Lynch Syndrome (LS). It is caused by either a mutation of the EpCAM gene or of the mismatch repair genes (MLH1, MSH2, MSH6, PMS2), resulting in microsatellite instability. Microsatellite instability is present in >90% of CRC with LS, whereas this is only seen in 12% of sporadic CRC (Jansen, Menko, Brosens *et al.*, 2014). The risk of CRC or extra-colonic cancers due to LS is dependent on which mismatch repair gene has been mutated. Colonic tumours typically present proximal to the splenic flexure (60-80%)(Giardiello, Allen, Axilbund *et al.*, 2014).

1.2.3.2. Familial adenomatous polyposis (FAP)

FAP is an autosomal dominant syndrome, which is caused by a germline mutation in the APC gene, where there are over 1000 variations of mutation that result in FAP (Half, Bercovich, & Rozen, 2009). The severity of presentation of FAP is either classical or attenuated, depending on the location of the APC gene mutation. The classical presentation is of large numbers of multiple adenomatous polyps, often numbering hundreds to thousands, whereas attenuated FAP typically averages 30 polyps or 10-100 cumulatively over time. Classical FAP has an average age of CRC presentation at 39years, whereas attenuated FAP has an average age of 51years (Trimbath & Giardiello, 2002). The syndrome again carries with it both benign and malignant extra-colonic manifestations of presentation.

1.2.3.3. MUTYH- associated polyposis (MAP)

MUTYH-polyposis is an autosomal recessive syndrome, which is caused by inheritance of both alleles of the MUTYH gene (MYH gene). The presentation is similar to attenuated FAP. The average age of CRC presentation is 48 years (Jones, Vogt, Nielsen *et al.*, 2009). Extracolonic malignancy is also associated with MAP.

1.2.3.4. Juvenile polyposis (JP)

JP is an autosomal dominant syndrome which is influenced by a polygenetic mechanism. The exact mechanism in all presentations is not completely understood. In 39% of these patients, germline mutations in the Bone Morphogenic Protein Receptors Type 1a (BMPR1A) and SMAD4 genes have been found to be the cause. It is characterised by the

development of juvenile polyps mainly in the colon, associated with a higher risk of CRC to that of the general population (Brosens, van Hattem, Hylind *et al.*, 2007).

1.2.3.5. Peutz-Jeghers syndrome (PJS)

PJS is a rare autosomal dominant syndrome caused by a germline mutation of the serine threonine kinase 11 (STK-11), which is a tumour suppressor. Presentation of multiple hamartomatous polyps are found in both the small and large bowel (Bogaert *et al.*, 2014). It is also typically associated with both colonic and extra-colonic malignancy.

1.2.3.6. Serrated polyposis syndrome (SPS)

The genetic basis of SPS is still unknown, however it is thought likely to have a polygenetic underlying aetiology (Gaiser, Meinhardt, Hirsch *et al.*, 2013). The diagnosis is made on criteria of number and size of serrated polyps present throughout the colon (Boparai, Mathus-Vliegen, Koornstra *et al.*, 2010). SPS has been associated with a higher incidence of CRC to that of the general population (Rex, Ahnen, Baron *et al.*, 2012).

1.2.4. Sex

In most parts of the world, rates of CRC are higher in males than females. Males have been shown to have both a 30% higher incidence and a 40% higher mortality than females (R. Siegel, Desantis, & Jemal, 2014).

1.2.5. Race

On the surface, there appears to be a significant difference in the incidence of CRC both between different countries and also ethnicities (Center, Jemal, Smith *et al.*, 2009; Favoriti, Carbone, Greco *et al.*, 2016). However, when looking at this further, there are many confounding variables which affect an accurate representation of worldwide incidence of CRC between populations. It should be considered that the ability to report the incidence of CRC between countries has wide variation, with particular thought to access to healthcare and screening ability. It has been demonstrated that there is a significant difference in incidence and mortality of CRC between race and ethnicity within regional sub-populations (Rozen, Liphshitz, & Barchana, 2011; R. L. Siegel *et al.*, 2017), which could possibly be explained through differences in socioeconomic status playing a role in healthcare access. Deprived regions or subpopulations have been shown to have a higher morbidity and mortality, in relation to CRC (Byers, Wolf, Bauer *et al.*, 2008). In countries where screening programmes are undertaken, there is seen to be higher uptake of participation amongst higher socioeconomic subgroups (de Klerk, Gupta, Dekker *et al.*, 2017). Within the US, the black subgroup population had higher rates of CRC than the white population. It could be argued that race alone does not increase risk of CRC but rather reflects an interplay of complex factors including environmental influences, access to screening/healthcare and socioeconomic status as confounding variables to this observation (Irby, Anderson, Henson *et al.*, 2006).

1.2.6. Epigenetics

Environmental factors interacting with genes have been shown to influence the risk of developing CRC. Interactions including physical activity, obesity, medication (such as aspirin and vitamin D), tobacco use and food and alcohol consumption have all been shown to influence risk of CRC (Marley *et al.*, 2016)**.**

1.2.7. Colorectal cancer and peritoneal metastasis susceptibility

The true incidence of PM is not completely known, which is in part due to the lack of reliability of traditional imaging modalities detecting small peritoneal deposits, asymptomatic patient cohorts and post-mortem examinations not being routinely carried out (Sanchez-Hidalgo, Rodriguez-Ortiz, Arjona-Sanchez *et al.*, 2019). One retrospective cohort group of 3019 CRC patients surgically treated reported a 13% rate of peritoneal metastasis, where 61% were synchronous and 39% metasynchronous metastases found on clinical, radiological and histological examination after initial treatment (Jayne, Fook, Loi *et al.*, 2002). Whilst autopsy studies do carry in themselves an inherent self-selecting cohort bias, the incidence of CRC PM have been reported in some autopsy series to be as high as 40-80% (Koppe, Boerman, Oyen *et al.*, 2006). In one autopsy study of 5817 patients with a diagnosis of CRC, 1675 were seen to have metastatic disease. Mucinous adenocarcinoma (MC) and Signet-ring cell carcinoma (SRCC) more frequently had peritoneal disease, whereas adenocarcinoma (AC) predominantly metastasised to the liver. Colonic tumours above the peritoneal reflection were seen to have a higher rate of PM, whereas rectal tumours were seen to more often metastasise to extra-abdominal sites (Hugen, van de Velde, de Wilt *et al.*, 2014).

It could be hypothesised that the overall frequency of involvement of the peritoneum in CRC dissemination is likely to be higher amongst patients than what may be reported in the literature.

1.3. Current Treatment Options for Peritoneal Metastatic Disease in CRC

1.3.1. Surgery

1.3.1.1. Cytoreductive surgery (CRS) with Hyperthermic Intraperitoneal Chemotherapy (HIPEC)

CRS with HIPEC has become a widely accepted technique for treating peritoneal metastases from several abdominal origin cancers. Due to the magnitude of surgery, patient selection is important for patients undergoing CRS with HIPEC. The patient performance status and co-morbidities are important considerations in the determination of suitability to undergo surgery. However, there is no clear guidance or criteria regarding absolute thresholds for patients who are not suitable for surgery. However major cardiac or renal impairment have been identified as potential serious contraindications (Klaver, Groenen, Morton *et al.*, 2017).

There are several scoring systems described in the assessment of peritoneal dissemination in CRC and other abdominal cancers. The Peritoneal Carcinomatosis Index (PCI) score (Figure 1.3) is the most accepted score for both evaluating the tumour burden and estimating prognosis. A series of 173 patients demonstrated that a PCI index of <10 showed the 5-year survival to be approximately 53%, a score between 10-20 indicated a 23% survival and >20

indicated only 12% survival (Faron, Macovei, Goere *et al.*, 2016). Therefore, with PCI indexes >20 serious consideration should be taken as to whether to proceed to CRS and HIPEC. Such scoring systems do carry an element of intra- and inter-observer variation, and consistency of scoring in units is an important element to assessing outcomes.

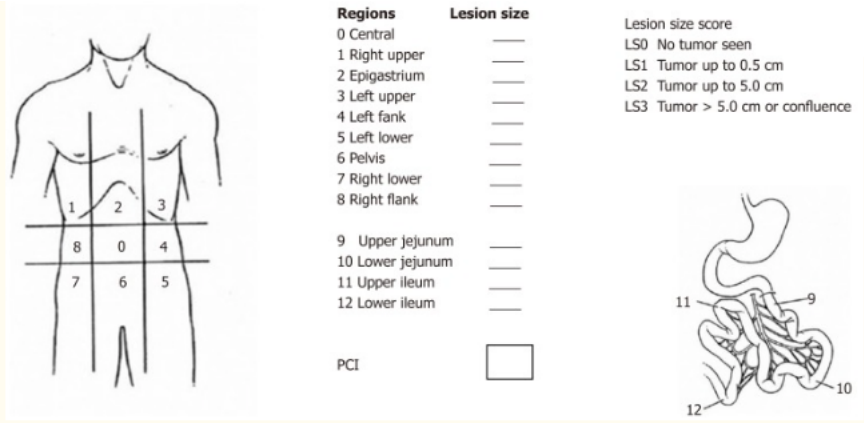

Figure 1.3. Peritoneal Carcinomatosis index scoring system as described by Sugarbaker (Jacquet & Sugarbaker, 1996). (Image taken from (Sanchez-Hidalgo *et al.*, 2019). The abdominal peritoneal cavity is split into nine regions and the small bowel is split into 4 regions of assessment. Peritoneal Tumour assessment and scoring is based on largest tumour deposits seen within the regions. Each assessment area is scored 0-3. 0 = no tumour, 1 = tumour up to 0.5cm, 2 = tumour up to 5cm, 3= tumour >5cm or confluent tumour.

Other predictors of prognosis include degree of lymph node infiltration, which is itself known to carry a poor prognosis for recurrence and reduced survival. Synchronous liver metastases need to be considered in treatment approach. Previously, PM with metastatic liver disease was considered a non-resectable entity however more aggressive treatment of liver metastases has seen an improvement in survival and is now not an absolute

contraindication for surgery (El-Nakeep, Rashad, Oweira *et al.*, 2017). Absolute contraindications to CRS with HIPEC include (Sanchez-Hidalgo *et al.*, 2019):

- Bulky and/or diffuse peritoneal metastasis
- Unresectable extra-abdominal metastatic disease.
- Vast small bowel serosal or small bowel mesenteric involvement (requiring an unaffected length of small bowel >150cm)
- Multi-segment small bowel obstruction
- Hepatic hilar PM involvement or unresectable liver metastasis

The process and principle of CRS involves resection of all macroscopic tumours from the intrabdominal cavity. This is achieved by parietal peritonectomy procedures and en-bloc resections of affected peritoneum and viscera. No residual macroscopic disease should be left.

The HIPEC phase of treatment, where heated chemotherapeutic regimens are delivered and circulated within the abdominal cavity, serves to treat any residual microscopic disease. However, there is lack of complete consensus as to the benefit of HIPEC in treating disease. The PRODIGE 7 trial directly compared CRS alone against CRS with HIPEC and demonstrated no significant survival benefit to CRS with HIPEC, with significantly increased morbidity in the HIPEC group (Quenet, Elias, Roca *et al.*, 2021). The results of this trial continue to be controversial. One of the key criticisms was that due to the trial being designed almost two decades ago, this has seen the evolution of chemotherapeutic regimens. Specifically, the dose and use of oxaliplatin has changed significantly and impact significantly in the assessment of morbidity. The use of mitomycin C has been shown to both have a better toxicity profile and be of benefit in animal studies (Koh, Ansari, Morris *et al.*, 2019).

1.3.1.2. Pressurised intraperitoneal aerosol chemotherapy (PIPAC)

Currently in experimental trials, PIPAC is an innovative drug delivery system being used for patients who have PM as the only region of metastatic disease from varying cancer origins. Patients whom are considered irresectable, and therefore not eligible for CRS & HIPEC, have been enrolled into experimental trials with PIPAC.

Pressurised aerosol derived chemotherapy delivery to the tissues is theorised, firstly, to boost the cytotoxic effect on the peritoneal tumours by increasing drug penetration, and secondly, serves to decrease the venous outflow due to the pressure facilitating more time in contact with the tumour tissues. Due to local tissues being affected, systemic side effects of the chemotherapeutic agents are reduced.

The outcomes, for patients with PM from CRC origin disease that undergo PIPAC therapy, are unclear in terms of improving overall survival. There are currently two trials involving PIPAC specifically looking at CRC origin and appendiceal origin tumours (Graversen, Detlefsen, Fristrup *et al.*, 2018; Lurvink, Rovers, Wassenaar *et al.*, 2021; Lurvink, Tajzai, Rovers *et al.*, 2021; Rovers, Lurvink, Wassenaar *et al.*, 2019; Rovers, Wassenaar, Lurvink *et al.*, 2021). There is one further trial looking at peritoneal metastatic tumours of various origins (Lurvink, Rovers*, et al.*, 2021; Lurvink, Tajzai*, et al.*, 2021).

Whether patients enrolled onto PIPAC regimens can be downstaged to a point where they can be considered for more radical CRS & HIPEC remains to be seen.

1.3.2. Chemotherapy

1.3.2.1. Conventional chemotherapeutic regimens

The role and the effectiveness of neoadjuvant and adjuvant systemic chemotherapy regimens for patients with CRC and PM has been controversial. Neoadjuvant chemotherapeutic regimens have not demonstrated clear improvement in survival in patients with isolated PM of CRC origin, without distant site systemic metastatic disease. The role of adjuvant systemic regimens is also unclear (Waite & Youssef, 2017). Part of the difficulty in assessing the benefit of systemic chemotherapeutic regimens in the context of CRS and HIPEC, is that to date, there are no clear standardised adjuvant protocols or regimens for patients undergoing CRS and HIPEC, and therefore treatment can potentially be haphazard and varied.

1.3.2.2. Novel treatment regimens

In advanced CRC, monoclonal antibodies (mAb) are available which specifically target phases of cancer growth, such as angiogenesis. Bevacizumab, which targets vascular endothelial growth factor (VEGF), was approved in 2004 and has been a mAb used in first-line therapy in mCRC (Grothey & Marshall, 2007). Other VEGF mAbs including aflibercept and ramucirumab have also been approved for second-line therapy (Mody, Baldeo, & Bekaii-Saab, 2018). Combination therapies of mAbs together with conventional systemic chemotherapeutic regimens have also been shown to provide a potential enhanced response to the addition of mAbs compared to systemic therapy alone (R. Cao, Zhang, Ma *et al.*, 2015; Choti, 2004; Hurwitz, Fehrenbacher, Novotny *et al.*, 2004; Y. Liu, Luan, & Wang, 2015).

Small case series have described a potential benefit of combination neoadjuvant therapy (Ceelen, Van Nieuwenhove, Putte *et al.*, 2014), but large-scale robust trials are still required. In the context of neoadjuvant treatment with mAbs, there is no clear data available concerning the safety of surgery following neoadjuvant treatment with such agents. One study described a two-fold increase in morbidity with the use of Bevacizumab prior to CRS and HIPEC and was likely associated with higher mortality (Eveno, Passot, Goere *et al.*, 2014).

1.3.3. Conservative and palliative approaches to patient care

Patients with mCRC who are untreatable, either surgically or systemically, can be considered principally for one of two approaches; the first of these being considered for palliative chemotherapy which would attempt to slow down the progression of disease. The second approach would entail symptomatic management of a patient with advanced CRC. The co-morbidity of the patient is likely to determine how aggressively symptoms can be managed. However, the burden of disease is also an important factor to consider when looking at the benefit of palliative chemotherapeutic regimens and the duration or timing of intervention a patient is likely to need.

Finally, the role of surgery in such palliative patients presenting with obstruction is also an area which is ambiguous. Stenting, defunctioning stomas or bypasses are possible options for patients who present with single point obstruction due to the metastatic process. However, patients with PM can present in situations where there are multifocal levels of

obstruction due to the burden of PM. This can often be a challenging scenario in which a multimodal approach should be considered for such patients, with the aim of improving quality of life. Both medical and interventional approaches have been found to be beneficial in some cases, including high calorie nutritional supplementation, drug therapy to reduce gastrointestinal secretions and antiemetic regimens have all served to help such patients. Some simple mechanical interventions such as NG tubes or venting gastrostomies may reduce nausea or vomiting for a patient. The underpinning principle towards approaching this is focusing on the patients' specific troublesome symptoms and finding a way to try to reduce the patient's symptoms, to improve quality of life

1.4. Genetic Pathways Involved in Colorectal Carcinogenesis

A complex range of molecular signalling pathways are attributed to tumorigenesis in CRC. At present, three predominant genetic pathways have been described in the underpinning aetiology of CRC.

1.4.1. The chromosomal instability (CIN) pathway

The CIN pathway is the most common route to colorectal carcinogenesis (Colussi, Brandi, Bazzoli *et al.*, 2013). Various mutations in the tumour suppressor genes such as APC, TP53 and 18q have been discovered in CRC. Similarly, mutations in the K-ras family oncogenes causing abnormalities in their expression and subsequent function are all seen to be part of the implicating key steps in carcinogenesis. The APC mutation is seen to disrupt the Wnt-signalling pathway that is responsible for cell growth and apoptosis (Behrens, 2005). TP53 mutations disrupt the transcription factor p53, which in normal function is responsible for

activating DNA repair proteins and initiating apoptosis when needed (D. Chen, Yu, Zhu *et al.*, 2006; G. H. Lee, Malietzis, Askari *et al.*, 2015). Alteration at 18q of chromosome 18 has been shown in 70% of primary CRC, particularly in advanced tumours (Fearon & Vogelstein, 1990). Tumour suppressors within the 18q gene, such as SMAD, DCC and Cables have also been studied in their involvement in various cancers including CRC (Kazemzadeh, Safaralizadeh, Feizi *et al.*, 2017; Korchynskyi, Landstrom, Stoika *et al.*, 1999; D. Y. Park, Sakamoto, Kirley *et al.*, 2007; Popat & Houlston, 2005; W. Xie, Rimm, Lin *et al.*, 2003). K-ras mutations cause persistent activation of the GTP (guanosine-5'-Triphosphate) protein, through RAS activation and subsequently affecting the Raf-MEK-ERK pathways, which causes persistent ongoing cell division (Pino & Chung, 2010). K-ras mutations are seen in 35-40% of CRC (Andreyev, Norman, Cunningham *et al.*, 1998; Santini, Loupakis, Vincenzi *et al.*, 2008).

1.4.2. Microsatellite instability (MSI) pathway

Microsatellites are repetitive DNA units of 1-5 base pairs, which are repeated over 15-30 times. Instability occurs where there is frequent change of the length of these sequences in DNA replication. Normally microsatellites are repaired by mismatch repair enzymes. However, where there are mutations in the genes responsible for sequencing of mismatch repair enzymes, microsatellite sequencing repair subsequently fails and instability ensues due to the failure to repair the errors (Konishi, Wheeler, Donaldson *et al.*, 2000). This is seen in only approximately 10-15% of sporadic CRC (Thibodeau, Bren, & Schaid, 1993) but in 90% of HNPCC (Aaltonen, Peltomaki, Mecklin *et al.*, 1994; Konishi *et al.*, 2000). It has also been seen in other types of cancers but less frequently than CRC.

MSI analysis is clinically useful to identify patients with hereditary non-polyposis colorectal cancer (HNPCC) as well as predict the likely cancer response to certain chemotherapy regimens. The Bethesda guidelines were a set of criteria developed to identify patients who should be tested for MSI and look to identify patients with HNPCC (Kaya, Basak, Sisik *et al.*, 2017; Murphy, Zhang, Geiger *et al.*, 2006; Rodriguez-Bigas, Boland, Hamilton *et al.*, 1997).

1.4.3. The CpG (cytosine-phosphate-guanosine) island methylator phenotype (CIMP)

CpG islands are present in human genes in an un-methylated form. Cancers have been found to have varying degrees of methylation, those with higher degrees of methylation carry a distinct epidemiology, presentation and histology (Nazemalhosseini Mojarad, Kuppen, Aghdaei *et al.*, 2013). It has also been seen that proximal and distal CRC have distinct methylation profiles. The exact pathophysiology of this mechanism is still not fully understood, however, epigenetic factors are thought to play a significant role in hyper-methylation leading to inactivation or downregulation of tumour suppressor genes (Chan, Issa, Morris *et al.*, 2002; Toyota, Ahuja, Ohe-Toyota *et al.*, 1999).

1.5. Signalling Pathways in Colorectal Cancer

The various signalling pathways involved in the pathogenesis of CRC are still being studied. There are several pathways known to play a role in tumorigenesis in CRC when they are disrupted. Research is ongoing into targeted treatment of suppressing or promoting steps within these specific pathways, to treat CRC, where abnormalities develop. The tumour microenvironment is an important factor when developing any treatment, as altering the pathway at a certain point may affect downstream cell signalling which may upregulate or downregulate tumour development.

1.5.1. Wnt signalling pathway

The Wnt proteins are regulators of cell proliferation amongst local cells, particularly with their usual short range of action. In humans, there are several subfamilies of Wnt proteins that regulate different genetic signalling dependent on the cells involved. They bind onto transmembrane proteins of cells to affect cell activity. The Wnt pathway is classified into β-catenin-dependent (canonical) and β-catenin-independent (non-canonical) pathways. The canonical pathway is influenced by the APC protein and in CRC plays a role in proliferation, migration, invasion, tumourigenesis and metastasis (Behrens, 2005; Rahmani, Avan, Hashemy *et al.*, 2017). Figure 1.4.

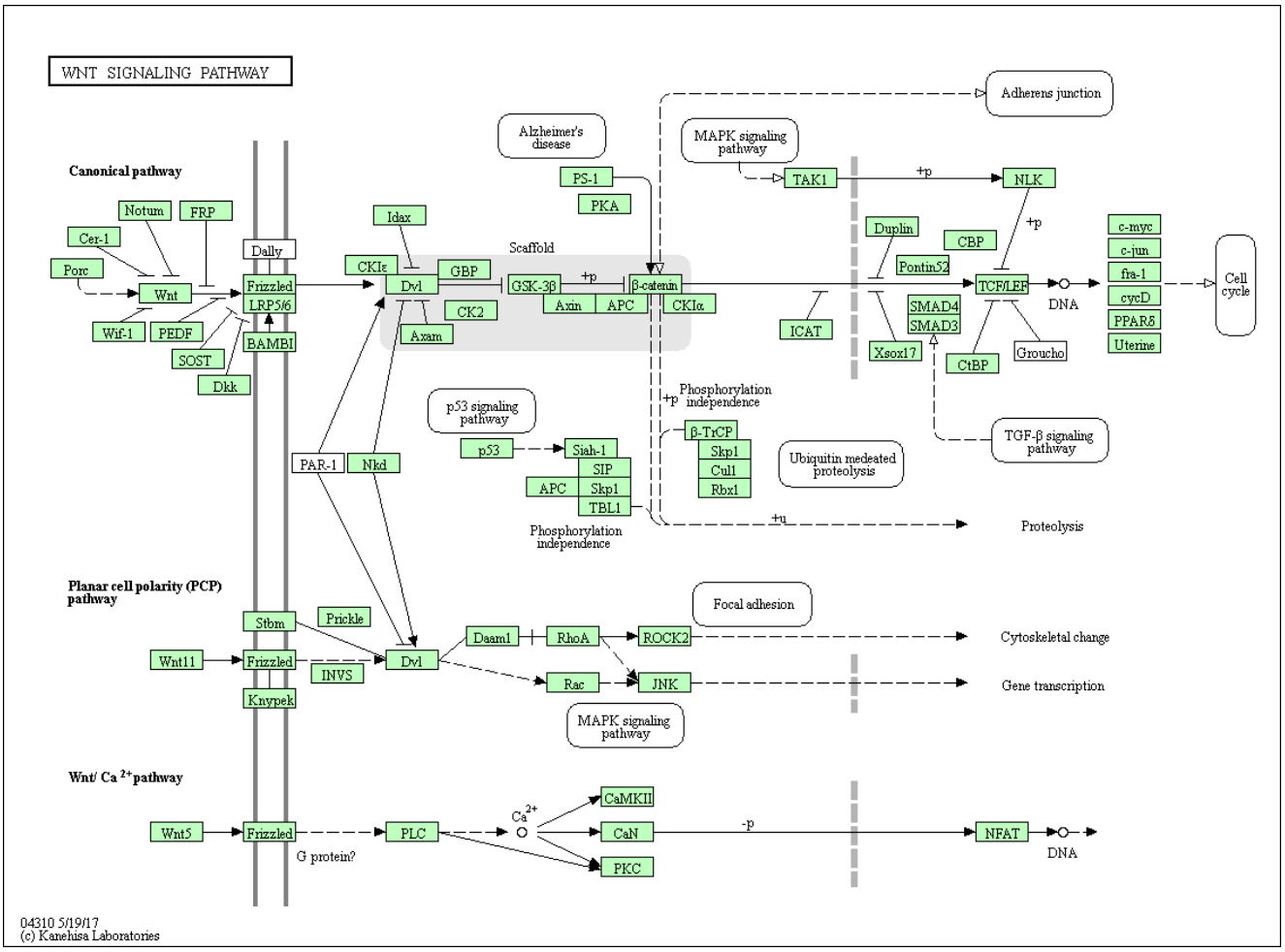

Figure 1.4. Wnt signalling pathway. Taken from GenomeNet.
http://www.genome.jp/kegg/pathway/hsa04310.png

1.5.2. TGF-β signalling pathway

TGF-β is an effective inhibitor of epithelial cell proliferation with activity on a wide range of cell types. Five isoforms of TGF-β s exist: TGF-β1-5. These are part of a superfamily of proteins which include inhibins, activins, müllerian inhibiting substance and BMPs (bone morphogenetic proteins) (Celeste, Iannazzi, Taylor *et al.*, 1990; Massague, 1990). TGF-β suppression is thought to lead to colorectal cancer by inhibition of TGF-β mediated growth control. It has also been shown that TGF-β is both an inhibitor and promotor of carcinogenesis and has a role in homeostasis (Akhurst & Derynck, 2001).

TGF-β receptors (TGF-β R1 & TGF-β R2) are equally important in the TGF-β signalling pathway and again can be seen to disrupt the signalling transduction of TGF-β (Lampropoulos, Zizi-Sermpetzoglou, Rizos *et al.*, 2012).

As seen in Figure 1.5, the SMAD proteins are integral in TGF-β signalling. Mutations in SMAD proteins have demonstrated a significant role in development of CRC (Korchynskyi *et al.*, 1999; O'Sullivan & Shanahan, 1999). Loss of SMAD signalling has been associated with advanced disease and poor prognosis in CRC (W. Xie *et al.*, 2003)

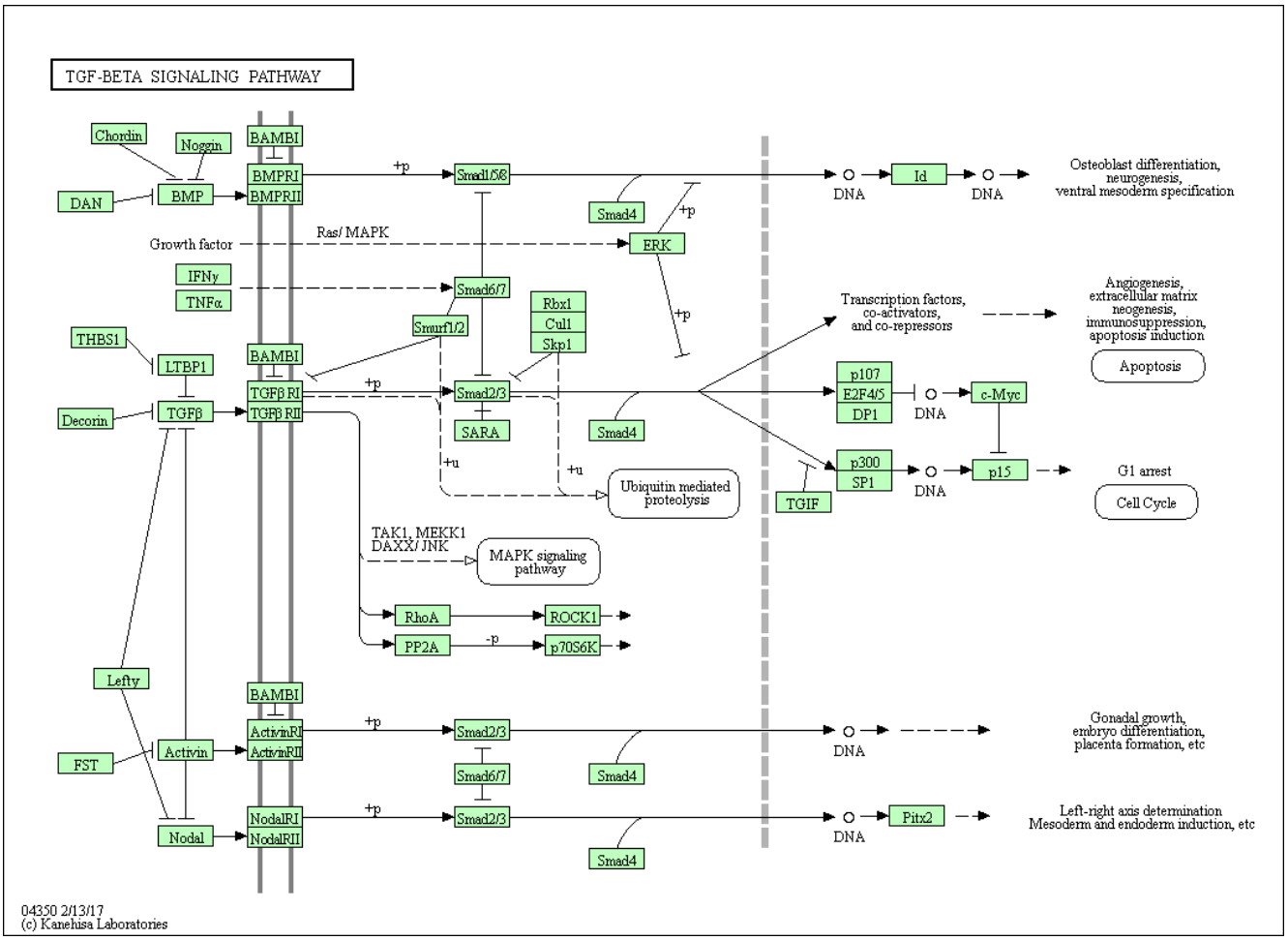

Figure 1.5. TGF signalling pathway. Taken from GenomeNet.

http://www.genome.jp/kegg/patI/hsa/hsa04350.png

1.5.3. P53 dependent signalling pathway

P53 is encoded by the *TP53* gene and is a tumour suppressor protein. The protein's molecular mass is 53 kilodaltons (kDa). It plays a role in preventing proliferation in many types of cancer and, when mutated, its regulatory functions in inhibiting angiogenesis, cell growth arrest, DNA repair and apoptosis are compromised. Figure 1.6.

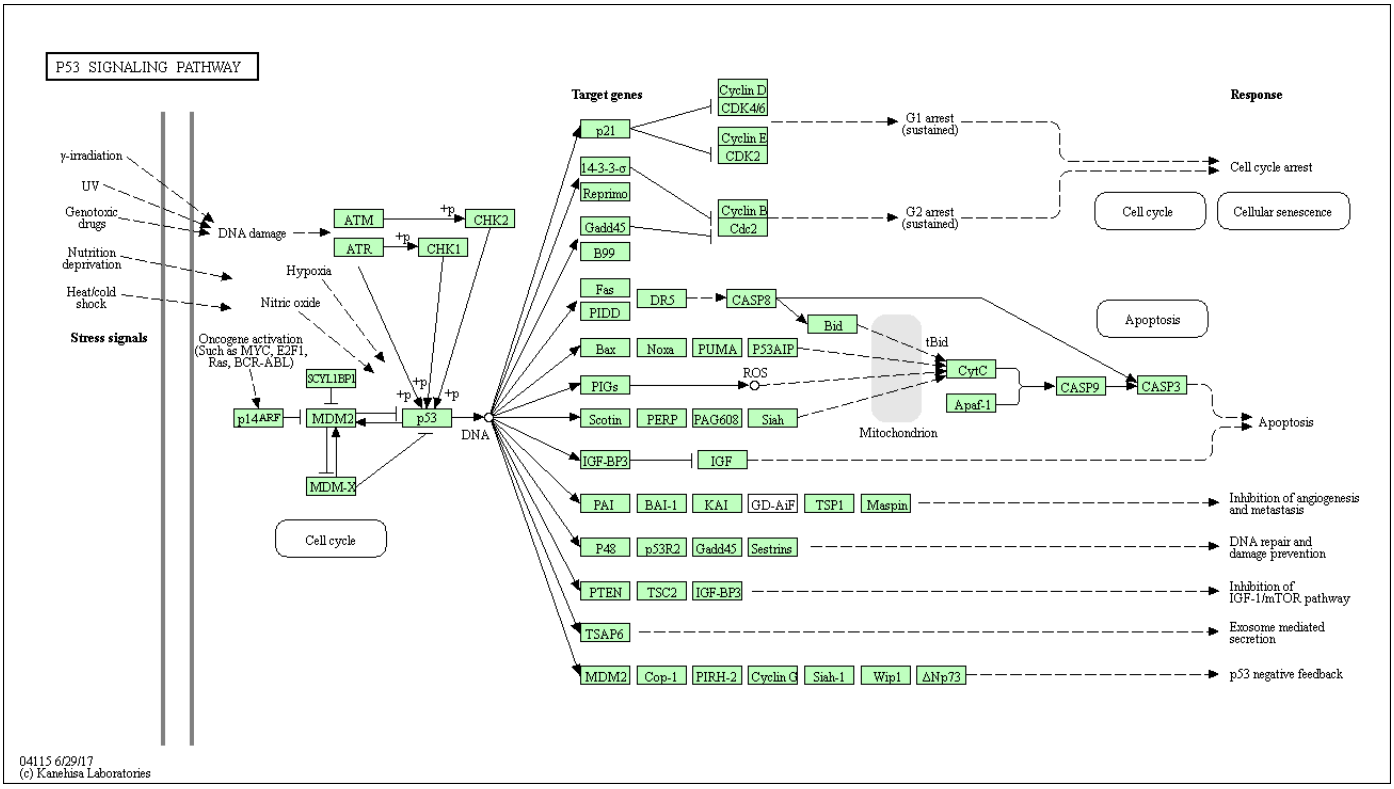

Figure 1.6. P53 signalling pathway. Image taken from GenomeNet

http://www.genome.jp/kegg-bin/show_pathway?hsa04115

1.5.4. MAPK signalling pathways

MAPK (mitogen-activated protein kinases) are seen to activate downstream proteins by phosphorylation. ERK (Extracellular signal-regulated kinase), P38 and JNK c-Jun N-Terminal kinase are three predominant MAPK pathways that regulate a wide array of cellular processes including cell proliferation (Figure 1.7). They are stimulated by both growth factors and cytokine/cell stress signals. In colorectal cancer, particular interest has been taken in the ERK pathway expression in disease states and inhibition (Fang & Richardson, 2005; Gulmann, Sheehan, Conroy *et al.*, 2009; Lascorz, Forsti, Chen *et al.*, 2010; Roux & Blenis, 2004).

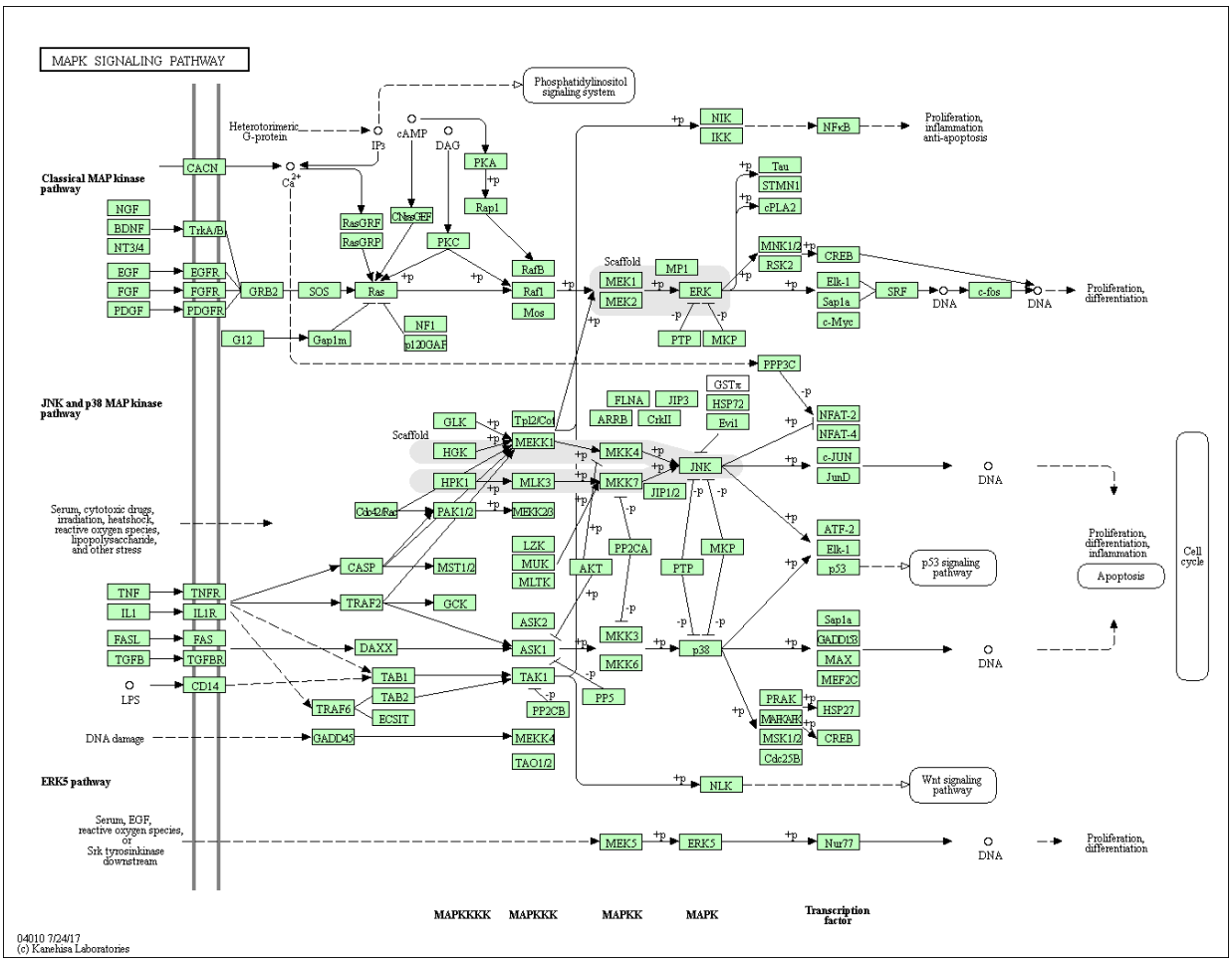

Figure 1.7. EGFR/RAS/RAF/MAPK signalling pathway. Taken from GenomeNet. http://www.genome.jp/kegIthway/hsa/hsa04350.png

1.5.5. PI3K-AKT signalling pathway

PI3K-AKT signalling has been demonstrated to contribute to apoptosis, cell cycle regulation and the P53 pathway. Activation of PI3k leads to phosphorylation and activation of AKT via PDK1/2 (phosphoinositide-dependent kinases), which in turn activate downstream intracellular proteins (Figure 1.8) that regulate cell survival and proliferation (Carnero, 2010; Choy, Fraga, Mackenzie *et al.*, 2016; Danielsen, Eide, Nesbakken *et al.*, 2015; Ke, Wei, Yeh *et al.*, 2015; Zhou, He, Jiao *et al.*, 2015).

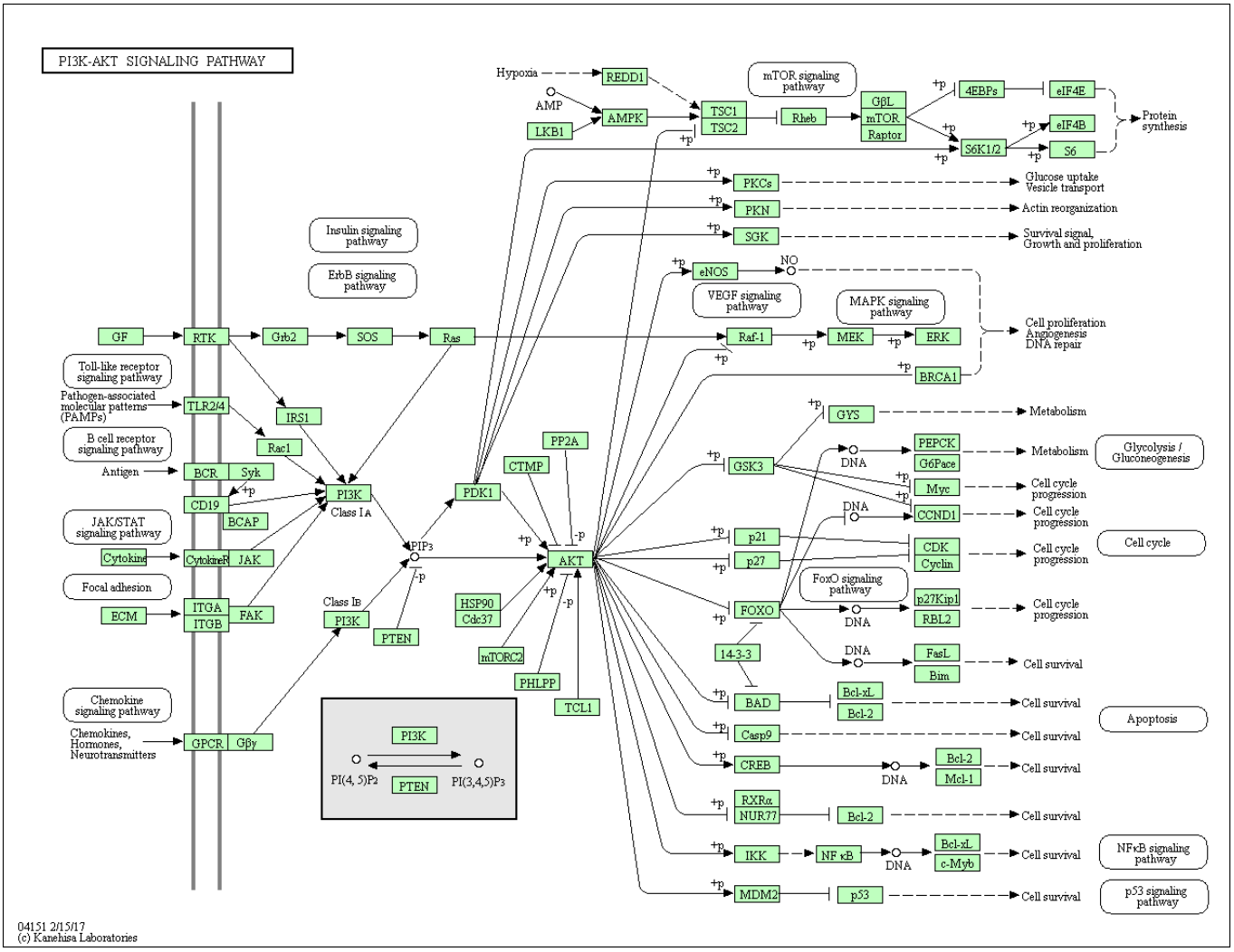

Figure 1.8. P13K Signalling pathway. Taken from GenomeNet.

http://www.genome.jp/kegg-bin/show_pathway?hsa04151

1.6 Mesothelial Cell Histology, Embryology, and Physiology

1.6.1. Histology

Within the abdominal cavity the peritoneum is split into two components, the parietal peritoneum and the visceral peritoneum. The parietal peritoneum lines the inner surface of the cavity, and the visceral peritoneum covers the visceral organs by integrating with the respective outer serosal layers. Both the visceral and parietal peritoneum are structurally similar. Both are composed of three fundamental layers: the mesothelium, the basal lamina, and the sub-mesothelial stroma. On top of the mesothelial cells sits a fluid film (Figure 1.9).

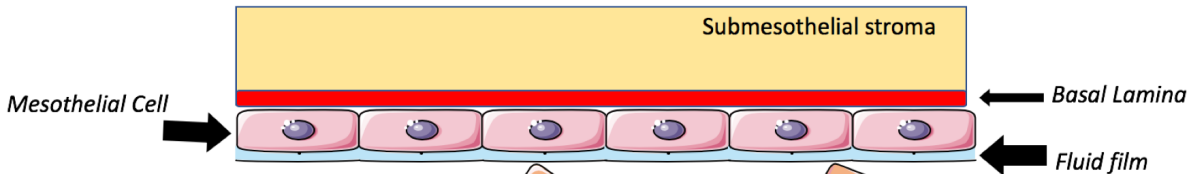

Figure 1.9: Histological structure of the peritoneum. Fluid film, Mesothelial cell layer, Basal Lamina and Sub mesothelial Stroma.

1.6.1.1. Fluid film

Sitting on top of the mesothelial cells is a glycoprotein called a glycocalyx, which serves to trap fluid and create a stagnant fluid layer. This layer is made up of proteoglycans and glycosaminoglycans (GAG). The hyaluronan family is the predominant GAG, which is seen to play a role in cell signalling and diffusion at the peritoneal surface (Evanko, Tammi, Tammi *et al.*, 2007; Knudson, Munaim, & Toole, 1995). The fluid film can influence both cell-cell adhesion and de-adhesion. It can serve to regulate tissue function including proliferation and locomotion of cells (Evanko *et al.*, 2007).

1.6.1.2. Mesothelium

This is a monolayer of mesothelial cells that have both epithelial and mesenchymal characteristics. These cells cover the entire surface of the three serosal surfaces of the body cavities in humans- the pericardium, the pleura and the peritoneum (Mutsaers, 2002). In males, it also surrounds the testis. The cells have a central round or oval nucleus and are roughly 25μm in diameter and can adapt their functional and structural characteristics depending on the conditions they are under (Mutsaers, 2002). Most cells are structured in squamous flattened arrangement, however under certain conditions or regions within the peritoneum, such as the 'milky spots' of the omentum, peritoneal side of the diaphragm and the parenchymal organs, the arrangement of cells is predominantly cuboidal (Mironov, Gusev, & Baradi, 1979; Mutsaers, 2002). The cells have been shown to play roles in fluid and cell transport, inflammation, tissue repair, lysis of fibrin deposition, as a protective barrier and as a frictionless interface for organs and tissues (Blackburn & Stanton, 2014; Mutsaers, Prele, Pengelly *et al.*, 2016; Waniewski, 2013).

1.6.1.3. Basal lamina

The basal lamina is thought to support the mesothelial cells at the basal surface. It is made up of an extracellular matrix composed of a mixture of collagens, with type IV collagen and laminin as predominant features. The binding of mesothelial cells to the basal lamina is weak, therefore detachment regularly ensues following minor trauma (Raftery, 1973; J. O. van Baal, Van de Vijver, Nieuwland *et al.*, 2017).

1.6.1.4. Interstitium

The interstitium is also referred to as the sub-mesothelial stroma. This provides further support to the peritoneal structure, particularly with type I collagen fibres. Fibronectin, proteoglycans, GAGs, fibroblasts, adipocytes, lymphatics and blood vessels are present within this structure. The interstitium is also a readily available source of immune cells which are activated in various pathologies.

1.6.2. Embryology

Peritoneal development begins in the fifth week, at the gastrulation stage, of gestation (Sadler, 2012). The peritoneum is derived from the mesodermal cells lining the body cavity of an early embryo, termed the intraembryonic coelom. The mesoderm splits into three components; the lateral plate mesoderm, the intermediate mesoderm and paraxial mesoderm. The peritoneum develops from the lateral plate mesoderm, where it separates into the visceral plate and parietal plate.

The visceral plate mesoderm together with the endoderm contribute to forming the gut wall and the mesodermal cells form the visceral peritoneum. The parietal plate, together with the ectoderm, contribute to form the embryonic body wall. The parietal plate mesodermal cells form the parietal peritoneum (J. O. van Baal *et al.*, 2017).

The visceral peritoneum forms a double layer which provides a structure or scaffold for mesenteries to develop in which vessels and lymphatics form to supply organs. The omentum is again formed from a double layer of visceral peritoneum.

1.6.3. Physiology

The role of the peritoneum is of significance in maintenance of homeostasis within the abdominal cavity. Peritoneal fluid is in constant contact with the peritoneum, which circulates within the abdominal cavity and creates a microenvironment for cells and molecules to interact. The lymphatic stomata serve as drainage channels for ascitic absorption of fluid and cells from the peritoneal cavities. They can be found on the greater omentum, falciform ligament, mesentery and throughout the peritoneal lining of the abdominal cavity.

Molecules have the ability to enter or leave via transudation, exudation or through the lymphatics. When pathology occurs (i.e. neoplasia, trauma, inflammation or infection), either the equilibrium is disrupted leading to abnormal function or alternatively the normal physiology of the peritoneum is exploited by a given pathology. In relation to metastatic spread in CRC, the physiological interaction of the peritoneum within the microenvironment is harnessed in peritoneal spread.

In response to injury, not only do mesothelial cells heal from the wound edges but have also been shown to demonstrate the ability to detach from distant sites, migrate and settle on a site of mesothelial injury (Mutsaers *et al.*, 2016). The concept of free-floating mesothelial cells in the peritoneal fluid is thought to increase the speed of repair of injured sites (Foley-Comer, Herrick, Al-Mishlab *et al.*, 2002). The peritoneum contains surface microvilli (Blackburn *et al.*, 2014) and as such covers a large surface area approximately 140cm^2 (+/- 80cm^2) (Albanese, Albanese, Mino *et al.*, 2009; Rubin, Clawson, Planch *et al.*, 1988).

1.7. Peritoneal Metastasis in Colorectal Cancer

The development of PM in CRC is thought to be caused by four principal mechanisms - direct invasion, intraperitoneal seeding, lymphatic spread and haematogenous embolic dissemination. Distant peritoneal metastasis in CRC is thought to be initially caused by individual or collections of cells being able to detach from the primary tumour and obtain access to the peritoneal space. Once free, these cells can be transported along the predictable physiological routes, which are responsible for clearance of fluid from the peritoneal circulation. It has been described that the dissemination of peritoneal metastases is dependent on the primary location of the tumour and the subsequent circulation of shedding or detached tumour cells from the primary tumour results in a relatively predictable pattern of peritoneal spread (Carmignani, Sugarbaker, Bromley *et al.*, 2003). Malignant mucinous ascites also has different peritoneal surface metastatic patterns to that of solid tumours.

Tumour cells must then next be able to attach to the distant peritoneum, before they then can invade and proliferate at the new site of attachment. This process and success of metastatic cells being able to achieve this is multifactorial. What this means is that the ability for a malignant cell free-floating in the peritoneal cavity to attach on to a distant site, away from the primary tumour, is dependent on both the biological properties of the cancerous cells themselves and also the biological conditions of the distant tissue (Cortes-Guiral, Hubner, Alyami *et al.*, 2021). This is termed the so called ‘soil and seed’ theory (Mikula-Pietrasik, Uruski, Tykarski *et al.*, 2018).

In the process of intraperitoneal seeding, two mechanisms of attachment to the peritoneum have been described. The first is via trans-lymphatic metastasis (TLM) and the second being trans-mesothelial metastasis (TMM) (F. Sun, Feng, & Guan, 2017). In TLM, free tumour cells find access to the sub-mesothelial lymphatics through openings at the junctions of mesothelial cells, called lymphatic stomata. In TMM, free tumour cells are believed to exploit the native cell surface receptor mechanisms to adhere to the mesothelium through possible upregulation of cell surface receptor molecules of the cancer cells, which express a distinct pattern of adhesion receptors. These mechanisms are thought to possibly share similarities in mechanisms of leukocyte migration in peritoneal inflammation (MacCarthy-Morrogh & Martin, 2020).

Cytokines normally released in reaction to peritoneal inflammation include tumour necrosis factor-α (TNF-α), Interleukin (IL)- 1β, IL-6 and interferon-γ and have been seen to create a beneficial environment for tumour cells interacting with mesothelial cells (Yonemura, Endou, Nojima *et al.*, 1997). This cytokine release increases the expression of cell adhesion molecules, including platelet-endothelial cell adhesion molecule-1 (PECAM-1) and intracellular adhesion molecule-1 (ICAM-1), allowing for more readily available ability of mesothelial cells to interact with tumour cells (Jayne, O'Leary, Gill *et al.*, 1999; Klein, Bittinger, Skarke *et al.*, 1995; Y. Liang & Sasaki, 2000).

1.7.1. Peritoneal metastatic model

The cycle of PM formation is theoretically split into four steps (Sluiter, de Cuba, Kwakman *et al.*, 2016) (Figure 1.10a):

1. Detachment, local invasion, and entry to peritoneal cavity:

Shedding of cancer cells from a primary colon cancer mass can either be spontaneous or iatrogenic. Spontaneous causes can involve downregulation of cell-cell adhesion properties within a tumour. Incomplete resection or breach of tumour integrity at surgical resection are potential modes of iatrogenic cancer cell detachment. Cells, once free, are then able to be transported around the peritoneum utilising the peritoneal circulation (Figure 1.10b). Cells are normally unable to survive following detachment since they require anchorage to the extracellular matrix (ECM) and surrounding cells in order to function optimally. Anoikis is a type of programmed cell death to prevent tissue proliferation when anchorage-dependent cells become detached and are unable to continue normal cell-cell signalling. Cancer cells have a multitude of mechanisms in which to evade cell death mechanisms. One such mechanism described includes the ability of an anchorage dependent cancer cell to aggregate into clusters with other cancer cells. This facilitates the ability for cells to both survive within a microenvironment of cell clusters whilst in suspension, providing time in which such cells can find a distant site to adhere to (Y. Liu, Bunston, Hodson *et al.*, 2017).

2. Adherence to peritoneal surface:

Detached malignant cells adhere to mesothelial cells of the peritoneum through interaction with adhesion molecules found on the cell surfaces of both the malignant cells and the mesothelial cells. Inflammatory mediators have been reported to promote the expression of adhesion molecules and increase the propensity for peritoneal dissemination at a distant site (Klein *et al.*, 1995; van Grevenstein, Hofland, van Rossen *et al.*, 2007). HA coating the mesothelial cells has also been described to facilitate cell-cell adhesive properties in both malignant and non-malignant cell interaction (Dechaud, Witz, Montoya-Rodriguez *et al.*, 2001; Misra, Hascall, Markwald *et al.*, 2015)

3. Invasion of the peritoneum:

Access to the sub-mesothelial layers of the peritoneum is thought to occur where there are disruptions of mesothelial continuity. This disruption could be iatrogenic, via local trauma. Alternatively, the cancer cells themselves can cause disruption to the mesothelial layer, such as through inducing apoptotic mechanisms of mesothelial cells (Heath, Jayne, O'Leary *et al.*, 2004). Another theory is the changing shape and rounding of mesothelial cells in response to inflammation and cytokine expression, which is thought to expose the basement membrane making it susceptible to invasion by malignant cells (Yonemura *et al.*, 1997).

4. Colonisation and angiogenesis:

Metastatic tumour deposits, once having breached the mesothelial layer, can proliferate through the production and utilisation of growth factors (Davies, Farmer, White *et al.*, 1994; Salomon, Brandt, Ciardiello *et al.*, 1995). In order to enrich tumour cells with nutrients and oxygen, tumour cells can produce angiogenic promoting molecules that induce angiogenesis in the patient and bring a blood supply to the tumour cells (Hanahan & Weinberg, 2011; Lemoine, Sugarbaker, & Van der Speeten, 2016).

All these steps are regulated by multi-molecular interaction and signalling mechanisms, which facilitate the process of peritoneal spread. Studies looking into individual influential molecules have demonstrated some degree of variability in the level of peritoneal dissemination when they are affected (Hanahan *et al.*, 2011). The next section discusses a selection of molecules that have previously been identified and described in the literature as potentially playing a role in process of PM.

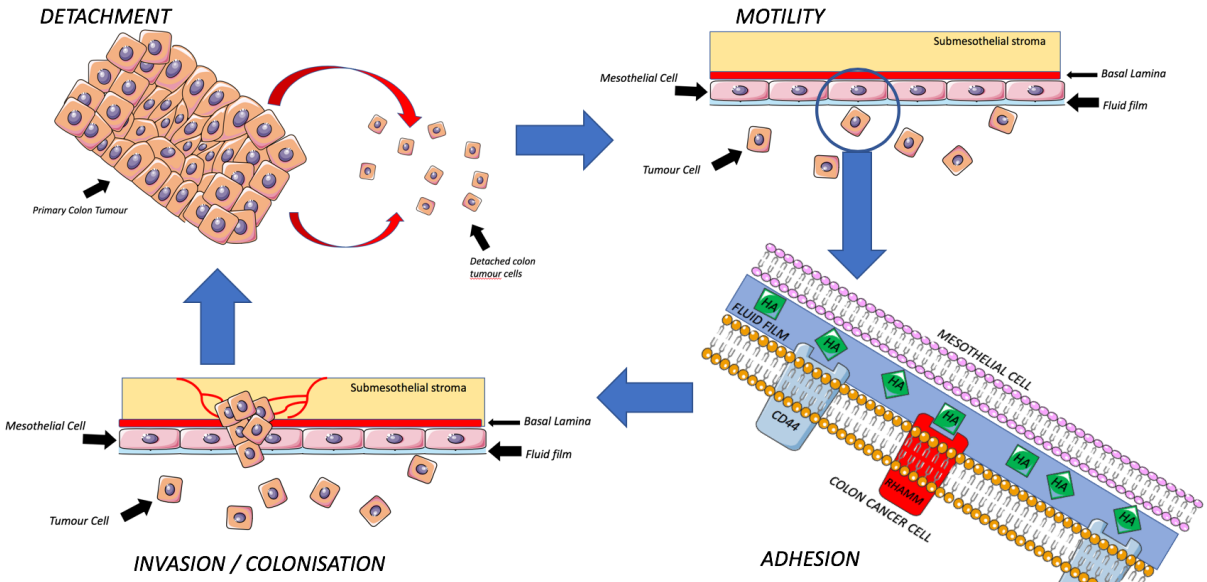

a.

b.

Figure 1.10: a. The peritoneal metastatic model of spread of cancer cells within the peritoneal cavity. b. Schematic figure of typical flow of fluid of peritoneal circulation which enables likely predictions of peritoneal metastatic spread. Image taken from (Levy, Shaw, & Sobin, 2009).

1.8. Molecules Involved in Stages of Peritoneal Spread

Peritoneal metastatic spread has been shown to be a multi-molecular signalling process with various avenues of progression, both dependent on the type of malignancy and due to interdependent polygenetic variables (Pretzsch, Bosch, Neumann *et al.*, 2019; Yonemura & Endou, 2000). Several different molecules have been identified as part of the process of PM at various stages of metastatic spread to the peritoneum.

1.8.1. Molecules involved in detachment and motility and migration

1.8.1.1. Met Proto-oncogene (c-MET)

In normal physiology c-MET is activated by hepatocyte growth factor (HGF) to initiate an invasive growth pattern seen in embryonic development and organ regeneration (Y. Zhang, Xia, Jin *et al.*, 2018). Hepatocyte growth factor receptor (HGFR) is encoded by the proto-oncogene c-MET. Malignancy appears to have utilised this process to enhance invasion. c-MET has been shown to be involved in peritoneal spread in ovarian malignancy (K. Sawada, Radjabi, Shinomiya *et al.*, 2007). Abnormal c-MET expression has been associated with poorer outcomes in CRC (Osada, Matsui, Komori *et al.*, 2010).

1.8.1.2. KLKs (Kallikrein-related peptidases)

A link has been found between KLK expression and cell clustering (de Cuba, Kwakman, van Egmond *et al.*, 2012). There are 15-proteins known to make up the KLK family. KLK7 expression has been seen in aggregation of malignant cells in ovarian cancer and also is thought to be prognostically relevant in CRC (Dong, Tan, Loessner *et al.*, 2010). Cell clustering has facilitated the evasion of anoikis mechanisms of free-floating adhesion-

dependent cancer cells, when detached from the primary tumour. The upregulation of KLKs in malignancy may promote cell survival for PM in the detachment phase.

1.8.1.3. V-Src (Sarcoma viral oncogene homologue)

V-Src (Sarcoma viral oncogene homologue (Src)) is a tyrosine kinase that has been shown to provide transient protection of colorectal epithelial cells from anoikis and Src expression is thought to increase such resistance (Hofmann, Lippert, Falk *et al.*, 2009; Sakamoto, Takamura, Ino *et al.*, 2001). Cell-cell adhesion is promoted by increased V-Src expression (de Cuba *et al.*, 2012), which may promote cell clustering in the peritoneal environment for free-floating cancer cells as part of anoikis evasion.

1.8.1.4. TWIST homologue 1 (TWIST1)

TWIST is a transcription factor which is found abundantly in mesodermal origin cells. Suppression of TWIST with siRNA has shown corresponding rates of migration, invasion, and adhesion to peritoneal mesothelium to be significantly lower in ovarian cancer cell lines and thus reducing peritoneal disease burden (Terauchi et al., 2007).

1.8.1.5. Epidermal growth factor receptor (EGFR)

When EGFR is activated, it initiates a signalling cascade which both initiates cell proliferation and is thought to downregulate E-cadherin activity. Experimental work, with ovarian cancer cell lines downregulating E-cadherin, demonstrated an invasive response of the malignant cells. This was thought to be precipitated by the down signalling induction of Matrix Metallopeptidases (Cowden Dahl, Symowicz, Ning *et al.*, 2008).

1.8.1.6. Hepatocyte growth factor (HGF)/scatter factor (SF)

HGF/SF has been seen to be secreted by fibroblasts (Stoker, Gherardi, Perryman *et al.*, 1987) and is thought to promote carcinoma cell migration. Tumour cells can exploit this process through the upregulation of expression of HGF/SF via secretion of molecules, such as Interleukins and growth factors themselves (T. Nakamura, Matsumoto, Kiritoshi *et al.*, 1997; Shimao, Nabeshima, Inoue *et al.*, 1999).

1.8.2. Molecules involved in peritoneal adherence and colonisation:

1.8.2.1. Integrins

In normal physiology, integrins are a group of receptors involved in cell-ECM (extracellular matrix) attachment and signalling. Several studies have demonstrated that integrins may have a role in peritoneal attachment of malignant cells. Blockade of integrin activity has shown reduced peritoneal attachment in *ex-vivo* and *in vivo* models (Holloway, Beck, Girard *et al.*, 2005; Oosterling, van der Bij, Bogels *et al.*, 2008).

1.8.2.2. Cadherin 1 (CDH1 or E-cadherin)

CDH1 is made up of glycoproteins that facilitate cell-cell adhesion in epithelial cells. Cancers including CRC, have shown reduced expression of CDH1, and consequently increased metastatic invasion. (Jie, Zhongmin, Guoqing *et al.*, 2013; S. Y. Park, Lee, Cho *et al.*, 2016; Pocard, Debruyne, Bras-Goncalves *et al.*, 2001)

1.8.2.3. Intracellular adhesion molecule 1 (ICAM-1)

There are five ICAMs which form a subfamily of the immunoglobulin superfamily of cell adhesion molecules. ICAM-1 is a single chain protein 80-114kDa with a core polypeptide structure of 55kDa. ICAM-1 has been found to act as a binding receptor for HA. The molecule has been found to share some basic amino acid clusters which are similar to both CD44 and RHAMM (Receptor for hyaluronan mediated motility) (McCourt, Ek, Forsberg *et al.*, 1994). Increased expression of ICAM-1 has been found to be associated with increased adhesion of malignant cells in CRC cell lines (Alkhamesi, Roberts, Ziprin *et al.*, 2007; Mikula-Pietrasik, Uruski, Kucinska *et al.*, 2017). This molecule is discussed further in relation to CRC in section 1.9.10.

1.8.2.4. Epithelial cell adhesion molecule (Ep-CAM)

High expression of Ep-CAM has been found to be associated with epithelial malignancy and has been demonstrated in CRC particularly in distant metastatic spread. Downregulation of Ep-CAM expression may potentially inhibit CRC proliferation. (Han, Zong, Shi *et al.*, 2017; Karanikiotis, Skiadas, Karina *et al.*, 2005; Qi, Zhou, Zhang *et al.*, 2015).

1.8.2.5. CD44

CD44 has also been referred to by several alternative names including homing cell adhesion molecule (HCAM), phagocytic glyocoprotein-1 (Pgp-1), lymphocyte homing receptor, Hermes antigen, Extracellular matrix receptor-III (ECMR-III) and HUTCH-1. CD44 is a glycoprotein which has been implicated in a wide array of cellular functions including many cell-cell interactions, cellular adhesion, and migration. Its significant role in cellular adhesion is discussed in section 1.9.

1.8.3. Molecules involved with invasion of the peritoneum

1.8.3.1. Matrix metalloproteinases (MMPs)

ECM is broken down by the proteolytic action of MMPs, both in normal and malignant physiology. This process is thought to facilitate tumour cell invasion to the stromal layer. In various types of malignancy, overexpression of certain MMPs has been seen. In animal studies, inhibition of MMP activity showed inhibition of peritoneal metastasis (Mizutani, Kofuji, & Shirouzu, 2000; Y. Wang, Wu, Pang *et al.*, 2017; Q. Zhao, Xu, Sun *et al.*, 2017). MMPs are linked to Cancer associated Fibroblasts. These smooth muscle fibroblasts appear to be a source of various lytic enzyme production, including MMPs, and are able to promote invasion through breaching the basement membranes after adhesion at distant sites (Glentis, Oertle, Mariani *et al.*, 2017; Martin, Pujuguet, & Martin, 1996).

1.8.4. Colonisation, survival, and angiogenesis induction

1.8.4.1. Insulin-like growth factors (IGF)

Expression of IGF's has been observed in CRC. There have been particular IGF proteins which have been found to be associated with more adverse survival rates (Yamamoto, Oshima, Yoshihara *et al.*, 2017).

1.8.4.2. Vascular endothelial growth factor (VEGF) and VEGF receptor (VEGFR)

VEGF and its isoforms have been shown to play a role in metastatic CRC neovascularisation and solid tumour formation (Bird, Mangnall, & Majeed, 2006; Hanahan *et al.*, 2011). Experimental models involving VEGFR blockade have been shown to inhibit metastatic proliferation and metastasis formation (Gille, Heidenreich, Pinter *et al.*, 2007) with drug therapy targeting such mechanisms having been trialled in metastatic CRC with some success (Hurwitz *et al.*, 2004; Kang, Kim, Lee *et al.*, 2009; Yeh, Tsai, Huang *et al.*, 2016).

1.8.4.3. Hypoxia inducible factor 1 (HIF-1)

HIF-1, amongst other molecules, plays a role in the regulation of VEGF expression (H. Chen, Feng, Zhang *et al.*, 2015). Hypoxic microenvironments in CRC have been shown to increase the expression of HIF-1 (Kaidi, Qualtrough, Williams *et al.*, 2006; L. Zhang, Hu, Xi *et al.*, 2016).

1.8.4.4. Immune aggregates

The immune microenvironment is increasingly thought to have significant importance in cancer development and progression. Presence of immune cell aggregates in solid tumours have been associated with poor prognosis. Tumours evading the host immune system from destruction within the tumour microenvironment has been hypothesised as being one of the hallmarks of cancer (Hanahan *et al.*, 2011). Within the peritoneal cavity the omentum is a common site of metastatic spread. Regions on the omentum containing clusters of immune aggregates have been identified as sites, or regions, where metastatic cells preferentially attach. Concentrated areas of immune aggregates have been found to contain a dense capillary network with markers of active angiogenesis. These areas on the omentum and peritoneum have been named milky spots and are a major implantation site for peritoneal metastases in various cancers (J. Liu, Geng, & Li, 2016). One study demonstrated that some mesothelial cells at these sites secrete vascular endothelial growth factor-A, with some hypoxic cells secreting HIF-1. Both of these molecules could further foster microenvironments which favour tumour cell survival and growth (Gerber, Rybalko, Bigelow *et al.*, 2006).

1.8.4.5. CCN protein family

CCN family of proteins is an acronym for cysteine-rich protein 61 (CYR61), Connective tissue growth factor (CTGF) and Nephroblastoma overexpressed (NOV). A total of 6 family members, exhibiting the same basic structure have been identified (CCN1-6). CCNs have been shown to mediate a range of cellular activities in both normal physiology and pathological conditions, including cell functions, embryonic development, angiogenesis,

wound healing fibrosis, inflammation, and tumorigenesis. This is primarily through binding and interacting with a range of receptors including integrins, IGFs, lipoprotein-receptor related proteins (LRPs) and HSPGs. These are then able to affect various signalling pathways including Wnt, TGF-ß and insulin receptor signalling (IRS). In CRC, CCN 1,4 and 6 have been seen to be upregulated and CCN5 downregulated. CCN 3 has shown varied results of both upregulation and downregulation, and the degree of upregulation or down regulation seen may be determined by the tumour stage (J. Li, Ye, Owen *et al.*, 2015). CCN2 has been identified as a key regulator of CRC invasion and metastasis and a prognostic marker in stage II and III CRC (B. R. Lin, Chang, Che *et al.*, 2005). CCN2 expression has also been reported by the same group as a biological marker for the prediction of CRC peritoneal metastases, alongside the role of integrin α5-dependent pathway in the adhesion ability of CCN2-modulating colon cancer cells (B. R. Lin, Chang, Chen *et al.*, 2011).

1.9. Hyaluronic Acid Dependent Adhesion and Associated Molecules

1.9.1. Hyaluronic acid (HA) structure & function

HA (also termed hyaluronan), is a repeating disaccharide unit of N-acetyl-D-glucosamine and D-glucuronic acid, leading to construction of a linear polysaccharide (Laurent & Fraser, 1992). It has been found to be present and play a role in many different tissues. Hyaluronan displays elastic properties, its elasticity increasing with the molecular concentration. In solution hyaluronan exists as randomly kinked coils, which entangle with each other when grouped together. This entanglement can form more complex secondary and tertiary structures, which in turn reinforce the strength of the molecule (Mikelsaar & Scott, 1994; Scott, Cummings, Brass *et al.*, 1991). It has also been demonstrated that the viscous

properties of complex polysaccharide networks influence and resist water movement between fluid compartments (Day, 1950). The full extent HA plays in physiological functions is still not fully understood. However, HA has been described to have a multifunctional role. Some of these functions include a matrix/scaffold role, water balance and osmotic buffering, lubrication between tissues, and acting as a scavenger of free radicals. The role of HA in regulation of cellular activity has been shown in various guises, including cell proliferation, cell locomotion, cell protection and wound healing (Laurent *et al.*, 1992; Laurent, Laurent, & Fraser, 1996). In most tissues HA has a relatively rapid turnover from a few hours to a few days. Intestine modelling has predicted the half-life of HA in the peritoneum to be 0.1-1.2days (Brown, Laurent, & Fraser, 1991).

The process of adhesion in PM is achieved utilising cellular adhesion molecules, which can interact with distant sites. Adhesion molecules can either be independent or important in a cascade of activation of a series of adhesion molecules. Broadly speaking, in the context of PM, adhesion can be split into HA-dependent and HA-independent adhesion.

HA has been shown to interact with three principal cell surface adhesion molecules, namely CD44, RHAMM and ICAM-1 (Aruffo, Stamenkovic, Melnick *et al.*, 1990; Entwistle, Zhang, Yang *et al.*, 1995; McCourt *et al.*, 1994). CD44 is considered to have greatest influence of the three HA-interacting adhesion molecules and has been extensively studied (Misra *et al.*, 2015). Studies looking into comparing the effects of expression of molecules following the addition of HA have shown CD44 upregulation. Other studies have reported that the introduction of HA causes upregulation of downstream signalling cascades, and therefore it

may be a key effector of certain signalling mechanisms (Jordan, Racine, Hennig *et al.*, 2015; Lokeshwar, Mirza, & Jordan, 2014).

1.9.2. CD44 structure

CD44 is a transmembrane glycoprotein that was first found to have cell adhesion and homing functions on lymphocytes (Sneath & Mangham, 1998). It has since been found to carry out a multifunctional role within most human tissues, both due to multiple binding sites on the protein molecule and isomer variants (Lesley & Hyman, 1998). It has also been shown to be involved in cell migration, extravasation, proliferation, haematopoiesis, and immune cell modulation (Johnson & Ruffell, 2009; Siegelman, DeGrendele, & Estess, 1999). CD44 is encoded on the short arm of chromosome 11 (Gao, Lou, Dong *et al.*, 1997), which can produce variations of the protein due to the combination of constant and variable exons within the sequence. There are 10 constant exons and 9 variable exons. The most common isoform of CD44 is CD44 standard (CD44s), in which there are no variable exons. In humans, there are nine variant exons (CD44v) that can be produced by alternative mRNA strands. These isomers can be produced by one or more of the nine variant exons, thus allowing many possible variant isomers to be produced (Figure 1.11).

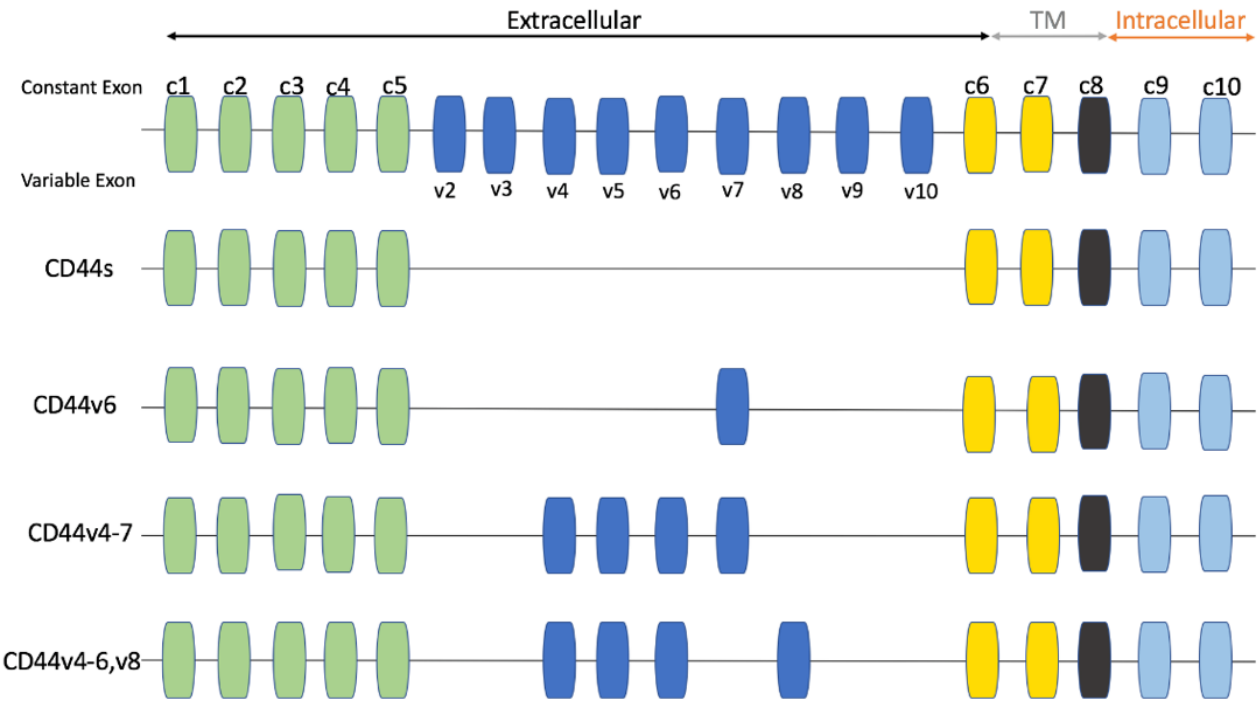

Figure 1.11. The genomic structure of CD44, with examples of variant isoform combinations. Multiple splice variant combinations facilitate many isoforms of CD44v. Image adapted from (Sneath *et al.*, 1998).

In normal colonic tissue CD44s has strong expression in the tissues. Variant isoforms of CD44 including CD44v6, CD44v7, CD44v8, CD44v7&8, CD44v7&9, CD44v7 v8 &v9 have all been shown to have moderate expression, in normal colonic tissue (D. L. Cooper, Dougherty, Harn *et al.*, 1992).

Interest was expressed in the early 1990s, when it was demonstrated that metastatic potential could be transferred to a non-metastatic pancreatic cell through transfection of a CD44 variant (Gunthert, Hofmann, Rudy *et al.*, 1991). The initial work involved identifying membrane proteins on metastatic rat adenocarcinoma using monoclonal antibodies. The antibodies were screened against a bacterial cDNA library, where a CD44 variant isoform

was found to be encoded. The cDNA was transfected to normal pancreatic rat cells, which did not express the specific CD44 variant. The normal cell line, now transfected, was found to have gained metastatic properties when injected into rats.

1.9.3. CD44 as cancer stem cell markers in cancer

The study of biomarkers to attempt to both diagnose and predict outcomes of malignancy is an ongoing and expanding field. There have been studies assessing and observing CD44 and isoform expression within cancer populations. CD44V6 has been implicated as a biomarker of distant and peritoneal dissemination of malignancy (Motohara, Fujimoto, Tayama *et al.*, 2016; Mulder, Kruyt, Sewnath *et al.*, 1994; Parker, 1995; Tjhay, Motohara, Tayama *et al.*, 2015; L. H. Zhao, Lin, Wei *et al.*, 2015). A retrospective study demonstrated that specific polymorphisms in genes encoding CD44 were found to be associated with time to recurrence of stage II and III colorectal cancer (Stotz, Herzog, Pichler *et al.*, 2017). Studies into ovarian cancer have found that low CD44 expression has been linked to a particular histotype of malignancy, and a recent meta-analysis demonstrated that CD44 expression was associated with a high TNM (tumour, node, metastasis) stage and a poorer overall survival at 5-years (Bartakova, Michalova, Presl *et al.*, 2017; J. Lin & Ding, 2017). In a study of pancreatic cancer, CD44, along with CD24, was observed to be upregulated in early pancreatic cancer. CD44 was seen to lose expression in more advanced stages of malignancy (Durko, Wlodarski, Stasikowska-Kanicka *et al.*, 2017). Further research is underway to establish whether CD44 may be a useful biomarker in the detection and prediction of various tumours.

1.9.4. CD44 as signalling regulators

Signalling in CD44 has been broadly split into HA-independent and HA-dependent signalling. HA-independent CD44 interaction has been shown to initiate intracellular signalling events through the intracellular CD44 cytoplasmic tail which is seen to interact with many intracellular signalling molecules, altering gene expression. HA-dependent signalling requires two CD44 molecules to be cross-linked to facilitate interaction with HA which in turn allows with other signalling proteins to also interact. Three mechanisms of molecular activity have been described into how CD44 carries out its intracellular functions (Ponta, Sherman, & Herrlich, 2003):

1) CD44 as a ligand binding surface protein:

CD44 as a transmembrane glycoprotein facilitates interaction with molecules within the ECM. One key molecule that has demonstrated interaction with CD44 from the ECM is hyaluronic acid (HA). Intracellular mitogenic stimuli are believed to regulate CD44 – hyaluronan affinity at the cell surface (Misra *et al.*, 2015).

2) CD44 as a co-receptor:

An emerging theory in signal transduction is that cell-adhesion molecules can act as co-receptors to extracellular stimuli. What this means is that CD44 variant isoforms can act as co-receptors whereby the molecule can be used to promote interaction of external molecules, such as growth factors, to the cell surface of the cancer cell to enhance metastatic ability and progression. Alternatively, CD44 can act as a co-receptor in the role to stabilise other cell surface molecular receptor interactions with external stimuli (C. Chen,

Zhao, Karnad *et al.*, 2018). These receptors traverse the cell membrane, and the cytoplasmic region has both catalytic kinase activities and phosphorylation motifs. When the cytoplasmic regions of these receptors are activated, they are able to form active receptor docking sites for the various components on the extracellular domains, which facilitate intracellular signalling (Ponta *et al.*, 2003). CD44 and its isoforms have been shown to function as co-receptors with C-met and EGFR family molecules (Orian-Rousseau, Chen, Sleeman *et al.*, 2002; Sherman, Rizvi, Karyala *et al.*, 2000).

3) CD44 as a link between the plasma membrane and actin cytoskeleton:

CD44 has been found localised to microvilli and regions of actin chains. The cytoplasmic domain does not have actin binding CD44 and is able to interact with other protein molecules. These bind to the actin cytoskeleton to mediate cell signalling indirectly. An example of this is the ERM (ezrin, radixin, moesin) and merlin proteins, which are able to bind to CD44. Regulation of these interactions can occur in three ways. Firstly, it can be regulated through the ability of ERM and merlin to have active and inactive receptor conformations. Secondly, regulation may take place through direct competition for CD44 binding via upregulation or downregulation of the interacting proteins with CD44. Thirdly, regulation may involve CD44 cytoplasmic tail phosphorylation, through intracellular cell signalling (Ponta *et al.*, 2003; Thorne, Legg, & Isacke, 2004).

1.9.5. CD44 and HA interaction

HA binding sites in the extracellular domain of CD44 have been identified through truncation mutagenesis techniques(Peach, Hollenbaugh, Stamenkovic *et al.*, 1993). CD44 and HA binding has been found to be stabilised by disulphide bonding, where cysteine residues have been thought to be important components of binding (D. Liu & Sy, 1996). One study demonstrated residues Cys77 and Cys97 being involved in this way. Destabilising or preventing such bonding from occurring through redox reactions has been shown to destabilise the CD44/HA interaction (Kellett-Clarke, Stegmann, Barclay *et al.*, 2015). Studies on the inhibitors of this CD44/HA interaction have looked at the treatment of various disease processes the molecules play a part in, including peritoneal spread in malignancy (Harada, Nakata, Hirota-Takahata *et al.*, 2006; Hirota-Takahata, Harada, Tanaka *et al.*, 2007).

1.9.6. CD44-HA interaction and peritoneal metastasis in colorectal cancer

Expression studies have demonstrated CD44 and its isoforms being present in CRC, with overexpression being associated with aggressive metastatic CRC phenotypes (Elliott, Rychahou, Zaytseva *et al.*, 2014). Tumour suppressors, such as NDRG1 (N-myc downstream-regulated gene 1), which regulate CD44 expression have been found to reduce the degree of dissemination of metastasis *in vitro*, in individual CRC cell lines (Wangpu, Yang, Zhao *et al.*, 2015). However, it has been observed that CD44 expression appears to be independent of P53 mutations in CRC (Zeilstra, Joosten, Vermeulen *et al.*, 2013). Isoforms of CD44, such as CD44V6, seen in CRC, have been shown to have increased preponderance to metastatic spread (Katoh, Goi, Naruse *et al.*, 2015; Weg-Remers, Schuder, Zeitz *et al.*, 1998; Wielenga, van der Voort, Mulder *et al.*, 1998; A. Yamaguchi, Goi, Taguchi *et al.*, 1998; Yamane,

Tsujitani, Makino *et al.*, 1999). It has been demonstrated that inflammatory cytokines including IL-1β and TNF-α can contribute to enhanced peritoneal tumour adhesion in CRC cell lines (van Grevenstein *et al.*, 2007). CD44 crosslinking and fragmented HA has been shown to upregulate adhesive molecules' expression of integrins, thereby enhancing adhesive properties of endothelial cells. In the same study c-MET expression was also increased, enhancing integrin-facilitated adhesion of CRC cell lines. It was thereby inferred that the expression of CD44 created an adhesion cascade for CRC cells to facilitate metastasis (Fujisaki, Tanaka, Fujii *et al.*, 1999).

1.9.7. CD44-HA interaction and peritoneal metastasis in other cancers

Within ovarian cancer (OvCa), high expression of CD44 in ovarian tumour cell lines has demonstrated adhesion to HA in *in vitro* models. Activity of HA has been found to be increased at metastatic sites in ovarian cancer and appears to correlate with degree of tumour grade (Hiltunen, Anttila, Kultti *et al.*, 2002; Jojovic, Delpech, Prehm *et al.*, 2002; Yeo, Nagy, Yeo *et al.*, 1996). The degree of adhesion appeared to be affected by the type of tumour cell line, rather than the degree of CD44 expression. Use of hyaluronidase or anti-CD44 antibodies, targeting the HA binding region, significantly reduced affinity for adhesion of OvCa cells *in vitro* on HA coated plate models (Gardner, Catterall, Jones *et al.*, 1996). The findings have also been replicated using immobilised fixed HA molecules (Catterall, Gardner, Jones *et al.*, 1997). Mechanisms of attachment through tumour derived exosomes are thought, in-part, to facilitate such attachments (K. Nakamura, Sawada, Kinose *et al.*, 2017). *In vivo* Xenograft models studying ovarian cancer have demonstrated that targeting CD44-HA interaction, using a monoclonal antibody targeting CD44, can affect tumour binding (Strobel, Swanson, & Cannistra, 1997).

High expression of CD44 in gastric cancer (GC) is seen as a poor prognostic marker regarding disease progression (Lu, Wu, Sun *et al.*, 2016). CD44 expression is thought to affect outcome and aggressiveness of GC. CD44 overexpression has been established as a marker of GC distant metastasis. In patients where resection intent was curative, again overexpression was associated with a poorer prognosis, increased recurrence, and a higher overall mortality (L. Cao, Hu, Zhang *et al.*, 2014; Y. Chen, Fu, Xu *et al.*, 2014; Mayer, Jauch, Gunthert *et al.*, 1993; Yoo & Noh, 2003).

Variants of CD44 have demonstrated different frequencies of expression in GC cell lines, with the degree of variant expression being predominantly dependent upon the TNM stage of GC, invasion depth and Lauren classification (Go, Ko, Lee *et al.*, 2016; J. W. Xie, Huang, Zheng *et al.*, 2013). Research looking specifically at GC cell lines has found expression of other molecules influencing expression of CD44. Several recent studies have demonstrated expression of several molecules including HMGA2 (High Mobility Group AT-hook 2), HIF-1α (Hypoxia-Inducible factor 1α), SALL4 (Sal-like-protein 4) and HOXA10 (Homobox A10) can regulate CD44 expression and again be associated with a poorer prognosis for patients with GC (G. Liang, Li, Du *et al.*, 2017; J. Sun, Sun, Zhu *et al.*, 2017; Wu, Li, Zhang *et al.*, 2015; Yuan, Zhang, Zhang *et al.*, 2016).

Whilst CD44 expression has been demonstrated in GC, little evidence exists on the significance of CD44 expression and how it influences behaviour of GC or how GC influences CD44 expression.

The exact mechanisms of pancreatic cancer metastatic disease are still not fully understood. CD44 has been shown to influence MMP (MT1-MMP) expression in pancreatic cell lines, where MMPs have been shown to influence tumour invasion through upregulation and downregulation in cell and *in vivo* models (Jiang, Zhang, Kane *et al.*, 2015). Overexpression of CD44 is thought to correlate with a poor survival in pancreatic cancer patients (Jiang *et al.*, 2015; X. P. Li, Zhang, Zheng *et al.*, 2015).

1.9.8. Receptor for hyaluronan mediated motility (RHAMM)

RHAMM, also called CD168, was originally identified on murine fibroblasts and fibrosarcoma cells. It is located on chromosome 5q33.2, where alternative splicing of its mRNA produces four known isoforms of the protein (Schutze, Vogeley, Gorges *et al.*, 2016). Initially, RHAMM was described as a protein involved in cell locomotion (Hall & Turley, 1995), however today RHAMM is also known to be implicated in many other functional roles at cellular level. It is found on the cell surface, in the cytoplasm and the nuclei of various types of cells. In normal tissue, RHAMM has been found to be responsible for cell signalling cascades, cell cycle progression and expression of genes regulating the extracellular matrix (Tolg, McCarthy, Yazdani *et al.*, 2014). The interaction of RHAMM with HA has been shown to induce tyrosine phosphorylation of cellular proteins including focal adhesion kinase ($p125^{FAK}$) in fibroblasts (Hall, Wang, Lange *et al.*, 1994; C. Wang, Thor, Moore *et al.*, 1998; S. Zhang, Chang, Zylka *et al.*, 1998). In CRC it has been implicated in unfavourable prognostic outcomes and thought to contribute to metastatic dissemination (Koelzer, Huber, Mele *et al.*, 2015; Lugli, Zlobec, Gunthert *et al.*, 2006; Mele, Sokol, Kolzer *et al.*, 2017; K. Wang & Zhang, 2016; Zlobec, Terracciano, Tornillo *et al.*, 2008). The underlying reason for this is still not fully understood.

The HA binding domain on RHAMM was first discovered by Turley and their interaction researched by her group (Turley, 1982, 1989, 1992; Turley, Moore, & Hayden, 1987; Turley & Torrance, 1985). The two binding domains found on RHAMM have been shown to contribute equally to the HA binding ability of this protein. A common HA binding receptor-protein motif has been demonstrated in both CD44 and RHAMM molecules, which was shown through site-directed mutagenesis techniques (B. Yang, Yang, Savani *et al.*, 1994).

Disease progression in many cancers has been linked with overexpression of RHAMM. RHAMM expression has even been ranked as a highly significant prognostic factor in terms of predicting overall outcome. In CRC, higher expression of RHAMM is correlated strongly with an overall poorer prognosis (K. Wang *et al.*, 2016). Literature describes RHAMM as being responsible for increased motility and invasion of metastatic cells and a significant factor driving metastatic spread (Mele *et al.*, 2017). However, little discussion is made directly towards influence on cell adhesion when interacting with HA specifically in CRC and the effect on peritoneal dissemination.

Increased surface expression of RHAMM has been shown to be amplified through the addition of HA (Misra *et al.*, 2015). RHAMM overexpression has demonstrated increased metastatic ability to migrate and colonise distant secondary sites (Koelzer *et al.*, 2015; Mele *et al.*, 2017; Rein, Roehrig, Schondorf *et al.*, 2003; D. Wang, Narula, Azzopardi *et al.*, 2016). Tumour buds, which are clusters of cells found at the invasive fronts of tumours, are seen as a more aggressive subpopulation of cells within a tumour. In CRC, RHAMM positivity within tumour budding cells has been associated with more aggressive tumour histopathological

features (Koelzer *et al.*, 2015). Conversely, silencing of RHAMM expression has been shown to decrease tumorigenicity within CRC cells both *in vitro* and *in vivo* (Mele *et al.*, 2017).

1.9.9. Intercellular adhesion molecule-1 (ICAM-1) and colorectal cancer

Intercellular adhesion molecule-1 (ICAM-1;CD54) is a member of the immunoglobulin superfamily (van de Stolpe & van der Saag, 1996). It has been identified as having roles in transmigration of leukocytes from the intravascular space out into tissues, in certain autoimmune diseases as well as cancer, and has been found to be present on endothelial cells. Levels of ICAM-1 have also been implicated as prognostic markers in various autoimmune disease states (Lawson & Wolf, 2009). ICAM-1 is the third adhesion molecule which is identified as having cell surface expression of the hyaluronic acid receptor molecule (McCourt *et al.*, 1994).

Increased expression of ICAM-1 has demonstrated increased adhesion of malignant cells in CRC cell lines (Alkhamesi *et al.*, 2007; Mikula-Pietrasik *et al.*, 2017). ICAM-1 is a single chain protein 80-114kDa with a core polypeptide structure of 55kDa. ICAM-1 has been reported as a binding receptor for HA (Soliman, Ye, Jiang *et al.*, 2021). The molecule has been found to share some basic amino acid clusters similar to CD44 and RHAMM (McCourt *et al.*, 1994).

ICAM-1 has been implicated in affecting cellular adhesive behaviours in various cancer biology studies. Regarding CRC, expression of ICAM-1 has been found to be shown to be increased in tumour associated fibroblasts in CRC *in vitro* and as a result adhesive capacity was found to be increased in culture experimentation (Schellerer, Langheinrich,

Hohenberger *et al.*, 2014). Cells put under oxidative stress have demonstrated increased expression of ICAM-1 and have been seen to promote adhesion of selected colorectal and pancreatic cell lines (Ksiazek, Mikula-Pietrasik, Catar *et al.*, 2010). High serum ICAM-1 and VCAM-1 expression have also been found in patients with more advanced CRC than early disease (Giannoulis, Angouridaki, Fountzilas *et al.*, 2004).

Interestingly, the literature on ICAM-1 is mixed. Although downregulating ICAM-1 expression has been shown to reduce CRC cell adhesion (Alkhamesi, Ziprin, Pfistermuller *et al.*, 2005), it has also been demonstrated that ICAM-1 negative tumours have a higher rate of metastasis to liver and lymph node than ICAM-1 positive CRC (Maeda, Kang, Sawada *et al.*, 2002). Interplay of other adhesion molecules in the enhanced dissemination of ICAM-1 negative CRC tumour cells is yet to be explored (Soliman *et al.*, 2021).

Another study has described upregulation of ICAM-1 gene expression correlating with inhibition of CRC tumour growth and reduction in development of liver metastases (Tachimori, Yamada, Sakate *et al.*, 2005). However, other research has shown that the expression of ICAM-1 was inversely related to CD44 expression, with lower expression of ICAM-1 being observed in metastasising tumours (Wimmenauer, Keller, Ruckauer *et al.*, 1997).

The varied conclusions drawn from expression of ICAM-1 in relation to CRC could in part be due to genetic polymorphisms of ICAM-1 and expression. One study demonstrated that various polymorphisms of ICAM-1 were expressed at a higher prevalence in cancer patients than non-cancer patients. The study therefore inferred that expression of certain

polymorphisms could be correlated with risk stratification for patients likely to develop CRC (Q. L. Wang, Li, Liu *et al.*, 2009). Another factor could be related to the timing of expression in relation to the early or advanced disease state, which could again show altered expression simply according to stage of disease. Alternatively differential expression could be related to where on the tumour the samples for *in vitro* studies have been taken, such as from the invasive front of a tumour.

1.10. Anchorage Dependent Cells and Anoikis in Colorectal Cancer

If CRC cells are impeded long enough to prevent attachment to host cells, such as using a competitive inhibitor, anoikis evasion may be disrupted and CRC cells will fail to survive in the peritoneal cavity environment. The KLKs (Kallikrein-related peptidases) and V-Src (V-Sarcoma viral oncogene homologue) family molecules have been implicated in cell-cell dependent clustering of CRC cells and resistance to anoikis (de Cuba *et al.*, 2012). It may be possible that inhibition of CD44-HA interaction may not only affect adherence to distant tissues, but also affect the cell-cell adhesive properties of the CRC cells themselves. While the cells may not undergo anoikis spontaneously, delayed adhesion in the peritoneal microenvironment could increase free-floating cell vulnerability to targeted treatment with multimodal therapy.

1.11. Targeting HA-mediated Interaction in Malignancy

Although not specifically targeting HA-dependent adhesion molecular interaction, there are two ongoing trials which describe utilising HA to enable increased delivery of chemotherapeutic agents in metastatic CRC (Clinicaltrials.gov, 2014, 2015; Gibbs, Clingan, Ganju *et al.*, 2011). Both trials are from the same group, in Australia, examining the delivery of Irinotecan which is used as a chemotherapeutic agent in metastatic colorectal cancer. Irinotecan is combined with HA in the treatment of metastatic CRC. The drug delivery platform is based on the use of HA as a novel excipient, in which formulation of Irinotecan with HA results in optimisation of cytotoxic drug uptake and retention within solid tumours. Early studies have shown enhanced efficacy in both non-clinical and early clinical studies. The first is a phase II single arm trial of FOLF(HA)IRI plus cetuximab in irinotecan-naïve second line patients with KRAS wild type metastatic CRC (Clinicaltrials.gov, 2014). The second is a randomised double blind phase III trial, comparing FolF(HA)IRI versus standard FOLFIRI chemotherapeutic regimens for second- or third-line therapy in Irinotecan-naïve patients (Clinicaltrials.gov, 2015).

Cisplatin based chemotherapeutic regimens have formed the basis of treatment of several cancers including colonic, gastric, and ovarian cancer. PIPAC (pressurised intraperitoneal aerosolised chemotherapy) has been a new novel treatment modality option for palliative patients with metastatic intraperitoneal disease. Modifying the chemotherapeutic aerosol to exploit the mechanism of CD44 over-expression on many tumour types, in combination with CD44-hyaluronic acid interaction, has led to the use of HA-linked cisplatin in some

PIPAC regimens, with the aim of more effectively enhancing the chemotherapeutic effect on tumour cells (Shariati, Lollo, Matha *et al.*, 2020).

In vivo Xenograft models studying ovarian cancer have demonstrated that targeting CD44-HA interaction, using a monoclonal antibody targeting CD44, can affect tumour binding (Strobel *et al.*, 1997). To date there has been one in-human phase I clinical trial published, using a monoclonal antibody (mAb) specifically targeting CD44-HA in advanced solid tumours. Whilst this study was not targeting peritoneal spread of GI tumours, it is relevant to mention simply due to being the only human trial targeting the specific CD44-HA mechanism of interaction. The antibody selectively binds near the HA-binding region of all CD44 isoforms. Solid tumours including colorectal, thymus and skin primary malignancies demonstrated a degree of modest tumour shrinkage in primary and distant disease, however, there was no significant overall treatment response. The patient response was evaluated through FDG-PET (fluorodeoxyglucose-Positron emission tomography) imaging. However, the study was stopped early, due to there being no evidence of a clinical response and no evidence of pharmacodynamic dose-response relationship with the treatment. There were no safety concerns identified with the treatment (Menke-van der Houven van Oordt, Gomez-Roca, van Herpen *et al.*, 2016).

The effects of this prior xenograft study, targeting CD44, could possibly have shown negligible results due to assessing the effects on already established solid tumours rather than examining the prevention of tumour from being established at a distant site. It may be more appropriate in the examination of adhesion molecules, such as CD44, to attempt to assess the disruption of distant site binding, before cancer cells are even able to establish as

distant tumours, by targeting this CD44-HA interaction, concentrating on the adhesion phase of the metastatic model. Many clinical trials, by examining drug response to novel agents, assess effect on established advanced solid tumours in what are, in effect, palliative patients. The timing of the cellular interaction and treatment initiation, which affects a different phase of the metastatic model, is crucial to consider. For example, adjusting the study following complete cytoreductive resection of peritoneal tumours and administering mAb targeting CD44-HA against a placebo. Alternatively a complementary study approach could examine the effect of local recurrence following initiation of mAb treatment that targets CD44-HA binding, following resection of a perforated or T4 tumour.

1.12. Summary

HA-dependent receptor molecules CD44, RHAMM and ICAM-1 have been independently associated with metastatic and peritoneal dissemination of many different primary cancers, as well as other autoimmune and inflammatory conditions. There is limited understanding and literature on peritoneal spread in CRC. Current chemotherapeutic strategies in peritoneal metastatic disease often utilise generic regimens, with no definitive gold standard to manage these. Delivery of chemotherapeutic agents systemically, locally or in combination is still being explored. However, a personalised approach, tailored to the genetic protein expression of cancer biology, is the standard to aspire toward. Radical surgery carries with it an inherent risk of peritoneal recurrence. Further consideration of refining the management of microscopic free-floating cancer cells following radical surgery, such as CRS & HIPEC, is most certainly a relevant question to explore further, considering the challenge and poor prognosis of patients presenting with peritoneal disease in CRC.

Targeting HA-dependent adhesion may have the potential to prevent, reduce or control peritoneal metastatic disease in CRC. Targeted immediate disruption of CRC-HA interaction at the time of cancer surgery could be beneficial, where macroscopic disease has been resected but where there is a risk of micro-metastases. Locally advanced or perforated colorectal tumours are highly likely to allow malignant cells to enter the peritoneal cavity. Prevention of adhesion and CRC-HA interaction could lead to reduced ability of cells to attach to distant tissues, such as the peritoneum. Disruption in adhesion of CRC cells and promoting anoikis is a direction to explore for new treatment options, with the aim of either

reducing deaths from PM due to locally advanced CRC, or optimising conditions in the multimodal treatment of PM.

Hypothesis

Expression

1) HA-dependent adhesion molecules, namely CD44, RHAMM and ICAM-1, are upregulated in CRC.

The nature of the peritoneal metastatic model and the abundance of naturally occurring hyaluronic acid lining the peritoneal cavity will see CRC cells upregulate expression of HA-dependent receptor molecules. The null hypothesis is that there will be no difference in the expression levels of these molecules when compared to normal tissues. Expression of HA-independent adhesion molecules will also be examined as a comparator.

Human CRC cell line investigation hypothesis:

1) Introduction of a competitive hyaluronic acid (HA)-receptor inhibitor can prevent colorectal cancer cellular adhesion.
2) Anchorage dependent CRC cells are unable to survive in suspension.

Targeting HA interaction with HA-dependent adhesion molecules by treating with a competitive inhibitor will prevent CRC cellular adhesion at the peritoneum in both *in vitro* peritoneal models and *in vivo*. The null hypothesis is that treatment with an inhibitor will not affect cellular adhesion.

1.13. Aims

The aims of this project are:

1. To screen RNA expression of molecules identified in the literature as being involved in peritoneal adhesion in various cancers from colorectal cancer tissue microarrays.

2. To examine whether there is any relationship between molecular expression and clinicopathological data.

3. To examine the expression of HA-dependent and HA-independent adhesion molecules

4. To examine the effects on adhesion when targeting hyaluronic acid and colorectal cancer adhesion *in vitro.*

5. To examine the effects on colorectal cancer cell survival, when targeting the hyaluronic acid receptor in vitro.

6. To examine the effects on peritoneal dissemination of colorectal cancer when targeting the hyaluronic acid receptor.

Chapter 2

Materials and Methods

2.1 Hyaluronic acid inhibitor and hyaluronic acid

2.1.1 Hyaluronic acid inhibitor (HAi)

Hyaluronic acid inhibitor (AnaSpec, Fremont, California, USA) is a twelve amino acid peptide, which is a direct competitive inhibitor to hyaluronic acid (HA), a high molecular weight glycosaminoglycan expressed abundantly in the extracellular matrix and on cell surfaces. This peptide shows specific binding to soluble, immobilised and cell-associated forms of hyaluronic acid. It has been shown to inhibit leukocyte adhesion to HA substrates almost completely (Mummert, Mohamadzadeh, Mummert *et al.*, 2000).

Molecular formula: C64H94N20O16

Molecular mass/weight: 1399.7

Sequence three letter code: H-Gly-Ala-His-Trp-Gln-Phe-Asn-Ala-Leu-Thr-Val-Arg-OH

2.1.2 Hyaluronic acid (HA)

High molecular weight hyaluronic acid (R&D Systems®, Minneapolis, USA. Cat. GLR002) is a naturally occurring linear polymer of the repeating disaccharide structure D-glucuronic acid-beta-1, 3-N-acetylglucosamine-beta-1,4(1-3). It is a glycosaminoglycan (GAG) that is abundantly present in the extracellular matrix of all vertebrates. HA synthases (HAS-1,2 and 3) synthesise HA. HA biological functions differ depending on the molecular weight of HA. High molecular weight HA (>500kDa) is anti-angiogenic, anti-inflammatory, and immunosuppressive. Low molecular weight HA (10-500kDa) is highly angiogenic and pro-inflammatory.

Source: Produced by microbial fermentation of Streptococcus pyogenes

Molecular mass/weight: >950kDa.

Formulation: White to off white powder which can be reconstituted in aqueous solutions.

2.2 Standard Solutions and Reagents

The standard chemicals and reagents used were obtained from Sigma-Aldrich (Sigma-Aldrich, Poole, Dorset, United Kingdom), unless stated otherwise.

2.2.1. Solutions for Cell culture work

Trypsin

Trypsin, at a stock concentration of 25mg/ml, was made up with 500mg (milligrams) of trypsin (Sigma-Aldrich, Poole, Dorset, UK) was dissolved in 20ml (millilitres) of 0.05M EDTA. The solution was mixed and filtered through a 0.2μm syringe filter (Sartorius, Epsom, UK). The solution was divided into 10ml aliquots and stored at -20°C. When required the trypsin was defrosted overnight in a fridge at -5°C and brought to room temperature when required for use.

PBS (Phosphate Buffered Saline)

10x concentrate, Sigma-Aldrich P5493. Diluted down with distilled water.

EDTA (Ethylenediaminetetraacetic acid) 0.02%

A stock solution of 1g KCl (potassium chloride), 5.72g Na_2HPO_4 (Disodium-Hydrogen-Phosphate), one-gram KH_2PO_4 (Potassium-Dihydrogen-Phosphate) 1.4g EDTA and 40g of NaCl (Sodium chloride). This was dissolved in distilled water to a total volume of 5-litres. The solution was buffered to pH 7.4 and autoclaved before storage.

Antibiotic and antifungal combination

Standard antibiotic and antifungal regimens for use with tissue culture included 12.5mg amphotericin B (2ml of 6.25mg/ml amphotericin B in dimethyl-sulphoxide (DMSO)), 3.3g penicillin and 5g of streptomycin. These components were dissolved in a total volume of 500ml with Balanced salt solution (BSS).

Foetal Calf Serum (FCS)

Foetal Bovine Serum Heat Inactivated, Sigma-Aldrich F9665.

DMEM (Dulbecco's Modified Eagle Medium)

DMEM/F12 Ham Sigma-Aldrich 500mls D8437. This was supplemented with 50mls FCS (10%) and 5mls Antibiotic.

Medium 199 (M199)

Sigma-Aldrich M4530 500mls. This was supplemented with 50mls FCS (10%), 5mls Antibiotic, Epidermal Growth Factor (EGF) 250µl (10ng/ml) and Hydrocortisone 200µl (0.4µg/ml).

2.2.2. Solutions for RNA/DNA molecular biology

75% Ethanol solution

Ethanol solution 75% was made up 750ml Ethanol and 250ml Distilled water.

1-Bromo-3-Chloropropane

1-Bromo-3-Chloropane (Sigma-Aldrich, 200ml, B9673) can be used instead of chloroform and is less toxic. It is used for RNA isolation.

2-Propanol

Molecular biology grade 2-Propanol (Sigma-Aldrich) 500ml I9516. It is used in DNA/RNA extraction.

TRI Reagent®

TRI reagent® (Sigma-Aldrich, 93289) also known as TRIzol is a monophasic solution of phenol and guanidinium isothiocyanate. It has potential to simultaneously solubilise biological material and denature proteins. It is widely used for deproteinising RNA and for DNA, RNA and protein isolation.

RT master mix

A standard X2 RT master mix was made up to 10 µl per reaction and was scaled up and calculated based on the number of reactions. The master mix was prepared on ice using the following components:

10x RT buffer	2µl
25x dNTPmix (100nM)	8 µl
10x RT random primers	2 µl
RNAse inhibitor	1 µl
MultiScribe Reverse Transcription	1 µl
Nuclease free H_2O	3.2 µl

PCR water

Double distilled, deionised, and autoclaved water was used to ensure nuclease free water is used, in order to prevent degradation of DNA

Diethylpyrocarbonate (DEPC) water

DEPC water was used to inactivate RNase enzymes which could contaminate water or laboratory equipment. A stock solution of DEPC water was prepared by dissolving 500µl of DEPC in 9500µl of dH_2O. The solution was autoclaved prior to use.

PCR Master Mix

PCR Master Mix (Thermofisher Scientific) is a 2x concentrated solution of Taq DNA polymerase, dNTPs and all of the components required for PCR, except DNA template and

primers. The pre-mixture saves time and reduces contamination by reducing pipetting required for PCR set up.

Transfer Buffer

Tris-Glycine Buffer 10x Concentrate. Sigma-Aldrich T4904.

Running Buffer

Tris-Glycine-SDS buffer 10x Concentrate. Sigma-Aldrich T7777.

Buffer QG (QIAGEN, Manchester, UK)

Buffer QG is a solubilisation and binding buffer (with pH indicator) for use in DNA clean-up procedures. The composition of Buffer QG is confidential and is a proprietary component of the QIAquick® gel extraction kit

Buffer PE (QIAGEN, Manchester, UK)

Buffer PE is a wash buffer for use in DNA clean-up procedures. The composition of Buffer PE is confidential and is a proprietary component of the QIAquick® gel extraction kit.

2.2.3. Primers

Primers used in polymerase chain reaction (PCR) are shown in Table 2.1.

Table 2.1. Primers for PCR

Gene	Primer	Primer Sequence 5`-3`
CD44	**CD44F10**	ACCATGGACAAGTTTTGGT
	CD44R10	TTACACCCCAATCTTCATGT
	CD44F3	ACCATGGACAAGTTTTGGTG
	CD44R3	TTACACCCCAATCTTCATGTC
	CD44SEQF1	CCAGCCTCTGCCAGGTTC
	CD44SEQR1	CACCTTCTTCGACTGTTGAC
	CD44SEQF2	AGCACTTCAGGAGGTTACAT
	CD44SEQF3	CTGCAGTAACTCCAAAGGAC
	CD44SEQF3	CTAGTGATCAACAGTGGCAAT
	CD44SEQR3	TTGGGTTGAAGAAATCAGTC
	CD44ZR1	ACTGAACCTGACCGTACACTGTAGCGACCATTTTTCTC
RHAMM	**RHAMMF1**	GCACCATCTCCAGGTGCTTAT
	RHAMMR1	CCATGCCTTCTTGCTTAGCC
	RHAMMZR1	ACTGAACCTGACCGTACATGATTTCTGAAAGGATACTGGTCCT
GAPDH	**GAPDHF8**	GGCTGCTTTTAACTCTGGTA
	GAPDHR8	GACTGTGGTCATGAGTCCTT
BACT	**BACTF**	ATGATATCGCCGCGCTCG
	BACTR	CGCTCGGTGAGGATCTTCA

2.2.4. Solutions for agarose gel electrophoresis

Agarose

Molecular biology grade. Melford Chemical and Biochemical Manufacturing. MB1200.

Tris-Borate-EDTA (TBE) Buffer

Ten percent 10x Concentration. Sigma-Aldrich T4415.

SYBR® Safe DNA gel stain

SYBR® Safe DNA gel stain (Invitrogen, Life Technologies Ltd) at a dilution of 1:10000 was used to stain DNA in the agarose gel following electrophoresis as specified by manufacturer.

2.2.5. Solutions and gels for Western blot

2.2.5.1. Transfer buffer

Transfer buffer was prepared by dissolving 15.15g Tris, 72g glycine and 1-litre methanol in 4-litres dH_2O.

2.2.5.2. Running Buffer

A (x10) stock solution was prepared by dissolving 303g Tris, 100g SDS and 1.44Kg Glycine in 10litres of dH_2O. The pH was adjusted to 8.3 using NaOH and the solution was stored at room temperature. A working solution was prepared by diluting 100ml of stock solution with 900ml dH_2O

2.2.5.3. Ammonium Persulphate (APS)

A 10% APS solution was prepared by dissolving 1g APS in 10ml of dH_2O. The solution was stored at 4°C until use.

2.2.5.4. Tris(hydroxymethyl)aminomethane (Tris) buffered saline (TBS)

A (x10) stock solution (200mM Tris;1.37M NaCl) was prepared by dissolving 24.228g Tris-Cl and 80.06g NaCl in 1 litre dH_2O. The pH was altered to 7.4 using hydrochloric acid and the solution was stored at room temperature until use.

2.2.5.5. Resolving gel

A standard 12% resolving gel, for SDS-polyacrylamide gel electrophoresis (SDS-PAGE), was prepared using 6.6ml dH_2O, 8ml 30% acrylamide mix, 5ml 1.5M Tris (pH8.8), 200µl 10% SDS. 200µl 10% APS, 8µl Tetramethyl ethylenediamine (TEMED) per gel.

SDS-PAGE requires altered percentage gel concentrations for different size proteins. Abcam protocol recommend gel percentages based on protein size and are summarised in Table 2.2.

Table 2.2. Resolving gel percentage for SDS-PAGE. Taken from Abcam.

Protein Size	Gel percentage
4-40kDa	20%
12-45kDa	15%
10-70kDa	12.5%
15-100kDa	10%
25-100kDa	8%

https://www.abcam.com/protocols/general-western-blot-protocol (accessed June 2021).

2.2.5.6. Blocking solution

Blocking solution was made up using 5% powdered milk 2.5g and 0.1% polyoxyethylene (20) sorbitan monolaurate (Tween 20) (Sigma-Aldrich, St. Louis, USA) in 50mls TBS.

2.2.5.7. Stacking gel

A 5% stacking gel for SDS-PAGE was prepared using 4.1ml dH_2O, 1ml 30% acrylamide mix, 705µl 1.5M Tris pH6.8, 60µl 10% SDS, 60µl 10% APS, 6µl TEMED per gel.

2.2.5.8. Laemmli sample buffer

2x Laemmli buffer is a premixed protein sample buffer for SDS-PAGE (Sodium dodecyl sulphate-polyacrylamide gel electrophoresis). Formulation is comprised of 65.8mM Tris-HCl, pH 6.8, 2.1%SDS, 26.3% (w/v) glycerol, 0.01% bromophenol blue.

2.3 Storage & maintenance of cells

2.3.1 Incubation

Cell lines were incubated at 37°C in 5% CO_2 in either Panasonic MCO-18AC-PE or Sanyo MCO-15AC incubators.

2.3.2 Storage of cell stock

Cells were stored for periods less than three-months at -80°C in 10% Dimethyl Sulfoxide (DMSO) and DMEM. For longer, than three-months, cells were stored in liquid nitrogen.

2.3.3 Revival of cells

Cells were thawed rapidly following removal from either liquid nitrogen or -80°C and transferred into a universal container containing 10mls of appropriate pre-warmed medium, to dilute the DMSO present in storage medium. This was centrifuged at 1700rpm for five-minutes to form a cell pellet. The medium was aspirated, removing all DMSO. The pellet was re-suspended in 5mls of medium and placed into a 25cm^2 cell culture flask and placed into an incubator overnight (15-17hours). Following examination under a microscope, assessing cell adherence, the medium was changed to remove non-viable floating cells and any residual DMSO and returned to the incubator.

2.3.4 Maintenance of cells

Cells were maintained in supplemented medium appropriate to each of the cell lines. Either a 25cm^2 or a 75cm^2 flask was used to grow cells. Cells were passaged on a weekly to bi-weekly basis to maintain a confluence of 10-90%. Assessment of confluence was with a light microscope and approximating area of flask covered by cells. All tissue culture was carried out inside a class II laminar flow cabinet which had been cleaned pre- and post- use with 75% ethanol. Aseptic technique was employed throughout.

2.3.5 Adherent cell detachment and counting

At confluences of 70-90%, adherent cells were detached from the tissue culture flask. This was by aspirating the medium, washing cells with PBS buffer, aspirating again and then incubating the flask with 1-2mls of trypsin/EDTA for 5-20minutes. Once detached the cell suspension was centrifuged at 1700rpm for 5minutes. The cell pellet was re-suspended in 1-

5ml fresh medium. Cells were counted using a haemocytometer counting chamber (Hawksley, Sussex, UK) using a light microscope (Ceti Microscopes, Medline, Oxon, UK) under 10x10 magnification. 10µl cell suspension was placed within the haemocytometer. Each sixteen-square area of the haemocytometer measured 1mm x 1mm x 0.2mm which allowed for calculation of the number of cells per ml, with the following equation:

$$\text{Cell number/ml} = \frac{\text{number of cells in 16 square area}}{} \times 10^4$$

The mean number of cells was calculated from counting three 16 square areas and used to calculate the number of cells per ml which was used to calculate the volume of cells required in the appropriate *in vitro* and *in vivo* function experiments. Remaining cells were re-seeded into cell culture flasks at appropriate confluences.

2.4 Cell lines

Cell lines used throughout were cultured under conditions listed in section 2.2.

- HT115

Cells were obtained from ECACC (European Collection of Authenticated Cell Cultures), which were obtained from a human colon adenocarcinoma. Morphology of the cells is epithelial, with adherent growth properties. Catalogue No. 85061104. Cells were cultured in supplemented DMEM. (Figure 2.1)

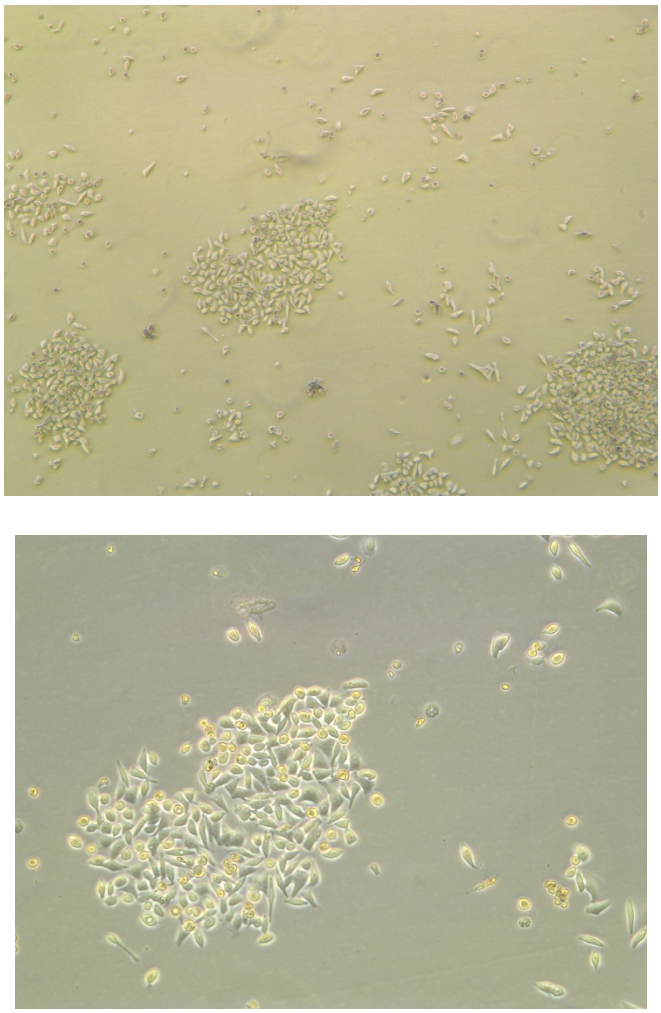

Figure 2.1. HT115 colorectal cancer cells under light microscopy at x5 and x10 magnification.

- HRT-18

Cells were obtained from ATCC (American Type Culture Collection), which were isolated from a human 67-year-old male with right colon adenocarcinoma, from a resected ileocaecal specimen. Morphology of the cells is epithelial, with adherent growth properties. Cells were cultured in supplemented DMEM. (Figure 2.2)

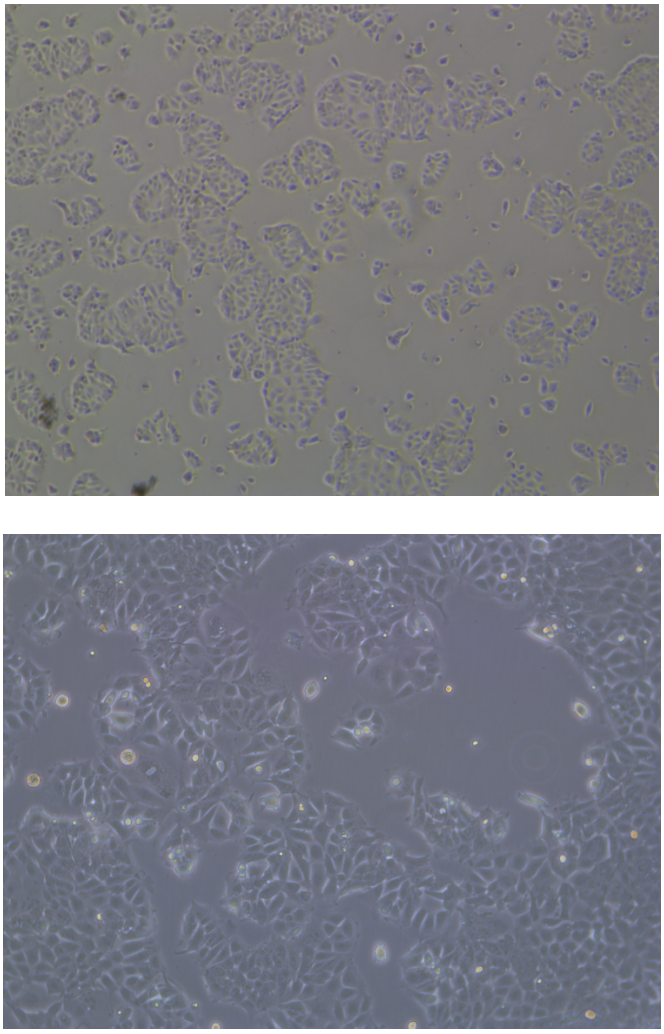

Figure 2.2. HRT-18 colorectal cancer cells under light microscopy at x5 and x10 magnification

- Caco-2

Cells were derived from ATCC (American Type Culture Collection), which were isolated from a human 72-year-old male with colorectal adenocarcinoma. Morphology of the cells is epithelial-like, with adherent growth properties. Cells were cultured in supplemented DMEM. (Figure 2.3)

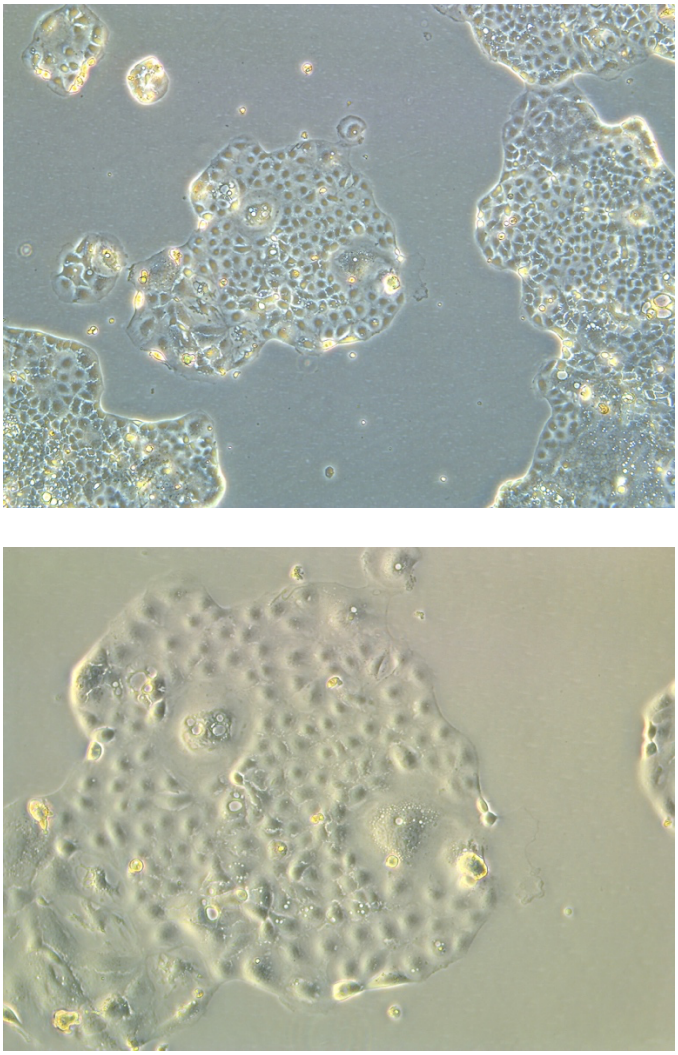

Figure 2.3. Caco-2 colorectal cancer cells under light microscopy at x5 and x10 magnification.

- LP-9

Cells were obtained from the Cornell Institute. Normal human mesothelial cells LP-9 retrieved from the peritoneum of a 26-year-old female with ovarian carcinoma. Cell morphology is fibroblast-like, with adherent growth properties. Cells were cultured in supplemented M199. (Figure 2.4).

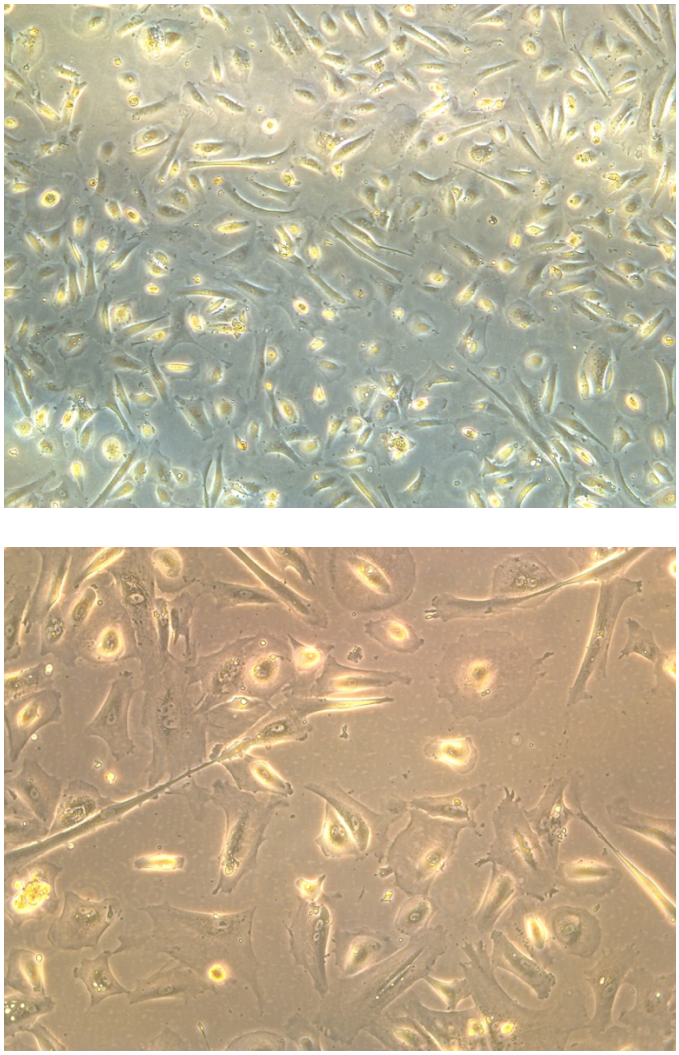

Figure 2.4. LP9 mesothelial peritoneal cells under light microscopy at x5 and x10 magnification.

2.5 RNA extraction

- Growth medium was aspirated from flask or well plate
- Cells were washed with PBS
- One millilitre of TRI reagent® was added to the flask/well plate
- Cells were scraped and lysate was passed through pipette several times to produce a homogenous fluid
- Samples were transferred to sterile 1.5ml Eppendorf tubes (can store at -20°C at this stage if needed)
- Samples were stood at room temperature for five-minutes
- Next, 0.2ml 1-Bromo-3-Chloropropane was added to samples
- Samples were vortexed for approximately 15seconds
- Samples were stood at room temperature for a further 5-10minutes
- Samples were centrifuged at 12000rcf (relative centrifugal force (g-force) for 15minutes at 4°C, in a pre-cooled centrifuge.
- Two layers formed: top RNA (clear layer), middle DNA (white layer), bottom protein (pink layer).
- RNA was extracted and placed into a new sterile 1.5ml Eppendorf tube.
- 0.5ml 2-propanol per ml TRI reagent® was added.
- Samples were vortexed and left to stand for 5-10minutes, at room temperature.
- Samples were then centrifuged at 1200rcf for 10minutes at 4°C
- The resulting fluid was discarded and concentrated white pellet at bottom of tube was preserved.
- The pellet was washed with 1ml 75% ethanol

- The pellet was vortexed and then centrifuged at 7500rcf for five-minutes at 4°C
- At this stage samples could either go on to be measured for their concentration with the Nanophotometer™, in preparation for reverse transcription, or frozen down at -80°C for storage for use at later date.

2.6 RNA concentration

RNA concentration was measured using a spectrophotometer, Nanophotometer™ from Implen.

2.7 Reverse Transcription

- The volume of RNA required was calculated using the formula 1/ 0. [concentration of RNA ng/μl] = volume
- RNA samples were diluted to a total volume of 10μl using PCR water (10μl-volume RNA = volume PCR water).
- Ten microlitres of RT mix was added
- The sample was added to the thermocycler under the following settings:
    - Step 1. held at 25°C for 5 minutes
    - Step 2. held at 42°C for 60minutes
    - Step 3. held at 70°C for 15minutes
    - Step 4. held at 4°C ∞
- Samples were either diluted to 1 in 4 or 1 in 5 by adding either 60μl or 80μl PCR water
- At this stage samples could either go on to PCR or be frozen down to -20°C.

2.8 Polymerase chain reaction (PCR)

To prepare samples and reduce pipette error (example 16µl final volume)

A. 1. PCR master mix =8-16µl
+
2. Forward Primer [500nM] = 1-2µl X no. of samples (+1 extra sample vol) = Volume
+
3. Reverse Primer [500nM] = 1-2µl

B. 1. Sterile H_2O = 5-10µl
+ X no. of samples (+1 extra sample volume) = Total Volume
2. Sample cDNA = 1-2µl

C. Control 6-12µl H_2O x no. of samples (+1 extra total sample volume) = volume

The thermocycler was warmed up to base temperature of 94°C prior to use for PCR. Using either PCR tubes or PCR plates, samples were placed in the thermocycler. The thermocycler cycle conditions are shown in Table 2.3.

Table 2.3: PCR thermocycler conditions

Thermocycler conditions set up
Step 1: Hold at 94°C for 5 minutes
Step 2: Hold at 94°C for 30 seconds, hold at 55°C for 30 seconds, hold at 72°C for 2 minutes and 30 seconds (repeated for 35-40cycles)
Step 3: Hold at 72°C for 10minutes
Step 4: Hold at 4°C ∞

2.9 Agarose gel electrophoresis

The correct amount of agarose, in 50-200mls of TBE, was microwaved/melted and placed into a flask to make the correct percentage gel. A standard agarose gel mixture with TBE is shown in Table 2.4.

Table 2.4: Agarose gel ratios

	50ml TBE	**150ml TBE**
Agarose	0.4g	1.2g
Agarose	0.5g	1.5g
Agarose	1g	3g

When cool enough to touch 5-10µl of SYBR safe® was added.

The gel was poured and left to set.

TBE was added to cover gel and the comb was removed.

Samples were loaded onto the gel, including an appropriate DNA ladder

The gel was run at the following settings:

- 100-140volts
- 100-130mA
- 50 watts

- The timeframe was variable depending on the products.

2.10 DNA extraction from polyacrylamide gels using QIAquick® gel extraction kit

Gel extraction of PCR products facilitates the ability to sequence products to confirm primers for the expression of the molecule of interest. The methodology is described below.

- The gel was excised containing the DNA band, with a clean sharp scalpel.
- Excess polyacrylamide was excised to reduce the gel size.
- The gel slice was weighed and 1-2volumes of diffusion buffer was added to 1 volume of gel. (i.e., 100-200µl for each 100mg of gel)
- Samples were incubated in a heating block at 50°C for 30minutes in an Eppendorf tube.
- Samples were centrifuged for 1 minute at 13000rpm, in a conventional tabletop microcentrifuge.
- The supernatant was carefully removed using a pipette. The supernatant was passed through a disposable plastic column or a syringe containing a Whatman-GF/C syringe filter to remove any residual agarose gel.
- The volume of the recovered supernatant was determined.
- Three volumes of Buffer QG were added to 1 volume of supernatant and mixed. The colour of the mixture was checked to ensure that it was yellow in colour.
    - If the colour was orange or violet 10µl 3M sodium acetate, pH5.0, was added.
- A QIAquick® spin column was placed in a provided 2ml collection tube.
- The DNA was bound by applying the sample to the QIAquick® spin column back into the same collection tube.
- 0.75ml of Buffer PE was then added to the column and centrifuged for 30-60 seconds.

- The flow-through was discarded and the QIAquick® spin column was placed back in the same tube.
- The QIAquick® spin column was pipetted into a clean 1.5ml Eppendorf tube.
- DNA was eluted by adding 50µl Buffer EB (10mM Tris-L, pH 8.5) to the centre of the QIAquick® spin column and then centrifuged for 1minute.
- The samples were quantified for DNA using a nanophotometer. The minimum concentration required was 10ng/µl for sequencing.
- The samples were then sent for sequencing to Source Bioscience Sequencing, Cambridge UK.

2.11 Immunofluorescent cell staining

Antibodies are a useful tool to demonstrate both the presence and the subcellular localisation of antigen or molecule. Cell staining is versatile and a sensitive method of detection. Cell staining can be divided in to four principal steps. Cell preparation, fixation, antibody application and evaluation.

In the first step, cells were attached to a solid support to facilitate the ability to handle the cells in subsequent examination. This was achieved with anchorage dependent and adherent cells by growing cells on a suitable solid support such as a coverslip or glass microscope slide. Alternatively, cells could be bound to a solid support using chemical linkers.

The second step was to fix +/- permeabilise the cells to ensure access of the antibody to its antigen. Ideal fixation would be to immobilise the antigens while maintaining the cellular

and subcellular structure, but still allowing unrestricted access to all cellular compartments for the antibodies. Organic solvents such as alcohol or acetone remove lipids and dehydrate the cells. Cross-linking reagents form intermolecular bridges and create a network of linked antigens. Cross-linking maintains cell structure better than organic solvents, but may reduce the ability of antibodies to reach some cellular components.

The third step involved incubation of cell preparations with antibody. Unbound antibody was removed by washing and the bound antibody was detected either directly or indirectly. The final step, staining, involved evaluation using a fluorescent microscope.

Immunofluorescent Staining Methodology:

- Cells were seeded using coverslip/chamber slide to the desired number of cells (approx. 30000-40000 cells) into 8-well chamber slide (Figure 2.5).
- Cells were incubated in a tissue culture incubator, at 37°C 5% CO_2, overnight.
- The medium was aspirated, and cells were fixed in either ice cold ethanol -20°C for a minimum of 20minutes. (Alternatively, 4% formalin could be used – ethanol can be stored for 3months prior to use and 4% formalin can be stored for one month)
- Cells were rehydrated using PBS for a minimum of 20 minutes at room temperature.
- Cells were permeabilised with 0.1% triton x100 (made in PBS) for 2-3minutes for transmembrane proteins and 5-minutes for non-transmembrane proteins.
- Cells were washed with PBS for 5minutes and placed on a rotator or gentle shaker. This was repeated for a total of three times.
- Dilutant was prepared with PBS and four drops 5-10% horse serum (blocking solution) with 20mls of PBS (1 drop/5mls).

- A total of 150µl serum/PBS mixture was added, after removing off a third of the PBS wash to the cells.
- The blocking solution was tapped off.
- The samples were incubated using primary and control antibodies (Ab) within wells.
    - Primary antibodies: CD44 Ab, $ITIH_3$ Ab
    - Control antibodies: Goat IgG Ab, Rabbit IgG Ab and Mouse IgG Ab
    - Antibodies to be made up to 1:20: 5µl Antibodies +95µl blocking solution/well
    - Control antibodies 1µl IgG control + 95µl blocking solution
- Samples were incubated either at 4°C overnight or at room temperature for 1 hour.
- The wells were washed three times with PBS for 5 minutes on a rotator.
- A secondary antibody was added, anti-mouse IgG TRITC (Sigma T5393) goat serum (Red).
    - 1:500 concentration Alexa secondaries (or 1:250 if using FITC/TRITC secondaries)
- Samples were incubated in the dark for one hour at room temperature.
- At this stage 1µl DAPI nuclear counterstain (blue), at 1:1000, was added.
- Samples were further washed, x3 times, in PBS
- The plastic frame was removed from the chamber slide and then a coverslip was mounted over the cells using fluorosave, avoiding air bubbles.
- The slides were placed on a tray, wrapped with foil (to prevent fading), and stored in a fridge at 4°C until viewed with the fluorescent microscope.

Figure 2.5. 8-well chamber slide used for cell imaging. Adherent cells are cultured in the chamber slide before the medium is aspirated, the plastic chamber frame detached from the coverslip, and cells are fixed for immunofluorescence using the methods described in 2.11.

2.12 Protein detection methodology

2.12.1 Protein extraction and cell lysate preparation

Once cells had reached appropriate confluence, the medium was removed with a vacuum aspirator and the cell monolayer was washed with PBS buffer. A sterile cell scraper was used to detach the cells from the flask surface and the resultant suspension was collected in a universal container. The samples were centrifuged at 2000rpm for 8minutes to deposit samples into a pellet. The pellet was resuspended in PBS and centrifuged twice more. After removal of the supernatant the pellet was resuspended in 100µl-300µl of lysis buffer (depending on pellet size) and transferred to a 1.5ml Eppendorf tube. The tube was placed on a Labinco rotating wheel (Woolf laboratories, UK) and rotated at room temperature. One hour later, the resulting suspension was centrifuged at 1300rpm for 15minutes, separating the sample into a supernatant containing proteins, which were transferred to a fresh Eppendorf tube. The protein samples were then either quantified or stored at -20°C until required.

2.12.2 Protein quantification and standardisation

Standardisation of protein concentration prior to analysis using SDS-PAGE and Western blotting techniques was done using the Bio-Rad DC protein assay kit (Bio-Rad Laboratories, Hemel Hempstead, UK). This assay produced a characteristic blue colour with absorbance read between 405-750nm on a EL x800 spectrophotometer plate reader (Bio-Tek, Wolf laboratories, UK). The standard used was bovine serum albumin.

Working reagent A (Alkaline copper tartrate solution) was prepared by adding 20µl of reagent S (Surfactant solution) to each 1ml of reagent A. In a 96-well plate serial dilutions of the protein standard of 50mg/ml bovine serum albumin (BSA) and the same lysis buffer which was used for the sample of proteins were prepared, in order to produce standards with a protein concentration gradient of 0.78mg/ml to 50mg/ml. Into the fresh wells 5µl of either the protein sample or standard were pipetted together with 25µl of Reagent A. Folin reagent (Reagent B) was also added at a volume of 200µl. The plate was agitated gently and left to rest for 20minutes at room temperature. A standard protein curve or protein concentration was prepared by plotting the graph of the BSA standards protein concentration versus absorbance, which was then used to determine the protein concentration of the protein samples. Protein samples were standardised to a final concentration of 1-2mg/ml using the appropriate volume of lysis buffer. Laammli x2 sample buffer concentrate was added on a 1:1 ratio to each standardised protein sample, prior to denaturation by boiling at 100°C for 50minutes. The boiled samples were either used immediately for SDS-PAGE or again stored at -20°C until required.

2.12.3 Sodium dodecyl sulphate polyacrylamide gel electrophoresis (SDS-PAGE)

The SDS-PAGE electrophoresis methodology was performed in line with the local lab protocol adapted from Abcam.

- Plates were washed with Hibiscrub® and ethanol, dried and set up in cast plates.
- Ethanol 70% was run between plates to check plates for leakage
- A resolving gel was made up based on concentration required.
- A comb was placed between plates, marking the bottom, and filling the resolving gel to bottom of marks.

- The gels were topped up with ethanol to ensure gel set straight and was left to set for 20minutes
- The ethanol was emptied.
- The stacking gel was made up and added to the top of plates with comb in-situ and left to set.
- The plates were added to an electrophoresis tank and filled with running buffer.
- The combs were then removed from the gel.
- The ladder and protein samples were added (10µl to each well).
- The gels were run on the electrophoresis settings of 90volts/200mA/50wats for 1-2.5hrs.
- The loading dye was checked intermittently during electrophoresis to ensure they did not run off end of gel.
- For any well unused for sampling, the well was loaded with Laemmli buffer to keep adjacent bands straight.
- When electrophoresis was complete the samples were immediately moved to the nitrocellulose transfer process.

2.12.4 Western blotting: transferring proteins from SDS-PAGE to a nitrocellulose a membrane

During the SDS-PAGE, the transfer process was prepared. The process is described as follows:

- The transfer plates (SD20 SemiDry Maxi System blotting unit (SemiDry, Wolf Laboratories, UK)) were cleaned with ethanol and left to dry.
- Four sheets of filter paper were cut to the same size as the gel and were soaked in x1 transfer buffer for 25-30minutes.
- The transfer membrane sheet was soaked in methanol.
- The SDS-PAGE gel once complete was removed from the cell with the glass plates gently opened to expose the gel. The stacking gel was discarded using a gel cutter.
- Once SDS-page was complete, two of the filter paper sheets were placed on the transfer plate, followed by x1 sheet of transfer membrane, followed by the SDS-PAGE gel placed on top and finally two more filter paper sheets.
- Tissue paper was used to remove excess transfer buffer and water from the transfer plate.
- The negative electrode plate was placed on top of the sheets and tightened down equally to ensure even distribution across the plate.
- The plate was activated at 15volts, 350-500mA, 5 watts for 30-60minutes.

2.12.5 Protein staining and immunoprobing

Successful transfer of the proteins from the gel to the nitrocellulose membrane was confirmed using Ponceau S staining. A 5% blocking solution was added to a 50ml Falcon tube (Fisher Scientific, Leicester, UK) along with the membrane. The membrane was orientated so that the side which had been facing the gel was towards the lumen of the tube.

The primary antibody was also added at this stage. The tube was left overnight at 4°C on a rotator to ensure equal distribution of the blocking solution on the membrane. The blocking solution was removed, and the membrane was washed with 5mls of TBST (Tris Buffered Saline with Tween), put on a roller for 5minutes at each wash and three washes were completed. A further 5mls of milk solution was added together with the secondary antibody and rolled at room temperature for 1-2hours. A further three washes of the membrane with TBST was completed and was followed by a fourth wash with TBS for 15minutes.

2.12.6 Protein visualisation

Protein detection was undertaken using the Luminata™ Forte Western HRP chemiluminescence substrate (Millipore, Billerca, USA). Horseradish peroxidase (HRP) catalyses the oxidation of luminol, which in the presence of peroxide releases photons which can be captured on a camera. The membrane was transferred to the UVITEC imager (UVITEC, Cambridge, UK) where 5-6mls of HRP were added and incubated for 2-5minutes at room temperature in the dark. The UVITEC imager was used to capture the chemiluminescence and recorded.

2.13 Tumour cell functional Assays

2.13.1 Live cell counting methodology

The methodology for trypan blue cell viability counting was adapted from the Sigma-Aldrich Trypan blue protocol (https://www.sigmaaldrich.com/technical-documents/protocols/biology/cell-quantification.html)

- Cells were harvested from cell culture plates with 2mls of trypsin
- Cells were resuspended in fresh DMEM to deactivate trypsin and spun down.
- An initial count was undertaken to determine dilution concentrations to split the cells at an appropriate number.
- Cells were spun down in a centrifuge and resuspended in 1ml PBS, to simulate the nutrient deficit peritoneal environment. Cells were broken down into a single cell suspension by gently pipetting the cell solution.
- Approximately 0.5-1million cells were harvested per experiment and placed into universal containers. Containers were placed in an incubator for the time required for each part of the experiment.
- Initial runs of the experimental technique had no further treatment added. Subsequent runs included HAi or HA to the suspension mixture.
- An equal volume of Trypan Blue (dilution factor =2) was added and mixed gently.
- The haemocytometer was cleaned.
- The coverslip was moistened with water or exhaled breath. The coverslip was slid over the chamber back and forth using slight pressure until Newton's refraction rings appear (Newton's refraction rings are seen as rainbow-like rings under the coverslip).

- Both sides of the chamber were filled with cell suspension (approximately 5-10µl) and viewed under an inverted phase contrast microscope using x20 magnification. Three large squares were counted for each sample within each experiment run and the mean was taken (Figure 2.6).
- Percentage cell viability was calculated by:

Percentage viability = (number of viable cells counted/total number of cells counted) x 100

- Percentage cells aggregated was calculated by:

Percentage Cells aggregated = (number of aggregated cells counted/Total number of cells counted) x100

a.

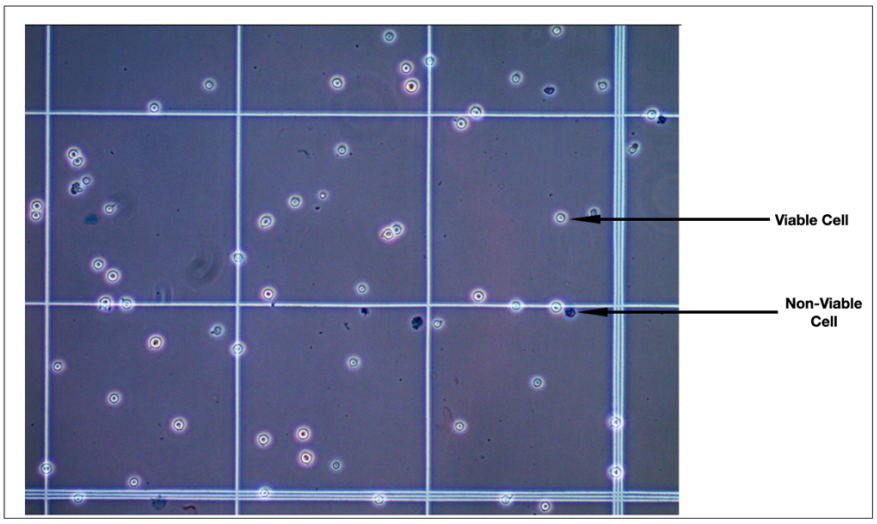

b.

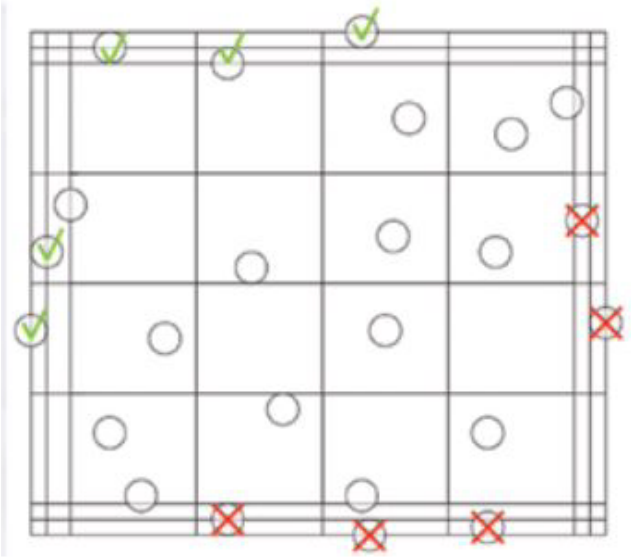

Figure 2.6: 2.6a. Trypan blue staining showing the view obtained from a Haemocytometer demonstrating a viable cell appearance versus a non-viable cell which has stained blue. Image taken from Sigma Aldrich data information online for trypan blue cell viability. 2.6b. Image demonstrating standardised field of view and cells to be included within the count of the Haemocytometer. Images taken and adapted from https://www.sigmaaldrich.com/technical-documents/articles/biofiles/cell-viability-and-proliferation.html.

2.13.2 A peritoneal model for free-floating colorectal cancer cells *in vitro*

The assessment of free-floating cancer cells, which are anchorage dependent, is needed in order to attempt to replicate free-floating cancer cells in the peritoneal environment. The use of non-adherent conical bottomed universal containers, which are not tissue culture treated, can mimic this environment and prevent cells adhering to their walls. Cells were harvested and quantified to appropriate cell numbers and placed into solutions, either with cell culture medium or alternatively PBS to attempt to replicate the free-floating peritoneal environment to a simplistic extent. Treatment was applied to the free-floating cells and compared to controls to assess cell viability, aggregation and apoptosis.

2.13.3 Cell adhesion assay

2.13.3.1. Adhesion assay: Matrigel™ coated plate preparation

- Five micrograms of Matrigel (BD Matrigel™ Matrix, Matrigel™ Basement membrane Matrix, Corning Inc, Flintshire UK) was seeded into each well, of a 96well plate (Applied Biosystems™, Life Technologies Ltd, Paisley, UK).
- Matrigel comes in a stock concentration of 9.2mg/ml and is then diluted to 50µl/ml in serum free medium ((9200µg/50 µg) x number of wells required including an error sample volume) to total volume required.
- The Matrigel was dried at 55°C for about 1-2hours.
- The coated plates could be stored at 2-8°C for up to a week, sealed with Parafilm™ to prevent dehydration, on a level surface.

2.13.3.2. Adhesion assay: HA coated plate preparation

- High molecular weight hyaluronic acid (Catalogue no. GLR002, R&D Systems®, Minneapolis, USA) made up to a stock concentration of 10mg/ml. Serial dilutions were made using PBS or DMEM to concentration required.
- The required concentration was seeded onto plate and incubated at 55°C to set HA on plate.

2.13.3.3. Adhesion Assay: LP9 Coated plate preparation

- Cells were trypsinised with 2mls trypsin.
- Once cells were detached 8mls of M199 was added
- Cells were centrifuged to a pellet at 15000rpm for five minutes.
- The medium was aspirated from the pellet
- Cells were re-suspended in medium
- Cells were counted
- The required number of cells was 12000cells/well
- The required number of cells were extracted for the number of wells required on the 96-well plate and added to required volume of medium (100µl/well).
- The cell mixture was pipetted at 100µl/well and incubated over 24-48hours at 37°C.
- The cells were checked for confluency prior to conducting adhesion assay.

2.13.3.4. HAi Concentration

HAi (AnaSpec Inc. Fremont, California, USA Cat 62622). Stock concentrations made at 400µM. Serial dilutions were made using DMEM as required

2.13.3.5. Adhesion assay: procedure

- The required number of CRC cells were harvested from the culture flask:
    - Trypsinised in 2mls trypsin
    - Once cells were detached 8mls DMEM was added
    - Cells were extracted to a universal container (UC) & centrifuged at 15000rpm for 5-minutes.
    - Medium was aspirated and the cells were re-suspended in DMEM.
- Cells were counted
- The appropriate number of cells were extracted and added to required volume of medium in the UC.
- DiI ($DiIC_{18}$) 20µl (5mg/ml) was added to the UC, mixed, and incubated for 40minutes at 37°C.
- The UC was centrifuged at 15000rpm for five-minutes and the medium was aspirated from the pellet.
- Five millilitres of PBS was added to wash the pellet, and then centrifuged for a further five-minutes at 10000rpm. The PBS was then aspirated from pellet.
- The wash was repeated once more (total two wash cycles with PBS).
- Cells were re-suspended with the required volume of DMEM.
- Either 100µl of HAi at required concentration or 100µl control PBS was added in DMEM to wells.
- One hundred microlitres of CRC cell suspension was added to wells.
- Cells were incubated at 37°C for 40minutes.
- The wells were aspirated gently

- The wells were washed gently with 400µl PBS and then gently aspirated.
- Cells were fixed in 100µl – 200µl Formalin 4%.

2.13.3.6. Results recording

The results were measured using one of two techniques to assess the degree of adhesion. Manual counting was used following imaging cells with EVOS fluorescent imaging microscopy and single cell culture models were stained with crystal violet to measure cell absorbance as an alternative method of cell counting.

Method 1:

1. Cells were imaged using EVOS fluorescent imaging analyser (M7000, Thermofisher scientific Inc.) using red fluorescence protein (RFP) and Trans-illumination imaging.
2. Adherent CRC cells were manually counted to plate using image J software.
3. Images were standardised into a grid pattern and manually counted using the same standard cell counting methodology as when counting on a haemocytometer in section 2.13.

Method 2 (for single cell type adhesion assays):

1. Cells on the 96-well plates were stained with 200µl crystal violet per well.
2. Crystal violet was washed off gently using water
3. The plate was left to dry.
4. Acetic acid 10% was then added at a volume of 200µl per well
5. Plate absorbance was then read using plate reader at appropriate light absorbance setting following the plate reader operating instructions.

2.13.4 Cell counting kit-8 (CCK-8): cell viability assay

Cell Counting Kit-8 (CCK-8) allows convenient assays by utilising Dojindo's highly water-soluble tetrazolium salt, WST-8 (2-[methoxy-4-nitrophenyl)-3-3(4-nitrophenyl)-5-(2,4-disulfophenyl)-2H-tetrazolium, monosodium salt]), which produces a water-soluble formazan dye upon reduction in the presence of an electron mediator.

CCK-8 is a one bottle solution without the requirement of premixing components. It is a sensitive colorimetric assay for the determination of viable cells in cell proliferation and cytotoxic assays. The amount of formazan dye generated by the dehydrogenases in cells is directly proportional to the number of living cells.

Cell viability assay using CCK-8 methodology modified as follows:

- Cell suspension at a volume of 100µl was dispensed (5000-7000cells/well or container) into an appropriate number of either universal containers or 96-well plates, depending on experiment. (If testing adherent cells pre-incubate the plate for 24hours to allow cells to settle)
- The addition of 10-20µl of treatment substances to be tested was added.
- The plate was incubated for the appropriate length of time for the viability assay
- Each universal container/well had 10µl of CCK8 solution added (it was ensured not to introduce bubbles during this)
- The plate was incubated for 1-4hours at 37°C
- The absorbance was measured at 450nm using a microplate reader.

2.13.5 Flow Cytometry

Flow cytometry is a technique used to detect and quantify physical and/or chemical characteristics of a population of cells or particles. For this study a sample of cells suspended in solution was injected into the flow cytometer to assess for viable, early apoptotic, and late apoptotic cell populations. Cells in suspension were stained with a variety of monoclonal antibodies with fluorescent dyes. The specific antibody combinations provide the specific information required for the cell populations. The stained cells were passed through the flow cytometer where a laser light was utilised to characterise the physical structure of the cell and measure the fluorescent staining.

It is possible to measure extrinsically mediated apoptosis induction involving the analysis of various receptor expression (Elmore, 2007). Flow cytometry can be used to differentiate apoptosis progression through each pathway to help determine an apoptosis mechanism.

12.13.6. Annexin V apoptosis detection assay

Apoptotic cells undergo morphological changes indicating progression of cell death, which can take place quite rapidly. An early indicator of apoptosis is the rapid translocation and accumulation of a membrane phospholipid called phosphatidylserine (PS), on the extracellular surface from the cell cytoplasm (Arur, Uche, Rezaul *et al.*, 2003). The apoptosis detection kit Annexin V (Santa Cruz Biotechnologies) binding properties can be used to detect cells progressing through apoptosis and can be assessed according to their Annexin V and propidium iodide (PI) staining pattern. Early apoptotic cells will bind annexin V but are

not sensitive to intracellular staining with PI. However, as cells progress in the apoptosis cascade, the integrity of the cell plasma membrane is lost, which allows PI to penetrate and label the cell with a strong yellow-red fluorescence.

The Apoptosis assay methodology was adapted from the Santacruz data sheet. A reduction of the staining volumes used were found to be more effective, than the volumes stated on the standard datasheet. The standard stain volumes were found to be too high and could not be used for interpretation. The procedure was carried out as follows:

- 500000 cells/500µl CRC cells were collected and spun down at low-speed centrifugation (1500rpm) for 5 minutes. Cells were washed twice with cold PBS and resuspended in 1x Assay buffer at a concentration of $1x10^6$cells/ml.
- 100µl aliquot of cells was transferred to 1.5ml Eppendorf tubes, which were foil wrapped.
- 2.5µl Annexin V FITC and 1µl of propidium iodide (PI) were added.
- Negative control samples included treatment samples, with various stain samples excluded, these were:
    - 1. No annexin V FITC and no PI stains
    - 2. Annexin V FITC stain alone
    - 3. PI stain alone.
- Samples were vortexed gently and incubated for 15minutes at room temperature in the dark and stored on ice.
- A further 400µl of 1x assay buffer was added to the samples.
- Samples were analysed immediately with Flow cytometry using a single laser emitting light at 488nm.

2.14 *In vivo* xenograft murine model

Athymic nude mice (CD1) were obtained from Charles River Laboratories (Charles River Laboratories International, Inc. Kent, England, UK). All mice were housed in filter-topped isolation cages and all procedures were carried out in a class-II cabinet.

Based on previous experience from the lab group with in vivo work, five-million colorectal cancer cells (HT115) were injected into the peritoneal cavities of the mice at a volume of 100μl in PBS. A further 5million cells were injected subcutaneously on the dorsal aspect of the mice to facilitate visual monitoring of tumour growth. The mice were formally monitored twice a week measuring body weight and subcutaneous tumour nodule growth. The mice were terminated after 4 weeks. Post-mortem laparotomies were undertaken to detect intraperitoneal tumour growth. Tumour nodules were photographed using a stereomicroscope (Olympus, Japan) and the volume of metastatic tumour was calculated with the formula:

Tumour volume (mm^3) = 0.5x tumour nodule $width^2$x tumour nodule length

2.15 Histology

Histological assessment can be undertaken through embedding tumours in wax paraffin fixation. Histological specimens can be sliced, fixed and stained to examine cell structure and morphology accurately. For routine assessment the use of Haematoxylin and Eosin (H&E) is a preferential stain to initially examine cellular and tissue structure detail. The stain can be varied in intensity and is often driven by the pathologists experience and also personal preference. Broadly speaking, the stain demonstrates a wide range of cytoplasmic, nuclear, and extracellular matrix features that can be visually assessed. Staining technique is as follows:

- The slide sections were deparaffinized through two changes of xylene for 5-minutes each.
- Slides were Re-hydrated through a series of graded alcohol (100%, 100%, 90%, 70%, 50%), for 5 minutes each, followed by a wash in distilled water for 5 minutes.
- Slides were stained in Gill's haematoxylin solution for 2-5 minutes.
- Slides were washed in running tap water for a further 5 minutes.
- The slides were counterstained in Eosin solution for 30 seconds to 1 minute.
- The slides were dehydrated through a graded series of alcohol (literally by dipping and shaking in 70% and 90% ethanol and finally into 100% ethanol, twice, for 5minutes). Eosin will dissolve out of sections when in water, but if overstained with Eosin it can be left longer in 90% alcohol to remove some of the excess stain.
- Slides were cleared in two changes of xylene for 5 minutes each.
- Slides were mounted with a xylene based mounting medium of Distyrene, plasticiser and Xylene (DPX).

2.16 Statistical analysis

Prism was the statistical package software used throughout the study (Prism 9 for mac OS version 9.3.0, GraphPad software LLC, San Diego, USA). Kaplan Meir survival assessment was conducted using SPSS software (SPSS standard version 13.0; SPSS Inc., Chicago, Il USA). T-tests were conducted when comparing two variables of normally distributed data. One-way ANOVA assessment was utilised when comparing three or more groups. Differences were statistically significant when $p<0.05$.

Clinical Significance of Hyaluronic Acid Dependent Adhesion Molecules CD44, RHAMM and ICAM-1 in Colorectal Cancer

Chapter 3

3.1. Introduction

The process of cellular adhesion in peritoneal metastases (PM), in colorectal cancer (CRC), can be achieved utilising cellular adhesion molecules, which are able to interact with distant sites. The role of hyaluronic acid (HA), in the context of cancer growth and progression, has been proposed as a potential target in cancer therapy (Lokeshwar *et al.*, 2014). Adhesion molecules can either act independently, or via a cascade of activation of a series of adhesion molecules and processes. Broadly speaking, in the context of PM, adhesion can be split into HA-dependent adhesion and HA-independent adhesion (Soliman *et al.*, 2021). Overall, relatively little is known on the potential molecules involved in the adhesion phase in PM and the processes involved in peritoneal spread. Sluiter *et al* (2016) conducted a systematic review of the literature to attempt to identify potential molecules involved in adhesion and peritoneal dissemination in various cancers (Sluiter *et al.*, 2016). This forms the basis in screening potential adhesion molecules within this Chapter in relation to colorectal cancer.

As described in Chapter 1, HA has been shown to interact with three principal cell surface receptors, namely CD44, RHAMM and ICAM-1 (Aruffo *et al.*, 1990; Entwistle *et al.*, 1995; McCourt *et al.*, 1994). The interplay involved in cellular adhesion molecules and cascades can be complex and current literature, attempting to untangle the mechanisms involved in CRC can, in some cases, draw contradictory or incomplete conclusions (Sluiter *et al.*, 2016).

Intracellular adhesion molecule -1 (ICAM-1) is part of the immunoglobulin family, along with Vascular endothelial adhesion molecule-1 (VCAM-1) and L1 Cell adhesion molecule (L1CAM). VCAM1 and L1-CAM, unlike ICAM-1, do not have a receptor for hyaluronic acid.

High expression of serum VCAM-1 has been implicated, along with ICAM-1, in CRC progression and with increasing the likelihood of disease recurrence (Alexiou, Karayiannakis, Syrigos *et al.*, 2001; Maurer, Friess, Kretschmann *et al.*, 1998; Yamada, Arao, Matsumoto *et al.*, 2010). Mesothelial VCAM-1 has been described to interact with $\alpha 1\beta 1$ and $\alpha 4\beta 7$ molecules in the process of cell adhesion and metastatic progression (Kong, Kim, Kim *et al.*, 2018). Over expression of VCAM1, mediated by TNF-α, ILβ and reactive oxygen species, could contribute to increased risk of PM formation after surgery, following trauma (ten Raa, van Grevenstein, ten Kate *et al.*, 2007; Yu, Tang, Yu *et al.*, 2010). Simvastatin is theorised to potentially prevent peritoneal dissemination, through downregulation of VCAM1 (Wagner, Lob, Lindau *et al.*, 2011).

L1CAM has been predominantly studied in ovarian cancer and peritoneal metastases. It has been associated with multifunctional roles within tumour progression, including tumour cell adhesion (Arlt, Novak-Hofer, Gast *et al.*, 2006). Inhibition with an anti-L1CAM antibody has been shown to reduce intrabdominal tumour burden in mouse models (Arlt *et al.*, 2006). L1-CAM expression has been shown to be related to the level of aggression on the invasive front of CRC (Kajiwara, Ueno, Hashiguchi *et al.*, 2011). Adhesion to the peritoneum with L1CAM is through interaction with Neutropilin-1 (J. van Baal, van Noorden, Nieuwland *et al.*, 2018).

Epithelial cellular adhesion molecule (EpCAM) is a homotypic independent adhesion molecule (Patriarca, Macchi, Marschner *et al.*, 2012) and is highly expressed in gastric cancer PM (Imano, Itoh, Satou *et al.*, 2013). It has been implicated in cell adhesion,

signalling, migration, proliferation and differentiation (Trzpis, McLaughlin, de Leij *et al.*, 2007).

The gene Cadherin 1 (CDH1) encodes for the protein E-cadherin. E-cadherin is described to be involved in cell-cell adhesion in peritoneal dissemination of gastric cancer. Decreased CDH1 expression results in reduced cell adhesion and is seen more predominantly in the detachment phase from the primary tumour (Ma, Shen, Kapesa *et al.*, 2016). Epithelial to mesenchymal transition (EMT) (Kalluri & Weinberg, 2009) partly explains the complexity in cellular changes in the process of PM, where E-cadherin has been shown to play a role.

Carcinoembryonic antigen-related cell adhesion molecule 1 (CEACAM1) is a cell adhesion molecule belonging to the CEA and immunoglobulin gene families. Expression is complex in cancer and could also be related to EMT change and disease stage (Beauchemin & Arabzadeh, 2013; Gebauer, Wicklein, Horst *et al.*, 2014). It is seen to be down regulated in the early stages of several epithelial cancers, including CRC, but is often re-expressed in metastatic stages of disease (Arabzadeh & Beauchemin, 2012).

P-Glycoprotein (P-gp) is encoded by the gene MDR1. It has been demonstrated to play a role in postoperative adhesion formation, cell proliferation, migration and differentiation (L. Deng, Li, Lin *et al.*, 2016). Expression of MDR1 in human CRC has been reported to be higher in well differentiated tumours (Mizoguchi, Yamada, Furukawa *et al.*, 1990). P-gp has also been reported to enhance tumour aggressiveness (Pirker, Wallner, Gsur *et al.*, 1993).

MUC 1 and MUC16 are part of a high molecular weight glycoprotein MUC family, which is broadly split into gel forming mucins or transmembrane mucins. Both MUC1 and MUC16 fall under the transmembrane glycoprotein sub-family domain. MUC16 gene has also been demonstrated to code for the CA125 antigen, which is more commonly associated to ovarian cancer. However, expression of MUC16/CA125 has also been demonstrated in other epithelial tumours including colon. Expression of both MUC1 and MUC16 has been associated with a mixed response of both adhesive properties and also contributes to de-regulation of cell-cell adhesion in epithelial cancers (Akita, Tanaka, Tanida *et al.*, 2013; Muniyan, Haridas, Chugh *et al.*, 2016; Rump, Morikawa, Tanaka *et al.*, 2004; H. S. Wang & Wang, 2015). MUC1 has been implicated in oncological progression and has been involved in regulation of CDH1. MUC16 silencing has been shown to reduce epithelial cancer cells' ability to form colonies, adhesion, migration and invasiveness (Reinartz, Failer, Schuell *et al.*, 2012), as well as be associated with adhesion in conjunction with interaction with mesothelin (Streppel, Vincent, Mukherjee *et al.*, 2012).

This chapter screens the panel of adhesion molecules, which have been identified in the literature, in various abdominal cancers and potentially have been seen to have a link with peritoneal metastases in CRC. These molecules were also screened in relation to clinicopathological outcomes that are linked to publicly available tissue microarray datasets. Particular attention is paid to molecules CD44, RHAMM and ICAM-1, which have been shown to have hyaluronic acid receptor binding in order to ascertain their potential involvement in CRC.

3.1.1. Chapter aims

The aims of this chapter to look at the following:

1. To examine RNA expression of panels of molecules identified in the literature which are associated with, or have been studied in, peritoneal adhesion in various cancers, from a publicly available tissue microarray
2. To examine whether there is any relationship between molecular expression and the associated clinicopathological data.
3. To examine the expression of the HA-dependent adhesion molecules in CRC:
    a. CD44
    b. RHAMM
    c. ICAM-1
4. To examine expression of HA-independent adhesion molecules in CRC.

3.2. Methods

Tissue microarray data facilitates large volume gene expression data to be collected and examined. This data can be uploaded to online publicly available databases and can allow others to further assess genes of interest, not originally looked at by the original researchers, due to the volume of data available. The Gene Expression Omnibus (GEO) is one database where raw data can be downloaded for further analysis (https://www.ncbi.nlm.nih.gov/geo/ (last accessed December 2021)).

GEO cohorts were searched for relevant human colorectal cancer datasets. Each dataset returned was assessed to include either cohorts containing colorectal cancer with matched normal tissue, matched clinicopathological outcomes, or primary CRC cell line expression. RNA expression profiles were matched to the clinicopathological datasets matched to the specimens collected. Data was downloaded, processed, and cleaned using Microsoft Excel to enable further analysis. Statistical analysis was carried out using GraphPad Prism, data analysis software. Cohorts were excluded based on experimental methodology and low sample numbers.

3.2.1. Cohorts

3.2.1.1. GEO dataset GSE 40967

There were 585 patients with unpaired colorectal adenocarcinoma, which were analysed for expression of identified genes for adhesion molecules with microarrays (Affymetrix U133 Plus 2.0), with GEO platform GPL570. Raw data was made publicly available through GEO dataset GSE40967 (Ligue Nationale Contre le Cancer, France. Made public 22nd May 2013. Last Updated 25th March 2019). The clinicopathological details of this data set is summarised in Table 3.1 and Section 3.2.2.

3.2.1.2. GEO dataset GSE44076

Ninety-eight paired normal colonic mucosae and colonic tumour samples were analysed for expression of selected genes with microarrays (Affymetrix HG-U219), with GEO platform GPL13667. A further fifty unpaired samples of colonic mucosae, biopsied from healthy individuals at colonoscopy, were also analysed. The tumour cases were early stage II, microsatellite stable colon cancers, from a homogenous patient group with more than three years of follow up, without neoadjuvant chemotherapy. The original data set series was available from colonomics.org, in the original study design, of which is summarised in Figure 3.1. Raw data is publicly available through GEO dataset GSE44076 (Catalan Institute of Oncology, Spain. Made public 14th March 2014. Last updated 1st July 2019). The clinicopathological details of this dataset is summarised in Table 3.2 and Section 3.2.2.

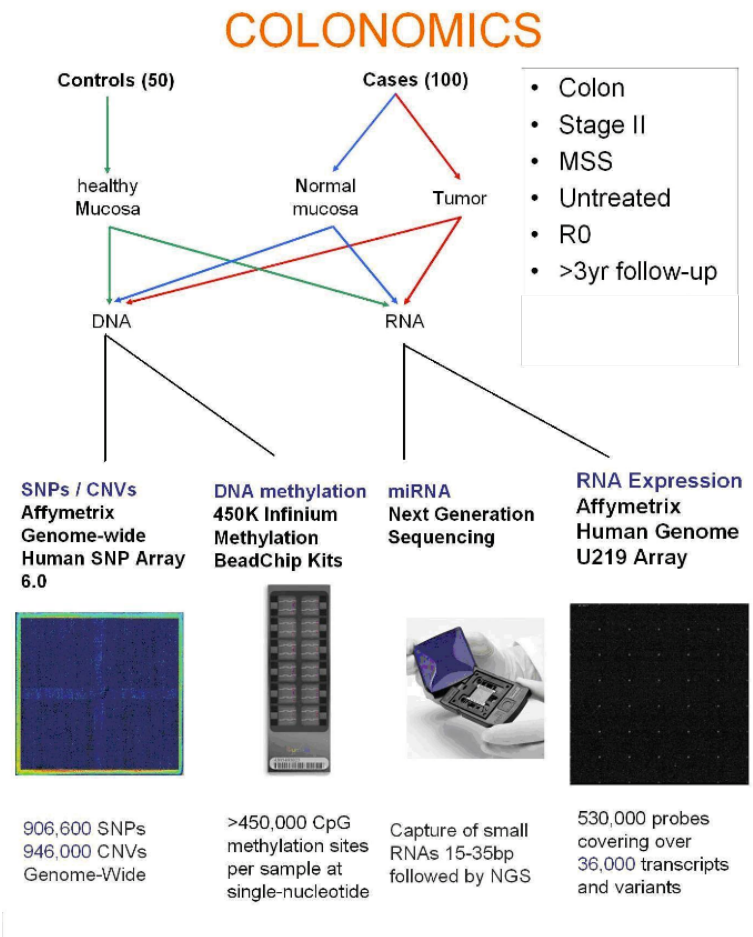

Figure 3.1. Dataset GSE44076 Colonomics original study design summary. Figure taken from www.colonomics.org.

3.2.1.3. GEO dataset GSE90830

Expression profiling of forty-four colorectal cancer cell lines by high throughput sequencing, comparing human CRC cell lines to primary tumours and normal tissues. Raw data was made publicly available through GEO dataset GSE90830 (Walter and Eliza Hall Institute of Medical Research, Australia. Made public 12th January 2018. Last updated 15th May 2019). The GEO platform used to analyse the data was GPL13534. The cell lines analysed and associated clinicopathological features are summarised in Table 3.3 and Section 3.2.3.

3.2.2. Clinicopathological data

3.2.2.1. GSE40967

There are 585 colorectal cancer specimens which were analysed for expression of identified adhesion molecules and assessed to the matched clinicopathological dataset. The clinicopathological features of the tumours included in this cohort are shown in Table 3.1. All tumour samples included were confirmed colorectal adenocarcinoma. The overall mean age was 66.9 years (range 22-97years).

Table 3.1. Clinicopathological features of colorectal cancer tissue samples GEO cohort GSE40967

		Number (Percent)
Total Samples	Total	585 (100%)
	Male	322 (55%)
	Female	263 (45%)
Overall Bowel Cancer Stage	I	38 (6.5%)
	II	271 46.3%)
	III	210 (35.9%)
	IV	60 (10.3%)
	Stage 0/Unknown	4 (0.7%)
T-Stage	T1	12 (2.1%)
	T2	49 (8.4%)
	T3	379 (64.8%)
	T4	119 (20.3%)
	T-stage unknown	26 (4.44%)
Nodal Status (N-stage)	N0	314 (53.7%)
	N1	137 (23.4%)
	N2	100 (17.1%)
	N-Stage unknown	34 (5.8%)
Metastatic Status (M-stage)	M0	481 (82.2%)
	M1	61 (10.4%)
	M-stage unknown	43 (7.4%)
Tumour Location	Proximal	232 (39.7%)
	Distal	351 (60%)
	Unknown	2 (0.3%)
BRAF Status	Wild Type	461 (78.8%)
	Mutated	51 (8.7%)
	Unknown	73 (12.5%)
KRAS status	Wild Type	328 (56.1%)
	Mutated	217 (37.1%)
	Unknown	40 (6.8%)
TP53 Status	Wild Type	161 (27.5%)
	Mutated	190 (32.5%)
	Unknown	234 (40.0%)

3.2.2.2. GSE44076

There are 98 colorectal cancer specimens which were analysed for expression of identified adhesion molecules and assessed to the matched clinicopathological dataset. From these patients 98 further samples were taken from adjacent non-tumour colonic tissue. A further 50 patient samples were taken from patients without colon cancer and the tissues were also included in the specimens as a further control for comparison. The clinicopathological features of the tumours included in this cohort are shown in Table 3.2. All tumour samples included were confirmed colorectal adenocarcinoma. The overall mean age was 68.9years (range 25-88years). The mean age for patients with tumour was 70.5years (range 43-87years) and without tumour was 62.5years (range 25-88years).

Table 3.2 Clinicopathological features of colorectal cancer tissue samples GEO cohort GSE44076

			Number (percentage)
Total Samples	Total		246 (100%)
	Tumour Tissue		98 (39.8%)
	Paired Normal Tissue		98 (39.8%)
	Normal Tissue		50 (20.3%)
Sex	Tumour Tissue	Male	71 (72.4%)
		Female	27 (27.5%)
	Paired Normal Tissue	Male	71 (72.4%)
		Female	27 (27.5%)
	Normal Tissue	Male	27 (54%)
		Female	23 (46%)
Anatomical Location	Tumour Tissue	Left	60 (61.2%)
		Right	38 (38.8%)
	Paired Normal Tissue	Left	60 (61.2%)
		Right	38 (38.8%)
	Normal Tissue	Left	23 (46%)
		Right	27 (54%)
Tumour Tissue Grade	IIa		90 (91.8%)
	IIb		8 (8.2%)

3.2.3. Colorectal cancer cell line cohort

3.2.3.1. GSE90830

Forty-four colorectal cancer cell lines were examined for expression of HA-dependent adhesion molecules CD44, RHAMM and ICAM-1 and compared for relative expression counts. Clinicopathological features of colorectal cell lines are summarised in Table 3.3.

Table 3.3. (Page 1 of 2) Colorectal Cancer Cell lines: Clinicopathological features

Cell line	Species of Origin	Cancer origin	Cell origin	Sex	Age as sampling (years)	Disease	Cell line type	Growth Properties	Dukes stage
C125PM	Human	Colon	Colon	-	-	Adenocarcinoma	Epithelial	Adherent	-
C135	Human	Colon	Colon	-	-	Adenocarcinoma	-	-	-
C70	Human	Colon	Sigmoid Colon	Female	60	Adenocarcinoma	Epithelial	Adherent	B
Caco-2	Human	Colon	Colon	Male	72	Adenocarcinoma	Epithelial-like	Adherent	-
COLO201	Human	Colon	Ascites	Male	70	Adenocarcinoma	Bipolar, refractile, fibroblast-like	Suspension, with few loosely adherent	D
COLO205	Human	Colon	Ascites	Male	70	Adenocarcinoma	Epithelial	Mixed adherent & suspension	D
COLO320	Human	Colon	Colon	Female	55	Adenocarcinoma	Rounded & refractile	Mixed adherent & suspension	C
DIFI	Human	Colon	Ascites	Female	46	Adenocarcinoma	-	-	-
DLD1	Human	Colon	Colon	Male	-	Adenocarcinoma	Epithelial	Adherent	-
GEO	Human	Colon	Colon	-	-	Adenocarcinoma	-	-	-
GP5D	Human	Colon	Colon	Female	71	Adenocarcinoma	Epithelial	Adherent	B
HCA7	Human	Colon	Colon	Female	58	Adenocarcinoma	Epithelial	Adherent	B
HCC2998	Human	Colin	Colon	-	-	Adenocarcinoma	-	-	-
HCT116	Human	Colon	Colon	Male	-	Adenocarcinoma	Epithelial	Adherent	-
HCT15	Human	Colon	Colon	Male	-	Adenocarcinoma	Epithelial	Adherent	-
HCT8	Human	Colon	Colon	Male	67	Adenocarcinoma	Epithelial	Adherent	-
HRA19	Human	Colon	Colon	-	-	Adenocarcinoma	Epithelial	Adherent	-
HT115	Human	Colon	Colon	-	-	Adenocarcinoma	Epithelial	Adherent	-
HT29	Human	Colon	Colon	Female	44	Adenocarcinoma	Epithelial	Adherent	-
HT55	Human	Colon	Colon	-	-	Adenocarcinoma	Epithelial	Adherent	-
IS1	Human	Colon	Colon	-	-	Adenocarcinoma	-	-	C
IS2	Human	Colon	Liver	-	-	Adenocarcinoma	-	-	C
IS3	Human	Colon	Peritoneum	-	-	Adenocarcinoma	-	-	C
LIM215	Human	Colon	-	-	-	Adenocarcinoma	-	-	-
LIM1863	Human	Colon	Ileocaecal valve	Female	74	Adenocarcinoma	Epithelial	Suspension	-
LIM1899	Human	Colon	Colon	Male	-	Adenocarcinoma	Epithelial	Adherent	-

Cell line	Species of Origin	Cancer origin	Cell origin	Sex	Age as sampling (years)	Disease	Cell line type	Growth Properties	Dukes stage
LIM2099	Human	Colon	Liver	Male	-	Adenocarcinoma	Epithelial	Adherent	-
LIM2405	Human	Colon	Caecum	Male	-	Adenocarcinoma	Epithelial	Adherent	-
LIM2537	Human	Colon	Transverse Colon	Male	73	Adenocarcinoma	Epithelial	Adherent	-
LIM2551	Human	Colon	Transverse Colon	-	-	Adenocarcinoma	Epithelial	Loose aggregates, some adherent, suspension	-
LS513	Human	Colon	Caecum	Male	63	Adenocarcinoma	Epithelial	Adherent	C
NCIH747	Human	Colon	Caecum	Male	69yrs	Adenocarcinoma	Epithelial	Adherent, floating aggregates	-
RKO	Human	Colon	Colon	-	-	Adenocarcinoma	Epithelial	Adherent	-
SNU175	Human	Colon	Peritoneum	Female	56	Adenocarcinoma	Epithelial	Adherent and suspension	-
SNUC2B	Human	Colon	Caecum	Female	43	Adenocarcinoma	Epithelial	Loose adherent	-
SW1116	Human	Colon	Colon	Male	73	Adenocarcinoma	Epithelial	Adherent	A
SW1222	Human	Colon	Colon	-	-	Adenocarcinoma	Epithelial	Adherent	C
SW480	Human	Colon	Colon	Male	50	Adenocarcinoma	Epithelial	Adherent	B
SW620	Human	Colon	Lymph Node	Male	51	Adenocarcinoma	Epithelial	Adherent	C
SW948	Human	Colon	Colon	Female	81	Adenocarcinoma	Epithelial	Adherent	C
T84	Human	Colon	Lung	Male	72	Adenocarcinoma	Epithelial	Adherent	-
V9P	Human	Colon	Colon	Male	67	Adenocarcinoma	Epithelial	-	-
VACO4S	Human	Colon	Rectum	Male	59	Adenocarcinoma	Epithelial	-	-
VACO5	Human	Colon	Caecum	Female	78	Adenocarcinoma	Epithelial	-	

Table 3.3 (page 2 of 2). Colorectal Cancer Cell lines: Clinicopathological features

3.2.4. Statistical analysis

Data obtained from GSE tissue sample cohorts, had been normalised by RNA concentration. Nonparametric data was analysed using the Mann-Whitney unpaired U-test or Kruskal-Wallis test and Dunn's test for comparison of multiple groups. Parametric data assessing multiple groups underwent One-way ANOVA testing with Tukey's test of multiple groups. Statistical analysis was performed using the statistical software Prism 8.2.0 (GraphPad Software, San Diego, Ca Software, La Jolla, CA).

Survival analysis was performed using Kaplan-Meir survival analysis. Colonomics (Colonomics.org) provides a Kaplan-Meir data tool to plot survival assessment of desired genes of interest, from the cohort data GSE44076. The gene of interest is split into three groups of low, medium and high expression. The patient cohorts are compared by Kaplan-Meir survival plots with the log rank p-value together with hazard ratio (HR) with 95% confidence interval calculated. Overall survival (OS) and disease-free survival (DFS) were assessed.

The threshold for statistical significance was a p value of <0.05 for all statistical assessments and the null hypothesis is rejected below this. See Table 3.4 for diagrammatic illustration and representation of p-values (Zhu, 2016).

Table 3.4. P-value legend denoting level of statistical significance shown within figures.

	P Value
*	<0.05
**	<0.01
***	<0.001
****	<0.0001

3.3. Results

3.3.1. CD44

3.3.1.1. CD44 expression is significantly increased in colorectal cancer

The expression of CD44 is significantly increased in tumour tissue compared to paired background colorectal tissue (adjusted p=<0.0001) and normal colorectal tissue (adjusted p=<0.0001). Expression in adjacent paired tissue was also seen to be significantly increased when compared to normal tissue (adjusted p=0.042). Data are shown in Figure 3.2.

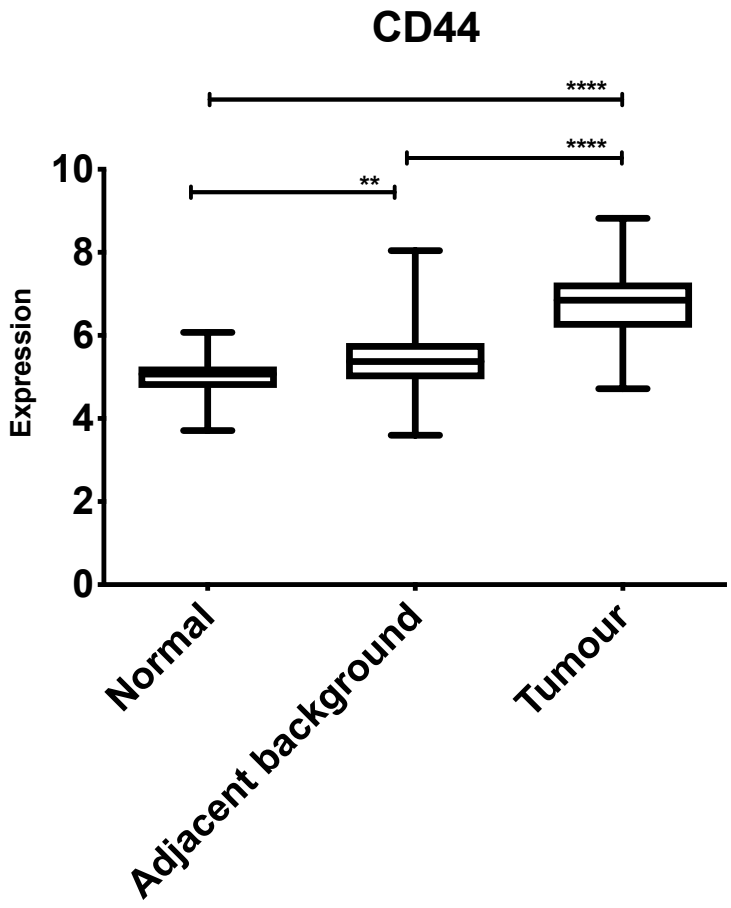

Figure 3.2. CD44 expression in colorectal cancer, paired adjacent tissue and normal tissue. In this figure and all subsequent figures in this chapter * indicates p<0.05, ** indicates p<0.01, * indicates p<0.001 and **** indicates p<0.0001. Data extracted are from GSE44076. Tumour tissue expression of CD44 is significantly upregulated when compared to both normal and adjacent background tissue (p=<0.0001 and p=<0.0001 respectively. CD44 expression is also found to be upregulated in adjacent background tissue when compared to normal colonic tissue (p=0.0042).**

3.3.1.2. CD44 expression is not related to overall colorectal cancer staging

The expression of CD44 in relation to cancer stage is shown in Figure 3.3. Expression of CD44 was not related to cancer stage (p=0.2519).

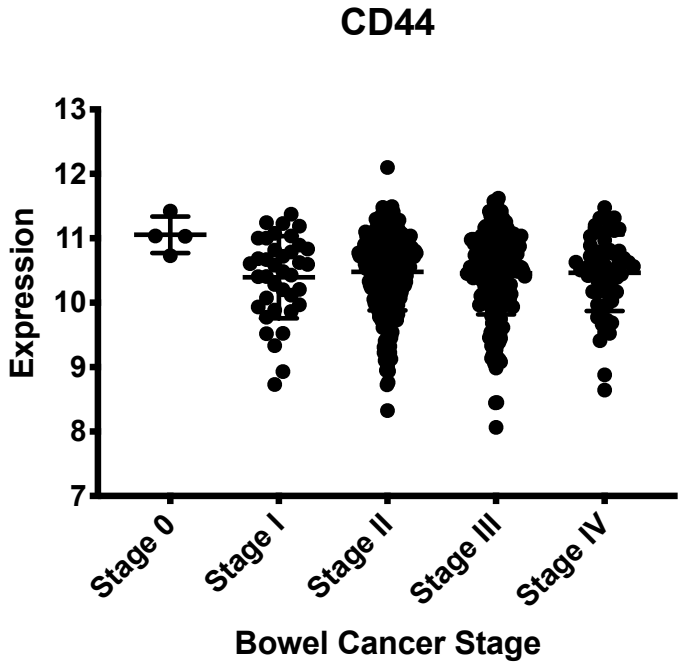

	Adjusted P Value
Stage 0 vs. Stage I	0.2196
Stage 0 vs. Stage II	0.3157
Stage 0 vs. Stage III	0.2827
Stage 0 vs. Stage IV	0.2984
Stage I vs. Stage II	>0.9999
Stage I vs. Stage III	>0.9999
Stage I vs. Stage IV	>0.9999
Stage II vs. Stage III	>0.9999
Stage II vs. Stage IV	>0.9999
Stage III vs. Stage IV	>0.9999

Figure 3.3. CD44 expression against overall cancer stage. Kruskal-Wallis test and Dunn's multiple comparisons test. Data extracted from GSE 40967.

3.3.1.3. CD44 expression and tumour TNM staging status

Comparing between T-stage groups there was seen to be no significant difference in CD44 expression (p=0.9934). CD44 expression in relation to T-stage is shown in Figure 3.4a. There was no significant difference between tumour nodal status and expression of CD44 (p= 0.8693) as shown in Figure 3.4b. There was no significant difference between tumour metastatic status and expression of CD44 (p= 0.9584) as shown in Figure 3.4c.

a.

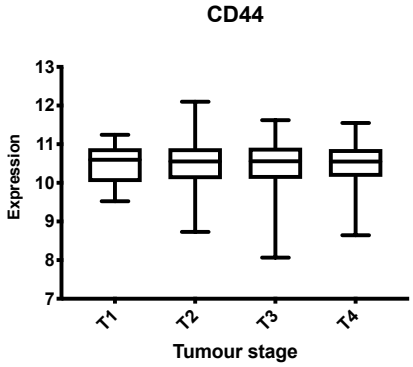

	Adjusted P-Value
T1 vs. T2	>0.9999
T1 vs. T3	>0.9999
T1 vs. T4	>0.9999
T2 vs. T3	>0.9999
T2 vs. T4	>0.9999
T3 vs. T4	>0.9999

b.

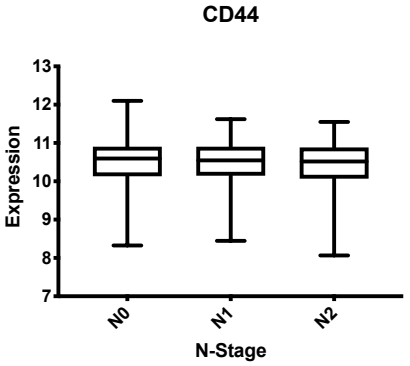

	Adjusted P-Value
N0 vs. N1	>0.9999
N0 vs. N2	>0.9999
N1 vs. N2	>0.9999

c.

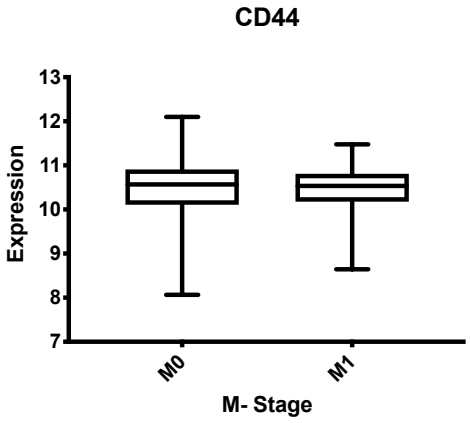

Figure 3.4. Expression of CD44 and tumour TNM status. Figure 3.4a Tumour T Stage and CD44 expression. Figure 3.4b Tumour Nodal Status and CD44 expression. Kruskal-Wallis Test and Dunn's test for multiple comparisons. Figure 3.4c Metastatic status and CD44 expression. Unpaired Mann-Whitney U-test. Data extracted from GSE 40967.

3.3.1.4. CD44 expression is not affected by gender

There was no significant difference between patient gender and expression of CD44 (p=0.3356). Results are shown in Figure 3.5.

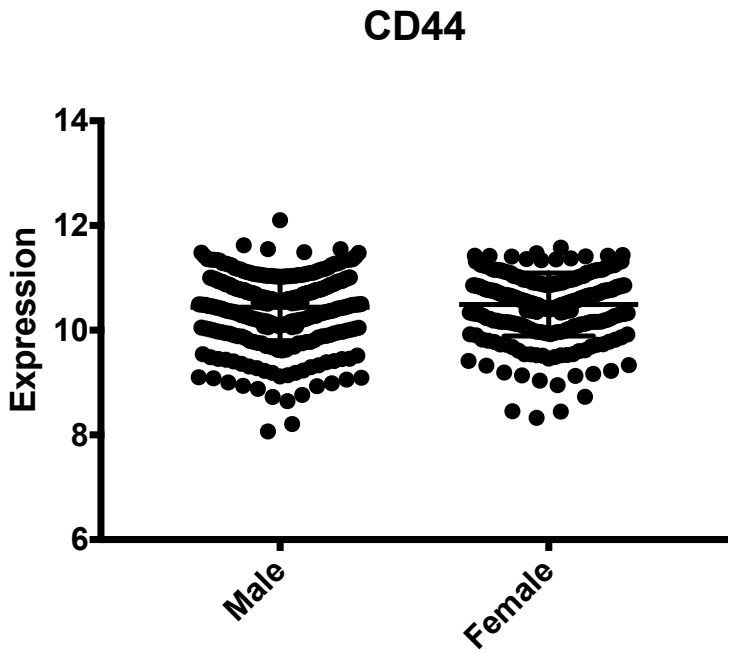

Figure 3.5. CD44 expression and sex. Unpaired T-test. Data extracted from GSE 40967.

3.3.1.5. CD44 expression and tumour location

There was seen to be no significant difference in CD44 expression between anatomical location in either normal tissue, paired adjacent tissue or tumour tissue. However, the same patterns of increased expression of CD44 as in section 3.3.1.1. were seen on the ipsilateral side between normal tissue against tumour tissue, and adjacent tissue against tumour tissue. There was however no change seen between normal tissue against adjacent tissue. Results in Figure 3.6.

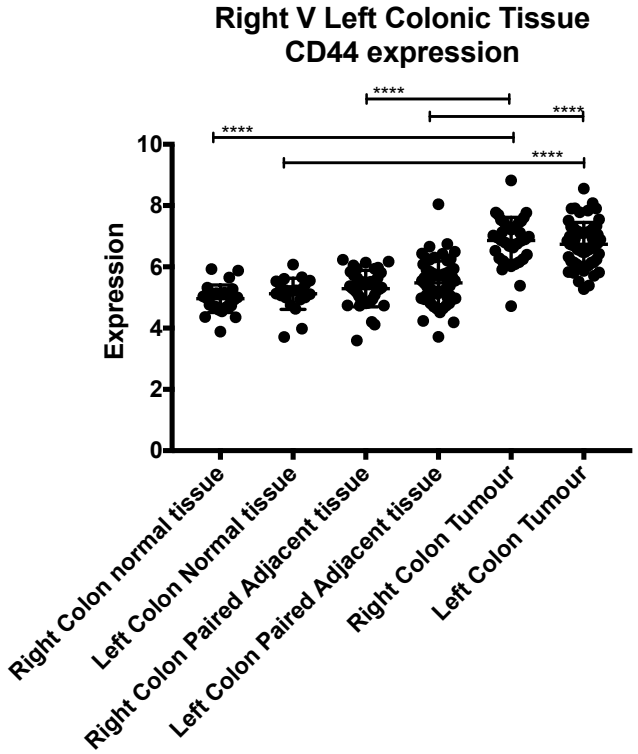

RHAMM Expression	Adjusted P-Value
Right Colon normal tissue vs. Left Colon Normal tissue	0.9994
Right Colon normal tissue vs. Right Colon Paired Adjacent	0.5321
Right Colon normal tissue vs. Left Colon Paired Adjacent	0.0130
Right Colon normal tissue vs. Right Colon Tumour	<0.0001
Right Colon normal tissue vs. Left Colon Tumour	<0.0001
Left Colon Normal tissue vs. Right Colon Paired Adjacent	0.9979
Left Colon Normal tissue vs. Left Colon Paired Adjacent	0.3577
Left Colon Normal tissue vs. Right Colon Tumour	<0.0001
Left Colon Normal tissue vs. Left Colon Tumour	<0.0001
Right Colon Paired Adjacent vs. Left Colon Paired Adjacent	0.9406
Right Colon Paired Adjacent vs. Right Colon Tumour	<0.0001
Right Colon Paired Adjacent vs. Left Colon Tumour	<0.0001
Left Colon Paired Adjacent vs. Right Colon Tumour	<0.0001
Left Colon Paired Adjacent vs. Left Colon Tumour	<0.0001
Right Colon Tumour vs. Left Colon Tumour	0.9991

Figure 3.6. CD44 expression and tumour location. One-way ANOVA. Data extracted is from GSE44076.

3.3.1.6. CD44 expression and patient survival

Cohort survival was assessed in terms of disease-free survival (DFS) and overall survival (OS). Follow up of cohorts were from stage II cancer patients for at least three years, taken from the Colonomics project and freely available raw data from the GEO database GSE44076. Expression was split into low, medium and high expression of CD44, assessing both adjacent colonic tissue and tumour tissue separately.

OS was seen to be reduced in highly expressed CD44 in adjacent colonic tissue when compared to tissue with low CD44 expression (Figure 3.7a). CD44 did not have low expression in tumour tissue. There was no difference demonstrated in tumour tissue between moderately expressed or highly expressed CD44 in relation to OS (Figure 3.7b).

For the matched adjacent colonic tissue, there was seen to be a significantly reduced DFS in high CD44 expression when compared to low expression CD44 tissue (Figure 3.7c). In tumour tissue CD44 was either moderately or highly expressed and there was not seen to be a significant difference in DFS between these groups (Figure 3.7d). Data are presented in Table 3.5 and Figure 3.7.

Table 3.5. Overall Survival and Disease-Free survival compared to level of CD44 expression in adjacent and tumour tissues. Data extracted from GSE 44076.

Overall Survival					
Tissue	CD44 Expression	N	HR	95% CI	P Value
Adjacent Mucosae					
	Low	43			
	Medium	53	2.07	0.40, 10.67	0.384
	High	2	17.85	1.61, Inf	0.019
Tumour					
	Medium	19			
	High	79	Inf	0.00, Inf	1
Disease Free	Survival				
Tissue	CD44 Expression	N	HR	95% CI	P Value
Adjacent Mucosae					
	Low	43			
	Medium	53	1.46	0.58, 3.67	0.42
	High	2	Inf	12.76, Inf	1.2e-5
Tumour					
	Medium	19			
	High	79	1.07	0.36, 3.16	0.9

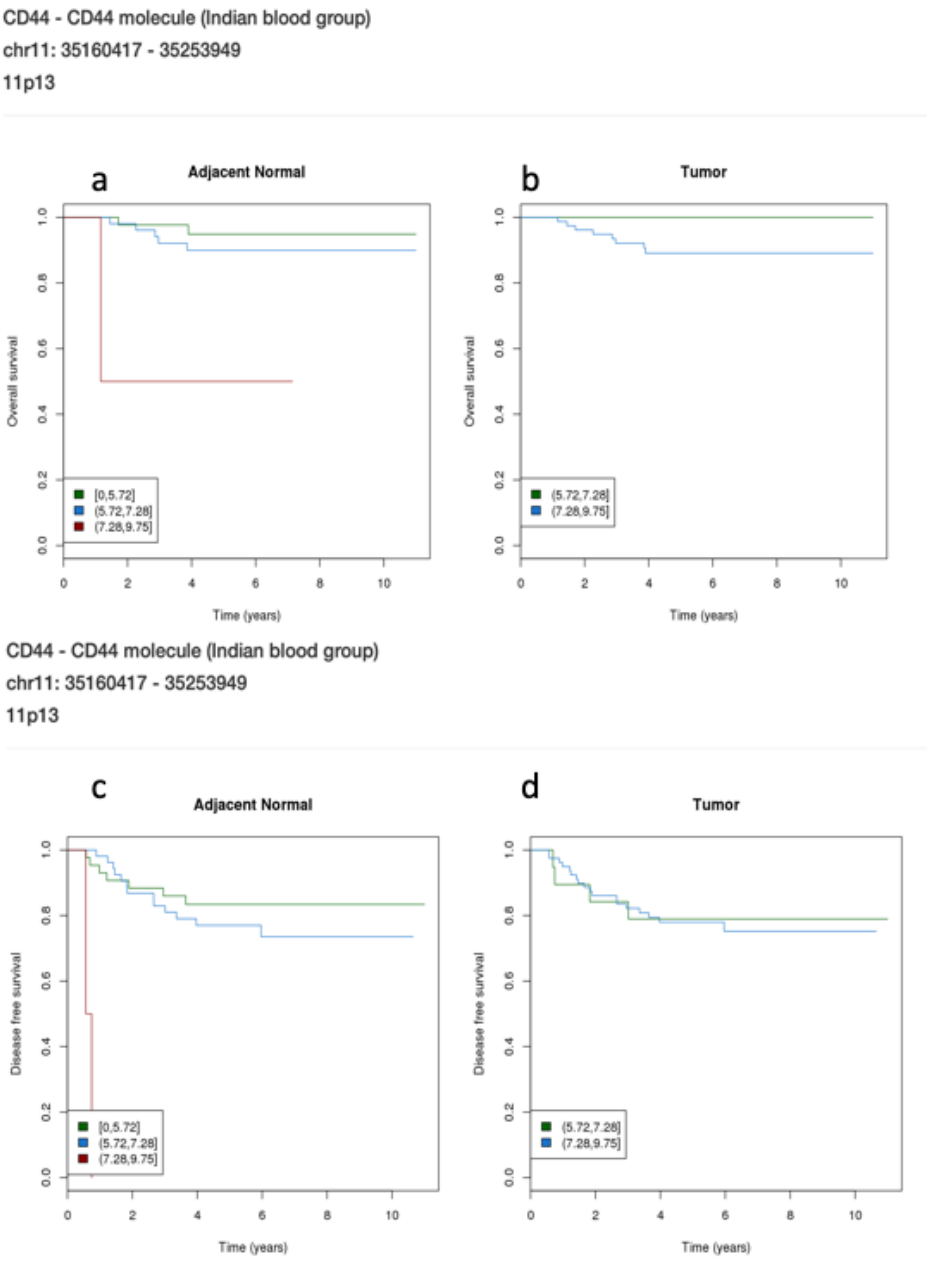

Figure 3.7. CD44 expression and survival: A cohort 98 matched adjacent normal background tissue and tumour tissue samples. Data were obtained from Colonomics website, a public access database of microarray expression data and survival outcomes. There was significant difference in overall survival (OS) and disease-free survival (DFS) related to CD44 expression for adjacent normal tissue. There was not a significant difference in OS or DFS related to CD44 expression in tumour tissue. Adjacent normal tissue: Low expression (0-5.72) n=43, Moderate expression (5.72-7.28) n=53, High expression (7.28-9.75) n=2. Tumour tissue: Low expression (0-5.72) n=0, Moderate expression (5.72-7.28) n=19, High expression (7.28-9.75) n=79.
a. Overall survival adjacent normal tissue and high CD44 expression correlates to lower overall survival (0-5.72 v 5.72-7.28, p=0.384 and 0-5.72 v 7.28-9.75, p=0.019). b. Overall survival tumour tissue and CD44 expression (0-5.72 v 7.28-9.75, p=1.00). c. Disease free survival adjacent normal tissue and CD44 expression (0-5.72 v 5.72-7.28, p=0.42 and 0-5.72 v 7.28-9.75, p=0.000012). d. Disease free survival tumour tissue and CD44 expression (0-5.72 v 7.28-9.75, p=0.90). Data extracted from GSE 44076.

3.3.1.7. CD44 expression and oncogene status

There was no significant difference in CD44 expression in either wild type (WT) or Mutated (M) BRAF or TP53 ($p=0.9706$ and $p=0.1829$). There was however a significant increase in expression of CD44 in mutated KRAS when compared to wild type ($p= <0.0001$). Results are shown in Figure 3.8.

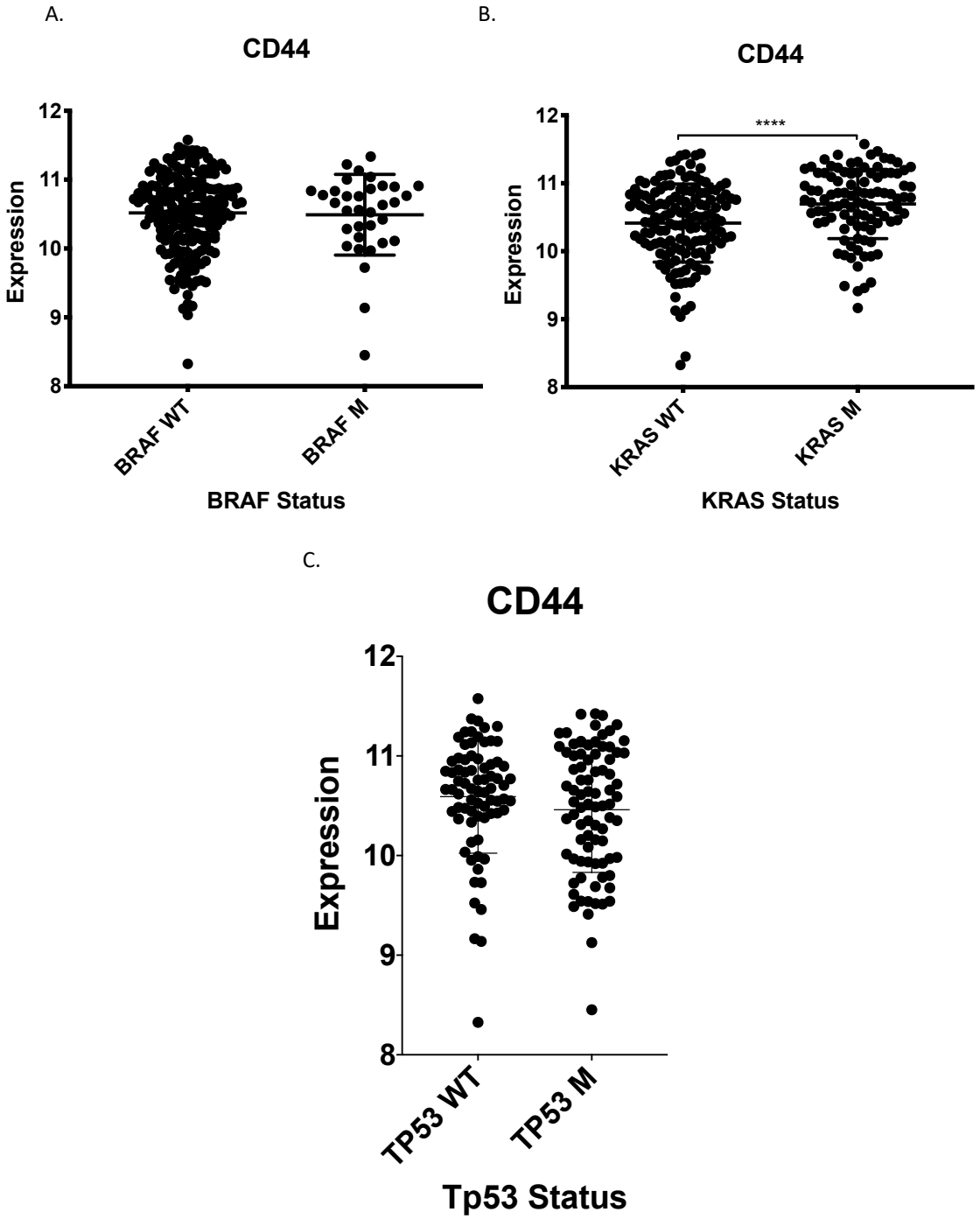

Figure 3.8. CD44 expression and oncogene status. A. Unpaired Mann-Whitney U-test of CD44 expression compared between BRAF Wild Type (WT) and BRAF mutated (M) (p=0.9706). B. Unpaired Mann-Whitney U-test of CD44 expression compared between KRAS WT and BRAF M (p=<0.0001). C. Unpaired Mann-Whitney U-test of CD44 expression compared between TP53 WT and TP53 M (p= 0.1829). Data extracted from GSE 40967.

3.3.2. RHAMM

3.3.2.1. RHAMM expression is significantly increased in colorectal cancer

The expression of RHAMM is significantly increased in tumour tissue compared to paired background colorectal tissue (Adjusted p=<0.0001) and normal colorectal tissue (Adjusted p=0.0004). However, RHAMM expression in adjacent paired tissue was seen to be significantly decreased when compared to normal tissue (Adjusted p=<0.0001). The data is shown in Figure 3.9.

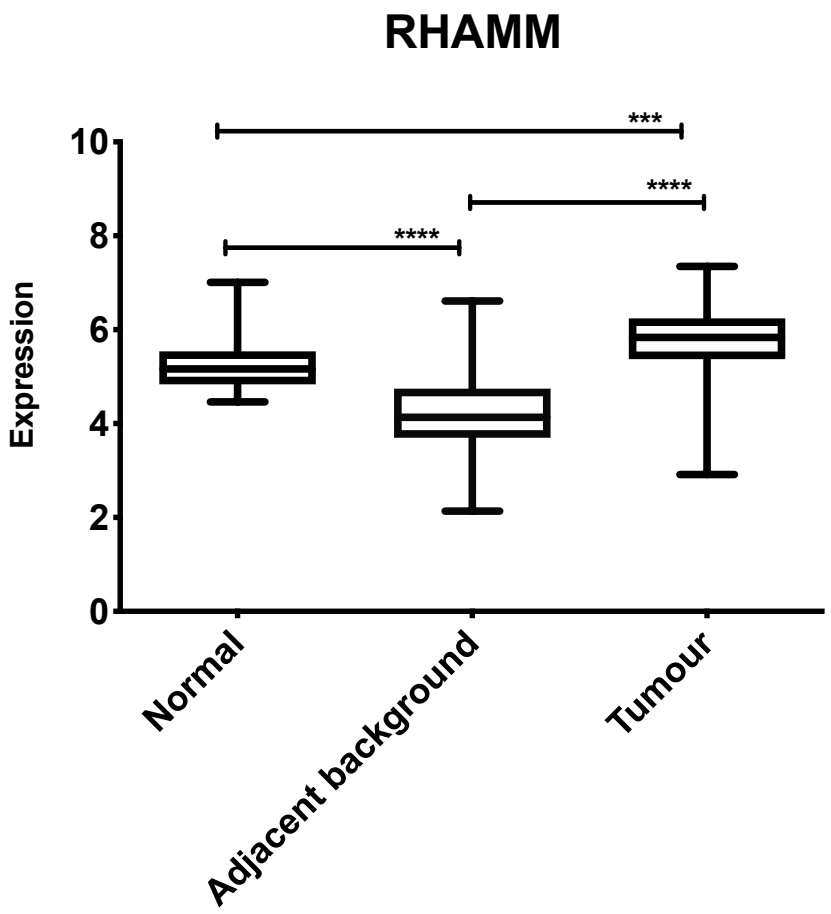

Figure 3.9. RHAMM expression in colorectal cancer, paired adjacent tissue and normal tissue. One-way ANOVA. Data extracted is obtained from the GSE44076 dataset. RHAMM expression in adjacent background tissue was downregulated when compared to normal tissue (p= <0.0001). Tumour tissue however, showed significantly upregulated RHAMM expression when compared to both normal and adjacent background tissue (p=0.0004 and p=<0.0001 respectively).

3.3.2.2. RHAMM expression is not related to overall colorectal cancer staging

The expression of RHAMM in relation to cancer stage is shown in Figure 3.10. Expression of RHAMM was not demonstrated to be related to cancer stage (p=0.9454).

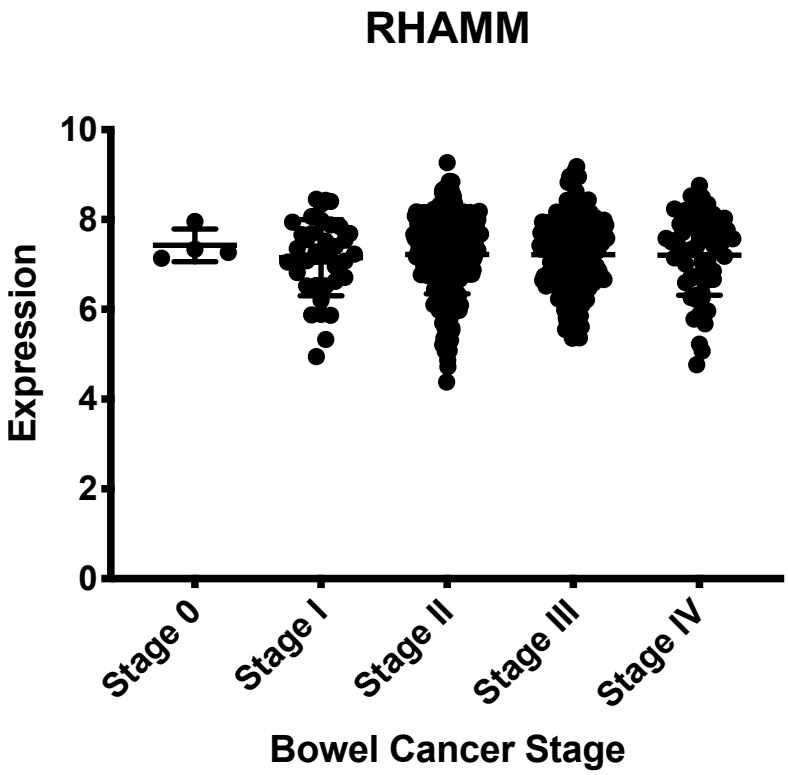

	Adjusted P Value
Stage 0 vs. Stage I	>0.9999
Stage 0 vs. Stage II	>0.9999
Stage 0 vs. Stage III	>0.9999
Stage 0 vs. Stage IV	>0.9999
Stage I vs. Stage II	>0.9999
Stage I vs. Stage III	>0.9999
Stage I vs. Stage IV	>0.9999
Stage II vs. Stage III	>0.9999
Stage II vs. Stage IV	>0.9999
Stage III vs. Stage IV	>0.9999

Figure 3.10. RHAMM expression against overall cancer stage. Kruskal-Wallis test and Dunn's multiple comparisons test. Data extracted from GSE 40967.

3.3.2.3. RHAMM expression and tumour TNM staging status

Comparing between T-stage groups there was seen to be no significant difference in RHAMM expression (p=0.4178). RHAMM expression in relation to T-stage is shown in Figure 3.11a. There was no significant difference between tumour nodal status and expression of RHAMM (p= 0.1063). Results in Figure 3.11b. There was no significant difference between tumour nodal status and expression of RHAMM (p= 0.6301). Results are shown in Figure 3.11c.

A.

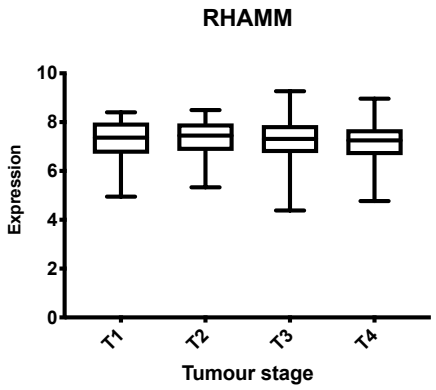

	Adjusted P-Value
T1 vs. T2	>0.9999
T1 vs. T3	>0.9999
T1 vs. T4	>0.9999
T2 vs. T3	>0.9999
T2 vs. T4	0.8345
T3 vs. T4	>0.9999

B.

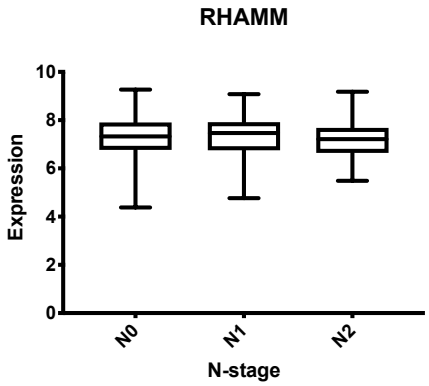

	Adjusted P-Value
N0 vs. N1	>0.9999
N0 vs. N2	0.2863
N1 vs. N2	0.1121

C.

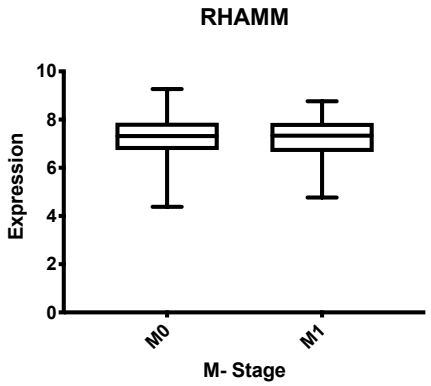

Figure 3.11. Expression of RHAMM and tumour TNM status. Figure 3.11a Tumour T Stage and RHAMM expression. Figure 3.11b Tumour Nodal Status and RHAMM expression. Kruskal-Wallis Test and Dunn's test for multiple comparisons. Figure 3.11c Metastatic status and RHAMM expression. Unpaired Mann-Whitney U-test. Data extracted from GSE 40967.

3.3.2.4. RHAMM expression is not affected by gender

There was no significant difference between patient gender and expression of RHAMM (p=0.9876). Results are shown in Figure 3.12.

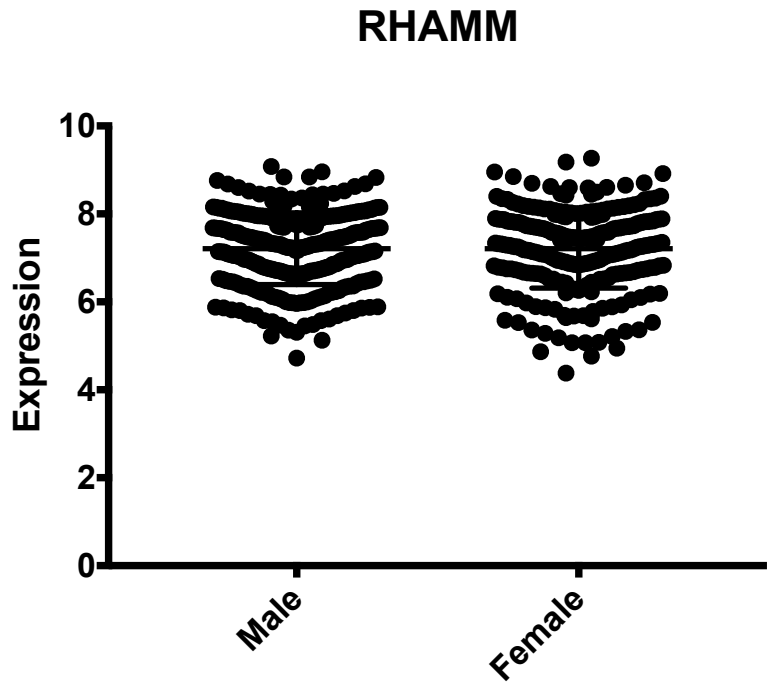

Figure 3.12. RHAMM expression and Sex. Unpaired T-test. Data extracted from GSE 40967.

3.3.2.5. RHAMM expression and tumour location

There was seen to be no significant difference in RHAMM expression between anatomical location for either normal tissue, paired adjacent tissue or tumour tissue. The same patterns of increased expression of RHAMM were demonstrated when biopsied from the ipsilateral anatomical side when comparing normal tissue. Results are shown in Figure 3.13.

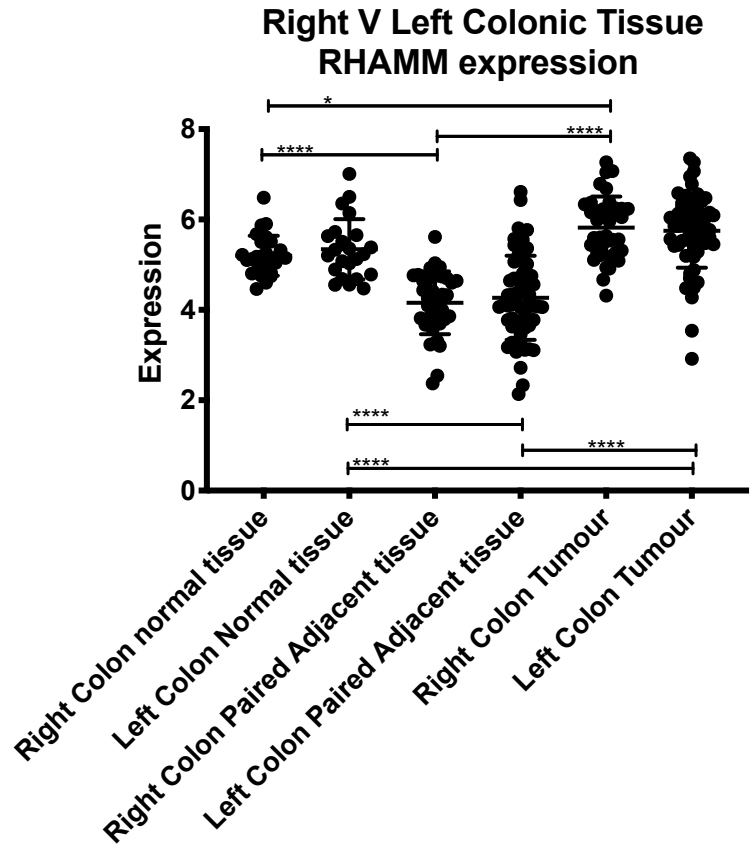

RHAMM Expression	Adjusted P-Value
Right Colon normal tissue vs. Left Colon Normal tissue	0.9856
Right Colon normal tissue vs. Right Colon Paired Adjacent	<0.0001
Right Colon normal tissue vs. Left Colon Paired Adjacent	<0.0001
Right Colon normal tissue vs. Right Colon Tumour	0.0179
Right Colon normal tissue vs. Left Colon Tumour	0.0258
Left Colon Normal tissue vs. Right Colon Paired Adjacent	<0.0001
Left Colon Normal tissue vs. Left Colon Paired Adjacent	<0.0001
Left Colon Normal tissue vs. Right Colon Tumour	0.1762
Left Colon Normal tissue vs. Left Colon Tumour	0.2588
Right Colon Paired Adjacent vs. Left Colon Paired Adjacent	0.9813
Right Colon Paired Adjacent vs. Right Colon Tumour	<0.0001
Right Colon Paired Adjacent vs. Left Colon Tumour	<0.0001
Left Colon Paired Adjacent vs. Right Colon Tumour	<0.0001
Left Colon Paired Adjacent vs. Left Colon Tumour	<0.0001
Right Colon Tumour vs. Left Colon Tumour	0.9978

Figure 3.13. RHAMM expression and tumour location. One-way ANOVA. Data extracted are from GSE44076.

3.3.2.6. RHAMM expression and survival

Cohort survival was assessed as described in 2.16 and 3.3.1.6.

There was no significant difference in survival demonstrated in either OS or DFS for either matched adjacent tissue or tumour tissue compared to RHAMM expression (Figure 3.14a to 3.14d). Data are presented in Table 3.6 and Figure 3.14.

Table 3.6 Overall Survival and Disease-Free survival compared to level of RHAMM expression in adjacent and tumour tissues. Data extracted from GSE 444076.

Overall Survival					
Tissue	RHAMM Expression	N	HR	95% CI	P Value
Adjacent Mucosae					
	Low	67			
	Medium	26	1.97	0.44, 8.81	0.37
	High	5	3.30	0.37, 29.56	0.29
Tumour					
	Low	8			
	Medium	28	0.51	0.05, 5.63	0.58
	High	62	0.57	0.07, 4.86	0.61
Disease Free	Survival				
Tissue	RHAMM	N	HR	95% CI	P Value
Adjacent Mucosae					
	Low	67			
	Medium	26	1.30	0.53, 3.23	0.42
	High	5	0.86	0.11, 6.55	1.2e-5
Tumour					
	Low	8			
	Medium	28	1.17	0.25, 2.78	0.84
	High	62	0.61	0.14, 2.78	0.53

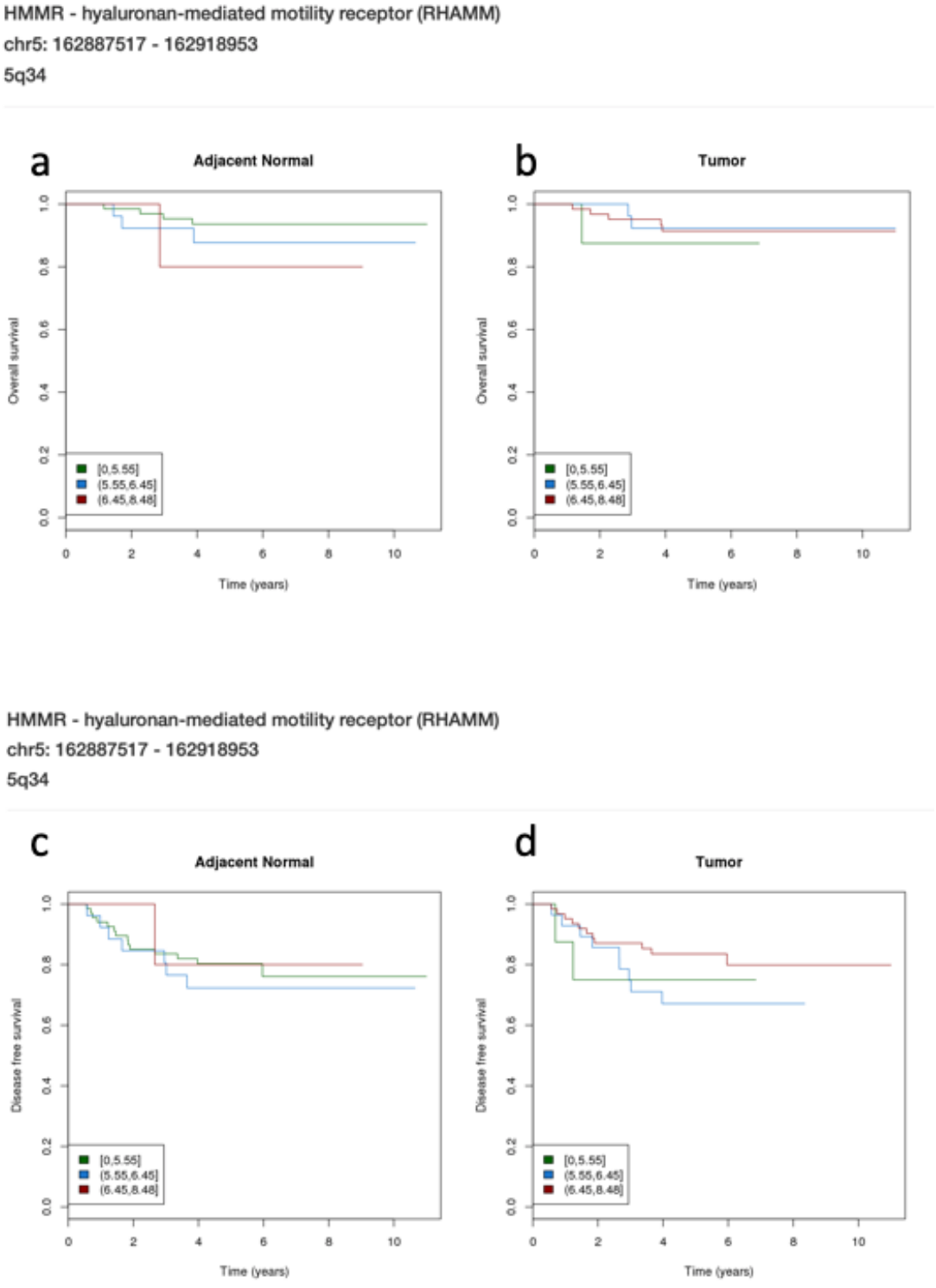

Figure 3.14 RHAMM expression and survival: A cohort of 98 matched adjacent normal background tissue and tumour tissue samples. There was no significant difference demonstrated in RHAMM expression and survival. a. Overall survival adjacent normal tissue and RHAMM expression (p=0.37). b Overall survival tumour tissue and RHAMM expression (p=0.29). c. Disease free survival adjacent normal tissue and RHAMM expression (p=0.58). d. Disease free survival tumour tissue and RHAMM expression (p=0.61). Data were obtained from Colonomics website, a public access database of microarray expression data and survival outcomes. Data extracted from GSE 44076.

3.3.2.7. RHAMM expression and oncogene status

There was no significant difference in RHAMM expression between wild type (WT) or mutated (M) BRAF and KRAS (p=0.1176 and p=0.6657). There was however a significant increase in expression of RHAMM in mutated TP53 when compared to wild type (p= 0.0092). Results are shown in Figure 3.15.

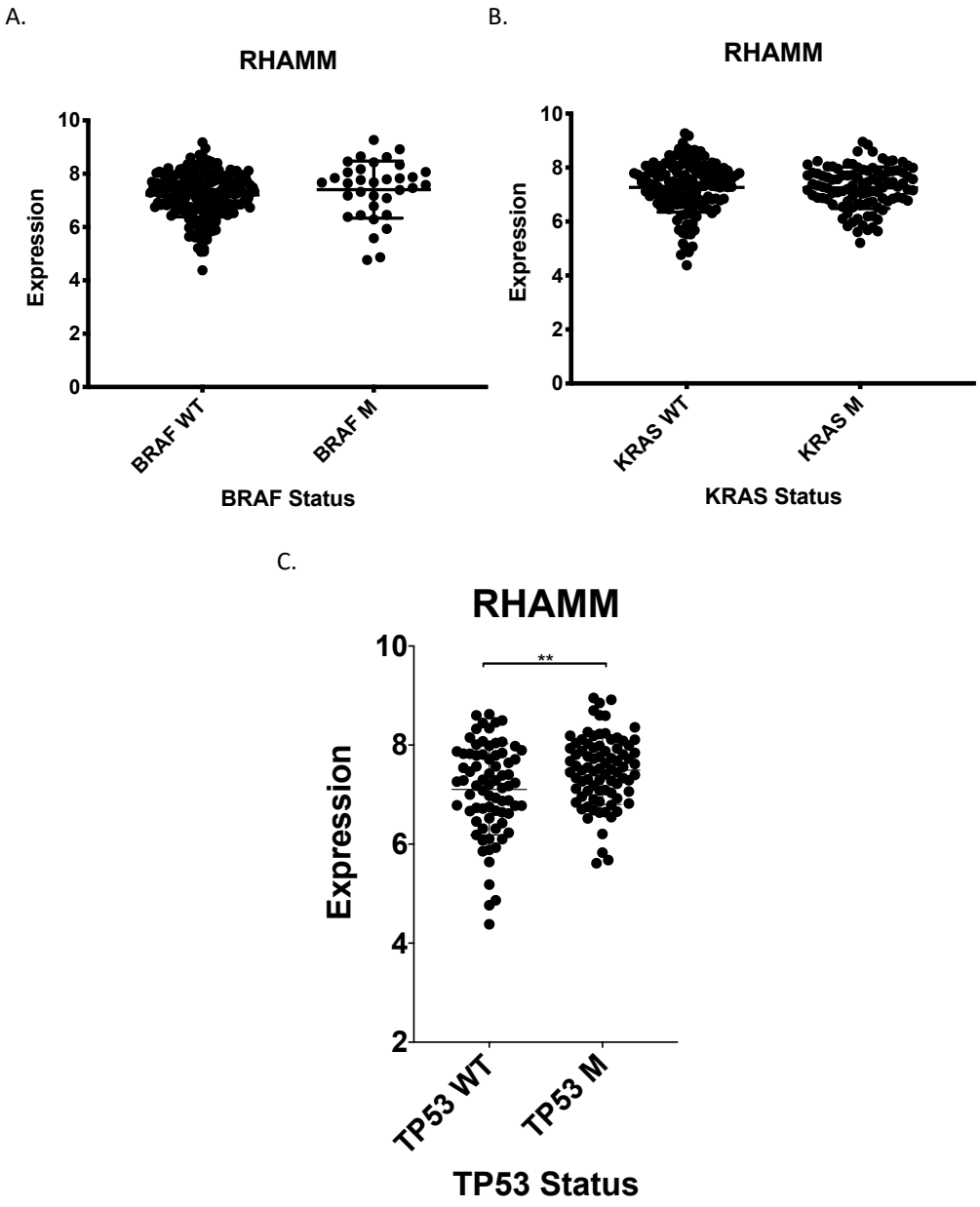

Figure 3.15. RHAMM expression and oncogene status. A. Unpaired Mann-Whitney U-test of RHAMM expression compared between BRAF Wild Type (WT) and BRAF mutated (M) (p=0.2124). B. Unpaired Mann-Whitney U-test of RHAMM expression compared between KRAS WT and BRAF M (p=0.8855). C. Unpaired Mann-Whitney U-test of RHAMM expression compared between TP53 WT and TP53 M (p= 0.0092). Data extracted from GSE 40967.

3.3.3. ICAM-1

3.3.3.1. ICAM-1 expression is significantly increased in colorectal cancer

The expression of ICAM-1 is significantly increased in tumour tissue compared to paired background colorectal tissue (adjusted p=<0.0001) and normal colorectal tissue (adjusted p=<0.0001). Adjacent paired tissue was also seen to be significantly increased when compared to normal tissue (adjusted p=<0.0001). Data are shown in Figure 3.16.

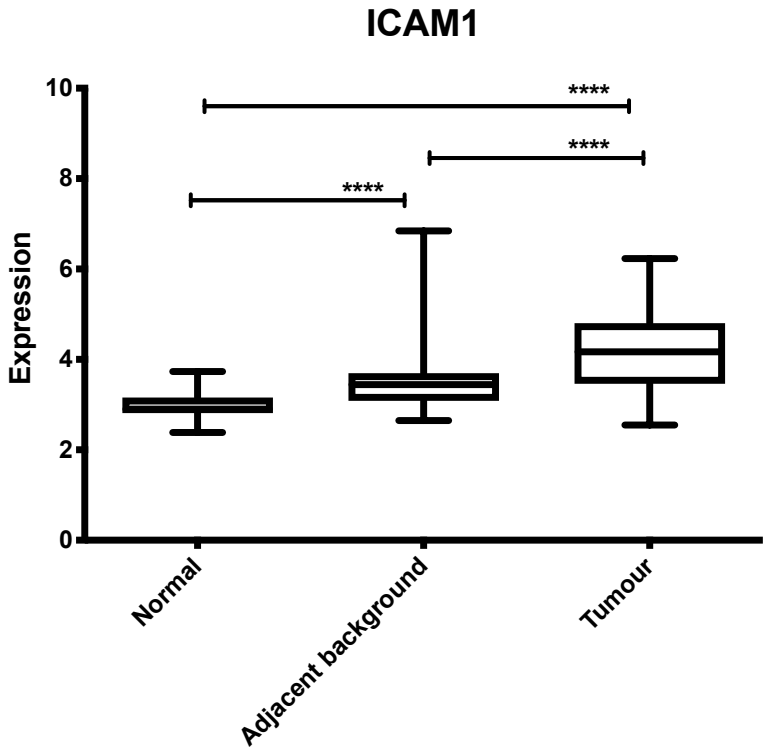

Figure 3.16. ICAM-1 expression in colorectal cancer, paired adjacent tissue and normal tissue. One-way ANOVA. Data extracted are from GSE44076. Tumour tissue expression of ICAM-1 was found to have significantly higher expression when compared to adjacent background and normal colonic tissue (p=<0.0001 and p=<0.0001 respectively). Adjacent background tissue also had higher expression than that of normal colonic tissue (p=<0.0001).

3.3.3.2. ICAM-1 expression is not related to overall colorectal cancer staging

The expression of ICAM-1 was not related to cancer stage (p=0.8437). Results are shown in Figure 3.17.

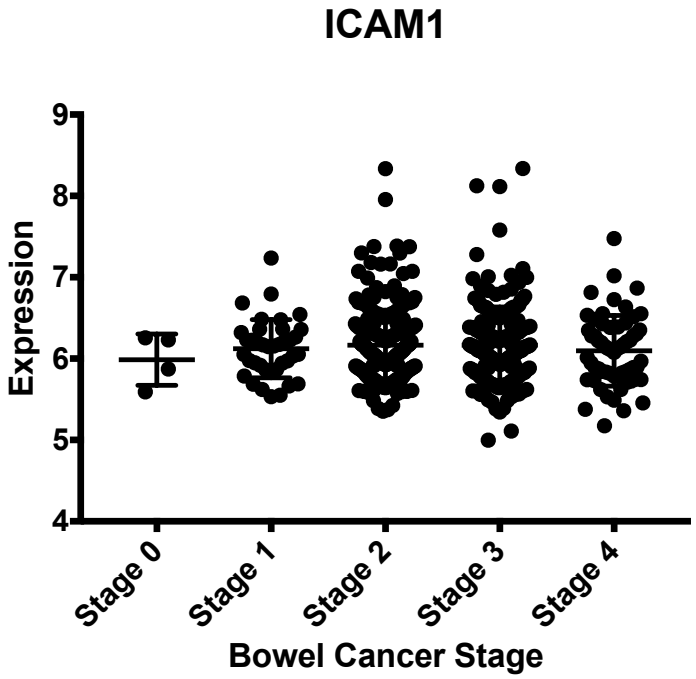

	Adjusted P Value
Stage 0 vs. Stage I	>0.9999
Stage 0 vs. Stage II	>0.9999
Stage 0 vs. Stage III	>0.9999
Stage 0 vs. Stage IV	>0.9999
Stage I vs. Stage II	>0.9999
Stage I vs. Stage III	>0.9999
Stage I vs. Stage IV	>0.9999
Stage II vs. Stage III	>0.9999
Stage II vs. Stage IV	>0.9999
Stage III vs. Stage IV	>0.9999

Figure 3.17 ICAM-1 expression against cancer stage. Kruskal-Wallis test and Dunn's multiple comparisons test. Data extracted from GSE 40967.

3.3.3.3. ICAM-1 expression and tumour TNM staging status

When comparing between T-stage groups, there was seen to be a significant difference in ICAM-1 expression (p= 0. 0.0117). Dunn's test of multiple comparisons demonstrated a significant increase in expression of ICAM-1 between T2 V T3 (p= 0.0289) and T3 V T4 (p= 0.0404) tumours. ICAM-1 expression in relation to T-stage is shown in Figure 3.18a. There was no significant difference between tumour nodal status and expression of ICAM-1 (p= 0.4596). Results are shown in Figure 3.18b. There was no significant difference between whether metastases were present or not, in relation to expression of ICAM-1 (p= 0.3522). Results are shown in Figure 3.18c.

a.

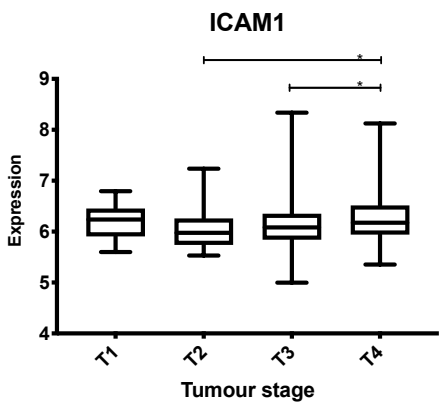

	Adjusted P-Value
T1 vs. T2	0.8844
T1 vs. T3	>0.9999
T1 vs. T4	>0.9999
T2 vs. T3	>0.9999
T2 vs. T4	0.0289 *
T3 vs. T4	0.0404 *

b.

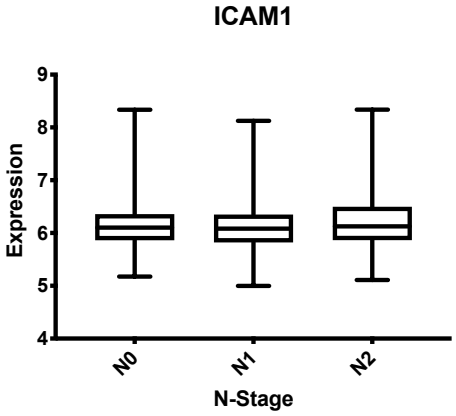

	Adjusted P-Value
N0 vs. N1	>0.9999
N0 vs. N2	>0.9999
N1 vs. N2	0.6476

c.

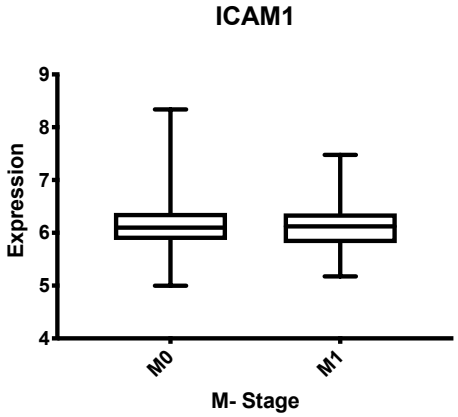

Figure 3.18 Expression of ICAM-1 and tumour TNM status. A. Tumour T Stage and CD44 expression. B Tumour Nodal Status and CD44 expression. Kruskal-Wallis Test and Dunn's test for multiple comparisons. C. Metastatic status and CD44 expression. Unpaired Mann-Whitney U-test. Data extracted from GSE 40967.

3.3.3.4. ICAM-1 expression and gender

There was no significant difference between patient gender and expression of ICAM-1 (p=0.8342). Results are shown in figure 3.19.

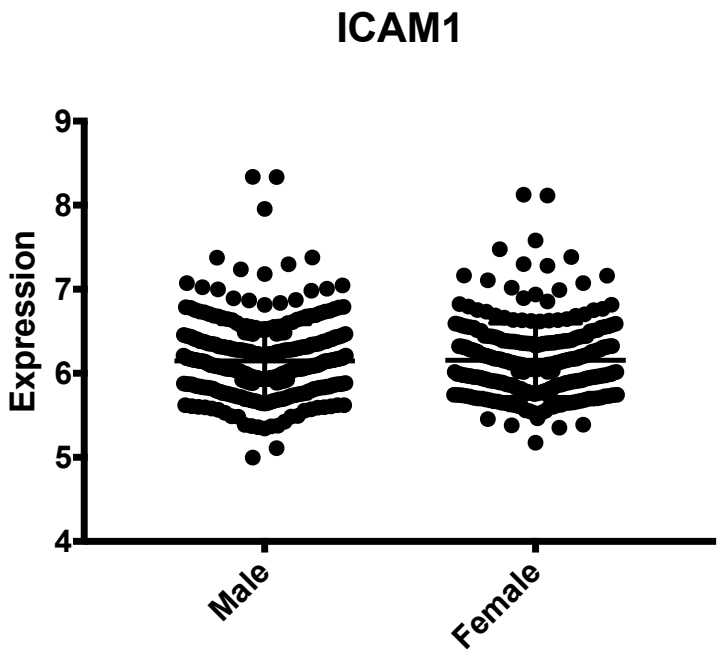

Figure 3.19. ICAM expression and gender. Unpaired T-Test. Data extracted from GSE 40967.

3.3.3.5. ICAM-1 expression and tumour location

There was seen to be no significant difference in ICAM-1 expression between anatomical location for either normal tissue, paired adjacent tissue or tumour tissue. The same patterns of increased expression of ICAM-1 were demonstrated when biopsied from the ipsilateral anatomical side when compared to normal tissue (Figure 3.20).

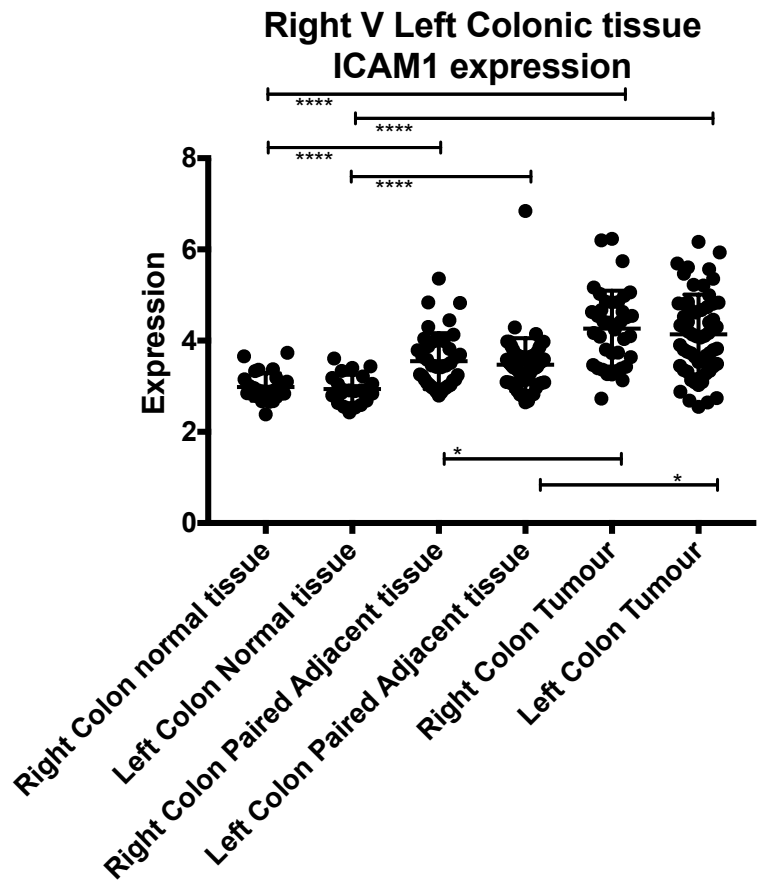

ICAM-1 Expression	Adjusted P-Value
Right Colon normal tissue vs. Left Colon Normal tissue	>0.9999
Right Colon normal tissue vs. Right Colon Paired Adjacent	0.0145
Right Colon normal tissue vs. Left Colon Paired Adjacent	0.0289
Right Colon normal tissue vs. Right Colon Tumour	<0.0001
Right Colon normal tissue vs. Left Colon Tumour	<0.0001
Left Colon Normal tissue vs. Right Colon Paired Adjacent	0.0109
Left Colon Normal tissue vs. Left Colon Paired Adjacent	0.0218
Left Colon Normal tissue vs. Right Colon Tumour	<0.0001
Left Colon Normal tissue vs. Left Colon Tumour	<0.0001
Right Colon Paired Adjacent vs. Left Colon Paired Adjacent	>0.9999
Right Colon Paired Adjacent vs. Right Colon Tumour	<0.0001
Right Colon Paired Adjacent vs. Left Colon Tumour	0.0006
Left Colon Paired Adjacent vs. Right Colon Tumour	<0.0001
Left Colon Paired Adjacent vs. Left Colon Tumour	<0.0001
Right Colon Tumour vs. Left Colon Tumour	0.9990

Figure 3.20. Anatomical location and ICAM-1 expression. One-way ANOVA. Data extracted are from GSE44076.

3.3.3.6. ICAM -1 expression and patient survival

OS was seen to be reduced in samples expressing high levels of ICAM-1 in matched adjacent colonic tissue (p=0.03) and for tumour tissue (p=0.059) when compared to low ICAM-1 expression (Figure 3.27a and 3.27b).

For the matched adjacent colonic tissue there was seen to be a significantly reduced DFS in high ICAM-1 expression, when compared to low expression ICAM-1 (Figure 3.27c). In tumour tissue ICAM-1 there was significant difference seen in DFS between the expression groups (Figure 3.27d). Data are presented in Table 3.7 and Figure 3.21.

Table 3.7. Overall Survival and Disease-Free survival compared to level of ICAM-1 expression in adjacent and tumour tissues. Data extracted from GSE 44076.

Overall Survival					
Tissue	ICAM-1 Expression	N	HR	95% CI	P Value
Adjacent Mucosae					
	Low	31			
	Medium	50	1.21	0.11, 13.30	0.88
	High	17	10.80	1.26, 92.48	0.03
Tumour					
	Low	7			
	Medium	27	0.23	0.03, 1.64	0.143
	High	64	0.19	0.04, 10.06	0.059
Disease Free	Survival				
Tissue	ICAM-1 Expression	N	HR	95% CI	P Value
Adjacent Mucosae					
	Low	31			
	Medium	50	0.57	0.20, 1.63	0.295
	High	17	2.36	0.85, 6.51	0.098
Tumour					
	Low	7			
	Medium	27	0.49	0.12, 1.97	0.32
	High	64	0.44	0.12, 1.53	0.20

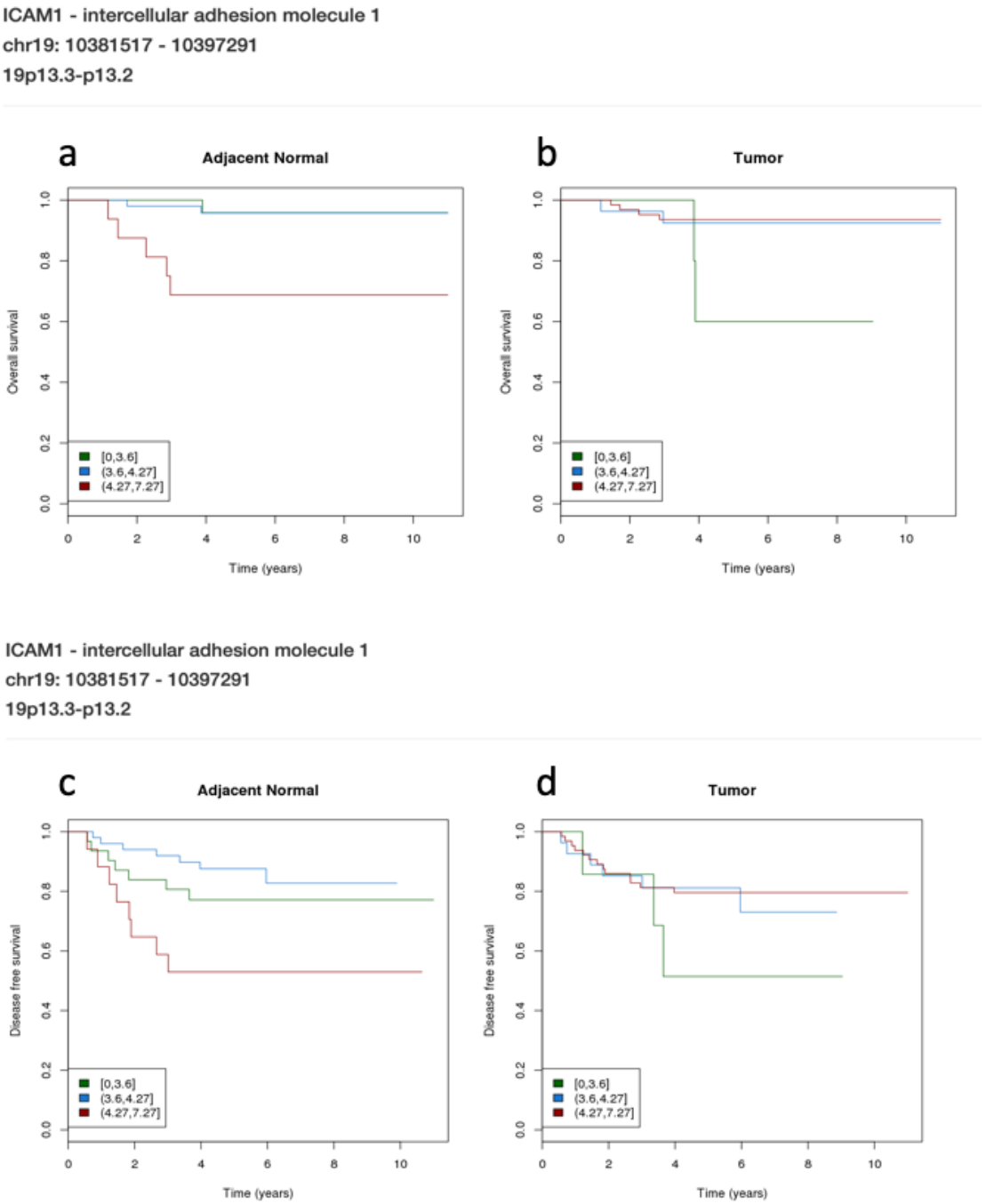

Figure 3.21 ICAM-1 expression and survival: Adjacent normal tissue: Low expression (0-3.6) n=31, Moderate expression (3.6-4.27) n=50, High expression (4.27-7.27) n=17. Tumour tissue: Low expression (0-3.6) n=7, Moderate expression (3.6-4.27) n=27, High expression (4.27-7.27) n=64. a. Overall survival adjacent normal tissue and high ICAM-1 expression correlates to lower overall survival (0-3.6 v 3.6-4.27, p=0.295 and 0-3.6 v 4.27-7.27, p=0.098). b. Overall survival tumour tissue and ICAM-1 expression (0-3.6 v 3.6-4.27 p=0.32 and 0-3.6 v 4.27-7.27, p=0.20). c. Disease free survival adjacent normal tissue and ICAM-1 expression (0-3.6 v 3.6-4.27 p=0.88 and 0-3.6 v 4.27-7.27 p=0.03). d. Disease free survival tumour tissue and ICAM-1 expression (0-3.6 v 3.6-4.27 p=0.143 and 0-3.6 v 4.27-7.27 p=0.059). Data extracted from GSE 44076.

3.3.3.7. ICAM-1 expression oncogene status

There was a significant increase in expression of ICAM-1 in mutated compared to WT BRAF ($p=0.0017$). KRAS or TP53 status demonstrated no significant expression of ICAM-1 ($p=0.3293$ and $p=0.6170$ respectively). This is illustrated in Figure 3.22.

A.

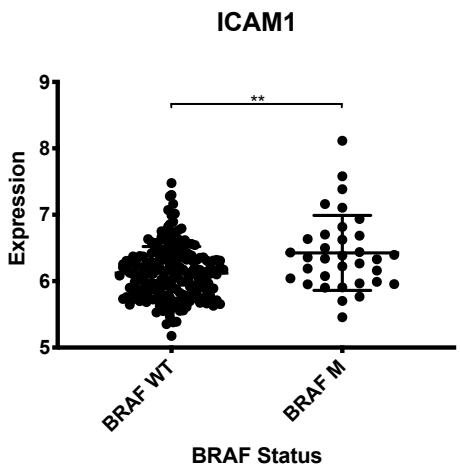

B.

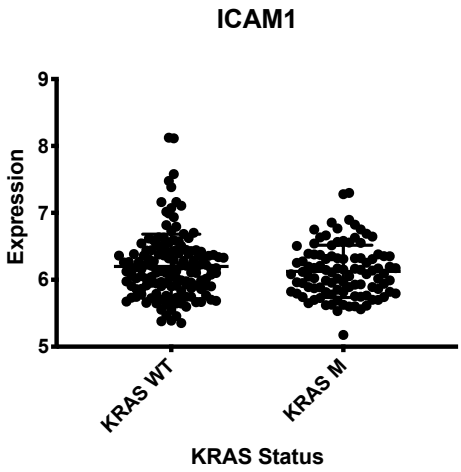

C.

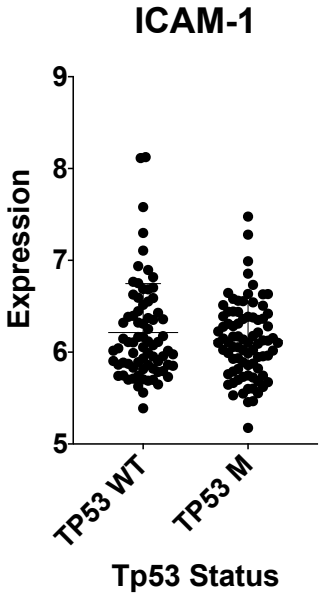

Figure 3.22 ICAM-1 expression and oncogene status. A. Unpaired Mann-Whitney U-test of ICAM-1 expression compared between BRAF Wild Type (WT) and BRAF mutated (M) (p=0.0017). B. Unpaired Mann-Whitney U-test of ICAM-1 expression compared between KRAS WT and KRAS M (p=0.3293). C. Unpaired Mann-Whitney U-test of ICAM-1 expression compared between TP53 WT and TP53 M (p= 0.6170). Data extracted from GSE 40967.

3.3.4. HA-independent adhesion molecules

3.3.4.1. HA-independent adhesion molecule expression is either significantly decreased or there is no difference in expression in colon cancer

Expression of MUC16, L1CAM, CEACAM1, EpCAM, MDR1 and MUC1 was significantly decreased in tumour tissue when compared to normal tissue. There was no significant difference in expression of VCAM1 and CDH1 between normal and tumour tissue.

Expression of VCAM1, L1CAM, CEACAM1, EpCAM, MDR1 and MUC1 was significantly decreased in tumour tissue when compared to paired adjacent tissue. There was no significant difference of expression between paired adjacent tissue and tumour tissue in MUC16 and CDH1.

There was significantly decreased expression of MUC16 in paired adjacent tissue when compared to normal tissue. There was however no significant difference in expression in the remaining studied HA-independent adhesion molecules. Data are shown in Table 3.8 and Figure 3.23.

Table 3.8. HA-independent adhesion molecule expression in colorectal cancer, paired adjacent tissue and normal tissue. Data extracted is from GSE44076.

Adhesion Molecule	Tissue	Expression	Adjusted P Value
VCAM1	Normal v Paired adjacent	-	0.0650
	Normal v Tumour	-	0.6413
	Paired Adjacent v Tumour	Decreased	0.0005
MUC16	Normal v Paired adjacent	Decreased	0.0001
	Normal v Tumour	Decreased	0.0039
	Paired Adjacent v Tumour	-	0.4870
L1CAM	Normal v Paired adjacent	-	0.9887
	Normal v Tumour	Decreased	0.0052
	Paired Adjacent v Tumour	Decreased	0.0002
CEACAM1	Normal v Paired adjacent	-	0.4706
	Normal v Tumour	Decreased	<0.0001
	Paired Adjacent v Tumour	Decreased	<0.0001
EpCAM	Normal v Paired adjacent	-	0.9338
	Normal v Tumour	Decreased	<0.0001
	Paired Adjacent v Tumour	Decreased	<0.0001
CDH1	Normal v Paired adjacent	-	0.9759
	Normal v Tumour	-	0.9005
	Paired Adjacent v Tumour	-	0.9593
MDR1	Normal v Paired adjacent	-	0.9727
	Normal v Tumour	Decreased	<0.0001
	Paired Adjacent v Tumour	Decreased	<0.0001
MUC1	Normal v Paired adjacent	-	0.9878
	Normal v Tumour	Decreased	<0.0001
	Paired Adjacent v Tumour	Decreased	<0.0001

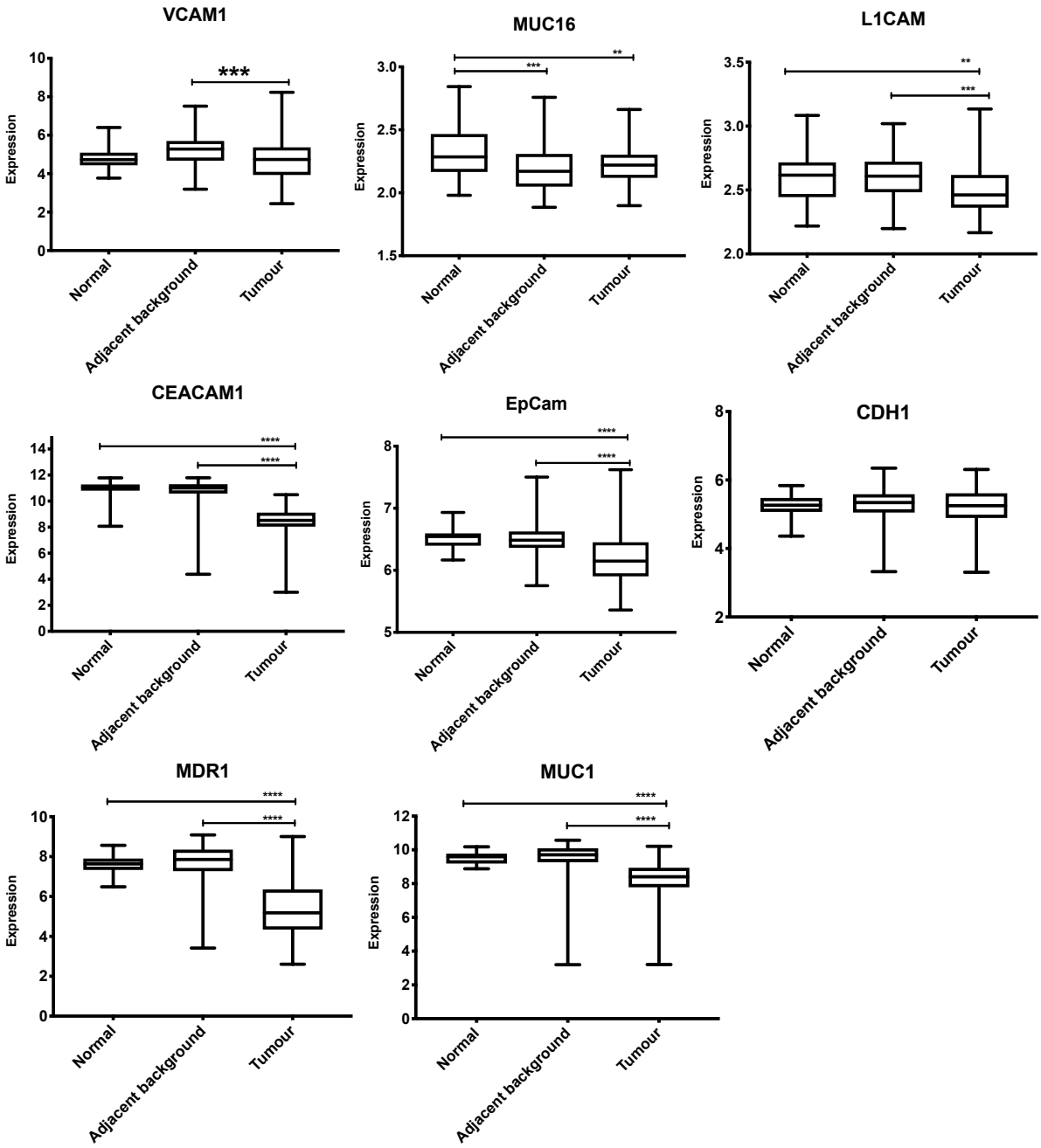

Figure 3.23. HA-independent adhesion molecule expression in colorectal cancer, paired adjacent tissue and normal tissue. Adhesion molecules VCAM1, MUC16, L1CAM, CEACAM1, EpCAM, CDH1, MDR1 and MUC1. There was either no difference in expression or reduced expression of adhesion molecules in tumour tissue when compared to normal tissue. One-way ANOVA. Data extracted are from GSE44076.

3.3.4.2. HA-independent adhesion molecule expression and overall tumour stage

There was found to be a significant decrease in expression of MUC1 between stage II and stage IV bowel cancer (p=0.0186, Adjusted p value p=0.0172). There was, however, no other significant difference in MUC1 expression when assessed against other bowel cancer stages.

There was no significant difference demonstrated between the remaining HA-independent adhesion molecules in relation to overall tumour stage (VCAM1 p=0.2982, MUC16 p= 0.3886, L1CAM p= 0.0536, CEACAM1 p= 0.6195, EpCAM p= 0.6156, CDH1 p=0.3146, MDR1 p= 0.2279). Results are illustrated in Figure 3.24.

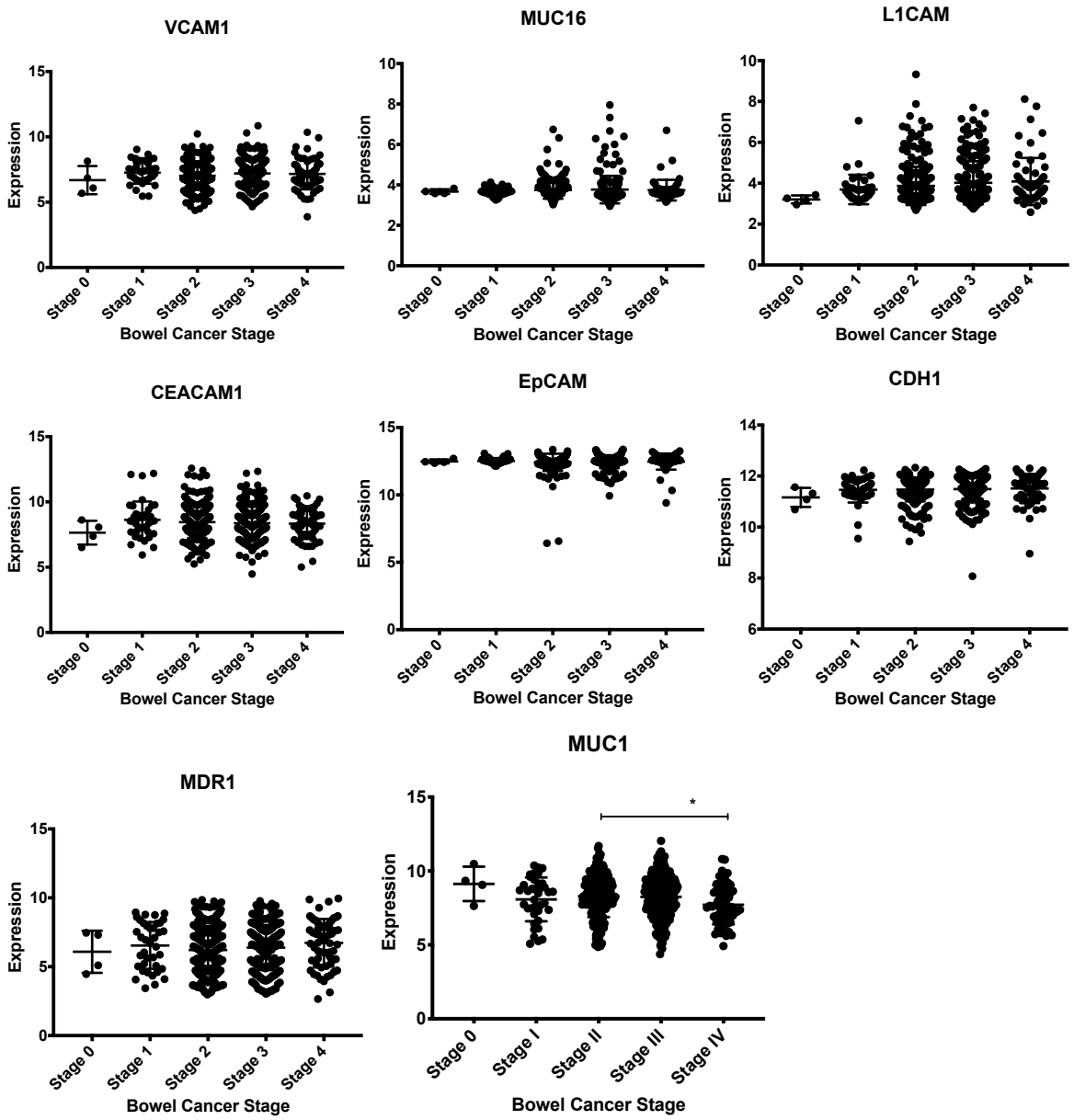

Figure 3.24. HA-independent adhesion molecule expression and overall bowel cancer stage. Adhesion molecules VCAM1, MUC16, L1CAM, CEACAM1, EpCAM, CDH1, MDR1 and MUC1. Kruskal-Wallis test and Dunn's multiple comparisons test. Data extracted from GSE 40967.

3.3.4.3. HA-independent adhesion molecule expression and tumour T-stage

There was found to be a significant decrease in expression of MDR1 between T3 and T4 tumours (p= 0.0021, Adjusted p value p=0.0037). There was, however, no other significant link demonstrated between MDR1 expression and T-stage.

There was no other significant difference demonstrated between the remaining HA-independent adhesion molecules, in relation to overall tumour stage (VCAM1 p=0.9529, MUC16 p= 0.2522, L1CAM p= 0.4497, CEACAM1 p= 0.5906, EpCAM p=0.2281, CDH1 p=0.1196, MUC1 p= 0.3357). Results are illustrated in Figure 3.25.

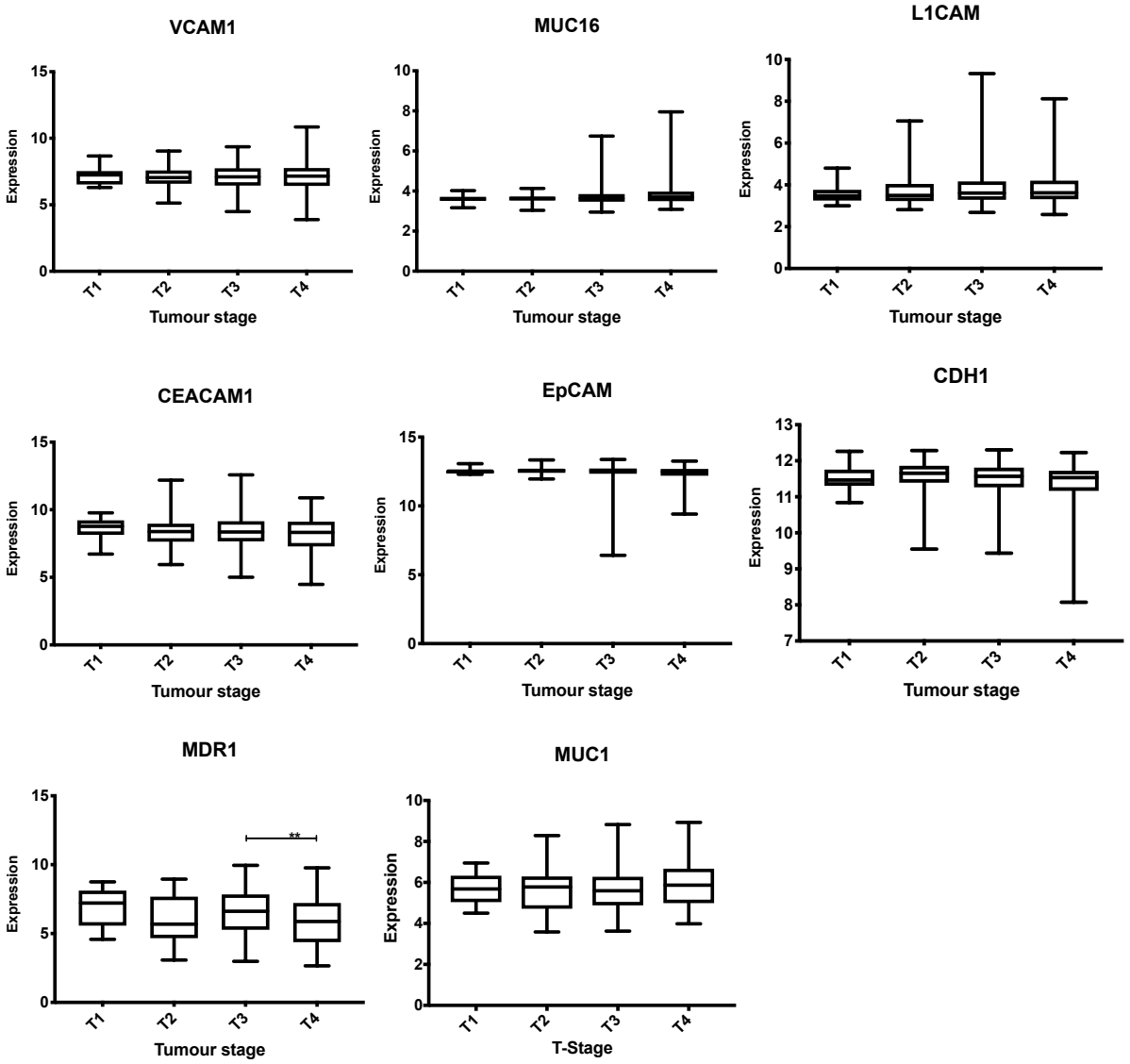

Figure 3.25. HA-independent adhesion molecule expression and tumour T-stage. Adhesion molecules VCAM1, MUC16, MUC1, L1CAM, CEACAM1, EpCAM, CDH1 and MDR1. Kruskal-Wallis test and Dunn's multiple comparisons test. Data extracted from GSE 40967.

3.3.4.4. HA-independent adhesion molecule expression and N stage

There was a significant increase in VCAM1 and L1CAM expression in nodal status N2 when compared to N0. There was otherwise no other significant difference found. CEACAM1 expression was decreased in N2 when compared to N1, but otherwise there was no other significant difference found. EpCAM expression was increased between N1 and N2. However, expression of EpCAM was decreased when N1 was compared to N0. There was no difference between N0 and N2.

There was found to be no significant difference between tumour N-stage and expression of MUC16, CDH1, MDR1 and MUC1. Results are summarised and illustrated in Table 3.9 and Figure 3.26.

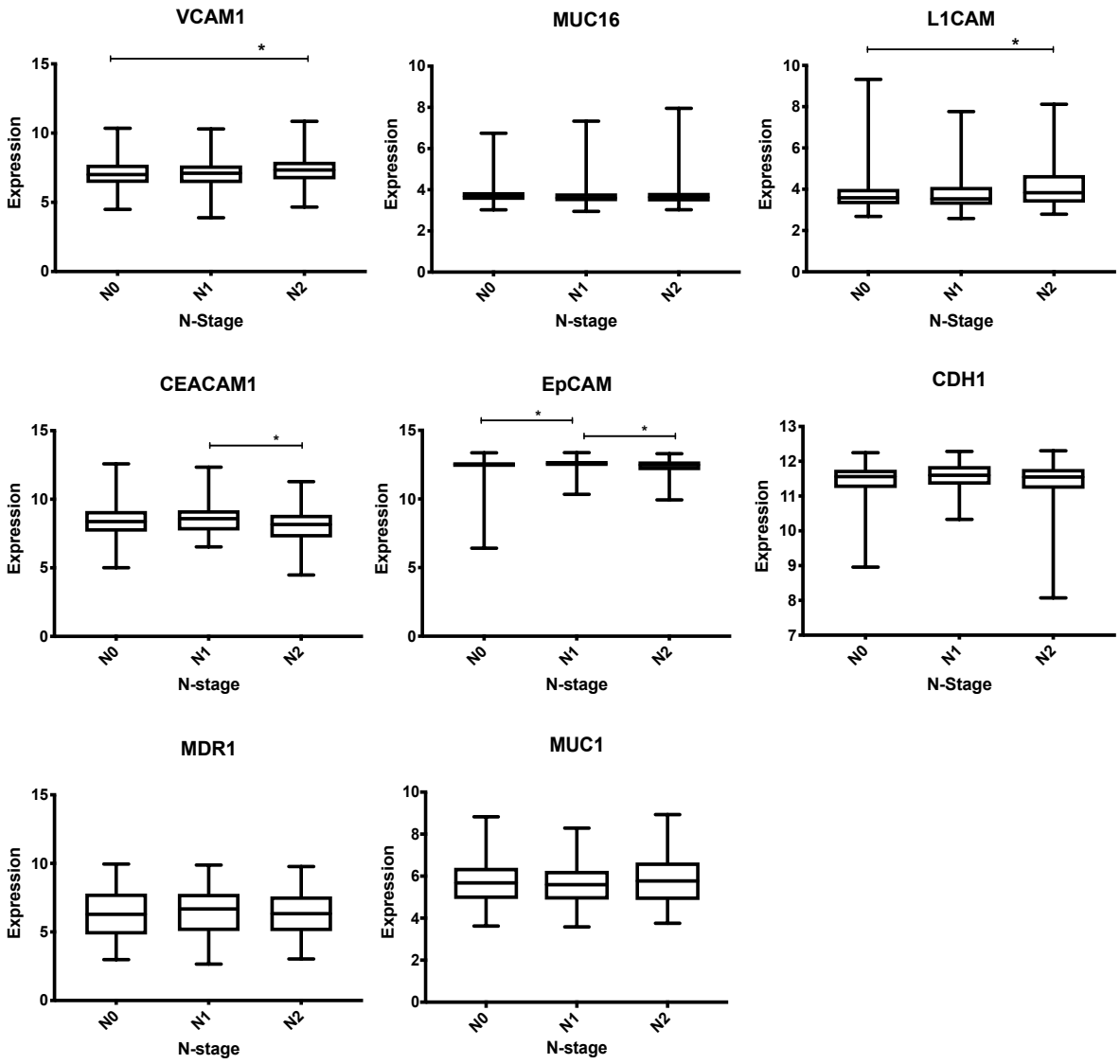

Figure 3.26. HA-independent adhesion molecules and tumour nodal status. Adhesion molecules VCAM1, MUC16, MUC1, L1CAM, CEACAM1, EpCAM, CDH1 and MDR1. Kruskal Wallis and Dunn's multiple comparisons tests. Data extracted from GSE 40967.

Table 3.9. N-stage and expression of HA-independent adhesion molecules. Kruskal Wallis and Dunn's multiple comparison tests. Data extracted from GSE 40967.

Adhesion Molecule	P-value	Sub-Group Analysis	Adjusted P-value	N-stage Expression
VCAM1	0.0337			
		N0 vs. N1	>0.9999	-
		N0 vs. N2	0.0414	Increased
		N1 vs. N2	0.0705	-
MUC16	0.1434			
		N0 vs. N1	0.1797	-
		N0 vs. N2	0.8479	-
		N1 vs. N2	>0.9999	-
L1CAM	0.0199			
		N0 vs. N1	>0.9999	-
		N0 vs. N2	0.0206	Increased
		N1 vs. N2	0.0584	-
CEACAM1	0.0410			
		N0 vs. N1	0.7635	-
		N0 vs. N2	0.1872	-
		N1 vs. N2	0.0358	Decreased
EpCAM	0.0190			
		N0 vs. N1	0.0430	Decreased
		N0 vs. N2	>0.9999	-
		N1 vs. N2	0.0379	Increased
CDH1	0.0659			
		N0 vs. N1	0.0965	-
		N0 vs. N2	>0.9999	-
		N1 vs. N2	0.1588	-
MDR1	0.4439			
		N0 vs. N1	0.7373	-
		N0 vs. N2	>0.9999	-
		N1 vs. N2	0.8520	-
MUC1	0.5501			
		N0 vs. N1	0.8568	-
		N0 vs. N2	>0.9999	-
		N1 vs. N2	>0.9999	-

3.3.4.5. HA-independent adhesion molecule expression and tumour M-stage

There was a significant decrease in expression of MUC1 seen in M1 staged tumours compared to M0 (p= 0.025). There was found to be no significant difference between tumour M-stage and expression of the remaining adhesion molecules (VCAM1 p=0.6540, MUC16 p=0.9028, L1CAM p=0.2052, CEACAM1 p=0.9028, EpCAM p=0.3188, CDH1 p= 0.3614, MDR1 p=0.0787). Results are illustrated in Figure 3.27.

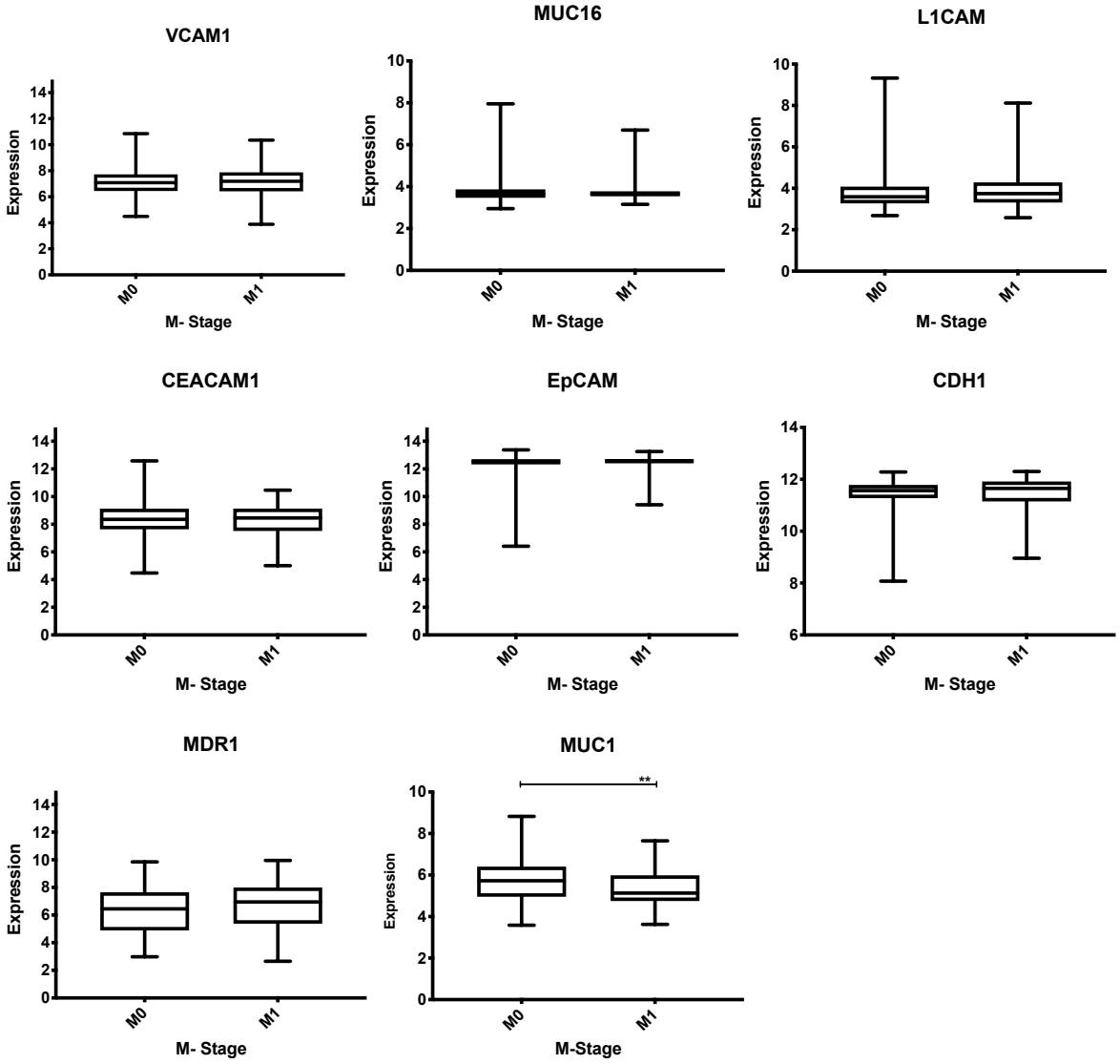

Figure 3.27. HA-independent adhesion molecule expression and tumour M-stage. Unpaired Mann-Whitney U-test. Data extracted from GSE 40967.

3.3.4.6. HA-independent adhesion molecule expression and gender

There was no significant difference between patient gender and expression of HA-independent adhesion molecules. Results in Table 3.10 and Figure 3.28.

Table 3.10. HA-independent adhesion molecule expression and sex. Unpaired Mann-Whitney U-tests.

	P value
VCAM1	0.2958
MUC16	0.5995
L1CAM	0.2178
CEACAM1	0.6952
EpCAM	0.7530
CDH1	0.5665
MDR1	0.1995
MUC1	0.7079

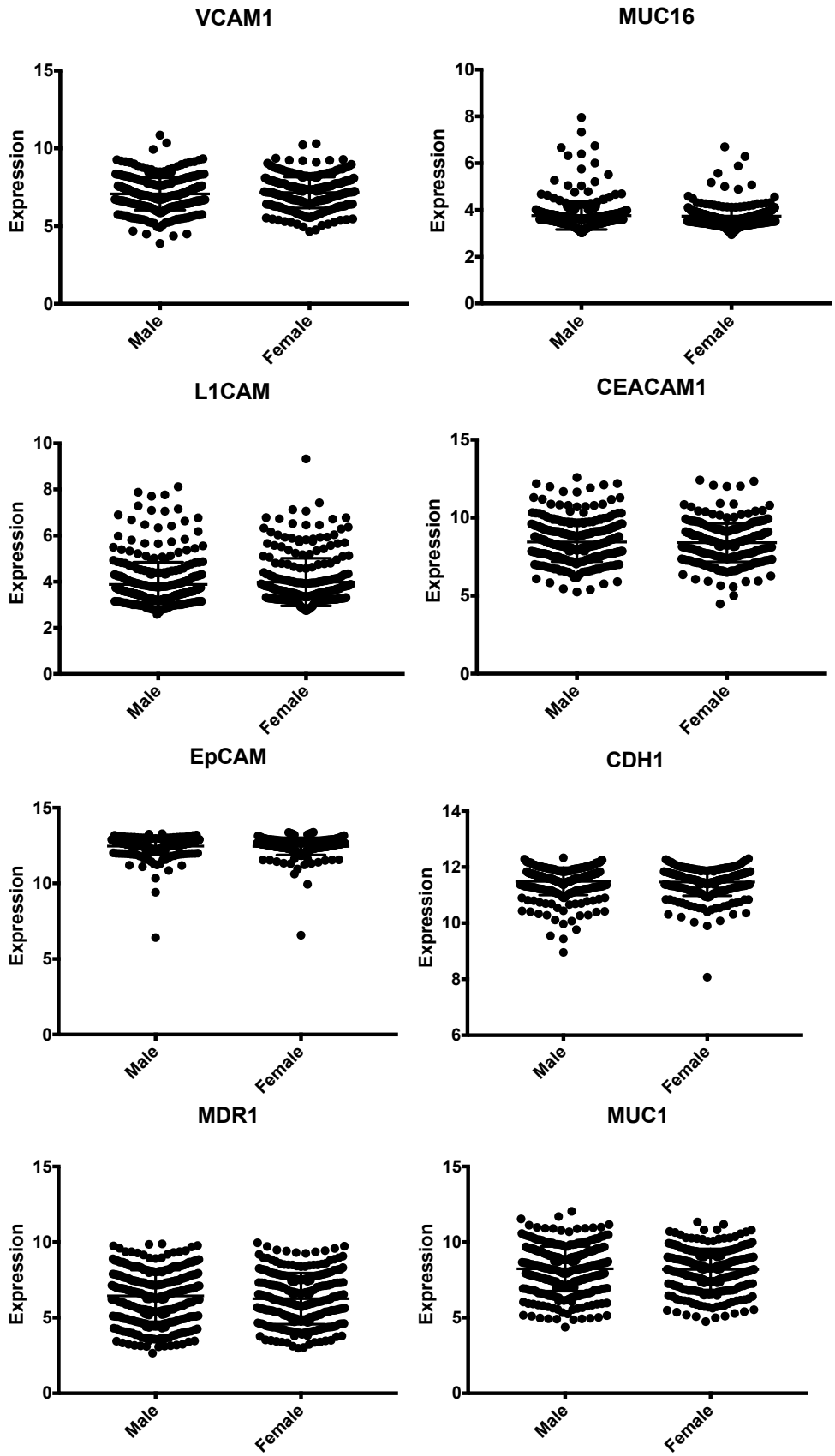

Figure 3.28. HA-independent adhesion molecule expression and sex. Adhesion molecules VCAM1, MUC16, L1CAM, CEACAM1, EpCAM, CDH1, MDR1 and MUC1. Data extracted from GSE 40967.

3.3.4.7. HA-independent adhesion molecule expression and tumour location

There was seen to be a significant decrease in expression of VCAM-1 in left-sided colon tumours compared to left-sided adjacent tissue (p=0.0066). In MUC16 there was a significant decrease in expression seen in right colon tumour tissue compared to right colon normal tissue (p= 0.046).

There was a significant decrease in expression in tumour tissue in both the right and left colon when compared to their respective ipsilateral anatomical sides when compared with both normal tissue and paired adjacent tissue for L1CAM (p=<0.0001), CEACAM1 (p=<0.0001), EpCAM (p=<0.0001), MDR1 (p=<0.0001) and MUC1 (p=<0.0001). There was no significant difference seen in CDH1 expression (p= 0.9688)

There was not seen to be a significant difference between tumour location between any of the studied molecules when comparing against contralateral side. Adjusted P-values are shown in Table 3.11 and Figure 3.29.

Table 3.11. Tukey's multiple comparison test of adjusted P-values. One-way ANOVA. Right versus Left Colon. Data from GSE44076.

Tukey's multiple comparisons	VCAM1 P value	MUC16 P value	L1CAM P value	CEACAM1 P value	EpCAM P value	CDH1 P value	MDR1 P value	MUC1 P value
Right Colon normal tissue vs. Left Colon Normal tissue	0.5994	0.7055	0.9997	0.5658	0.9572	0.9694	0.9950	0.9997
Right Colon Paired Adjacent vs. Left Colon Paired Adjacent	0.8730	0.6037	0.9987	0.0940	0.9362	0.9996	>0.9999	0.9987
Right Colon Tumour vs. Left Colon Tumour	>0.9999	>0.9999	0.8340	0.9019	0.9997	>0.9999	0.7056	0.8340
Right Colon normal tissue vs. Right Colon Paired Adjacent	0.4538	0.0554	>0.9999	0.9993	0.8563	0.9809	0.9981	>0.9999
Right Colon Paired Adjacent vs. Right Colon Tumour	0.5144	>0.9999	**<0.0001**	**<0.0001**	**0.0072**	>0.9999	**<0.0001**	**<0.0001**
Right Colon normal tissue vs. Right Colon Tumour	0.9999	**0.0460**	**<0.0001**	**<0.0001**	**0.0003**	0.9783	**<0.0001**	**<0.0001**
Left Colon Normal tissue vs. Left Colon Paired Adjacent	0.9286	0.1021	>0.9999	0.9845	0.9916	0.9978	>0.9999	>0.9999
Left Colon Normal tissue vs. Left Colon Tumour	0.5576	0.6909	**<0.0001**	**<0.0001**	**0.0032**	>0.9999	**<0.0001**	**<0.0001**
Left Colon Paired Adjacent vs. Left Colon Tumour	**0.0066**	0.6462	**<0.0001**	**<0.0001**	**<0.0001**	0.9995	**<0.0001**	**<0.0001**
Right Colon normal tissue vs. Left Colon Paired Adjacent	0.0370	0.0001	>0.9999	0.0721	0.9984	0.9963	0.9973	>0.9999
Right Colon normal tissue vs. Left Colon Tumour	>0.9999	0.0140	<0.0001	<0.0001	<0.0001	0.9745	<0.0001	<0.0001
Left Colon Normal tissue vs. Right Colon Paired Adjacent	>0.9999	0.8553	0.9975	0.7040	>0.9999	>0.9999	>0.9999	0.9975
Left Colon Normal tissue vs. Right Colon Tumour	0.6750	0.8244	<0.0001	<0.0001	0.0175	>0.9999	<0.0001	<0.0001
Right Colon Paired Adjacent vs. Left Colon Tumour	0.3517	0.9999	<0.0001	<0.0001	0.0006	>0.9999	<0.0001	<0.0001
Left Colon Paired Adjacent vs. Right Colon Tumour	0.0319	0.6577	<0.0001	<0.0001	<0.0001	0.9995	<0.0001	<0.0001

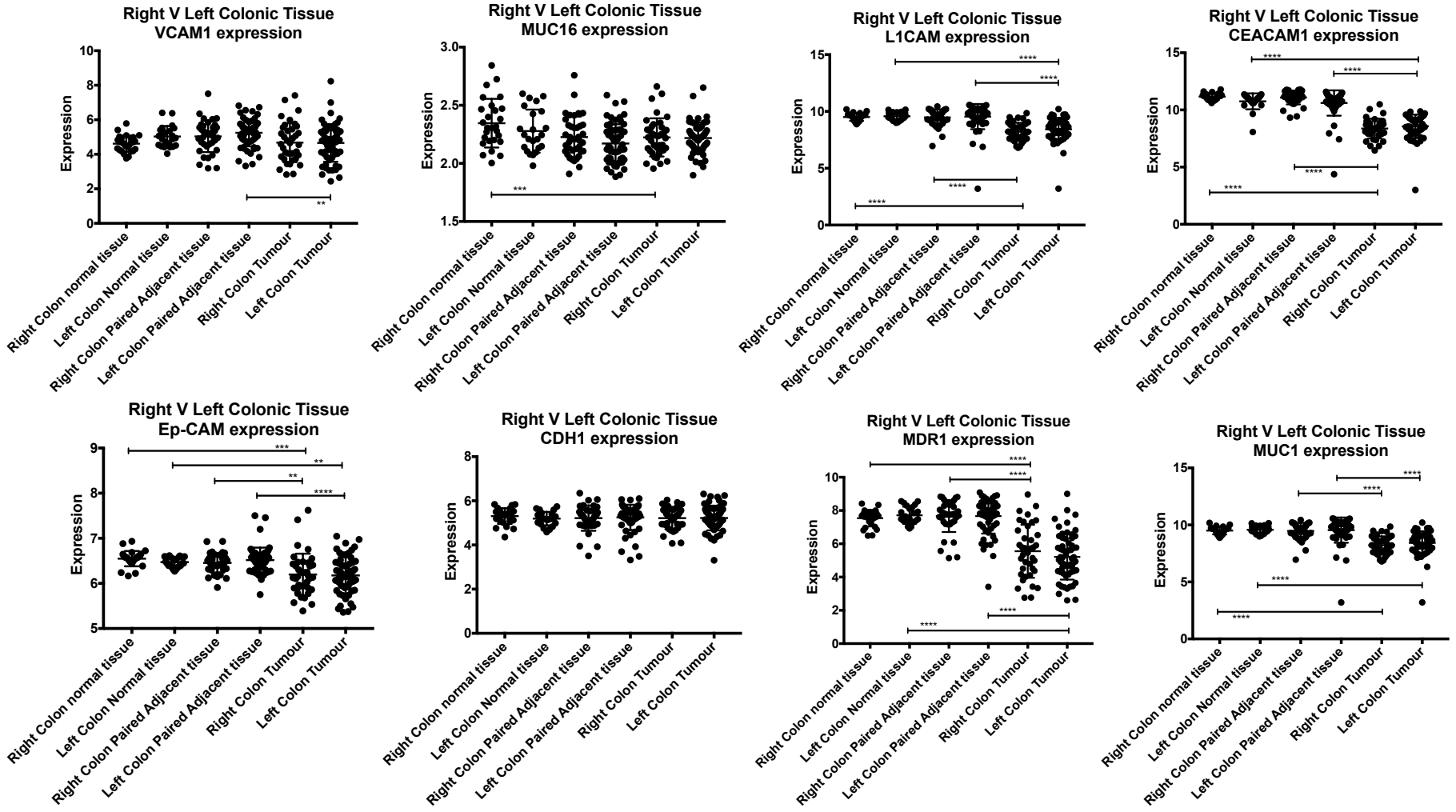

Figure 3.29 HA-independent adhesion molecule expression in relation to anatomical location and tumour status. One Way ANOVA.

Data extracted are from GSE44076.

3.3.4.8. HA-independent adhesion molecule expression and oncogene status

3.3.4.8.1. BRAF status

There was a significant decrease in expression of MDR1, CDH1 and EpCAM in mutated BRAF compared to WT samples (p=0.0001, p=0.0001 and p=0.0023 respectively), whereas MUC16 demonstrated a significant increase in expression in BRAF M compared to BRAF WT (p=0.0197).

There was no significant difference in BRAF status and expression of the remaining HA-independent adhesion molecules studied (VCAM1 p=0.1189, L1CAM p=0.1311, CEACAM1 p=0.1107, MUC1 p=0.1052). Results are illustrated in Figure 3.30.

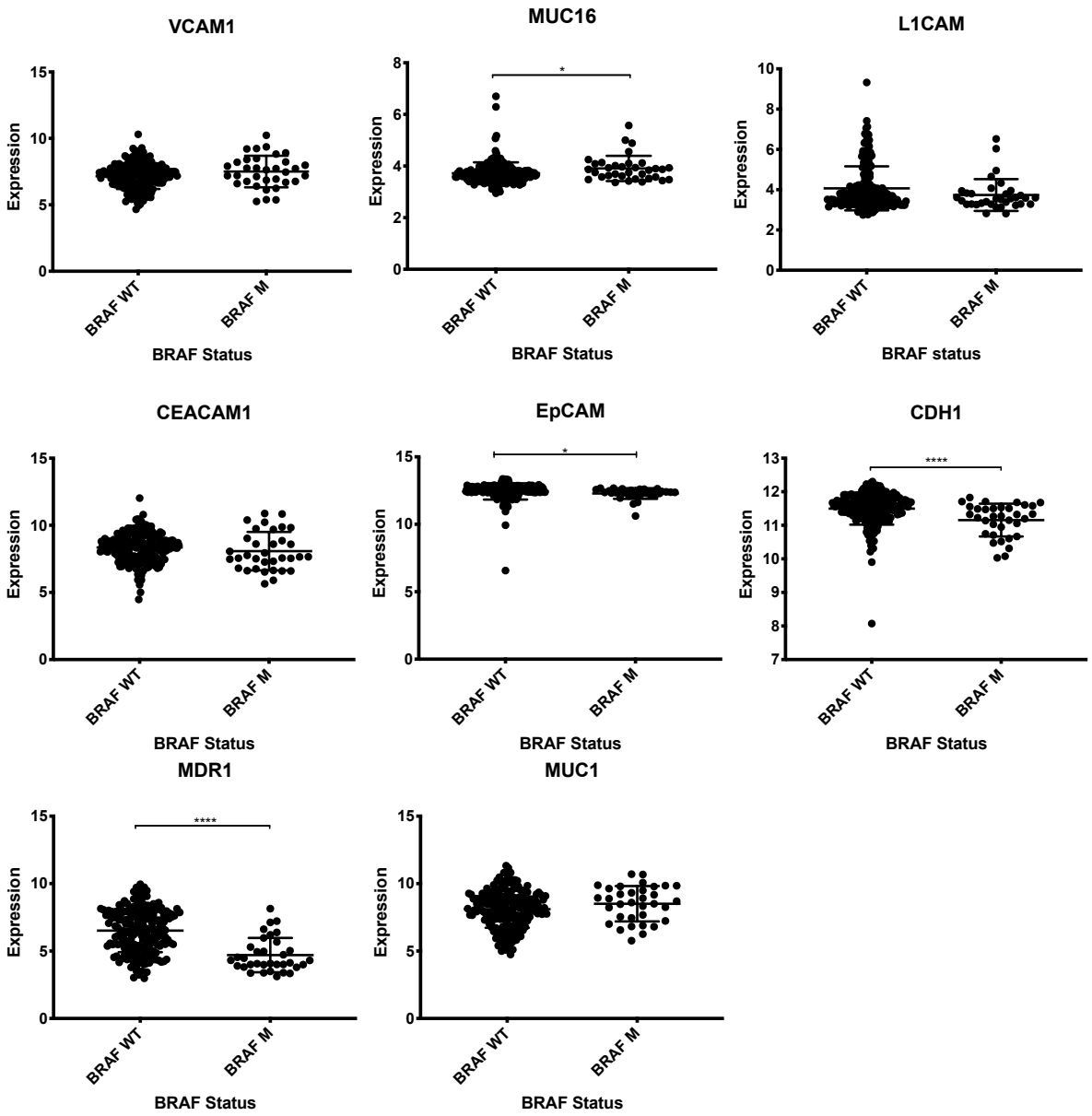

Figure 3.30. HA-independent adhesion molecule expression and BRAF status. Data extracted from GSE 40967.

3.3.4.8.2. KRAS status

There was significantly decreased expression of VCAM1 in mutated KRAS compared to KRAS WT samples (p=0.0026). Conversely there was significantly increased expression of MDR1 in mutated KRAS compared to WT (p=0.0367).

However, there was no significant difference in the remaining expression of adhesion molecules studied and KRAS status. (MUC16 p=0.6670, L1CAM p= 0.51196, CEACAM1 p=0.2989, EpCAM p= 0.9149, CDH1 p= 0.6976, MUC1 p= 0.0734). Results are demonstrated in Figure 3.31

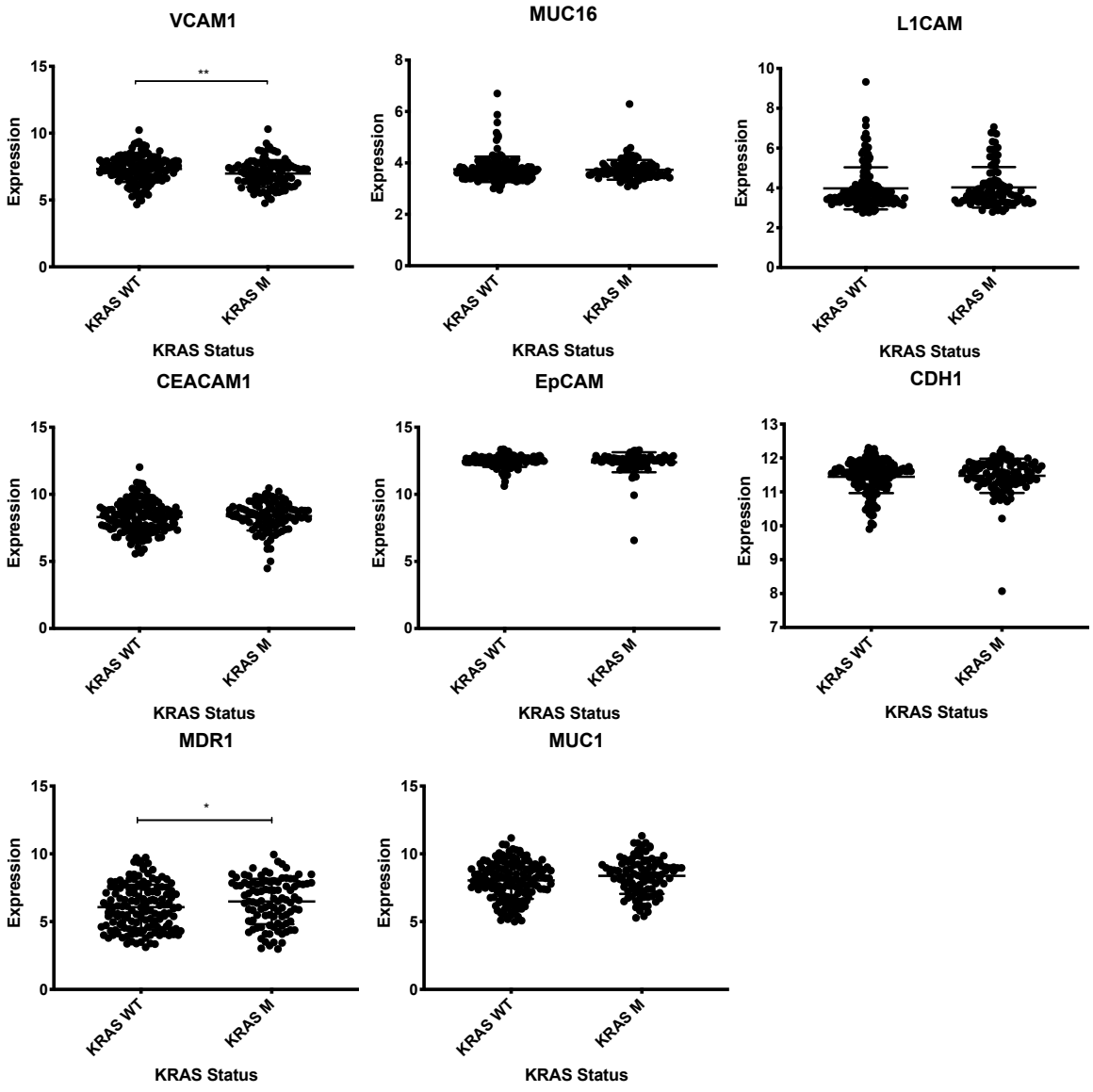

Figure 3.31. HA-independent adhesion molecule expression and KRAS status. Data extracted from GSE 40967.

3.3.4.8.3. TP53 status

There was a significant increase in expression of CDH1 in mutated TP53 compared to WT ($p=0.0074$).

However, there was no significant difference demonstrated in expression of TP53 and the remaining HA-independent adhesion molecules studied (VCAM1 $p=0.0751$, MUC16 $p=0.3832$, L1CAM $p=0.2720$, CEACAM1 $p=0.2527$, EpCAM $p=0.7408$, MDR1 $p=0.7051$, MUC1 $p=0.0664$). Results are illustrated in Figure 3.32.

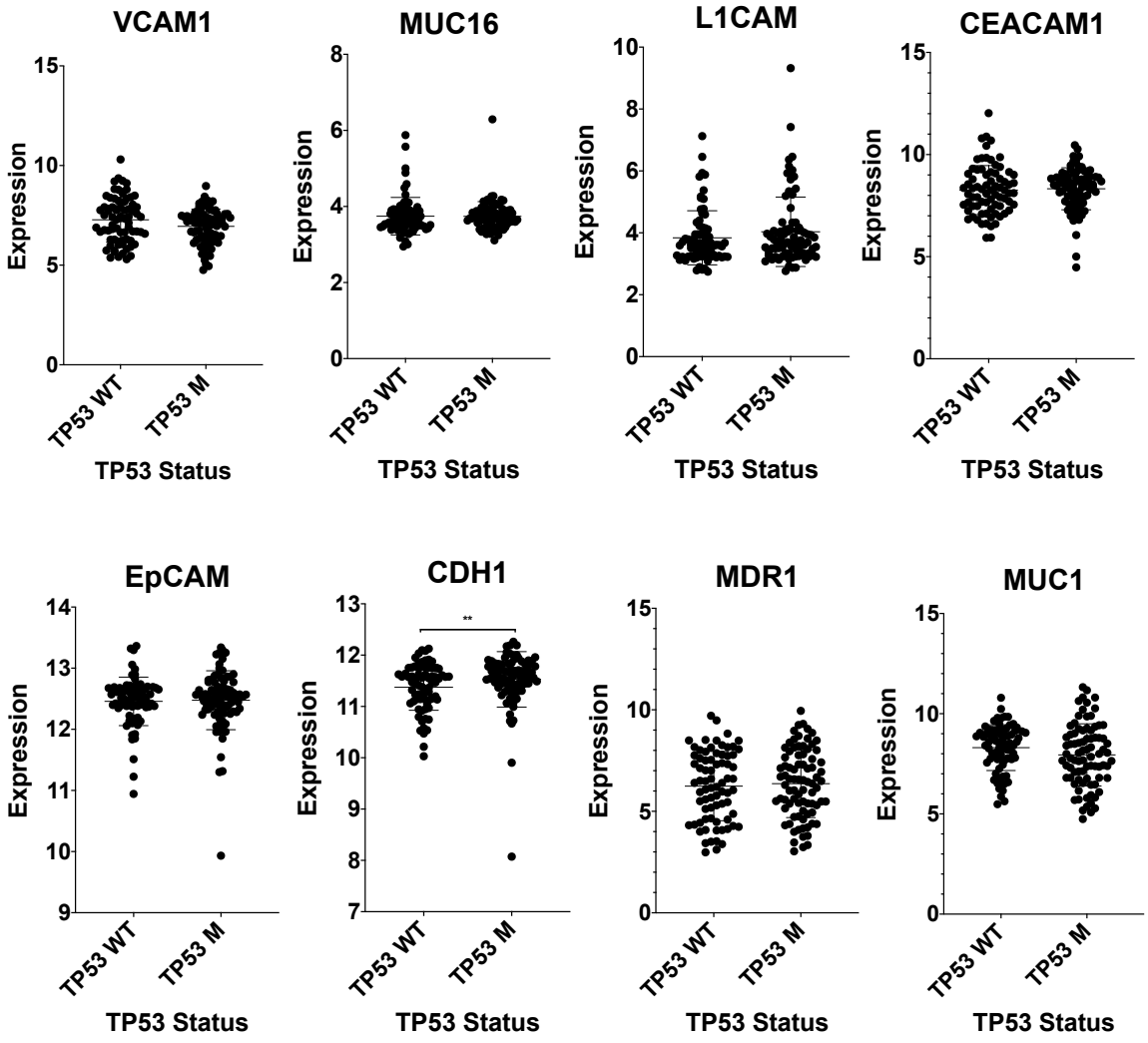

Figure 3.32 HA-independent adhesion molecule expression and TP53 status. Data extracted from GSE40967. CDH1 demonstrated an increase in expression in mutated KRAS compared to wild type KRAS (p-0.0074). The remaining HA-independent adhesion molecules (VCAM1, MUC16, L1CAM, CEACAM1, EpCAM, MDR1 and MUC1) demonstrated no significant difference.

3.3.5. Expression of hyaluronic acid-dependent adhesion molecules CD44 RHAMM and ICAM-1 in primary colorectal cancer cell lines

Whilst the presence of HA-dependent adhesion molecules is seen in primary colorectal cancer cohorts, it is important to determine relative expression in primary CRC cell lines, as part of planning future *in vitro* work. One important factor determining cell lines chosen for experimentation was presence of HA-dependent adhesion molecule expression, which was reflective of colorectal cell line cohorts. Relative gene count expression is summarised in Figure 3.33. For individual gene counts see Appendix 1.1 and 1.2.

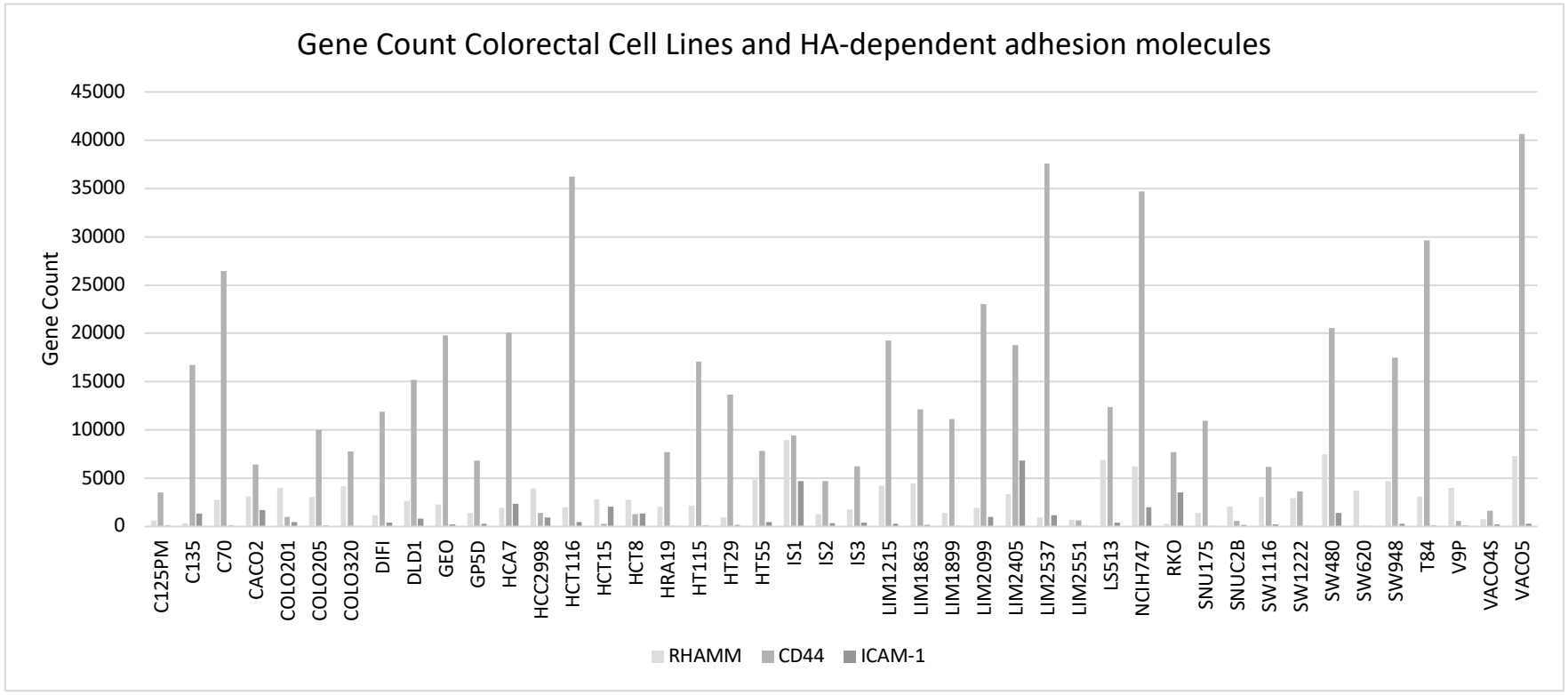

Figure 3.33. Colorectal Cancer Cell lines and gene expression count for CD44, RHAMM and ICAM-1. Data extracted from GSE90830

3.4. Discussion

3.4.1. General discussion

The GSE cohort 44076 studied 98 matched tumour and adjacent normal tissues in patients with stage II colon cancer, and in a further 50 non-cancer patient colon tissues. Within this cohort, all three identified HA-dependent adhesion molecules studied demonstrated increased expression within tumour tissue, compared to normal tissue and adjacent matched background tissue. For CD44 and ICAM-1, adjacent tissue was also seen to be significantly increased when compared to the non-cancer tissue, whereas RHAMM was significantly decreased.

There have not been any studies specifically looking at HA-dependent adhesion molecules CD44, RHAMM and ICAM-1, as a group, within CRC. Each molecule, individually, has been demonstrated as having influence on CRC development and dissemination (Bendardaf, Algars, Elzagheid *et al.*, 2006; Furuta, Zahurak, Goodman *et al.*, 1998; Koelzer *et al.*, 2015; Maurer *et al.*, 1998; Mele *et al.*, 2017; Wimmenauer *et al.*, 1997; Zlobec *et al.*, 2008). It is interesting to see the upregulation of CD44, ICAM-1 and RHAMM together, which all share expression of the HA-binding receptor. The possible relationship of HA-dependent adhesion molecules may be an important factor within metastatic dissemination of CRC, and future therapeutic modalities may need to target all three molecules to have effect.

Expression profiling in relation to several of the various molecules studied has been examined previously, occasionally with some conflicting results. ICAM-1 for instance has

been shown to reduce cell adhesion when down-regulated (Alkhamesi *et al.*, 2005). On the other hand, ICAM-1-negative tumours have been shown to have a higher rate of metastasis to liver and lymph nodes (Tachimori *et al.*, 2005).

Tissue samples from cohort GSE44076 do not specify the depth of sampling biopsy taken for the analysis of expression. Furuta et al (1998) demonstrated CD44s and V6 splice variant are differentially expressed in the epithelium when compared to the stromal matrix, which again highlights the importance of the tumour microenvironment potentially influencing both disease dissemination and interpretation of results (Furuta *et al.*, 1998). One could assume that sampling for cohorts were taken using the same biopsy technique and, as such, are comparable across the sampled cohort. However, on the other hand it is more than likely that sampling techniques could vary widely. A whole series of confounding variables could account for this, with the most likely sampling variation simply due to different clinicians taking samples, to contribute to the tissue array datasets.

Demonstrating increased expression of all identified HA-dependent adhesion molecules (RHAMM, ICAM-1 and CD44) is potentially significant. One possible consideration as to why they are upregulated is the possibility that they may indicate the common HA receptor shared between the molecules does indeed have a significant role within CRC. It is important to compare differential expression in tumour tissue against paired adjacent tissue, as carried out for the cohort GSE44076, since interaction between tumour and either surrounding stromal microenvironment, or systemic expression, can play a significant role in tumour dissemination. The comparison between the two demonstrates upregulation of HA-

dependent adhesion molecules CD44, RHAMM and ICAM-1 (Section 3.7.1.1, 3.7.1.5, 3.7.2.1, 3.7.2.5, 3.7.3.1, 3.7.3.5, 3.7.4.1 and 3.7.4.7)

The following adhesion molecules were downregulated in tumour tissue when compared to both paired adjacent and normal colonic tissue:

- L1CAM
- CEACAM1
- EpCAM
- MDR1
- MUC1

L1CAM is predominantly studied in ovarian cancer. Within colorectal cancer, expression of L1CAM has also been associated to metastatic initiating ability of cells and, high expression identified patients potentially at risk of metastatic disease at early disease presentations (Ganesh, Basnet, Kaygusuz *et al.*, 2020; Tampakis, Tampaki, Nonni *et al.*, 2020). In pancreatic cancer, L1CAM is seen to inhibit cell proliferation and invasion as well as arrest the cell cycle (Ben, An, Fei *et al.*, 2014). A recent publication has also demonstrated decreased L1CAM expression in 229 CRC specimens from stage I-IV cancers, when compared to 145 normal control patients (L. Y. Chu, Guo, Chen *et al.*, 2020).

Significantly, CEACAM1 is known to be downregulated in early stages of CRC but upregulated in metastatic stages of disease. (Arabzadeh *et al.*, 2012; Nittka, Gunther, Ebisch *et al.*, 2004; Song, Cao, Yoon *et al.*, 2011). In gastric cancer loss of CEACAM1 is associated

with poor prognosis and peritoneal dissemination (Takeuchi, Yokoyama, Nakamori *et al.*, 2019).

EpCAM expression in colon cancer has been shown to decrease in tumour tissue when compared to normal tissue. Another study confirmed that protein expression is decreased in tumour tissue when compared to normal tissue, through immunostaining, and was able to correlate tumour stage to level of EpCAM expression (Mokhtari & Zakerzade, 2017). This provides a degree of correlation to both RNA expression and protein expression. Complete loss of EPCAM has been linked to a small subset of Lynch Syndrome- associated colorectal cancers (Kim, Bae, Kim *et al.*, 2014), whereas partial loss of EPCAM is linked to tumour aggressiveness and poorer prognosis in CRC (Kim, Bae, Song *et al.*, 2016).

MDR1 expression has been related to the degree of tumour differentiation, with higher MDR1 expression seen in well differentiated CRC tumours (Mizoguchi *et al.*, 1990). Whilst high expression in adhesion fibroblasts is seen in post-operative adhesion formation following abdominal surgery (L. Deng *et al.*, 2016), there is limited data in the literature to relate MDR1 as a significant adhesion molecule in CRC. The significance seen in downregulation would need to be explored more completely to draw conclusions.

The role of MUC1 in colorectal cancer is not completely clear. It has been shown to be expressed in a wide variety of tumours and is considered to function as an anti-adhesion molecule inhibiting cell-cell interactions (Makiguchi, Hinoda, & Imai, 1996). MUC1 has been shown to interact or regulate E-cadherin through β-catenin binding. The two molecules are seen to compete at binding sites and MUC1 is able to disrupt E-cadherin mediated cell-cell

interaction (Niv, 2008). Intracellularly, the complex of MUC1-β-catenin can enhance cellular proliferation and decrease cell-cell adhesion, through activation of T-cell factor/leukocyte enhancing factor 1 (Tcf/LEF-1) (Baldus, Monig, Huxel *et al.*, 2004). MUC1 has been shown to interact with domain-1 of ICAM-1 and has a potential role in metastases of epithelial tumours (Hayashi, Takahashi, Motoya *et al.*, 2001). This could provide some explanation as to the mixed conclusions of ICAM-1 expression and prognosis in malignancy, as discussed in Chapter 1, as expression of ICAM-1 is interdependent on expression of molecules such as MUC1. ICAM-1 expression in the presence of either MUC-1 positive or negative tumours could be a potential prognostic indicator to explore further in PM in CRC. The data demonstrated downregulation of MUC1 expression in tumour cells, which could either represent promotion of cellular adhesion within the tissue sampled in the microarray or that the tumour tissue taken may not necessarily be at the invasive front of the tumour in which cells detach, if following the peritoneal metastatic model.

The data demonstrated VCAM-1 to be downregulated in tumour tissue when compared to adjacent normal tissue, however no difference was demonstrated when compared to normal colonic tissue. The role of VCAM1 in the progression of CRC remains largely unknown. One recent study demonstrated that upregulation of VCAM1 being associated with aggressive phenotypic characteristics of CRC and regulated invasion and metastasis of CRC through activation of Epithelial Mesenchymal Transition (EMT) (D. Zhang, Bi, Liang *et al.*, 2020). In contrast to the data presented within this Chapter, Zhang et al (2020) demonstrated that VCAM1 was upregulated in human CRC tissues compared with matched adjacent tissues (D. Zhang *et al.*, 2020). Why this is could be for a variety of reasons, which could include where the samples were taken from the tumour tissue or the stage of the

tumour or even considering other epigenetic factors which may have influenced the patient cohorts sampled.

However, this data was able to demonstrate increased expression of VCAM1 in nodal status in N2 disease when compared to nodal status N0. This could possibly correlate with VCAM1 expression being associated to lymphogenous metastatic spread in CRC and may go some way to corroborating the findings seen in Zhang et al (2020). This would correlate with the increased expression of nodal metastases reported in section 3.3.4.4. It should however be noted, that increased expression for VCAM1 was not seen within N1 disease when compared to N0 disease in this chapter.

MUC16, which codes for CA125, demonstrated downregulation of expression in tumour tissue when compared to normal colonic tissue, but there was no significant difference between adjacent tissue and tumour tissue. With the mixed effects this gene plays regarding adhesion described in the literature (Akita *et al.*, 2013; Muniyan *et al.*, 2016; Rump *et al.*, 2004; H. S. Wang *et al.*, 2015), this is potentially difficult to interpret. However, downregulation could contribute to cell-cell adhesive stability.

CDH1 demonstrated no difference between any of the cohorts. Reduced expression of CDH1, as described in section 3.1, results in reduced cellular adhesion, which can be found at the invasive front of a cancer. Specifically, where samples were taken from tumour tissue for the microarray could be particularly important in assessing differences in expression in the context of PM formation. A way to further assess this would be to take samples from

different regions from a tumour to assess for differences within a single tumour, or even differences in phases of the cell cycle.

There appeared to be no significant difference between overall cancer stage or TNM stage for expression of either CD44 or RHAMM. ICAM-1 showed increased expression between T2 and T3 tumours compared to T4 tumours. However overall cancer stage, N-stage and M-stage demonstrated no difference. There appears to be conflicting data in the literature assessing expression and stage of tumour advancement. Weg-Remers et al (1998) corroborated the findings that CD44 expression was independent of cancer stage and no different in control patients (Weg-Remers, Hildebrandt, Feifel *et al.*, 1998). However, CD44 has been shown to be related to tumour progression or more advanced disease states in several studies (Weg-Remers, Schuder*, et al.*, 1998; Wielenga, Heider, Offerhaus *et al.*, 1993; Wimmenauer *et al.*, 1997).

Wimmenauer et al (1997) demonstrated an inverse relationship between ICAM-1 expression and tumour staging (Wimmenauer *et al.*, 1997). RHAMM overexpression has been demonstrated to be an independent marker of tumour progression in all CRC stages. It has also been shown, *in vivo,* that downregulation of RHAMM abolishes metastases in mouse models and also affects both growth and dissemination in primary and metastatic CRC (Mele *et al.*, 2017).

The interplay of confounding variables within the literature, to the data processed from GSE40967, could be related to sampling size, sampling technique, tissue processing, prior

treatment or cohort epigenetic factors being addressed between samples. Consideration of data in the literature as to whether controls included matched adjacent tissue as a comparative factor in data analysis is important. Some papers analysed primary colorectal cancer data, whereas others looked at *in vivo* mouse data with human CRC cell lines, which in themselves have limitations.

Within the HA-independent cohort there were some differences seen between staging and expression. VCAM1 and L1CAM increased expression was seen when comparing N0 to N2 tumours. This seems to uphold some of the conclusions drawn from other work, (Kajiwara *et al.*, 2011; Maurer *et al.*, 1998) regarding disease progression. However, with no differences seen in increased expression in overall cancer stage, T-stage or M-stage, further work specifically addressing these questions would need to be undertaken.

EpCAM demonstrated an unclear relationship when analysing nodal status. In N1 disease expression was decreased when compared to N0. However, in N2 nodal disease expression significantly increased when compared to N1 disease. N2 disease was not significantly different to N0 disease. This could possibly reflect either EMT change in the tumour microenvironment or the multifunctional role EpCAM plays in cancer dissemination (Trzpis *et al.*, 2007). (Sections 3.7.1.2 - 3.7.1.3, 3.7.2.2 - 3.7.2.3, 3.7.3.2- 3.7.3.3 and 3.7.4.2-3.7.4.5)

For all molecules studied, there was no difference demonstrated between patient gender and expression. However, Iseki et al (2017) demonstrated, in a cohort of 49 patients (26:23 M:F), a significant difference in expression of CD44 between the sexes. In this cohort all

patients had unresectable metastatic colorectal malignancies and underwent primary chemotherapy (Iseki, Shibutani, Maeda *et al.*, 2017). There were either no other studies assessing expression related to sex, or no other studies found which found a significant difference in expression between the sexes (Pirker *et al.*, 1993)

In relation to survival, high expression in paired adjacent tissue of CD44 in stage II CRC demonstrated a significantly worse outcome, in both OS and PFS. This was not seen within the tumour tissue. This may be due to most of the tumour tissue expressing moderate or high CD44 expression and, as such, providing an inappropriate comparator. This appears to be consistent with Bendardaf et al (2006), that demonstrated that CD44s expression in metastatic CRC is associated with a shorter disease-free survival (DFS) (Bendardaf *et al.*, 2006).

DFS and OS were significantly poorer in high expression of ICAM-1 compared to low expression in adjacent colonic tissue. This conflicts with survival data from the matched tumour tissue. Within the tumour tissues, low expression appeared to correlate with decreased DFS and OS. For the tumour tissue matched data, prognosis was significantly poorer in ICAM-1 negative tumours than ICAM-1 positive (Maeda *et al.*, 2002) .

RHAMM did not demonstrate difference in survival between high or low expression in either adjacent tissues or tumour tissues from our data. However, literature data reports that high expression is an independent prognostic marker in CRC outcomes, where high RHAMM expression carries a poor prognosis (Z. P. Chu, Dai, Jia *et al.*, 2018; Ishigami, Ueno,

Nishizono *et al.*, 2011; Zlobec *et al.*, 2008). One possibility of conflicting survival data is due to the cohort being taken from stage II cancers alone and also relatively small groups analysed, such that it is difficult to establish robust comparisons or definite conclusions. To verify this further, a prospectively collected tissue bank including both serum samples and tissue samples taken from different sections of tumour tissue would be required. The tissue bank would ideally have tumour samples directly from peritoneal metastases of both colorectal origin tumours and other abdominal origin tumours. The analysis of such samples would look specifically for adhesion markers, would provide a more systematic approach toward examination of the hypothesis.

Oncogenes have been markers of prognostic outcomes in many different cancers. Outcomes in colorectal cancer are significantly affected by genomic instability. Within the umbrella of microsatellite instability (MSI), CpG island methylator phenotype (CIMP), and chromosomal instability (CIN), mutations in several different proteins and genes affecting proliferation and survival pathways have been identified. Three oncogenes studied within this chapter are KRAS, BRAF and TP53.

KRAS is commonly mutated in colon, lung, and pancreatic cancer. It is suggested that KRAS mutations detected in CRC may predict responses to monoclonal EGFR-targeted treatments (Santini *et al.*, 2008). From the CRC tissue array there is significantly higher CD44 expression in KRAS M tumours when compared to KRAS WT tumours ($p = <0.0001$). In one small study approximately 50% of KRAS mutated tumours were found in CRC peritoneal carcinomatosis (Gillern, Chua, Stojadinovic *et al.*, 2010), which indicates no clear preponderance for KRAS

WT or KRAS M in CRC PM. However, KRAS mutated tumours have been identified to have a high degree of correlation with worse prognostic outcomes, in metastatic colorectal cancer (Diez-Alonso, Mendoza-Moreno, Gomez-Sanz *et al.*, 2021). KRAS M has also been associated with unfavourable outcomes associated with CD44, along with CD166, overexpression (Ribeiro, da Silva Zanetti, Ribeiro-Silva *et al.*, 2016), in concordance with the data. The significance of this association has not been fully explained.

BRAF mutations are seen in approximately 10% of advanced colorectal cancers (Clarke & Kopetz, 2015) and seen more commonly in peritoneal metastatic disease (Yaeger, Cercek, Chou *et al.*, 2014). BRAF mutations are seen more commonly in elderly, female proximal tumours (Gonsalves, Mahoney, Sargent *et al.*, 2014). There is limited literature on the association of ICAM-1 expression and BRAF expression and there is no data comparing BRAF-WT against BRAF-M variants, when comparing ICAM-1 expression, which this dataset demonstrates as upregulation of ICAM-1 in BRAF-M. However, ICAM-1 variation and BRAF-WT and BRAF-M variants have been linked as possible prognostic markers to predict response to Bevacizumab-based treatment in mCRC (Papachristos, Kemos, Katsila *et al.*, 2019).

TP53 is the gene which transcribes the tumour suppressor protein p53. In ovarian cancer it has been demonstrated that mutant P53 promotes ovarian cancer adhesion to mesothelial cells via integrin β4 and Akt signalling (J. G. Lee, Ahn, Jin Kim *et al.*, 2015). In gastric cancer TP53 mutations were associated with aggressive PM patterns of disease (R. Wang, Song, Harada *et al.*, 2020). RHAMM has been shown to be downregulated by p53 tumour

suppressor expression. Sohr et al (2008) used mutant p53 as a control, but did not demonstrate downregulation RHAMM when compared to WT-p53. However, it is unclear whether upregulation was looked into (Sohr & Engeland, 2008). The data from this chapter demonstrated upregulation in RHAMM expression for mutated TP53, when compared to WT-TP53. This difference seen could be due to RNA expression as against protein expression. To examine whether this is the case using a prospectively collected tissue bank which not only looks at RNA profiling but also protein expression of adhesion molecules, together with oncogene status, would specifically assess this further.

Further examination, via collection of prospective tissue of CRC PM, is needed to assess if there is an association with either expression of BRAF, KRAS or TP53 mutated tumours. It could be hypothesised that, in CRC PM, there could be an association with at least one out of the three being expressed. The presence of one of the three mutated oncogenes could enhance the expression of one of the three HA receptor molecules. The presence or absence of the HA receptors could be an independent predictor to PM in CRC.

Data from GSE dataset GSE90830 demonstrated gene counts in CRC cell lines, relative to the expression of the HA-dependent adhesion molecules CD44, RHAMM and ICAM-1. This would serve to aid cross reference with the available cell lines within the lab, to consider for initial examination *in vitro*. Several cell lines demonstrate expression of all three HA-receptor molecules to be considered. Relative to CD44 and RHAMM the gene count for ICAM-1 in CRC cell lines has a lower expression (Appendix 1.1).

3.4.2. Limitations

There are several limitations of this dataset to be considered, when attempting to draw conclusions from this data. The first is to consider the limitations of a retrospectively analysed, publicly available dataset. The ideal would be to prospectively collect matched tissue samples to address the specific question at hand. However, it should be accepted that the constraints on time and regulation to prospectively collect sufficient tissue samples for such a purpose, can present challenges of their own.

Tissue cohorts are taken from primary tumour and are therefore not comparable to peritoneal metastatic deposits, where there could be differential expression. Four types of tissue would ideally be matched, in order to fully assess differential expression of PM in advanced CRC patients, which would include:

1. Control patient normal colonic tissue
2. Primary tumour tissue
3. Matched adjacent tumour tissue
4. Matched Peritoneal tumour tissue
5. Matched Peritoneal normal tissue

The data demonstrates expression of mRNA, which codes for respective proteins. Increased or upregulated mRNA expression should, in theory, correlate with increased protein expression. However, if considering the tumour microenvironment and possibly other molecular interactions not identified within this Chapter, mRNA expression may not truly

reflect, for example, the actual surface protein expression of the various adhesion molecules seen on a cell. The initial screening of RNA expression of molecules can give an indication as to where to target further study, in this case the HA-dependent adhesion molecules. A tissue data bank, with access to matched colonic and peritoneal tumour tissue, would be able to also examine for surface protein expression of protein molecules. Freely available microarray datasets are easily and quickly available, but in some ways are retrospective datasets, as tissue is already collected for potentially a different question intended by the original researchers.

Data comparing patient ethnic origin were not able to be analysed, as this was not available within the datasets. It has been described that there is disparity in outcomes between African American and Caucasian CRC patients (Govindarajan, Shah, Erkman *et al.*, 2003; R. L. Siegel, Miller, & Jemal, 2015). Exact reasoning is not fully understood, as there is a wide range of confounding variables to consider, including socioeconomic and epigenetic factors. One study utilising oncotype Dx colon cancer assay (12-gene assay Genomic Health Inc, Redwood City, California), found no difference in tumour biology between different races, where there was no difference in demographic or clinical factors (Govindarajan, Posey, Chao *et al.*, 2016).

3.4.3. Future work

The work from this chapter highlights that there may be a link to HA-dependent adhesion molecules being upregulated in colorectal cancer through RNA expression profiling. However, to further examine this area more completely, mRNA expression profiling should also be correlated to protein expression of both HA-dependent and HA-independent adhesion molecules. This should be looked at in CRC tissue, matched normal tissue, and in established peritoneal tumours of colorectal origin.

From the literature, cellular adhesion in PM is undoubtedly a complex multimolecular process. The interplay of adhesion molecule expression and the influence of signalling cascades at different points of tumour progression, might indicate that the analysis individual molecules and proteins in isolation may not be as important as looking at the relationship between the adhesion molecule on each other and where on the tumour and what stage the tumour is sampled. To attempt to analyse this using a multivariate model may provide further predictors of PM in patients with CRC.

3.4.4. Conclusions

The expression of HA-dependent adhesion molecules CD44, RHAMM and ICAM-1 has been shown to be increased in stage II CRC, when compared to normal and matched associated tissue. This indicates that these changes are not only present within colorectal tumour, but also involved in tumour cellular processes in the surrounding tumour microenvironment. High CD44 and ICAM appear to have a reduced DFS and OS, when compared to patients with low expression. There is however no difference related to patient gender or tumour location. There are no consistent significant differences to conclude definitively that there is any strong association between expression and tumour stage progression, correlating with the assorted conclusions from current published literature. Interestingly, mutations in oncogenes KRAS are associated with increased CD44 expression, TP53 with increased RHAMM expression and BRAF with ICAM-1 when compared to wild type forms, which warrants more detailed evaluation, particularly with potential for targeted subtype assessment and therapy.

However, it must be appreciated that the expression of all molecules may not be completely homogenous throughout an individual tumour particularly, as tumours progress and/or metastasise, that expression could change. Multimolecular pathways may account for overlapping phenotypic cellular functions, which may also contribute to some of the conflicting literature for certain molecules, regarding over- and under-expression.

Targeting HA-dependent adhesion will be explored in later chapters, to examine whether the ability of CRC to adhere to the mesothelium in the peritoneal environment can be disrupted, using a competitive inhibitory approach. Models mimicking the peritoneal environment *in vitro* will be explored. Then, if indeed, adhesion can be disrupted, it will be important to ascertain whether the cancer cells' ability to survive or adhere to other cells is affected. Furthermore, if it is possible to disrupt adhesion, this could potentially affect and change EMT expression.

Effects on cell adhesion and survival *in vitro* when targeting hyaluronic acid binding receptors

Chapter 4

4.1. Introduction

4.1.1. Anchorage and cellular survival

Folkman and Greenspan (1975) demonstrated cellular anchorage in many normal cells is extremely important for cell growth control (Folkman & Greenspan, 1975). This can also be translated, for many cancers, in terms of cellular physiology and cancer progress. Loss of attachment of various cells can induce cell death. The type of cell death can largely be dependent on the cell type, and includes apoptosis, non-apoptotic cell death and cell cycle arrest (Z. Deng, Wang, Liu *et al.*, 2021) The apoptotic process of cell death, in suspended epithelial cells, was termed “anoikis”, which means “homelessness” in ancient Greek (Frisch & Francis, 1994). While cancer cells may have mechanisms to avoid anoikis whilst in suspension, for peritoneal metastatic cells to proliferate in colorectal cancer they require the ability to reattach to an accommodating microenvironment (Mikula-Pietrasik *et al.*, 2018). This is a complex multimolecular process with many facets, with primary and alternative pathways, but it is often simplified to the “soil and seed” theory of peritoneal metastases, as described in Chapter 1.

4.1.2. Cell mechanisms of survival in colorectal cancer metastatic cells - stress and survival mechanisms

Detachment is a critical step for cancer metastases. However, in order to develop metastases at distant sites the cells need to be able to survive. Once cells are detached, they are exposed to different environmental and chemical conditions. These new stresses, which can include hypoxia, loss of nutrients, ATP deficiency and altered mechanical forces, can all affect cell behaviour.

Multiple signalling pathways are activated during cellular detachment and contribute to anchorage-independent survival, such as activation of the RAS-ERK and PI3K/AKT pathways, shown in Chapter 1.

Hypoxic CRC cells in solid tumours have been shown to have a higher metastatic capacity, through the expression of HIF1α and matrix metalloproteinases (MMP's) than cells in a normoxic state. The expression of these molecules has also been shown to promote migration, invasion and metastatic capacity of normoxic cells. IL-8 has been identified as a molecule involved within this process along with p65 through AKT mediated signalling regulation (Mi, Mu, Huang *et al.*, 2020; Rankin & Giaccia, 2016).

Within ovarian cancer (OvCa), it has been further verified that surgical peritoneal stress facilitates a pro-metastatic environment which exacerbates resistance to apoptosis via IL-8 through the AKT pathway (Pasquier, Vidal, Hoarau-Vechot *et al.*, 2018; Y. Wang, Xu, Zhang *et al.*, 2012). Where OvCa cells have been able to detach from primary tumours they are able to float passively to distant sites, during which time the host has time to recognise and eliminate these cells with intraperitoneal inflammatory cells. However, most cancerous cells are able to form clusters, in which they are able to attach to other cancerous cells, to promote survival within the peritoneal environment (Steinkamp, Winner, Davies *et al.*, 2013). The properties of cell-cell adhesion within the peritoneal environment thus prevent cell anoikis and increase the ability to survive in a free-floating state.

4.1.3. Anoikis evasion in anchorage-dependent colorectal cancer cells

Cell death is crucial in tissue homeostasis, organism development and host defence. Apoptosis is a programmed cell death mechanism. Cancer metastases can evade the 'cell death' mechanisms through activation of various cell signalling pathways and translocation mechanisms (J. Cooper & Giancotti, 2019; Fujii, Shimizu, Katoh *et al.*, 2021; Guha, Saha, Bose *et al.*, 2019). Integrin-associated signalling has been described to facilitate cell survival during cell detachment, which in turn can alter cell shape, proliferation and aid the ability to adhere at a distant site (Hehlgans, Haase, & Cordes, 2007). Cells having the ability to adapt to the changing environment facilitates survival. Several mechanisms have been described including, amongst others, cell cytoskeleton reorganisation to adapt to altered mechanical forces, adapting to ATP and nutrient deficiency to enhance cell metabolic efficiency, or alternatively supress metabolic activity and modify cell signalling , which are all associated with cell death evasion mechanisms (Z. Deng *et al.*, 2021).

4.1.4. Interruption to cell anchorage

Re *et al* (1994), demonstrated in endothelial cells that when suspended cells are prevented from adhering, cells rapidly lose viability with a half-life of approximately ten hours (Re, Zanetti, Sironi *et al.*, 1994). Cancer cells can evade cell anoikis mechanisms when free-floating. However, evasion mechanisms are unlikely to be indefinite while in suspension, particularly for the majority of cells that are anchorage-dependent. Cells which undergo cell cycle arrest or undergo dormancy typically undergo growth arrest while maintaining proliferative ability. More conventional drug therapy targets fast dividing cells, whereas dormant or quiescent cancer cells remain largely unaffected by such treatments (Damen, van Rheenen, & Scheele, 2021). Dormant cells will still require nutrition and the ability to

generate ATP. If such cells are anchorage-dependent, in order to proliferate and thrive, they will require an anchorage site to facilitate this. When considering this further, spilt or detached tumour cells during surgical tumour resection are unlikely to have undergone such rapid changes to adapt fully to a free-floating environment and are likely to attempt to adhere in order to survive. These cells are likely to be more susceptible to undergo anoikis if their ability to adhere is impeded. Delaying or disrupting adhesion may have a role in reducing local peritoneal recurrence at surgery for CRC.

4.1.5. Caspases and anoikis

Caspases are a family of proteases crucial for initiating and executing apoptosis within a cell. Initiation of apoptosis is multifactorial, and several signalling pathways converge on the activation of caspases, through both the intrinsic and extrinsic pathways (Figure 4.1). Anchorage-independent growth and epithelial mesenchymal transition are two factors associated with resistance to anoikis. Cancer cells develop anoikis resistance through a plethora of varied mechanisms facilitating survival.

Caspase-8 is the most upstream protease participating in the anoikis cascade. Activated caspase-8 can directly stimulate caspase-3 activity, via the extrinsic pathway, but can also contribute to the intrinsic pathway by cleaving Bid (BH3 interacting domain), which is a pro-apoptotic protein. This promotes mitochondrial pro-apoptotic factors leading to activation of caspase 9 (Paoli, Giannoni, & Chiarugi, 2013).

In caspase-3, cleaved and uncleaved forms are strong indicators of cell death induction. Cleaved caspase-3 propagates an apoptotic signal through protease activity on downstream

targets (Jelinek, Balusikova, Schmiedlova *et al.*, 2015). However, levels of cleaved caspase-3 have also been shown to correlate with cancer progression in tumour specimens (Hu, Peng, Liu *et al.*, 2014).

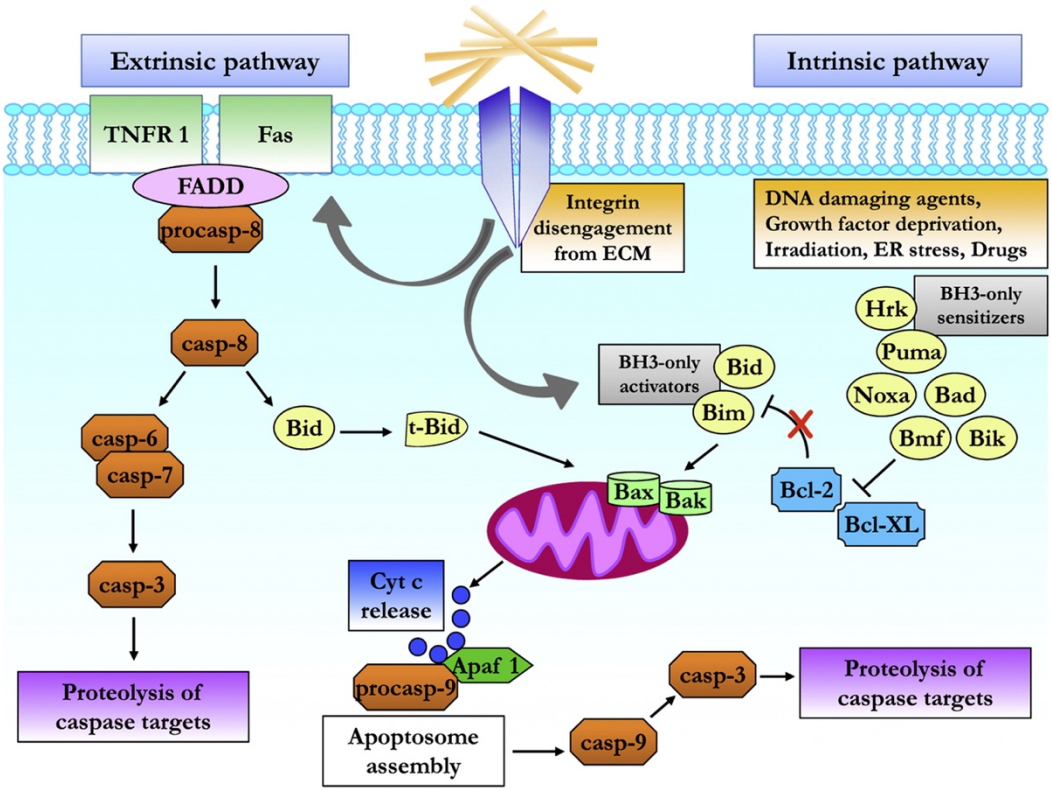

Figure 4.1. Molecular extrinsic and intrinsic pathways of anoikis and caspase cell signalling. Image taken from (Paoli *et al.*, 2013). The molecular abbreviations shown within the diagram are listed within the abbreviations section.

4.1.6. Chapter aims

The aims of this chapter are to:

1. Develop a peritoneal model in which to examine CRC cellular adhesion *in vitro*
2. Assess the effects on adhesion of treatment with a hyaluronic acid inhibitor
3. Examine the effects on survival when CRC cells lose anchorage
4. Assess the effects on CRC cellular aggregation when in suspension
5. Examine the response of CRC cells in suspension when treated with a hyaluronic acid inhibitor
6. Attempt to establish whether cells that are prevented from adhering in suspension undergo apoptosis

4.2. Materials and methods

4.2.1. Immunofluorescent cell staining

Immunofluorescence staining is a method to study subcellular and surface detection of proteins in fixed biological samples. It provides the ability to both detect and examine the distribution of proteins on and within cells. The methodology is described in Chapter 2.

4.2.2. An *in vitro* model of peritoneal cellular adhesion

The peritoneum is coated in a fluid film rich in glycosaminoglycans, of which HA is a predominant molecule. Cellular adhesion assays attempting to replicate the peritoneal environment must serve to provide a form of adhesion that replicates this environment.

One method to attempt to replicate this includes coating the bottom of plates with hyaluronic acid which is placed in solution on the plate and dried to fix to the plate bottom. The concentration of hyaluronic acid adherent to the plate bottom can be altered.

A second method to replicate this environment is to culture mesothelial cells to the plate, before adding CRC cells or treatment to this. The peritoneal cells will serve to mimic the peritoneum. The challenge with a co-culture model is differentiating mesothelial cells from CRC cells. To identify CRC cells adherent to the plate, the use of Dil stain (1,1'-Dopctadecyyl-3,3,3',3'-Tetrametylindocarbocyanine Perchlorate) is used to stain the CRC cells. Dil is a lipophilic membrane stain that diffuses to stain the entire cell. It is weakly fluorescent until incorporated into membranes. It provides an orange-fed fluorescent dye. It can be detected

using a EVOS M7000 cell imaging system (Thermofisher scientific Inc.). Figure 4.2 demonstrates an example of the plate image capture with Dil fluorescently stained HRT-18 colorectal cancer cells on the LP9 co-culture model

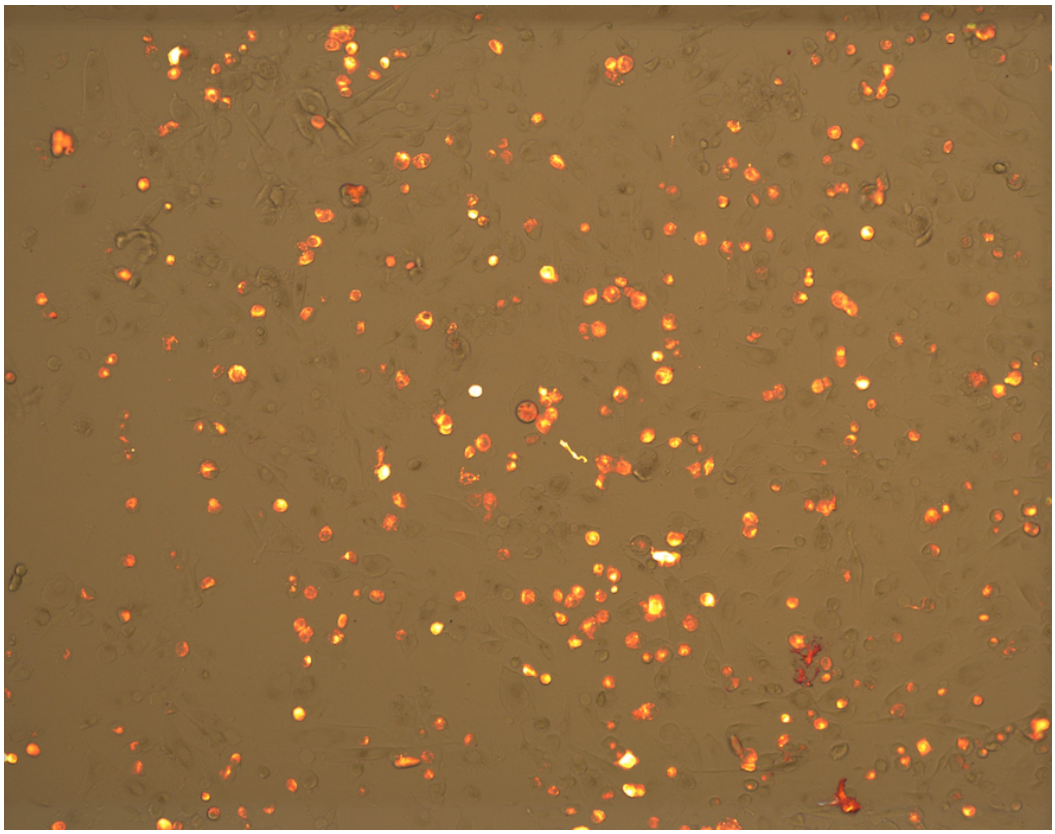

Figure 4.2. Dil stained HRT-18 colorectal cancer cells on the LP9 mesothelial coated co-culture model.

Matrigel is a soluble basement membrane matrix. When incubated in plastic tissue culture labware, the Matrigel proteins polymerise, which results in a recombinant basement membrane. This facilitates a way to study the complex cellular behaviour of anchorage-dependent cells that may not be replicated on plastic culture plates. Matrigel in this instance would serve as a positive control promoting cellular adhesion. An uncoated plate was used as a negative control comparator.

4.2.3. Examining cell survival in suspension

4.2.3.1. Trypan blue cell counting

Trypan blue is one of several stains recommended for viable cell counting. The method is based on the principle that viable cells do not take up certain dyes and non-viable cells do. Staining facilitates assessment and viewing of cell morphology. Cell counting methods using trypan blue are described in Section 2.13.1.

4.2.3.2. Cell viability

Free-floating CRC cells were examined in suspension as described in Sections 2.13.2 and 2.13.4. For cell viability, cells were pipetted gently to form a single cell suspension and placed into universal containers. Both viable and non-viable CRC cells were counted in triplicate, within each sample in each run of the experiment. For the HAi treated samples a concentration of 2µM within the 1ml suspension was used, based on previous adhesion assay experimentation. Two different concentrations of excess HA were used in treatment testing of cells: 312µg/ml and 624µg/ml respectively. Suspension samples of 10µl were taken at 0 minutes, 30 minutes, 1 hour, 4 hours, 6 hours, 12 hours, 24 hours, 48 hours, and 72 hours respectively.

4.2.3.3. Cell aggregation

Free-floating CRC cells were examined in suspension as described in Section 2.13.2. For cell aggregation, the cells were pipetted more extensively than in the cell viability assay, to ensure the proportion of cells commencing the experiment at time zero as a single cell suspension was maximised. Viable single cell and viable aggregated cells were counted in

triplicate within each sample. The experiment was repeated in triplicate. The same dosing concentrations of HAi and HA were used as set out in Section 4.2.3.2.

4.2.3.4. Cell Counting Kit-8

Cell counting kit-8 (CCK-8) is an assay based on detecting the dehydrogenase activity in the detection of viable cells, conditions, or chemicals. CCK-8 is a single solution allowing sensitive colorimetric assays for the determination of viable cells within cytotoxic and proliferation assays. The mechanism utilises Dojindo's water-soluble tetrazolium salt (WST-8). This produces a water-soluble formazan dye upon reduction in the presence of an electron mediator. When WST-8 is reduced by dehydrogenases in cells it produces an orange-coloured product (formazan) which is soluble in tissue culture medium. The amount of formazan produced is directly proportionate to the number of living cells. This can be measured using a plate reader at 450nm filtration. Fifteen wells from a 96-well plate were used, including both a positive and negative control.

4.2.4. Annexin V apoptosis detection assay and flow cytometry:

Treatment courses were undertaken of cells in free-floating suspension. Three treatment groups were examined, a HAi treated group, HA 312µg/ml and HA 624µg/ml. This was compared to both a negative control, with PBS and a positive control treated with sodium chlorite (NaClO). Cell suspensions following treatment, were processed, and transferred to the flow cytometer (BD FACS Canto II Flow Cytometer, Becton Dickenson & Co. Franklin, USA) following the Annexin V apoptosis assay protocol as set out in Section 12.13.6.

4.2.5. SDS-PAGE and Western blotting

SDS-PAGE electrophoresis and Western blotting was carried out in line with methods described in Section 2.12.

4.3. Results

4.3.1. Cell Lines

4.3.1.1. Expression of CD44 in colorectal cancer cell lines

Data from PCR shows that CD44 is strongly expressed in HT115, HRT-18 and Caco-2 cells.

The expression of CD44 in colorectal cancer cell lines is shown in Figure 4.3.

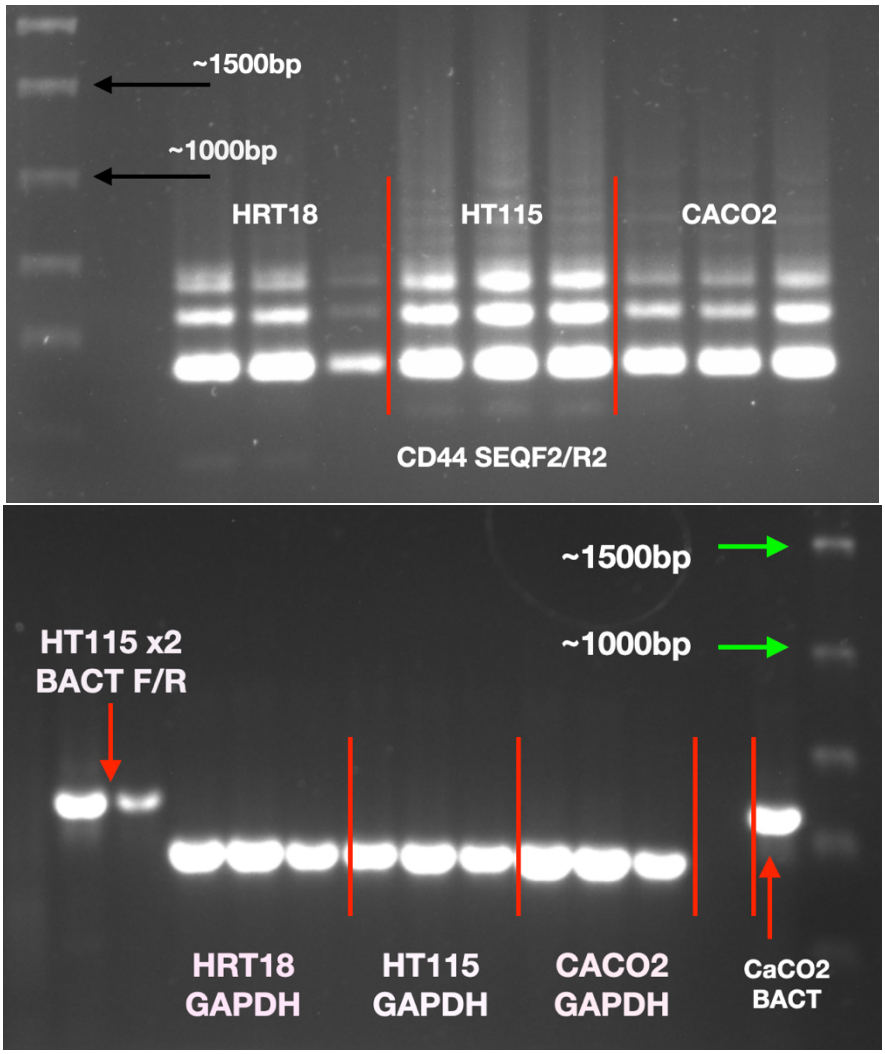

Figure 4.3. Expression of CD44 SeqF2/R2 in colorectal cancer cell lines – PCR results

Repeat agarose gel electrophoresis and gel extraction was undertaken for HT115 cells. Gels were sent for DNA sequencing to confirm primers used and to attempt to ascertain the CD44 variant for the primers, due to the many isoforms of CD44 described. Gel extraction was carried out as described in Section 2.10.

Three bands were obtained and quantified using a nanophotometer.

Large band: 16ng/µl

Medium band 35ng/µl

Small band 23ng/µl

DNA sequencing was undertaken by an in-house sequencing department. The sequencing was cross-checked using primer-blast. The large band was confirmed to be CD44v3. The medium band was found to be non-specific to any molecule. The small band was matched with several CD44 variants. The most likely variant is CD44v4. However, CD44 with various isoforms was confirmed present on the cell lines. The sequencing findings are summarised in Table 4.1.

Table 4.1. DNA sequencing of extracted PCR bands to examine CD44 and isoforms identified by PCR primers

Gel band size	CD44 Variant	Base pairs matching	Percentage match
Large	CD44v3	-	-
Medium	Nonspecific	-	-
Small	CD44v8	1173/1173	96%
	CD44v4	1173/1173	96%
	CD44 v7	1061/1061	86%
	CD44 v2	1059/1176	96%
	CD44 v6	1057/1174	96%
	CD44v1	1057/1174	96%
	CD44 v3	1057/1174	96%

Western blot to demonstrated protein expression was challenging. Several technique refinements were made, with particular attention to setting up the resolving and stacking gels. However, the protein bands for CD44, although present, were not clearly demonstrated due to background artifact as seen in Figure 4.4.

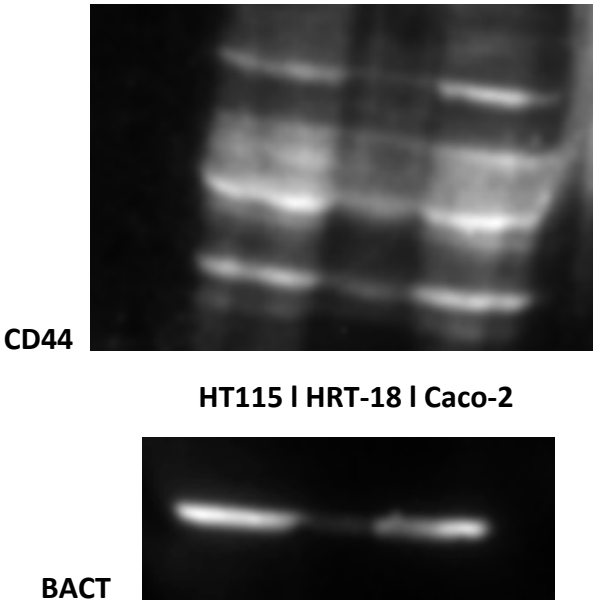

Figure 4.4. CD44 protein expression in HT115, HRT-18 and CACO cell lines

4.3.1.2. Expression of RHAMM in colorectal cancer cell lines

Data from PCR shows that RHAMM is strongly expressed in HT115, HRT-18 and Caco-2 cells. with two isoforms. The expression of RHAMM in colorectal cancer cell lines is shown in Figure 4.5. Western blot also confirmed two isoforms of RHAMM in the three cell lines, shown in Figure 4.6.

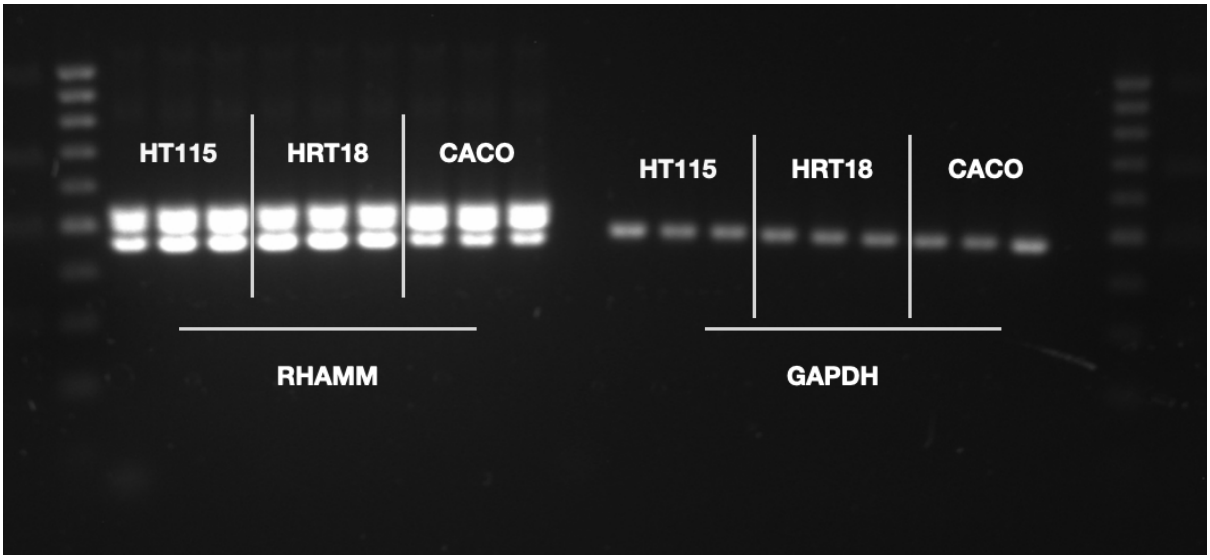

Figure 4.5. Expression of RHAMM in colorectal cancer cell lines. – PCR results. RHAMM expression: Channels 1-3 HT115, 4-6 HRT-18 and 7-9 Caco-2. 10 RHAMM Negative Control. GAPDH housekeeping gene expression: Channel 11-13 HT115, 14-16 HRT-18, 17-19 Caco-2. 20 GAPDH negative control. Two isoforms of RHAMM expressed

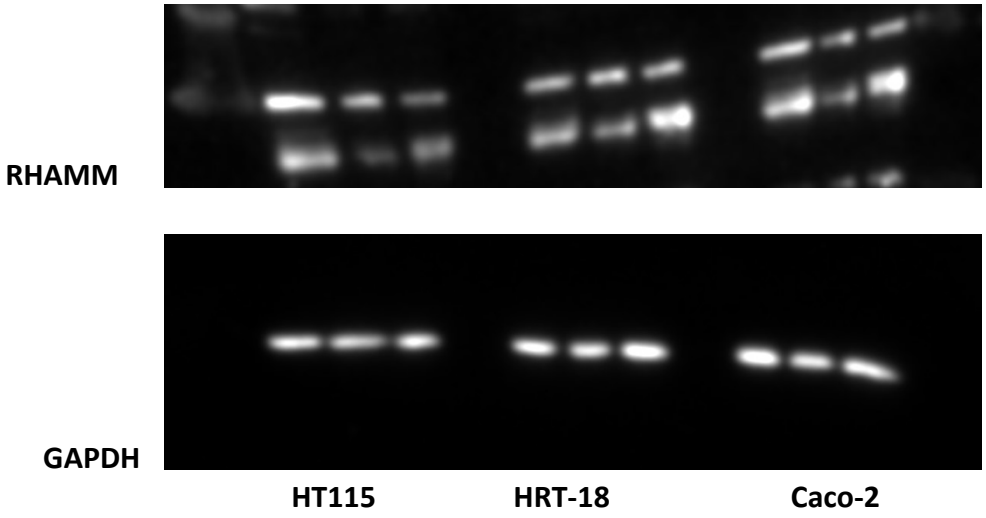

Figure 4.6. RHAMM protein expression in HT115, HRT-18 and Caco-2 colorectal cancer cell lines. Two isoforms are demonstrated.

4.3.1.3. Expression of CD44 in LP9 mesothelial cells

Expression of CD44 in LP9 mesothelial cells was demonstrated by PCR (Figure 4.7). Surface expression of CD44 was confirmed in LP9 cells by immunofluorescence and photographed using a fluorescent microscope at x40 magnification (Figure 4.8). Red fluorescence denotes CD44 antibody staining.

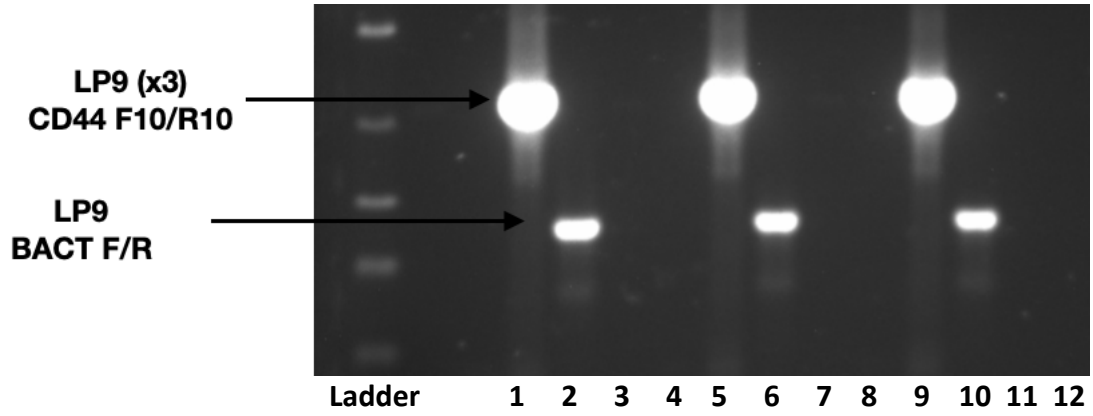

Figure 4.7. Serum electrophoresis demonstrating CD44 expression in LP9 mesothelial cells- PCR results. Row 1,5 and 9 shows LP9 expression. Rows 2,6 and 10 BACT control expression. Row 3,7 and 11 negative control LP9. Rows 4,8 and 12 negative control BACT. One Isoform of LP9 expressed at approx. 1000Kda

a. b.

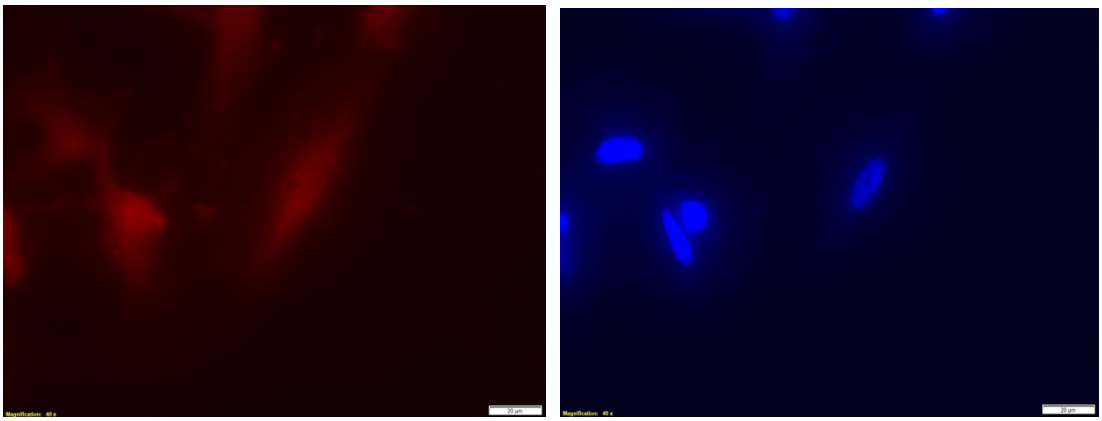

c.

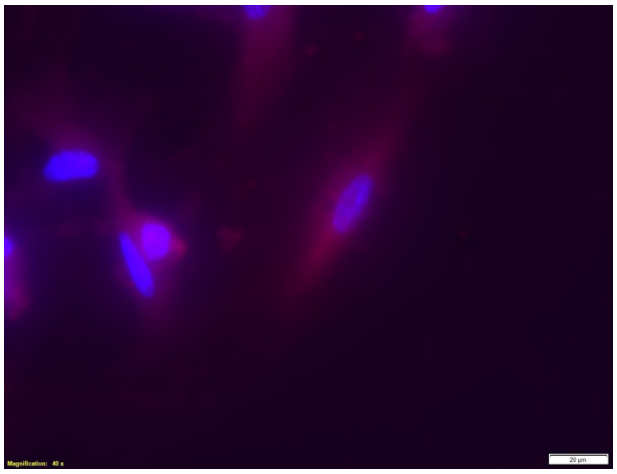

Figure 4.8. CD44 Antibody staining of LP9 mesothelial cells. 4.7a. Demonstrates CD44 expression shown with the red staining. c. Stained in blue denotes DAPI nuclear staining. c. Merged CD44 and DAPI staining. Fluorescent microscope images taken at x40 magnification.

4.3.2. Colorectal cancer cellular adhesion

4.3.2.1. Effect of hyaluronic acid coated plate on CRC cellular adhesion

The first peritoneal model was a hyaluronic acid coated plate. The plate was prepared using high molecular weight hyaluronic acid placed in solution with PBS at a set concentration into each of the wells being tested. The plate was dried in a plate drier at 60-80°C to evaporate the PBS solution. The hyaluronic acid was left set dried onto the bottom of the plate and was ready to be used for adhesion experimentation. Concentration selection assessed a sequenced range of HA concentrations and assessed cellular adhesion through both cell counting and absorbance. A preliminary experiment assessed untreated cellular adhesion, with a range of five concentrations of HA coating. This demonstrated a reduction in CRC cellular adhesion (Figure 4.9). This was further expanded to assess a greater range of HA coating concentrations and the technique was refined, in terms of coating the plates and cell seeding numbers for each experiment.

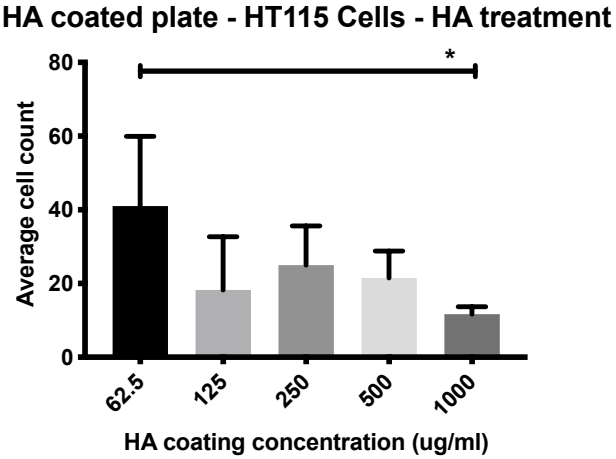

Figure 4.9. Preliminary experiment assessing HA plate coating and cellular adhesion of HT115. A reduction in cell adhesion was demonstrated at increases in HA concentration when compared to the lowest concentration used at 62.5µg/ml and was statistically significant at 1000µg/ml.

As expected, lower concentrations of HA demonstrated a reduced number of CRC cells adherent to the plates. As concentration increased cellular adhesion also increased and peaked at a concentration of 78.125µg/ml. This was demonstrated in both cell counting and crystal violet absorbance of HT115 cells (Figure 4.10).

The unexpected finding from this initial testing was that above 78.125µg/ml there was a significant reduction in cellular adhesion as HA concentration continued to increase. This optimal dose response indicated that a threshold concentration may prevent or hinder cellular adhesion. When considering this further, by flooding the system with excess exogenous HA, there will be a proportion of HA molecules in solution unbound to the bottom of the plate. As a result, these free-floating molecules of HA can in themselves act as a competitive inhibitor to the HA molecules anchored to the bottom of the plate. As a result, it may be possible to utilise excess exogenous HA to prevent CRC adhesion to the peritoneum.

To take this further, treatment with HA, as well as a hyaluronic acid inhibitor (HAi), would be used in further experimentation. For the HA coated plate experiments, to maximise cell adhesion to the plate, a concentration of 80µg/ml was chosen as a result of this.

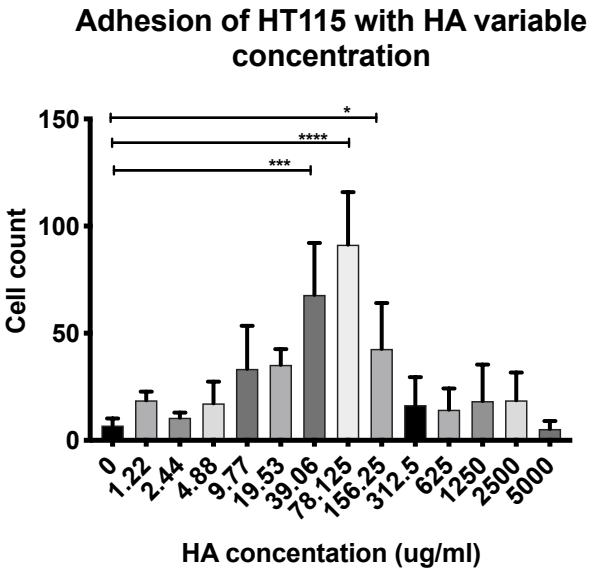

a.

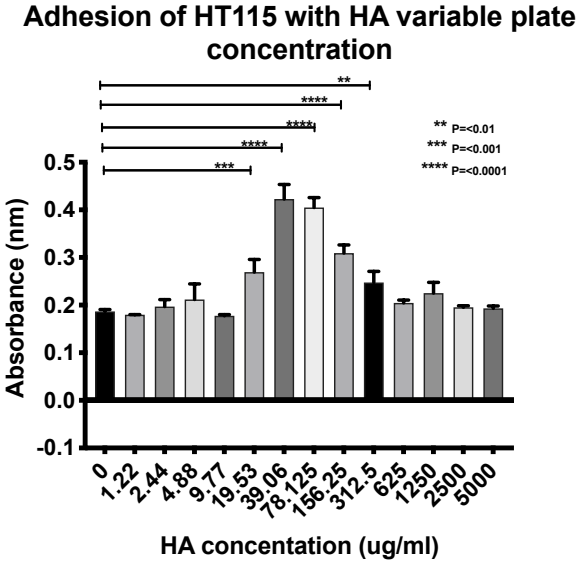

b.

Figure 4.10. HA-coated plate and examination of HT115 cellular adhesion. Figures demonstrate the peak HA concentration of maximum adhesion of HT115 cells. 4.10a cell counting methodology using EVOS and image J. 4.10b Crystal violet absorbance plate reading adhesion assay cell count of HT115 cells on a HA-coated plate with incremental dose increases of excess hyaluronic acid (HA). There is an optimum dosing concentration which demonstrates maximum cellular adhesion to the plate which peaks. At higher doses the levels of adhesion decrease. A greater than 50% decrease in adhesion is seen at a HA concentration of 156.25µg/ml or more, when compared to peak concentration of 78.125µg.ml.

4.3.2.2. Matrigel-coated plates and CRC cellular adhesion

Matrigel was set on the plates, the same as was carried out with hyaluronic acid described in Section 4.3.2.1. A range of Matrigel concentrations were tested on with Caco-2 and HRT-18 cells (Figure 4.11). Higher yields of cells were found to be adherent at concentrations of 20-40µg/ml in comparison to an uncoated plate. A Matrigel coated plate at 20µg/ml was prepared and 20,000 HT115 cells were seeded. This produced replicable results which were not significantly different. The range of mean cell count for three independent repeats was between 60-94 cells and would be reasonable for manual counting methods (Figure 4.12).

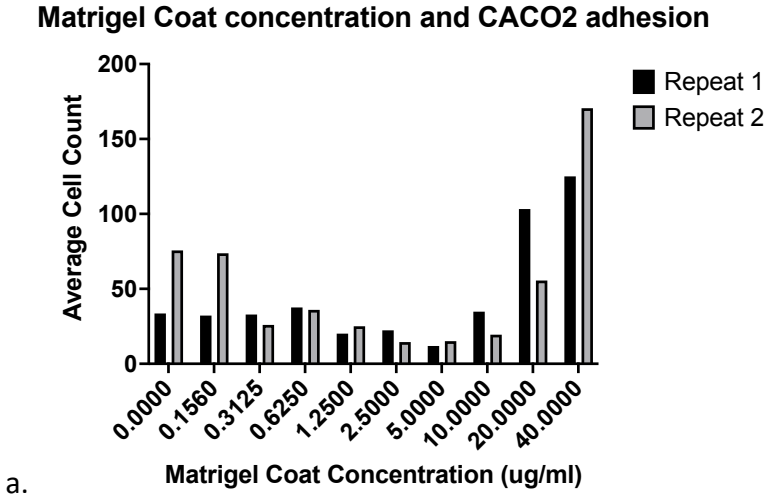

a.

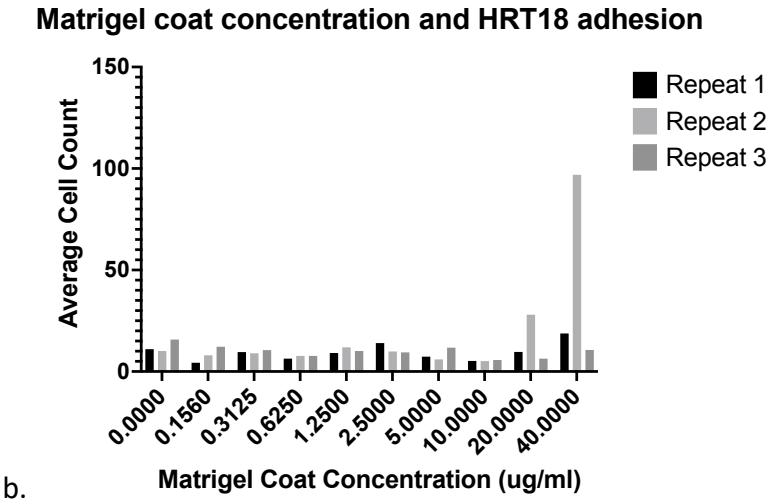

b.

Figure 4.11. Adhesion assays with Matrigel coated plates at a range of concentrations and colorectal cancer cell lines Caco-2 and HRT-18. 4.11a. Caco-2 cells completed in triplicate with two independent repeats. 4.11b. HRT-18 cells completed in triplicate three independent repeats.

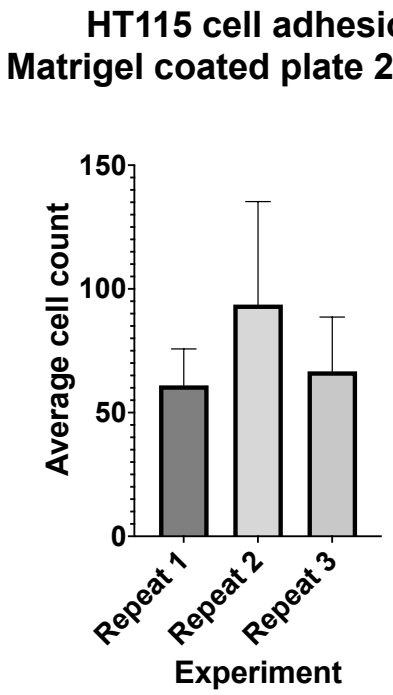

Figure 4.12. Matrigel coated plate at 20 µg/ml and Colorectal cancer cell adhesion. Mean cell count completed in triplicate of three independent repeats.

4.3.2.3. CRC cell lines and co-culture adhesion assay model

For initial testing of the co-culture model 20,000 CRC cells, which were untreated, were seeded on an LP9 coated plate and the degree of adhesion was assessed. All three cell lines had a reasonable degree of cellular adhesion to the peritoneal model (Figure 4.13). HRT-18 was significantly more adherent than Caco-2 (p=<0.0001) and HT115 (p=<0.0001) CRC cells. There was no significant difference between HT115 and Caco-2 (p=0.1934).

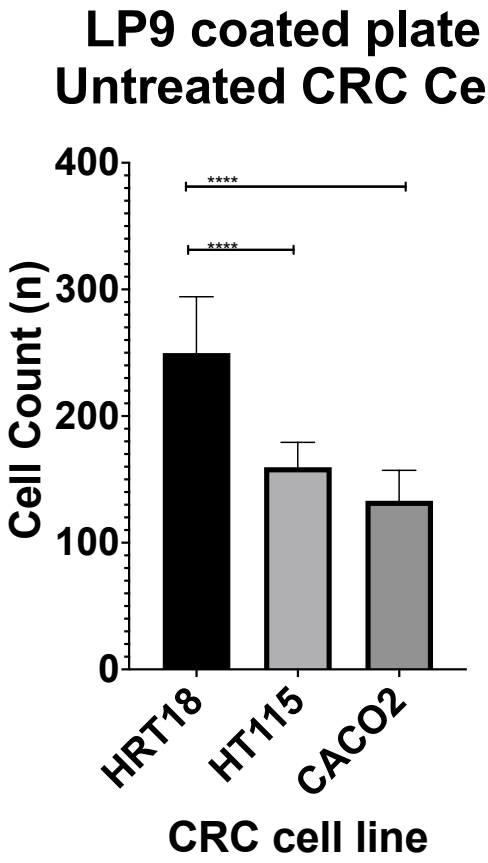

Figure 4.13. LP9 co-culture peritoneal model using DiI staining and EVOS plate reading, to differentiate CRC cells from peritoneal cells. Cells were seeded in equal numbers (20,000 cells). There was no significant difference between adhesion of HT115 and Caco-2 cell lines to LP9 (p=0.1934). There was a significant difference between HRT-18 adhesion to LP9 and both HT115 (p=<0.0001) and Caco-2 (p=><0.0001).

4.3.2.4. Dose dependent response of hyaluronic acid inhibitor on adhesion

When examining potential dose regimens of HAi to administer to cell lines, a range of HAi concentrations were used. A stock concentration of 400µM of HAi (AnaSpec Inc, Fremont, California, USA) was diluted down using DMEM or PBS. An initial concentration range of 0.156µM-20µM was used and compared to an untreated control. A HA-coated single cell culture peritoneal model was used, and absorbance was assessed. There was a significant reduction in cellular adhesion when compared to control (Figure 4.14)

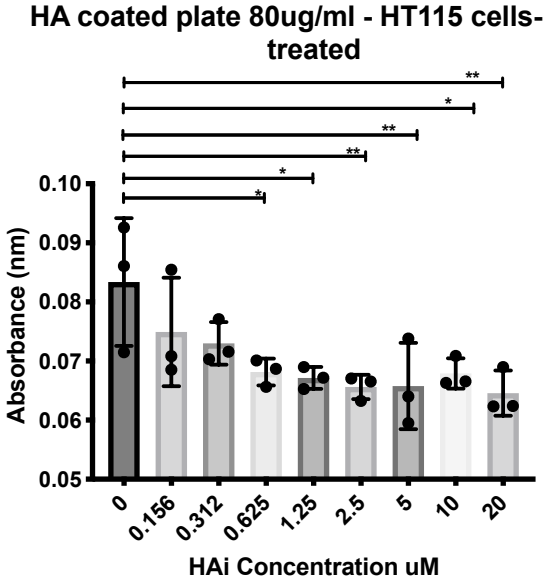

Figure 4.14. Adhesion assay absorbance of HT115 cells on a HA coated plate with dose increases of hyaluronic acid inhibitor (HAi). At doses of 0.625µM HAi there was a significant reduction in HT115 cellular adhesion compared to control (p=0.0277)

4.3.2.5. Effect of hyaluronic acid inhibitor on adhesion with HT115 cell line

HT115 cells were treated with HAi as described in Chapter 2 and 4.2.2. using a 96-well plate. A total of 10,000cells/well were seeded. The experiments were repeated in triplicate with three independent repeats. For the non-coated plate and the Matrigel coated plate there was no significant difference found in adherent cell count when compared to the controls.

However, in the peritoneal models both the HA-coated plate and the LP9 co-culture plates there was found to be a significant reduction in adhesion, when treated with HAi and the degree of adhesion reduced as the concentration of the inhibitor was increased. This was statistically significant (Figure 4.15 Appendix 2.1-2.4). For the HA-coated plate, when the experiment was normalised to the untreated control, there was a mean reduction of 65.6% in adhesion, in the HA-coated plate at a maximum HAi treatment concentration of 20µM. For the LP9 coated plate, there was a mean reduction of HT115 adhesion of 59.4% at the HAi treatment concentration of 20µM, when compared to the normalised control (Figure 4.16)

The inference taken is that the peritoneal *in vitro* models attempting to mimic HA-dependent adhesion have shown a reduction in cellular adhesion, when treated with a competitive inhibitor, compared to an untreated control.

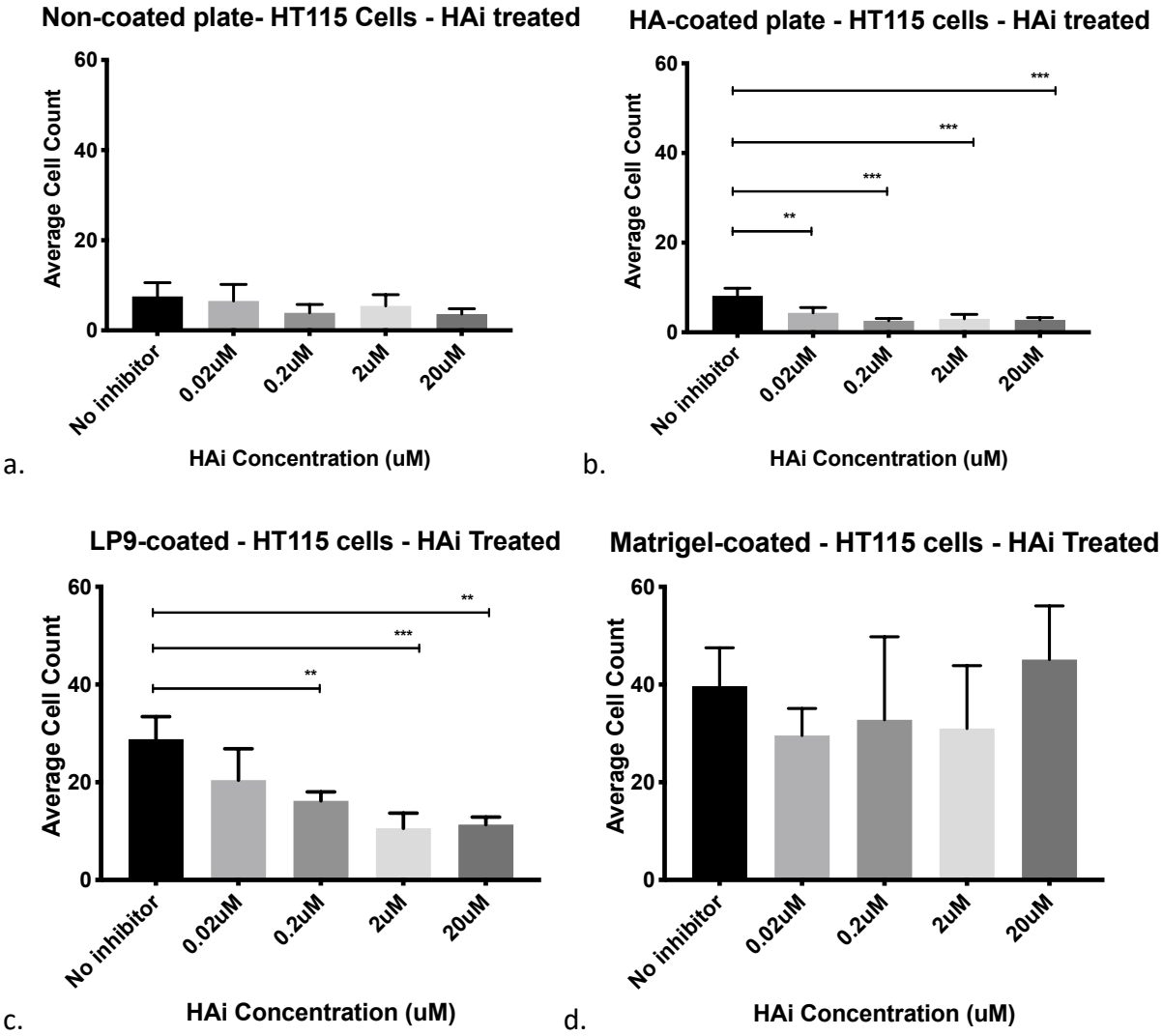

Figure 4.15. HT115 cells treated with HAi. 4.15a non-coated plate. 4.15b HA-coated plate, 4.15c LP9-coated plate, 4.15d. Matrigel-coated plate. There was a statistically significant reduction in CRC adhesion with HAi treatment in the peritoneal LP9-coated and the HA-coated plates.

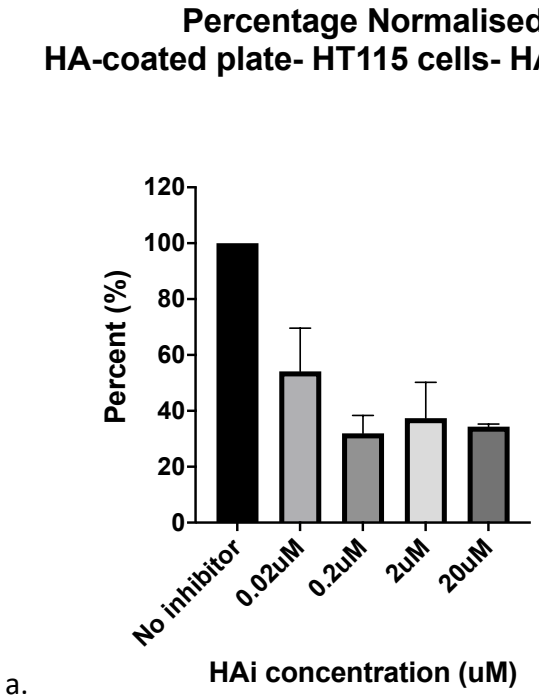

a.

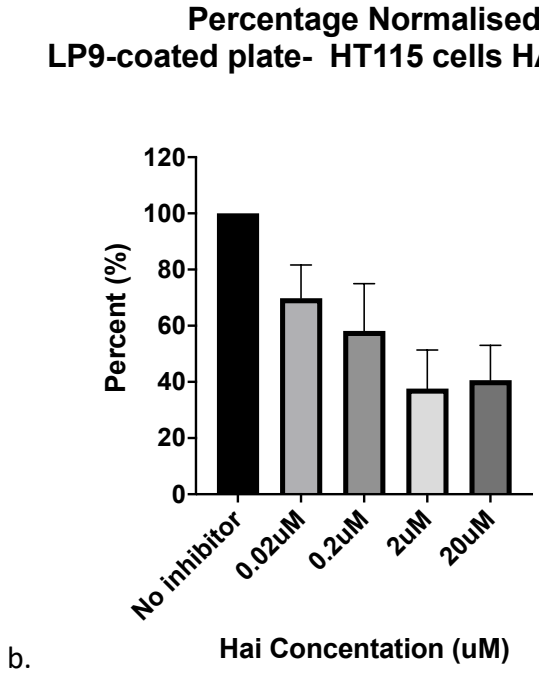

b.

Figure 4.16. Percentage change in adhesion with treatment of HAi when compared to a normalised untreated control. 4.16a HAi treatment of HT115 cells on a HA-coated plate. 4.16b. HAi treatment of HT115 cells on an LP9-coated plate.

4.3.2.6. Effect of hyaluronic acid inhibitor on adhesion with HRT-18 cell line

HRT-18 cells were treated with HAi on the co-culture LP9 seeded model. There was an observed 28.7% reduction in adhesion at 20µM HAi treatment when compared to the normalised untreated control. There was a similar reduction in adhesion at all HAi treatment concentrations. (Figure 4.17)

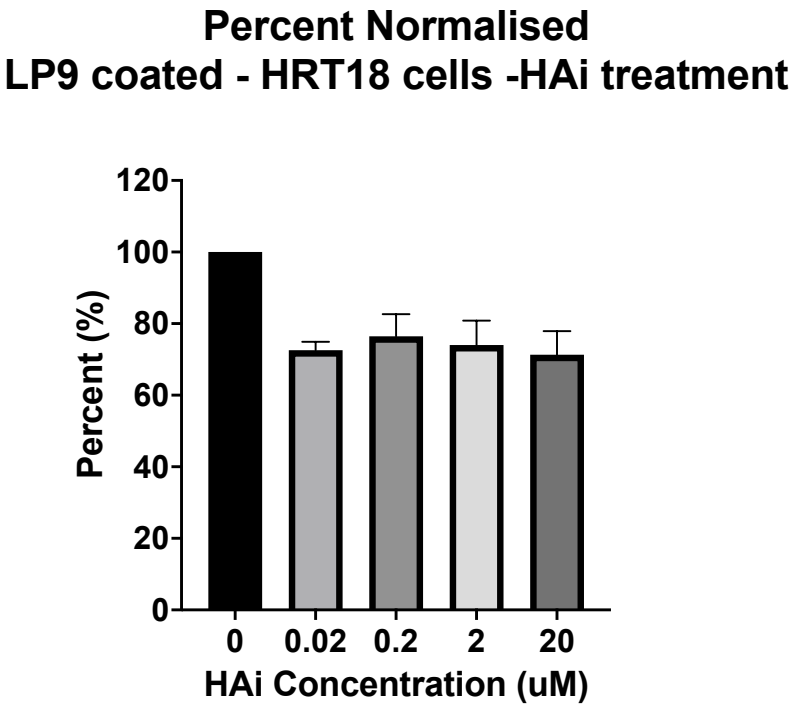

Figure 4.17. LP9 mesothelial co-culture peritoneal model. HRT-18 cells treated with HAi and compared to an untreated control. Percentage comparison was normalised to the untreated control. There was a reduction in adhesion in the HAi treated group.

4.3.2.7. Effect of hyaluronic acid inhibitor on adhesion with Caco-2 cell line

Caco-2 cells were treated with HAi on the LP9 seeded co-culture peritoneal model. There was seen to be a 19.1% reduction in cellular adhesion at 20µM HAi when compared to the untreated control, where the control was normalised. (Figure 4.18). All HAi treated groups had a reduction in cellular adhesion when compared to the untreated control.

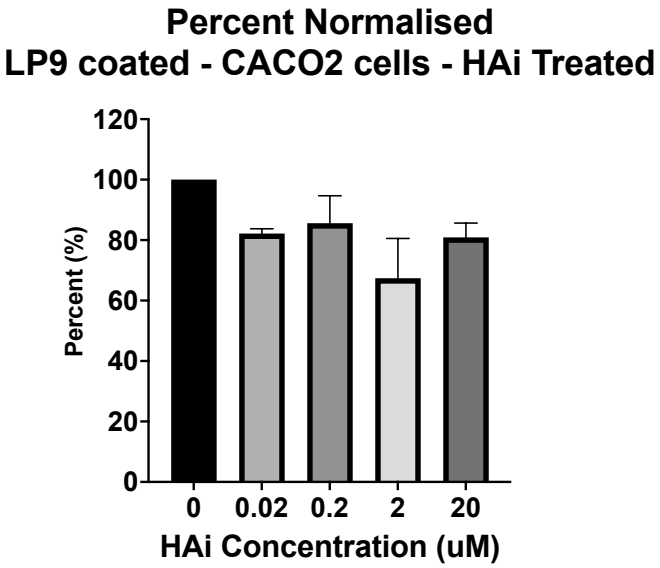

Figure 4.18. LP9 mesothelial co-culture peritoneal model. Caco-2 cells treated with HAi and compared to an untreated control. Percentage comparison was normalised to the untreated control. There was a reduction in adhesion in the HAi treated group.

4.3.2.8. Effect of excess exogenous hyaluronic acid on CRC cellular adhesion

LP9 co-culture plates treated with excess exogenous hyaluronic acid were tested in the three CRC cell lines. There was a reduction in cellular adhesion in all three cell lines with increasing concentration of excess HA. The largest reduction was at 1250µg/ml in all three cell lines. Experiments were repeated in triplicate with three independent repeats. Figure 4.19 demonstrates average percentage reduction in cellular adhesion when normalised to the untreated control.

For Caco-2 cells there was an average 49.2% reduction in CRC adhesion when compared to the untreated control at 1250µg/ml excess HA. For HRT-18 cells there was an average 49.0% reduction in CRC adhesion when compared to the untreated control at 1250µg/ml excess HA. Finally, for HT115 cells there was an average 36.1% reduction in CRC adhesion when compared to the untreated control at 1250µg/ml excess HA.

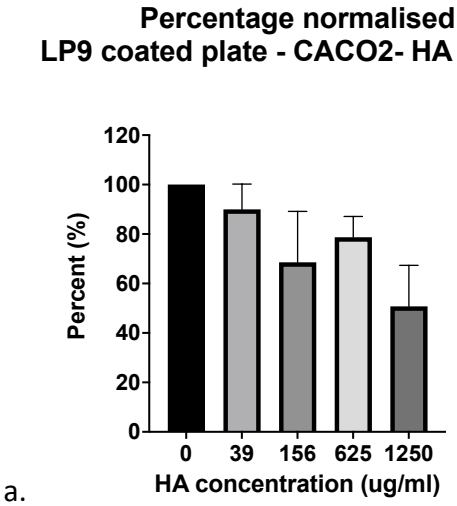

a.

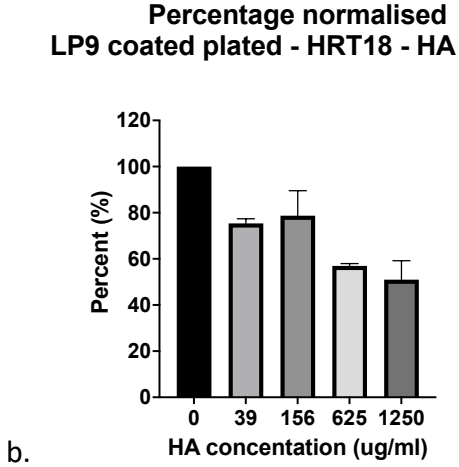

b.

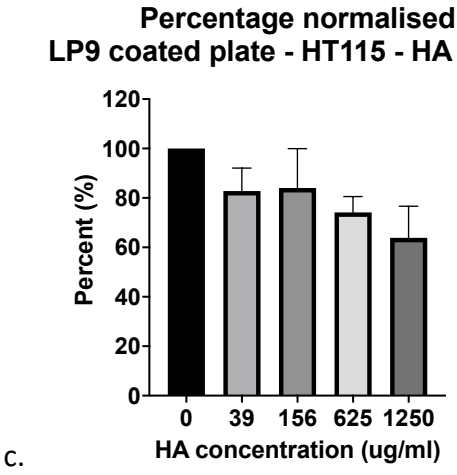

c.

Figure 4.19. LP9 co-culture treated with excess exogenous hyaluronic acid (HA). Percentage adhesion reduction normalised to untreated control. 4.19a. Caco-2 cells. 4.19b. HRT-18 cells. 4.19c. HT115 cells.

4.3.3. A peritoneal model for free-floating colorectal cancer cells *in vitro*

Three CRC cell lines were examined over time, to assess their response to survival when in an uncoated non-adherent container, whilst untreated. For the method to be able to be interpreted when the cells were treated, it was important to start with a high percentage of cells viable at time zero, as well as a high percentage of cells in single cell suspension. Initial examination assessed three CRC cell lines undergoing treatment and were compared to a control.

4.3.3.1. Preliminary experimentation with HRT-18

Initial experimental runs of the trypan blue cell count experiment initially demonstrated low yields of viable cells at 0hrs time point (Mean 59.12%, SD ± 18.53%), whereas, within the cell aggregation experiment, there were high yields of clumped cells from the outset of the experiment (Mean 63.50% SD ± 6.25%) (Figure 4.20). It was hypothesised that the reasons for this were likely down to experimental technique. Several steps of the technique were modified as described in 4.3.3.2 and repeat results were obtained.

a.

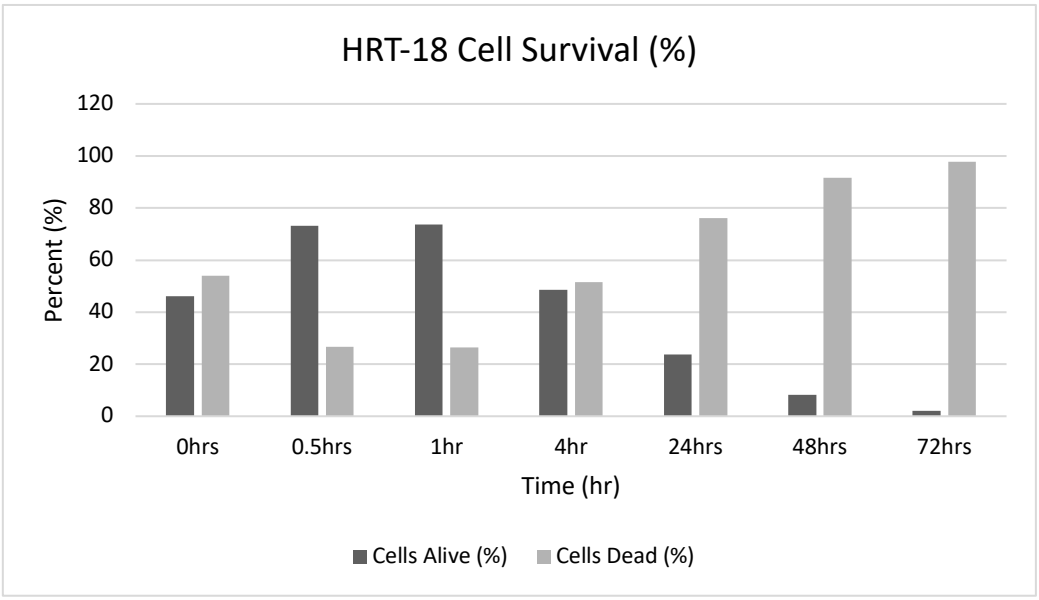

b.

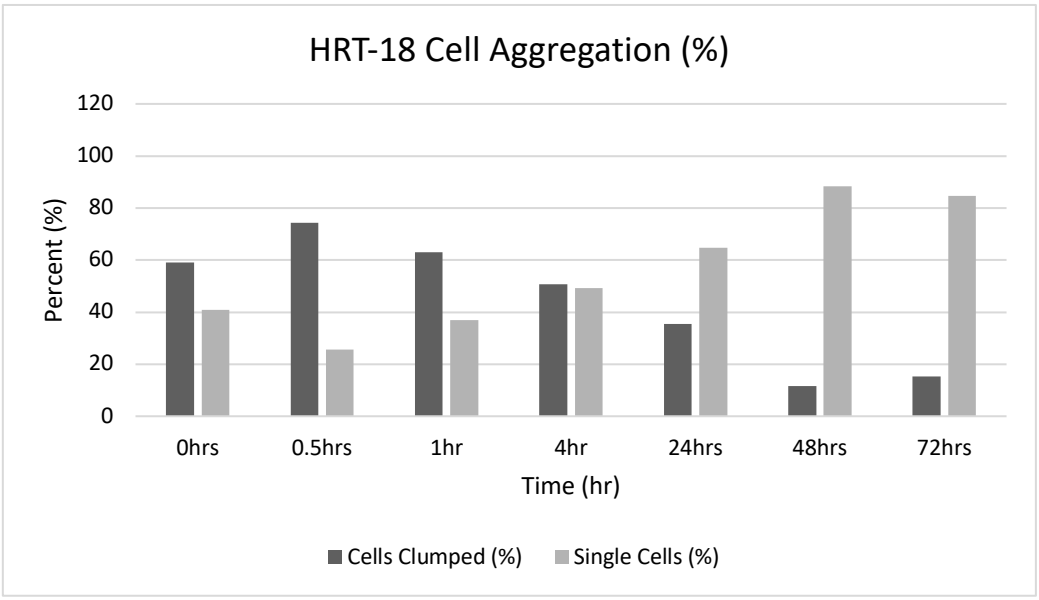

Figure 4.20: 4.20a Untreated HRT-18 CRC cells in suspension with assessment of cell viability over time following refinement of cell harvesting technique. 4.20b Untreated HRT-18 CRC cells in suspension with assessment of cell aggregation over time. Figures are representative of two independent repeats undertaken in triplicate.

4.3.3.2. Trypan blue cell counting optimisation

Starting with a viable percentage of cells at time zero, at 46% would not provide reliable results in which to compare to when cells underwent treatment. Several changes were made to modify the cell preparation technique. Firstly, the cells used for harvest were ensured to have only 60-70% maximum flask coverage, to reduce non-viable floating cell contamination extracted directly from the flasks. Secondly, the overall time taken to prepare the cells was able to be reduced, as the technique became familiar to perform reducing overall time. Thirdly the duration the cells were detached from the flasks using trypsin was reduced and standardised. Next, the time taken to incubate the cells in trypsin was also decreased. This standardisation in processing facilitated an increased yield of viable cells at time zero of the experiment which was reflected in repeat experimentation. For HRT-18 cells viable cells were able to be increased initially from 46.02%, to 72.22% to finally a mean of 88.34% ± 4.03% over two independent experiments.

Regarding aggregation experimentation, the trypsinisation time was increased by a few minutes longer than the viability assay and, pipetting technique was standardised to break up cells from clusters in both a more effective way to minimise cell lysis at when commencing the experiment.

4.3.3.3. Untreated free-floating HRT-18 CRC cells and effects on cell viability and aggregation

After refining the suspending cell assay methodology with HRT-18 CRC cells a much higher percentage of viable cells from the outset of the experiment at time zero, was yielded (Mean 88.3% SD ±4.03%). As the time course progressed in the viability assay, there was a trend towards decreased cell viability and increased non-viable cells over time. The most significant drop in cell viability was seen at 24 hours. By 72 hours there remained a mean of 28.2% (SD ±0.17%) of cells viable (Figure 4.21a).

In terms of aggregation, at time-0 there were a higher percentage of free-floating cells obtained than during the preliminary experiments (82.5%) and only 17.5% of cells were found adherent to other cells. Over time, the percentage of untreated viable cells increased in the percentage of aggregated cells when compared to single cells in the suspension. At 72-hours the percentage of aggregated cells had increased to 45.3% and single cells had decreased to 54.7%. (Figure 4.21b).

Subjectively, it was observed that HRT-18 CRC cells were particularly adherent and require a longer time period in order to detach from incubation flasks when compared to HT115 cell lines. However, HRT-18 cells overall behaved in a similar manner to that of HT115 cells under the experimental conditions.

a.

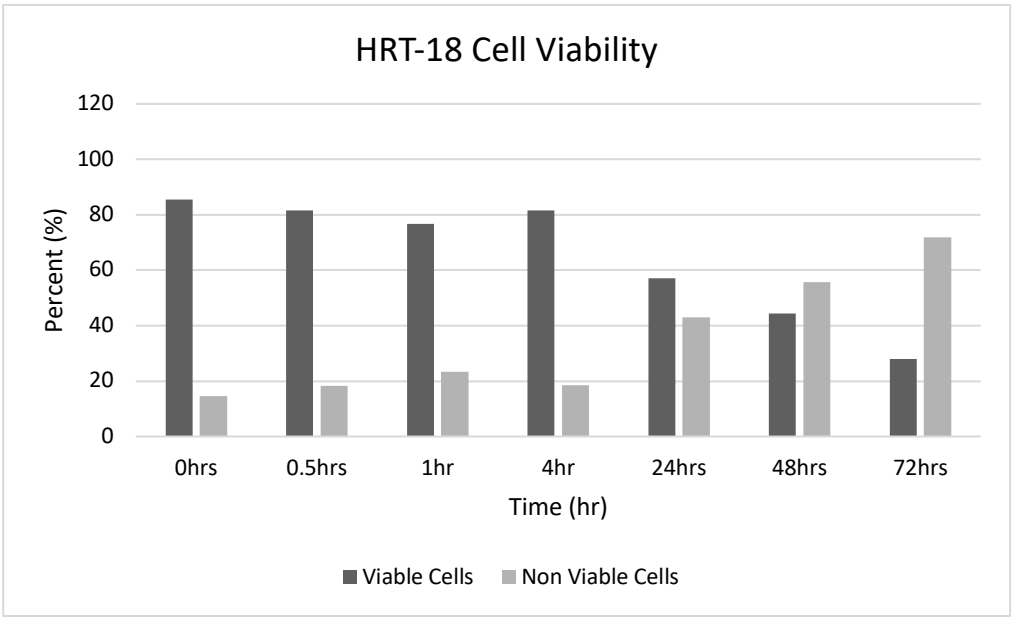

b.

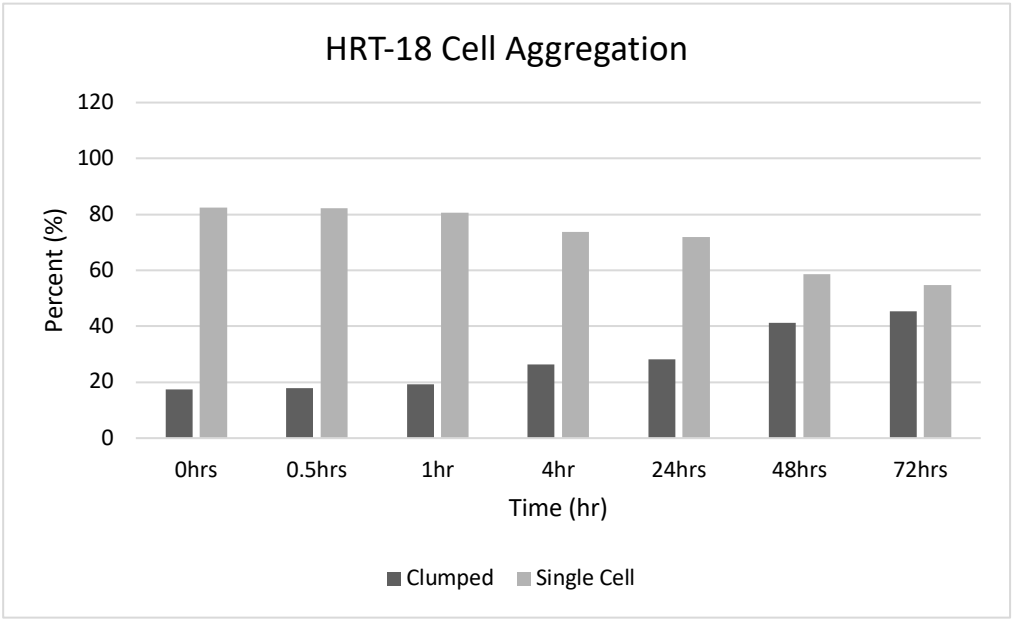

Figure 4.21: 4.21a Untreated HRT-18 CRC cells in suspension with assessment of cell viability over time following refinement of cell harvesting technique. 4.21b Untreated HRT-18 CRC cells in suspension with assessment of cell aggregation over time. Figures are representative of two independent repeats undertaken in triplicate.

4.3.3.4. Untreated free-floating HT115 CRC cells and effects on cell viability and aggregation

Subjectively, as described in 4.3.3.3, the HT115 cells were easier cells to detach and handle within this experimentation than HRT-18 cells in terms of cell detachment from plates and producing a single cell suspension.

Figure 4.22a demonstrates cell viability over time during the experimental time course of 72-hours. Overall cell viability decreased over time and non-viable cell counts increased over the time course of the experiment. Cell survival for untreated cells at time-zero showed 99.8% of cells were viable. At four hours there was a decline in cell viability of 11.84% and by 24 hours viability had reduced by 19.5% (80.3%). By 48 hours cell viability was at 19.7% and at 72 hours 8.1%. This demonstrated that the viability of anchorage dependent CRC cells reduced the longer they were left in suspension and were free-floating.

Figure 4.22b demonstrates HT115 cell aggregation over time during the 72-hour time course. At time-zero, on commencing the experiment a yield of 90.3% of cells were in single cell suspension and 9.7% were aggregated cells. At 24hours there was a decrease in free-floating viable single cells to 74.2%, with an increase to 25.8% of aggregated cells. By 48hours, aggregated cells had increased to 54.4% and single cell viable cells had decreased to 45.5%.

a.

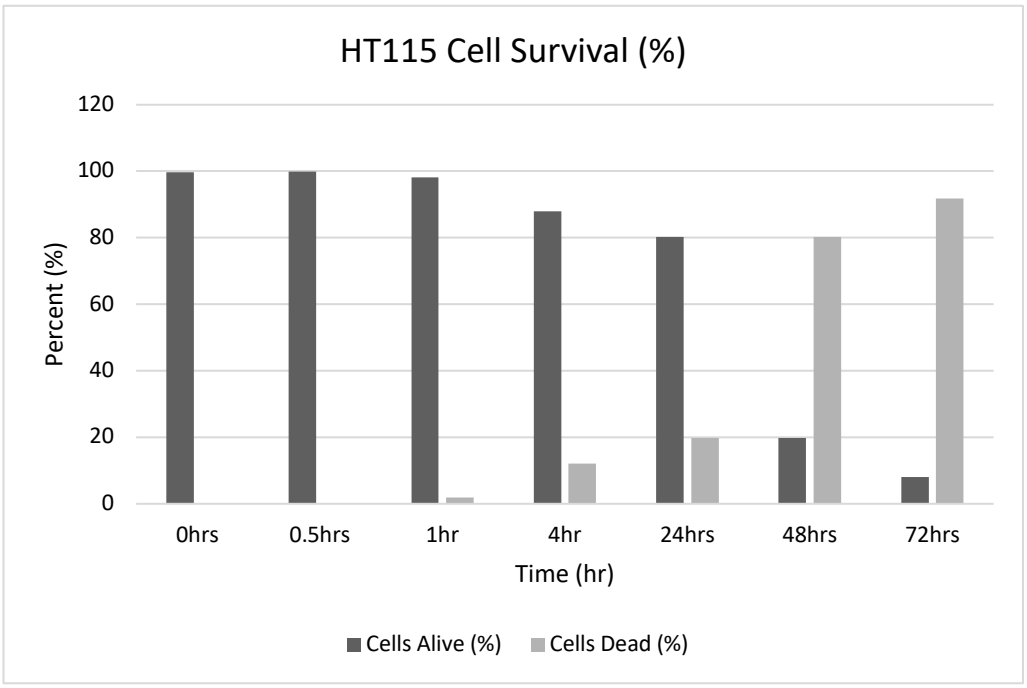

b.

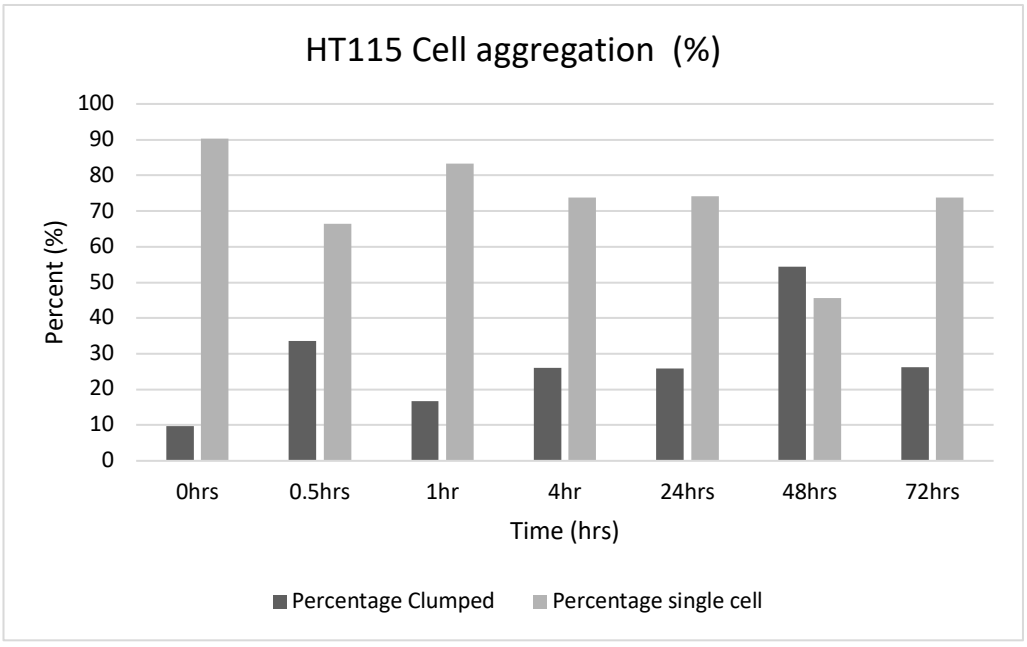

Figure 4.22: 4.22a Untreated HT115 CRC cells in suspension with assessment of cell viability over time following refinement of cell harvesting technique. 4.22b Untreated HT115 CRC cells in suspension with assessment of cell aggregation over time. Figures are representative of two independent repeats undertaken in triplicate.

4.3.3.5. Untreated free-floating Caco-2 CRC cells and effects on cell viability and aggregation

Caco-2 CRC cells behaved differently in respect to cell clumping compared to HRT-18 or HT115 cells. Cells readily clumped together to such a great extent by 48hours that it was not possible to individually count the cells. As a result, viability of the cells was able to be extended for a much longer period of time when compared to HT115 and HRT-18 cells. Two independent experiments were repeated, which verified these findings. At 24hours of cells in suspension the mean percentage of cells viable was 76.99% ± 0.21% (Figure 4.23a). The level of aggregation in Caco-2 cells was large at 4-hours and were aggregated to the extent that it was not possible to assess separate clumps of cells accurately (Figure 4.23b). In order to examine cells under treatment further and be able to compare them to control experimentation it was not possible to examine Caco-2 cells further for this series of experiments. (Figure 4.23).

a.

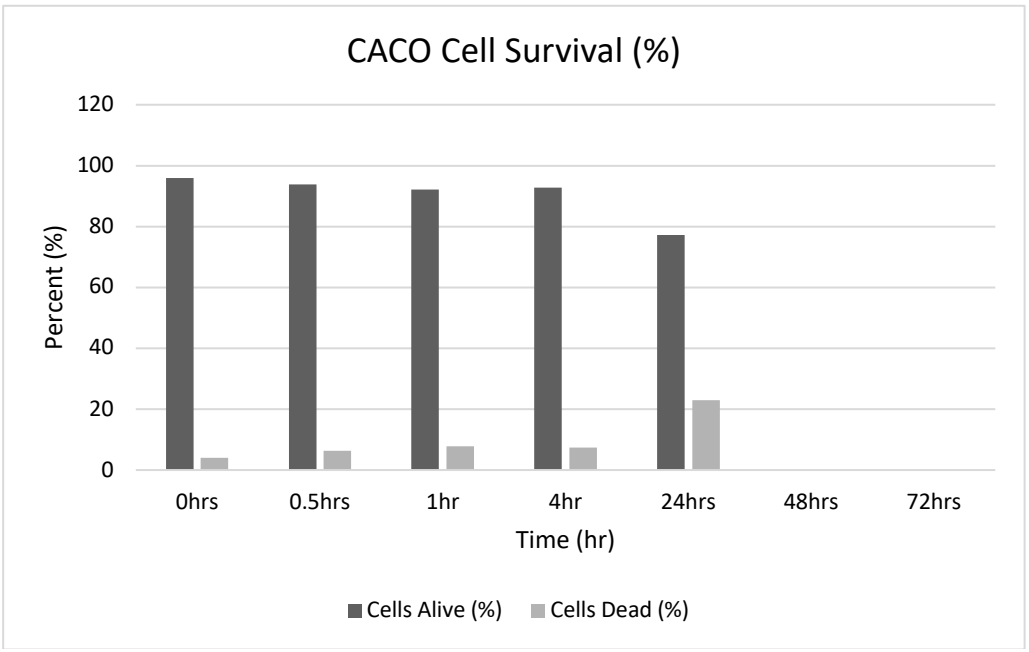

b.

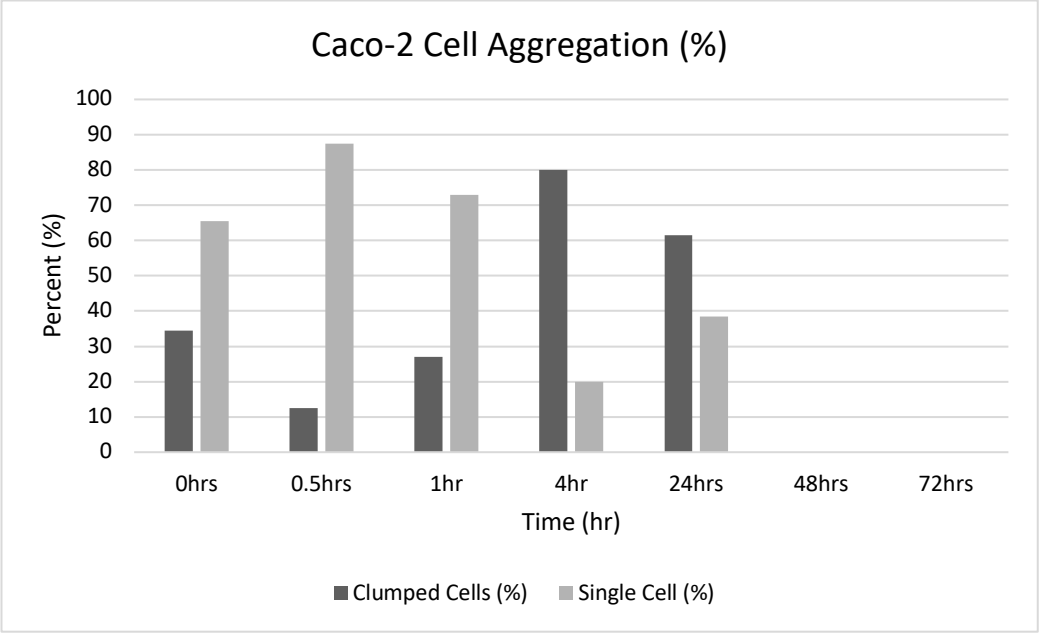

Figure 4.23: 4.23a Untreated Caco-2 CRC cells in suspension with assessment of cell viability over time following refinement of cell harvesting technique. 4.23b Untreated Caco-2 CRC cells in suspension with assessment of cell aggregation over time. Figures are representative of two independent repeats undertaken in triplicate.

4.3.4. Effects on cell viability when targeting the HA binding receptor in CRC

4.3.4.1. Cell viability assessment using trypan blue

Treatment with HAi and HA of free-floating cells was undertaken with a repeat time course study. Trypan blue stain was used to assess cell viability and morphology. Cell counting methodology was used to quantify viable cells. HAi treatment was at a concentration of 2µM. HA treatment was undertaken at concentrations of 312µg/ml and 624µg/ml respectively. There was an observed early drop in cellular viability with HAi treatment, which was statistically significant at 6 hours ($p=0.0044$). At 24 hours treatment there was a statistically significant reduction in viable cells in all treatment groups, when compared to the untreated control (HAi $p=0.0015$, 312µg/ml HA $p=0.0039$ and 624µg/ml $p=0.0019$). This may represent the effect on cell-cell interaction affecting the CRC cell ability to survive in suspension. (Figure 4.24).

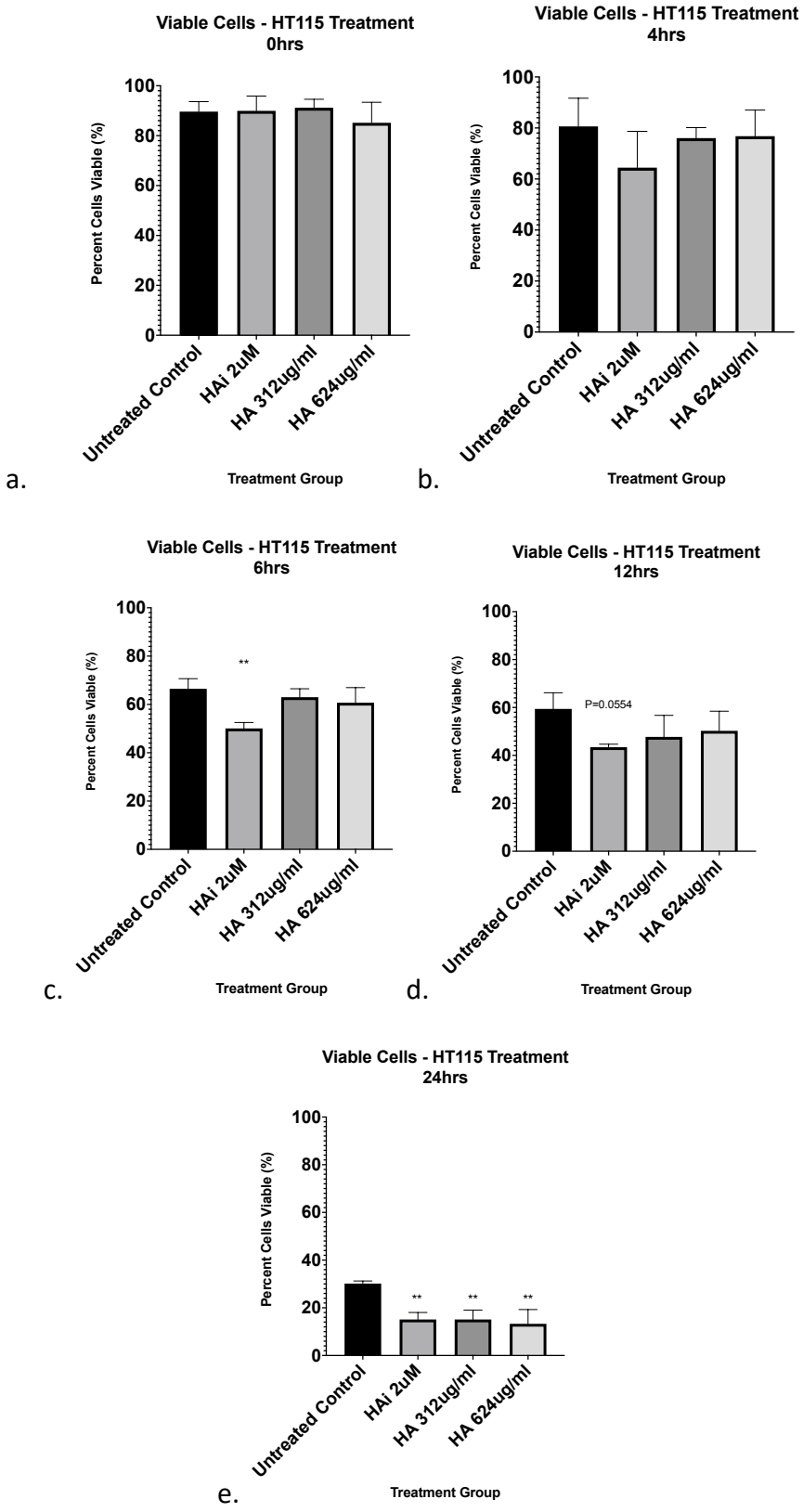

Figure 4.24. HT115 CRC cells and assessment of cell viability over time when treated with HAi or excess HA and compared to a PBS control group. One-way ANOVA and Dunnett's multiple comparisons. There was found to be a statistically significant reduction in cell aggregation with HAi treatment at 6 hours (p=0.0044) and at 24 hours (p=0.0015) compared to the control group. At 12 hours the trend in reduction of cell viability remained present but did not achieve statistical significance (p=0.0554). There was also found to be a significant reduction in cell viability in the HA treated groups at 24 hours, at both tested doses of 312ug/ml (p=0.0039) and at 624ug/ml (p=0.0019). Results are taken from percentages of means from three independent repeats, undertaken in triplicate. 4.24a Cell viability at 0 hours. 4.24b Cell viability at 4 hours. 4.24c Cell viability at 6 hours. 4.24d Cell viability at 12 hours. 4.24e Cell viability at 24 hours.

4.3.4.2. Cell viability assessment using cell counting kit-8 (CCK-8)

Cell viability assay cell counting kit 8 (CCK8) was used to verify the findings in 4.3.4.1 regarding treatment with either HAi or HA and the effect on cell viability whilst cells were in suspension. Methodology for CCK8 is described in Chapter 2. HAi at 2µM and HA at 312µg/ml were used for treatment. Both HT115 and Caco-2 cell lines were used. Time points were taken at 4 hours and 24 hours of treatment.

For HT115 cells there was a significant decrease in cell viability demonstrated in the treatment groups at 24 hours when compared to the untreated control (HAi treated $p=0.0156$ and HA treated $p=0.0362$).

For the Caco-2 cell line there was no demonstratable difference in cell viability in the treatment groups when compared to controls. (Figure 4.25).

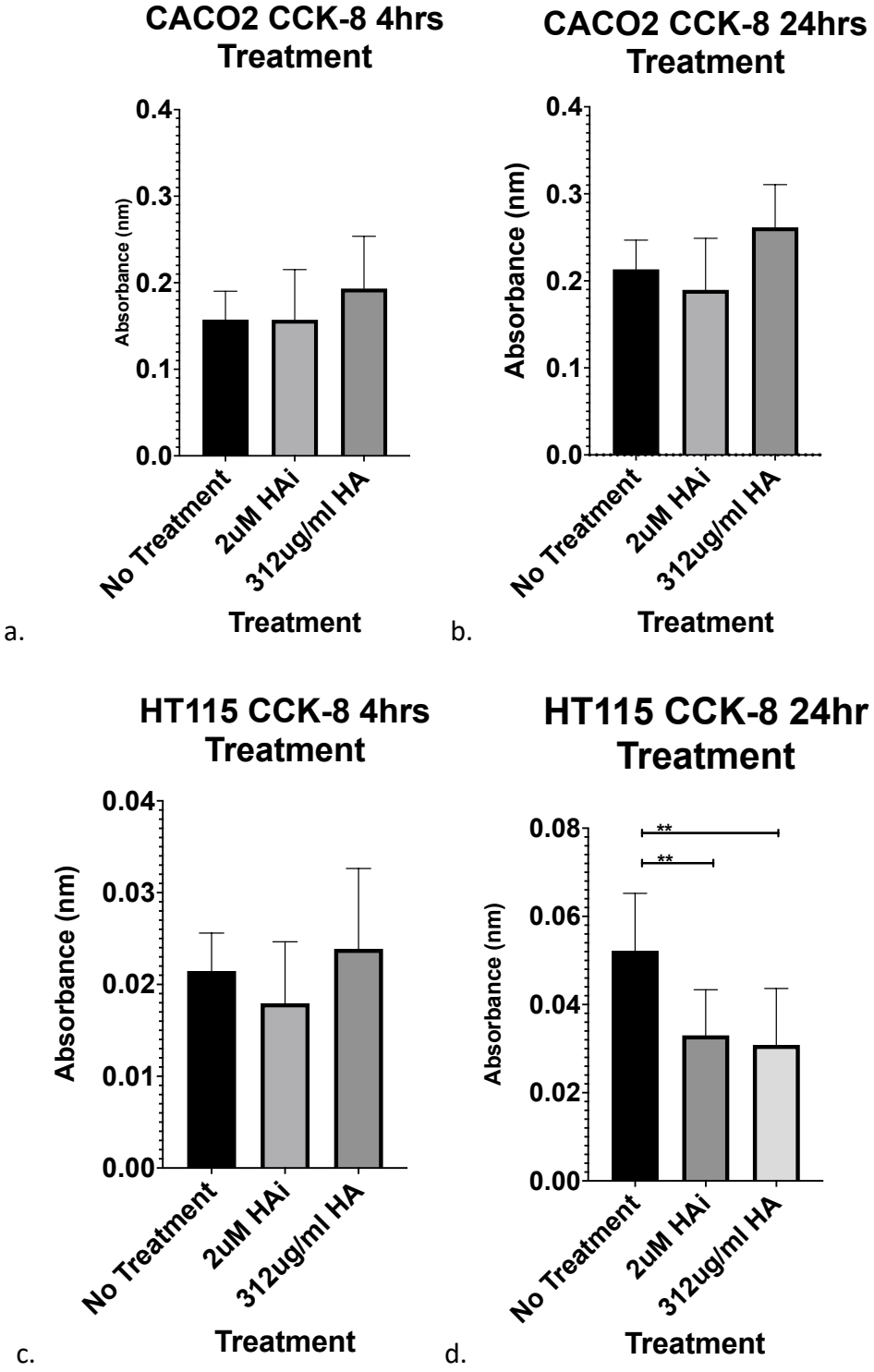

Figure 4.25: Cell counting kit-8 cell proliferation and cytotoxicity assay, to assess cell viability of free-floating CRC cells in suspension. One-Way ANOVA and Dunnett's multiple comparisons test. 4.24a. Caco-2 cells at 4 hours of treatment. 4.24b. Caco-2 cells at 24 hours of treatment. 4.24c. HT115 cells at 4 hours of treatment 4.24d. HT115 cells at 24hours of treatment.

There was no significant difference in cell viability of Caco-2 at either 4 hours or 24 hours of treatment compared to the control. There was no significant difference at 4 hours however, at 24 hours there was a significant reduction in HT115 cell viability in both the HAi treated group (p=0.0156) and the HA treated group (p= 0.0362) when compared to the control.

4.3.5. Effects of targeting the HA binding receptor in CRC on cell aggregation

HT115 cell aggregation and the effect of treatment with either HAi or HA was studied, as described in 4.2.3.3, over a 24-hour time period. Experimentation was carried out in triplicate with three independent repeats. Three treatment groups were examined: HAi treatment at 2μM, HA treatment at 312μg/ml and HA treatment at 624μg/ml.

At 12 hours there was a significant reduction in cell aggregation, of the viable cells in suspension with HAi 2μM treated cells when compared to the control. There was a mean reduction in cell aggregation of 17% ($p=0.0236$).

At 24 hours, HT115 cells in all three treatment groups demonstrated a significant reduction in cell viability when compared to the untreated control. Mean percentage aggregation of viable cells reduced by 16.1% for HAi 2μM, 14.6% for HA 312μg/ml and 15.8% for HA 624μg/ml when compared to the untreated control (HAi 2μM $p=0.0015$, HA 312μg/ml $p=0.0027$, HA 624μg/ml $p=0.0017$) (Figure 4.26).

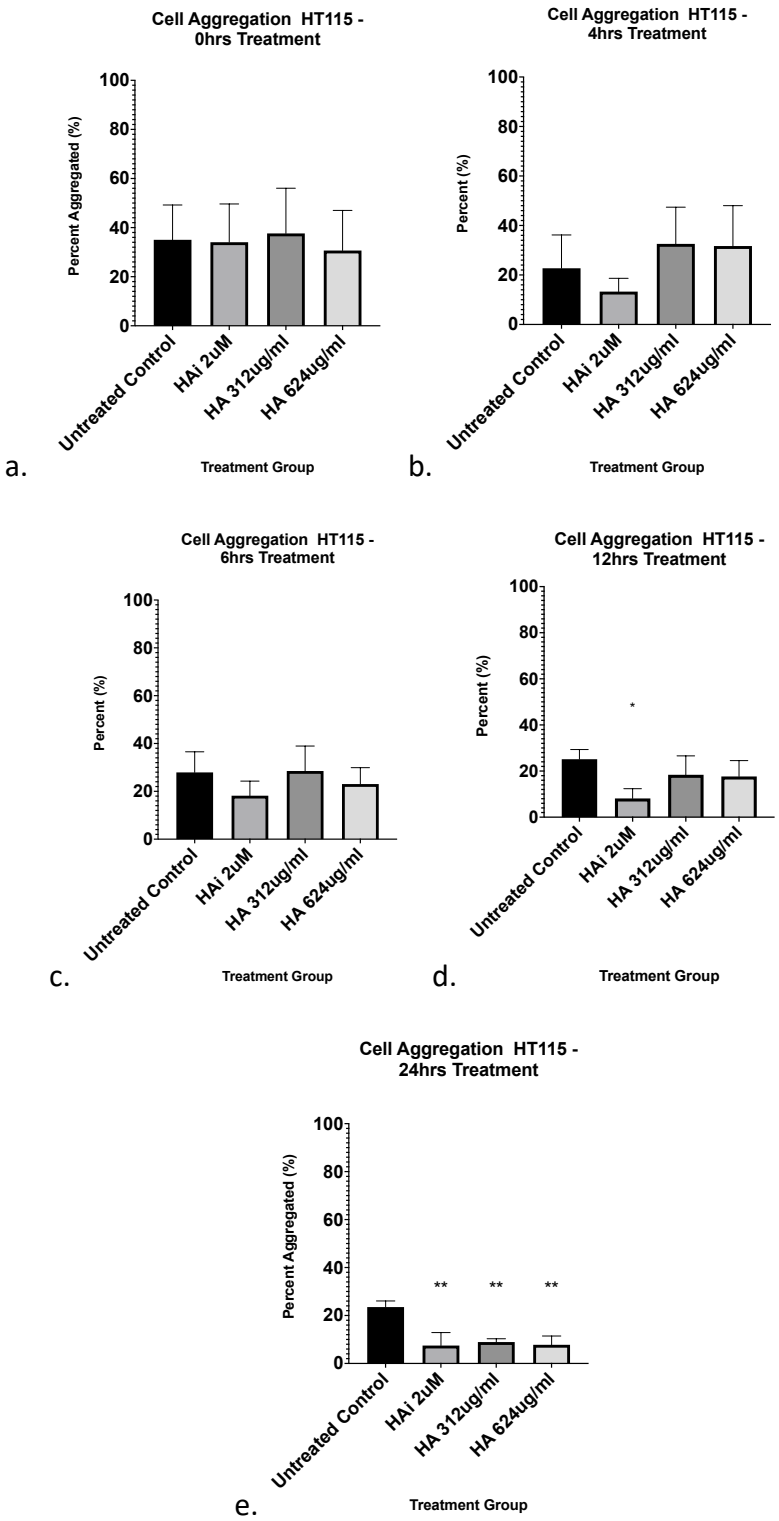

Figure 4.26: HT115 CRC cells and assessment of cell aggregation over time when treated with HAi or excess HA and compared to a PBS control group. One-way ANOVA and Dunnett's multiple comparisons. There was found to be a statistically significant reduction in cell aggregation with HAi treatment at 12 hours (p=0.0236) and at 24 hours (p=0.0015) compared to the control group. There was also found to be a significant reduction in cell aggregation in the HA treated groups at 24 hours at both tested doses of 312ug/ml (p=0.0027) and at 624ug/ml (p=0.0017). Results are taken from mean percentages from three independent repeats.4.26a Cell aggregation percentage at 0 hours. 4.26b Cell aggregation percentage at 4 hours. 4.26c Cell aggregation percentage at 6 hours. 4.26d Cell aggregation percentage at 12 hours. 4.26e Cell aggregation percentage at 24 hours.

4.3.6. Examining apoptosis and anoikis in CRC cells in suspension

HT115 cells were re-examined in suspension. There were three treatment groups (HAi 2µM, HA312µg/ml and HA624µg/ml) and an untreated cohort. Cells were treated in suspension for 12hours. At this point cells were processed in accordance with the Annexin V apoptosis detection kit, for assessment of early apoptosis. A positive control of NaClO and a negative control of unstained adherent cells were also sampled. (Figure 4.27).

There was a significant increase in early apoptosis of both the HA treated cells when compared to the untreated cohort (HA 312µg/ml p=0.0171 and HA 624µg/ml p= 0.0240). There was no significant increase in early apoptosis demonstrated in the HAi treated cohort (p=0.6058) (Figure 4.28).

As expected, overall apoptosis demonstrated a significant increase in cell death in the positive NaClO treated group (P=<0.0001). There was no difference in early apoptosis in the positive control compared to the untreated cohort (p=0.9418).

The identification of early apoptosis in the HA treated cohort led the next inquiry to ascertain whether caspase proteases, associated with the process of apoptosis (anoikis), could be detected.

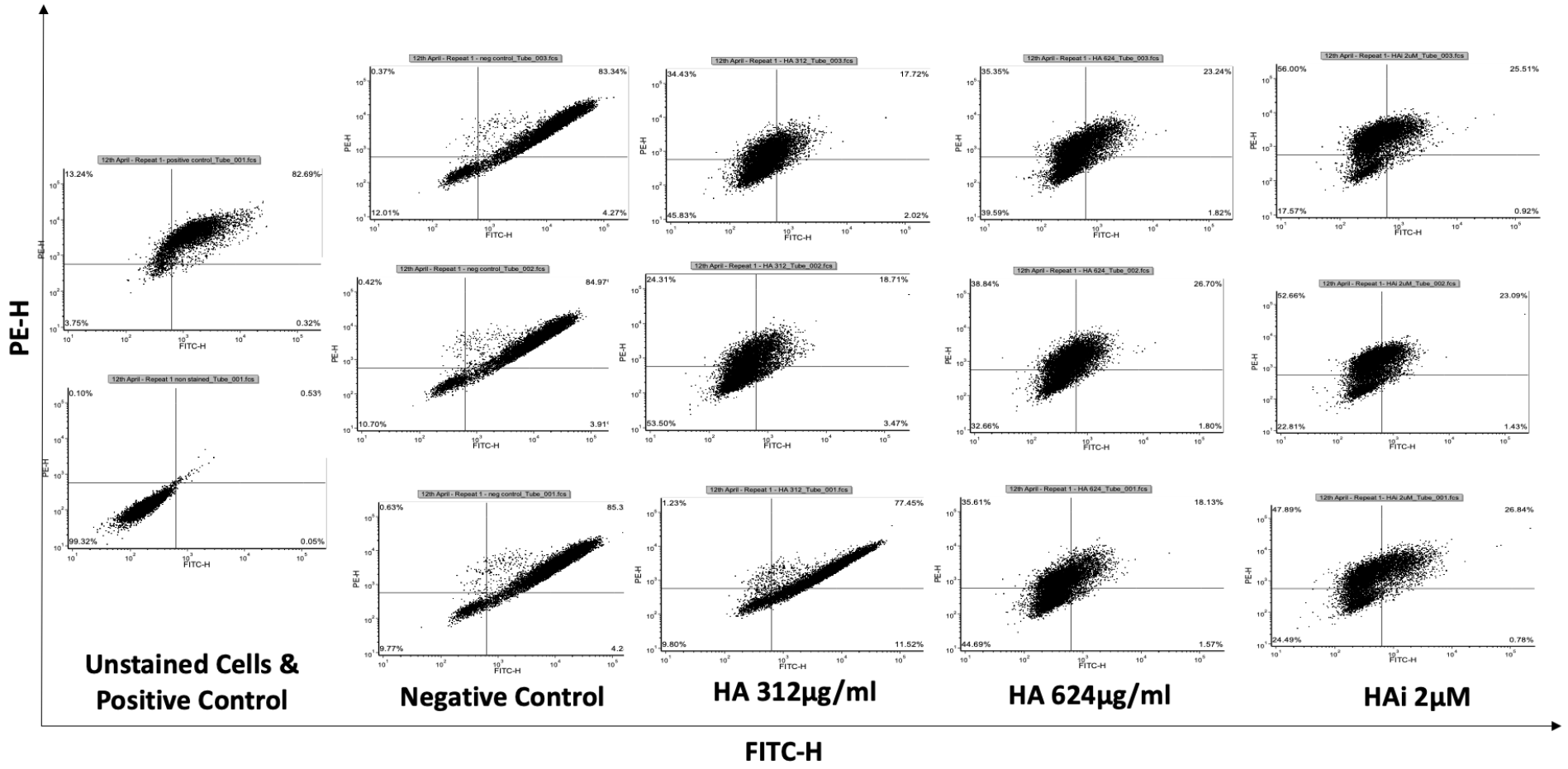

Figure 4.27: Cell populations annexin-V apoptosis detection assay assessed with flow cytometry at 12-hours of treatment. The untreated control and three treatment groups were repeated in triplicate. Bottom left quadrant represents live cells, bottom right the early apoptotic population, top right the late apoptotic cell population.

a.

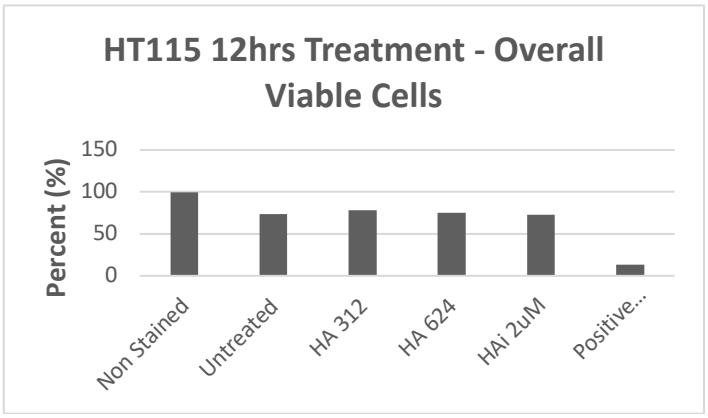

b.

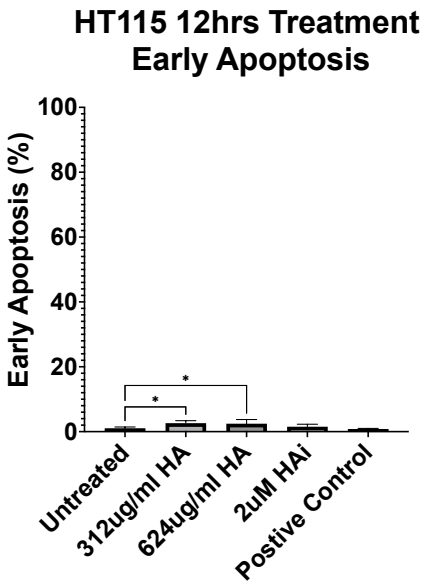

c.

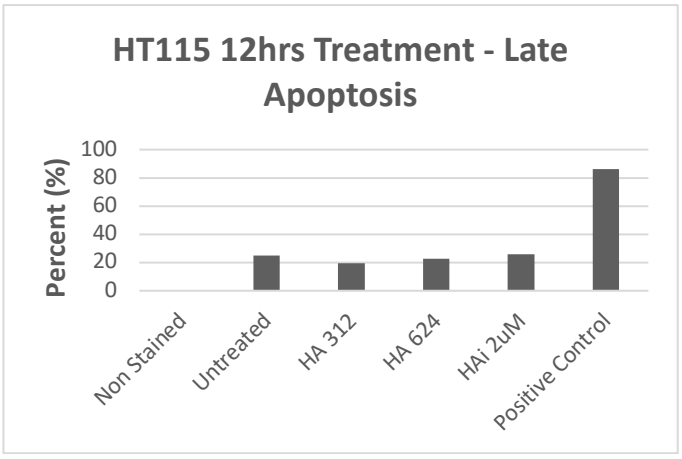

d.

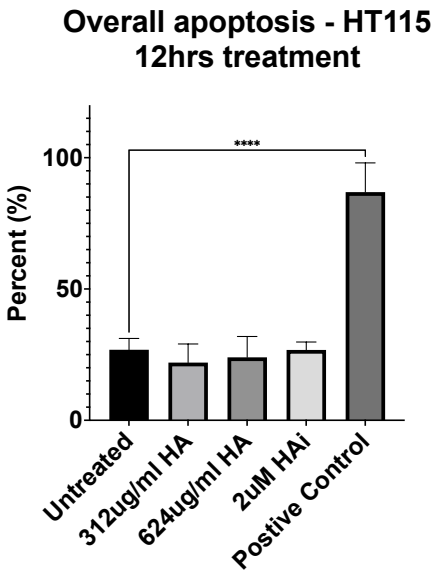

Figure 4.28: Graphical representation of Annexin V cell populations demonstrating cell viability and apoptotic populations at 12hours treatment. Non stained cells served as a negative control and the positive control cell populations had been treated with NaClO. 4.28a. Overall viable cells. 4.28b. Early apoptotic cell populations. 4.28c. Late apoptotic populations and relative comparisons. 4.28d. Overall apoptosis of cell populations.

4.3.7. Expression of caspase-3, caspase-8, and caspase-9 in suspended cells

Uncleaved caspase-3 gives a band at 35kDa, and cleaved caspase-3 at 17kDa and 19kDa. The suspended cells demonstrated both a 35kDa band and a 46kDa band (Figure 4.29). Uncleaved caspase 3 was demonstrated at 35kDa with strong bands seen in all suspended cells, with no one clear treatment group expressing significantly more than the other suspended cell treatment groups. The 46kDa band is not described in the caspase-3 antibody datasheet in terms of cleaved or uncleaved caspase-3 as an expected band to be seen. It is either non-specific band or relates to a larger molecule protein, which cleaved at a different site. This non-specific band of 46kDa has been described in the literature, when examining caspase-3, and the finding of different sized bands may represent different cellular events occurring (Witek & Fung, 2013).

Caspase-8 also appeared to be activated in all suspended cells (Figure 4.29), which was indicated by the appearance of 43kDa anti-caspase-8 band, which is one of the reported molecular weights of activated casepase-8 subunits. However, the pro-enzyme is reported to be 55kDa in the literature (Sanchez, Xu, Juo *et al.*, 1999) but was not present

Caspase-9 appeared present at 49kDa (Figure 4.29), but expression was not as strong as either caspase-3 or caspase-8.

Finally, GAPDH as the control was demonstrated at the expected 37kDa product across all samples (Figure 4.29).

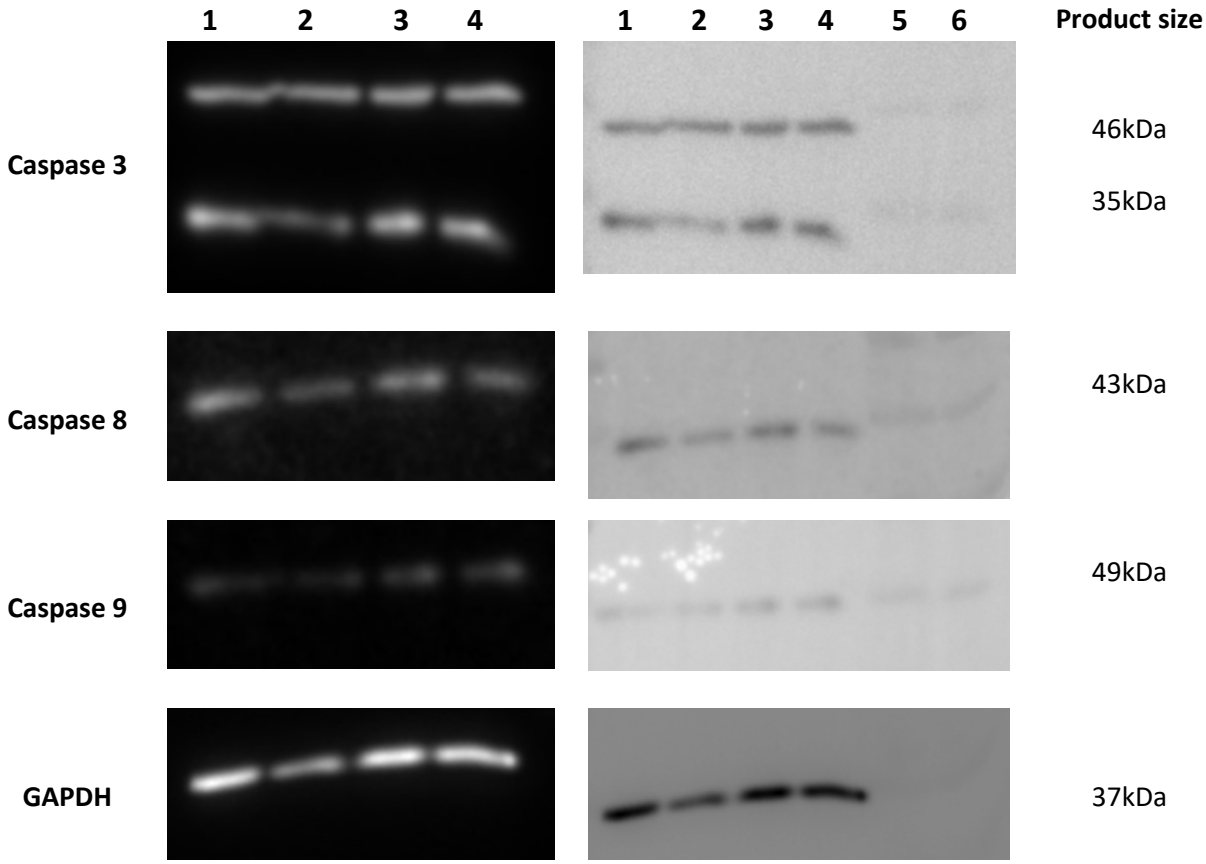

Legend	
1	Control
2	HAi Treated 2µM
3	HA treated 312µg/ml
4	HA treated 624µg/ml
5	Ladder
6	Ladder

Figure 4.29. Western blot assessment of caspase protein expression of suspended HT115 cells subject to treatment. The legend below denotes the protein band in relation to the treatment group.

4.4. Discussion

4.4.1. General Discussion

Cellular adhesion of anchorage-dependent cells is a key step in the peritoneal metastatic model. This chapter builds on Chapter 3 whereby HA-dependent adhesion molecules in CRC are seen to be upregulated. This chapter verifies the presence of HA-dependent adhesion molecules on both CRC cells and mesothelial cells. The presence of CD44 on the cell surface of mesothelial cells has been described in the literature previously (Gardner, Jones, Catterall *et al.*, 1995), which this work also confirms in the RNA, protein and immunofluorescent experiments. This chapter also demonstrates that cellular adhesion can be influenced by targeting the HA receptor and that by preventing adhesion the ability for CRC cells to survive is also affected.

A peritoneal model *in vitro,* in both HA coating of testing plates and a co-culture model served as the basis to examine CRC cellular adhesion and the effect of treatment, with either HAi or excess exogenous HA. This demonstrated a reduction in CRC cellular adhesion when treated with competitive inhibition. Based on the background work in Chapter 1 and Chapter 3, it is reasonable to infer that interaction with the HA receptor proteins is likely to be the underlying mechanism. However, it may be possible that an alternative pathway may be interfering with cell adhesion or that HA or HAi interacts with other surface molecules on the CRC cell. At this stage, the significant reproducible reduction in cellular adhesion with the treatment of either HAi or HA is worth exploring further.

When CRC cells are placed in suspension, the ability for CRC cells to survive is reduced. When CRC cells have treatment targeting the HA receptor, which targets cell-cell anchorage, it is shown that the ability for the CRC cells to survive is significantly reduced further. As described in the introduction to this chapter, cell anoikis evasion mechanisms by colorectal cancer cells facilitate the ability for cells to remain dormant in the peritoneal cavity. However, the process of EMT change, to trigger cell anoikis evasion mechanisms, to these cells is not likely to be immediate. In the context of a surgical resection of a tumour where there is tumour cell spillage at the microscopic level, tumour cells are likely to be more vulnerable to cell anoikis than tumour cells at the invasive front of a tumour, in which there has been time for cells to adapt and change morphology during the cell cycle, before detaching from the main tumour body.

CRC cells in suspension appear to undergo anoikis and the presence of caspases suggests that apoptotic mechanisms play a role to CRC cells in suspension. Further analysis directly comparing adherent CRC cells to free-floating cells would be worth examining further to directly compare the expression of caspases between the cell conditions.

4.4.2. Limitations

Whilst time consuming, cell counting methodology for adhesion assays proved the most consistent and accurate way in which to assess colorectal cancer cell adhesion. Absorbance assays with crystal violet in the single cell culture models, although were quicker and generally demonstrated the same trends as the cell counting method, the degree of sensitivity was lesser than with cell counting.

Unfortunately, the EVOS II cell plate reader malfunctioned during work and prevented further adhesion assay analysis of co-culture adhesion assays, to further explore cellular adhesion and the effect of treatment.

Western blotting proved problematic and as a result time consuming. Techniques were required to be refined and repeated multiple times to obtain consistent protein bands. Further analysis of protein band expression, such as with image J could have provided a method of semi quantification to examine protein expression and look for if there were any significant differences between the treated HT115 cells and the control HT115 cells. Expression of a strong non-specific band at 46kDafor caspase-3 was unusual and unexpected but, as described in 4.3.7, there are studies which have shown a 46kDa band associated with caspase-3. Alternative assessment of caspase expression could be undertaken through flow cytometry and could be used to quantify cell populations with expression of cleaved and uncleaved caspase-3, caspase-8 or caspase-9 (Crowley & Waterhouse, 2016).

For the flow cytometer anoikis examination, initial processing time was labour intensive and, processing the number of samples across three treatment groups in triplicate, potentially added to extra treatment time in some samples. If repeat experimentation were to be carried out, assessment of one treatment group to the control would potentially reduce sample processing time through the flow cytometer and potentially reduce sampling errors.

Overall, there are obviously limitations toward recreating the stromal tumour microenvironment *in vitro*. Experiments can be over-simplistic and exclude the many other significant molecular interactions, which affect dissemination of peritoneal metastatic disease in CRC and other malignancies.

4.4.3. Future Work

Epithelial-mesenchymal transition (EMT), is a key step in the differentiation process of solid cancers (Das, Bhattacharya, Chikkaputtaiah *et al.*, 2019). This is a crucial process where epithelial cells obtain properties of mesenchymal cells that possess morphological changes which increase motility and enhance communication and interaction with neighbouring cells. The changing environment and the stresses placed on free-floating CRC cells is a further area to explore *in vitro.* E-cadherin, Snail, Slug, Vimentin, N-cadherin, and TWIST-1 have been reported to play a role in the process of cell detachment from solid tumours. The changes potentially affecting anchorage dependent CRC cells in suspension that remain viable are an important aspect to examine further.

Assessment of expression on molecules responsible for anoikis evasion on the stresses to treatment, such as Hypoxia inducible factor HIF-1α, TGF-ß2 and other molecules responsible for chemoresistance may need to be examined to see if they are upregulated when subjected to treatment with HAi or HA. A rebound effect to treatment, enhancing the chemo resistant properties of CRC tumour cells should be considered.

If HAi and HA have the potential to affect cell-cell interaction, further work could look at the effect on invasion, migration, and growth of CRC cells subject to treatment. Functional growth, migration, and invasion assays to explore this further is an important line of further investigation.

HA is a naturally occurring compound present throughout mammalian cells. The effect of a naturally occurring compound is unlikely. That being said, formal cytotoxicity, as a direct result of either HA or HAi on cells, is important to evaluate. Boekel, Shinkai *et al*., (2014) evaluated the cytotoxicity of HA using an MTT assay. Their results suggested a decrease in cell viability in the presence of HA for osteoblastic bone cells (Boeckel, Shinkai, Grossi *et al.*, 2014). However, is reduced cell viability simply the result of loss of cell anchorage and cell-cell aggregative properties, as opposed to irreversible cell damage from the cytotoxic effect of treatment? This question would be one to look into further.

Consideration of Gastric, Ovarian, primary peritoneal and pancreatic cancers which commonly give rise to peritoneal metastases, would be another area to further explore, to see if this translates to the same outcomes. HA-dependent adhesion is not exclusive to CRC and similar outcomes could potentially be seen.

Alternative cell viability assays could be used to verify cell viability, such as real-time assay for viable cells using EVOS and luminescent cell viability assays, to explore the effects to treatment on CRC cells (Riss, Moravec, Niles *et al.*, 2004).

Genetically modified experimentation where CD44, RHAMM and ICAM-I are knocked down or upregulated in CRC cell lines to explore the subsequent effect on cellular adhesion, would be a further way to validate the HA/HA-receptor interaction. It would be expected that similar effects on CRC cellular adhesion would be demonstrated if the hypothesis is indeed correct.

The next chapter, Chapter 5, develops the work demonstrated in this chapter to examine a preliminary *in vivo* model of the effect of treatment with HAi and HA in PM of colorectal cancer cell lines. If reduction in CRC cell adhesion can be translated *in vivo* it would drive potential to examine this area further and consider clinical application in cancer treatment.

Targeting Hyaluronic Acid-Dependent Peritoneal Adhesion of Colorectal Cancer *in vivo*

Chapter 5

5.1. Introduction

5.1.1. Approaches to murine modelling

There are several methods of constructing murine models which have been developed to study the effects of human diseases including cancer. Models have been used to examine both the malignant process and response to therapy. Immunocompromised xenograft murine modelling allows assessment of factors involved in malignancy including malignant transformation and metastatic disease. It is one of the most widely-used and simplest models, in which tumour cells from humans are transplanted into an immunocompromised mouse. For many years xenograft modelling has been used as a pre-clinical screening process for the development of novel cancer treatments, following preliminary work conducted *in vitro*.

Immunodeficient mice are usually either athymic or severely compromised immunodeficient (SCID) mice, in order readily to accept the implanted human cell lines. It is the least expensive and least time-consuming type of murine model and generates reliable results which can be rapidly examined and reproduced. There has been debate whether xenograft models can realistically predict clinical response due to the use of single cell lines which do not necessarily represent true tumour behaviour, and concerns that the stromal component is rodent in origin rather than human with corresponding differences in biological behaviour (Sausville & Burger, 2006). Another concern in xenograft modelling is that, due to mice being immunocompromised, the stromal microenvironment cannot be truly replicated due to the loss of the host immune system (Richmond & Su, 2008).

One study (Gremonprez, Willaert, & Ceelen, 2016) reviewed pre-clinical models of peritoneal metastasis (PM) originating from colorectal cancer (CRC) which reported 164 studies involving animal models up to 2015. However, *in vivo* studies looking into PM of CRC were considerably less studied than when compared to either studies looking at CRC liver metastasis or ovarian origin peritoneal metastatic tumours. Relatively few genetically-modified murine models have been reported in CRC PM research and most of these xenograft models utilised HCT116, LS174T or HT29 CRC cancer cells. Using patient cells lines, rather than immortalised CRC cell lines, results in patient derived xenograft (PDX) models. These are more costly and more suited to investigating personalised treatment for patients.

There are other methods which provide a more realistic tumour microenvironment in which to examine cancer behaviour *in vivo.* These include either xenograft models in humanised mice, or genetically engineered (GEM) models.

Humanised immunodeficient mice are transplanted with human cells or tissues which may be ideally suited for direct investigation of human malignancy. Successful models depend on avoiding tissue rejection and maximising tissue function to facilitate replication of the microenvironment. These methods can potentially be expensive and time-consuming to achieve validation.

Genetically engineered animal models (GEM) are broadly split into two categories; knock-down models where a specific gene is targeted to lose function, and transgenic animal models where DNA from another source is incorporated into the DNA of the mouse. The new DNA becomes incorporated into all cells and tissues of the mouse. In early GEM, mice

were genetically engineered to express dominant oncogenes. GEM models have questionable value to be able to interpret the clinical results of treatment response and there is currently limited work within colorectal cancer models in examining PM (Sausville *et al.*, 2006). GEM models also do not necessarily reflect the clinical response to treatment seen in the mice cohort to that observed in humans, however, they are useful in examining the effect of specific genes in cancer development and progression.

When assessing responses to therapy it is important to get at least a 50% reduction in tumour growth to achieve a 'qualified' response to therapy. Adverse drug reactions at therapeutic doses are important to monitor in conjunction with therapeutic response (Talmadge, Singh, Fidler *et al.*, 2007).

With the benefits and limitations mentioned and summarised in Table 5.1, the effect of a treatment on the rate of tumour growth, tumour survival or regression can be assessed through murine modelling. Each of the various animal models described has both benefits and limitations in their use (summarised in Table 5.1). The choice of animal model should therefore be chosen carefully when considering the specific scientific question being asked, as well as with the timeframe available in which to address the question being considered.

Table 5.1: Summary of main murine mouse models with benefits and limitations.

Murine model	Advantages	Disadvantages
Xenograft immunodeficient	• Rapid analysis feasible within few weeks • Simplest technique • Realistic heterogeneity of tumour cells • Can predict human drug response	• Immunocompromised- less realistic tumour microenvironment • Single cell tumour lines
Xenograft in Humanised mice	• Competent immune system • More realistic tumour microenvironment • Realistic tumour heterogenicity • Can predict human drug response • Multiple therapies can be tested from single tumour biopsy	• Technique is complex • Expensive • Time consuming • Immune system not fully restored
Genetically Engineered Mouse (Transgenic)	• Competent immune system providing more realistic microenvironment • Mutations can translate to known human mutations • One or several genes can be mutated • Tumour progression can be studied over time • Can 'knock-out' or 'knock-in' specific genetic modifications	• Technique is complex • Expensive • Time consuming to develop GEM achieve validation before drug testing. • Tumour development in animals can be slow and variable • Limited number of genes can be targeted each time • Response to treatment in mice not necessarily reflective of human response

5.1.2. Murine mouse modelling and targeting hyaluronic acid

The specific question being asked within our experiment is whether peritoneal dissemination of CRC cells can be reduced by targeting the HA receptor molecules. As a preliminary test the simplest technique which facilitates rapid analysis which can predict human drug response is by using the xenograft immunodeficient murine model. This is accepting the limitations that the model brings.

There are some limited studies in animal models where either treatment with hyaluronic acid or targeting the hyaluronic acid receptor have been studied. The use of cross-linked hyaluronic acid gel was shown to inhibit metastatic growth in xenograft nude murine models of gastric and hepatic cancer, *in vivo* (Lan, Pang, Wu *et al.*, 2016).

Within colorectal cancer, to date there are three studies looking at hyaluronic acid in murine models with different outcomes and none has looked at a competitive hyaluronic acid inhibitor. Yamaguchi et al (2001) assessed a xenograft murine model, using CT26 CRC cells and BALB/c mice. The changes described a higher HA concentration with induction of a CO_2 pneumoperitoneum than when compared to laparotomy. This study further concluded that increased hyaluronic acid may be associated with port-site metastases (K. Yamaguchi, Hirabayashi, Suematsu *et al.*, 2001). Serafino et al assessed HA as a macromolecular drug delivery system utilising the HA receptor on CD44 for the anticancer drug SN-38, to target cancer by delivering chemotherapeutic agents using a rat colon tumour (DHD/K12/TRb in a BDIX rat) model (Serafino, Zonfrillo, Andreola *et al.*, 2011). Finally, Hubbard et al (2002) reported the only study to look at HA as a possible method to reduce CRC PM. The study

used BALB/c mice and KM12L4 CRC cells. The study looked at three groups; a control group, a group inserting Seprafilm® (a hyaluronic acid-based mesh), into the peritoneal cavity under the laparotomy incision and a third group where vicryl mesh was inserted. All mice underwent laparotomies and the peritoneal cavity inoculated with human KM12L4 CRC cells. The study concluded that whilst Seprafilm® was not directly associated with tumour metastasis, the associated trauma when applying biomaterials, such as Seprafilm® or vicryl mesh, was associated with an increased rate of local tumour growth. It was concluded that local trauma from such biomaterial insertion may stimulate local tumour growth (Hubbard & Burns, 2002). No further animal studies have examined this further.

5.1.3. Hyaluronic acid and intra-abdominal scar adhesion formation

It has been reported that surgical trauma increases the risk of peritoneal recurrence in many cancers including colorectal cancer (Behrenbruch, Shembrey, Paquet-Fifield *et al.*, 2018; J. W. Lee, Shahzad, Lin *et al.*, 2009; Pasquier *et al.*, 2018). The repercussions of trauma to the peritoneal cavity have also been demonstrated with respect to intrabdominal scar adhesion formation which has been studied extensively over the years (Ellis, 1962; Poerwosusanta, Gunadi, Oktaviyanti *et al.*, 2020). Intrabdominal adhesions are fibrous tissues which develop after trauma to serosal membranes and the peritoneal lining. They are a potentially serious problem following intrabdominal surgery as they can lead to bowel obstruction or other intrabdominal complications.

Adhesion scar formation is thought to be due to an underlying inflammatory multimolecular process involving interleukins, macrophages and other chemical mediators, along with hypoxia and cell damage to serosal or peritoneal cells and alteration to the fibrinolysis cascade (Maciver, McCall, & James Shapiro, 2011).

Hyaluronic acid has been studied both in murine and human studies as a possible method to prevent adhesion formation (Diamond, 1996; Johns, Rodgers, Donahue *et al.*, 1997; Kocak, Unlu, Akcan *et al.*, 1999; Rodgers, Johns, Girgis *et al.*, 1997; T. Sawada, Hasegawa, Tsukada *et al.*, 1999; Thornton, Johns, Campeau *et al.*, 1998). These studies have shown promising outcomes regarding a significant reduction in abdominal scar adhesion formation. It is not completely clear from the current literature whether there is one clear underlying mechanism of how introducing excess hyaluronic acid reduces scar formation, or whether this is a multimodal process.

5.1.4. Chapter aims

The aims of this chapter are:

1. To evaluate and compare peritoneal dissemination of CRC HT115 cell line between three cohorts of mice in a pilot study. –

- HAi treated group
- HA treated group
- Untreated control group

2. To assess whether the methodology of intraperitoneal CRC cell injection facilitates CRC peritoneal cellular growth
3. To assess whether the methodology of intraperitoneal injections is a viable treatment approach
4. To assess and demonstrate whether CRC cellular adhesion can be reduced *in vivo* by targeting the HA receptor

5. To assess whether there is a reduction in viable free-floating cells in treatment groups when compared to controls

5.2. Materials and methods

5.2.1. Project licence

In vivo experimentation was carried out under Home Office project licence (PPL: PE9445FC2). A Home Office Personal Licence was granted after completing training with the Royal Society of Biology, Charles River UK Ltd and Cardiff University under the UK and EU frameworks for animal handling (Individual licence: I89ED0784).

5.2.2. Mouse cohort

A total of eighteen athymic (CD1) nude mice were obtained from Charles River Laboratories (Charles River Laboratories International Inc, Kent UK). All mice were stored in filter-topped isolation cages and all procedures were conducted in a class II extractor cabinet. Mice were weighed on a weekly basis. They were cared for daily by a dedicated mouse laboratory team, as well as inspected regularly and cared for by investigators. Mice were settled into the designated laboratory for one week prior to commencing experimentation. CD1 nude mice were developed from the transfer of the nude gene from crl:NU-Foxn1nu to a CD-1 mouse through a series of crosses and backcrosses beginning in 1979 at Charles River Laboratories, Wilmington, MA. Due to the lack of a thymus the mice are unable to produce T-cells and therefore immunodeficient.

Charles River laboratories provide an estimated growth chart guideline from which to compare estimated expected growth chart weights, seen in Figure 5.1

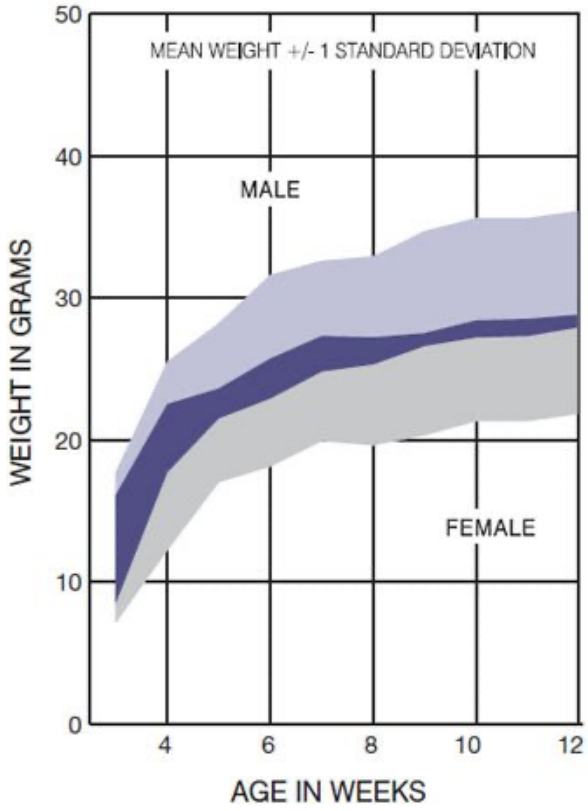

Figure 5.1: Image reproduced from Charles River website (criver.com). Estimated growth chart data. The shaded areas on each chart are the mean weight plus or minus one standard deviation at a given age averaged across all production facilities. Representing 67% of the population, with remaining 33% falling outside this weight range.

The eighteen mice were randomly split into three cohort groups of six mice. There were two treatment groups and one control group:

Group 1: Control group

Group 2: HA inhibitor treated group

Group 3: Excess exogenous hyaluronic acid treated group

5.2.3. Cell harvest

A total of 100-125 million colorectal cancer HT115 cells were harvested from *in vitro* cell culture. Three million colorectal cancer HT115 cells were harvested per mouse for intraperitoneal (IP) injection and a further two million cells were harvested for subcutaneous injection to monitor tumour growth. Cells were harvested with 1ml of trypsin, and then initially pooled in a suspension of DMEM in a universal container. Cells were spun down using a centrifuge, washed in phosphate buffered saline (PBS) and finally resuspended in chilled PBS and placed on ice.

5.2.4. Hyaluronic acid Inhibitor

From initial adhesion assay experimentation (Section 4.3.2.4), a concentration of 2.5µg/ml of HAi was selected as the dosing concentration to translate for *in vivo* experimentation. Therefore, the dosing required scaling for an equivalent murine dose. Each mouse weighed approximately 20g, which was taken as the assumed standard weight of a 4-week-old mouse. In order to calculate the dose required for a mouse it is necessary to estimate how to convert the various components of a mouse from weight (g) to volume (ml) by the following formula:

Murine equivalent dose = *in vitro* optimum dose (µg/ml) x (animal weight (g)/density (g/ml))

= 2.5µg/ml x (20/1g)

= 2.5 x 20

= 50µg HAi per mouse

A stock concentration of 400mM Hai was used to make up a total of 50µg of HAi in 125µl/mouse. Therefore, a total 300µg in a volume of 750µl PBS, split between six mice in the HAi treated cohort.

5.2.5. Hyaluronic acid

From initial adhesion assay experimentation, a concentration of approximately 156.25-312.5µg/ml of excess high molecular weight hyaluronic acid *in vitro* (**Chapter 4.3.2.1)** was demonstrated as the lowest effective dose. For the purposes of *in vivo* this was set to 200µg/ml. The dosing was again upscaled and converted to the *in vivo* model by applying the same formula to estimate the murine equivalent dose.

Murine equivalent dose = *in vitro* optimum dose (µg/ml) x (animal weight (g)/density (g/ml))

= 200µg/ml x (20/1)

= 200 x 20

= 4000µg HA per mouse

A stock of 100mg powdered HA was diluted with PBS and used to make a solution of 4000µg of HA in 200µl PBS for each mouse. A total of 1200µl was used for all six mice in the HA treated cohort. No further top up of PBS solution were required.

5.2.6. Intraperitoneal injection

Mice were inoculated on day zero with five million HT115 cells intraperitoneally in 100µl of PBS solution. Concurrently the respective treatment injections were also administered to each of the mice for each of the cohorts.

- Control group – 200µl PBS
- HAi treatment group – 200µl HAi in solution with PBS
- HA treatment group – 200µl HA in solution with PBS

The injection sites on the mice were cleaned, and IP injections were performed in the right iliac fossa (right lower quadrant) of the abdomen with a 12 -gauge needle. Mice underwent daily treatment injections for the first five consecutive days (week 0-1), followed by IP bi-weekly top-up treatment injections for the remaining three weeks (weeks 1-4). The treatment regimens are summarised in Table 5.2.

Table 5.2. Inoculation of CRC and treatment schedule for *in vivo* xenograft model

Treatment Week	Control Group	HAi treatment group	HA treatment Group
Week 1	1. Day 0 - Inoculation CRC cells subcutaneously (s/c) and intraperitoneal (IP) injection. 2. Injection of control treatment PBS SC 3. Day 1-5 – Daily single injection of PBS control treatment via IP injection	1. Day 0 – Inoculation CRC cells s/c and IP to all mice. Injection of HAi treatment IP. 2. Day 0 – Injection of HAi treatment via IP injection 3. Day 1-5 – Daily single injection of HAi treatment via IP injection	1. Day 0 – Inoculation CRC cells s/c and IP to all mice. 2. Injection of HA treatment IP injection. 3. Day 1-5 – Daily single injection of HA treatment via IP injection
Week 2	Monday & Thursday top up treatment of PBS via IP injection	Monday & Thursday top up treatment of HAi via IP injection	Monday & Thursday top up treatment of HA via IP injection
Week 3	Monday & Thursday top up treatment of PBS via IP injection	Monday & Thursday top up treatment of HAi via IP injection	Monday & Thursday top up treatment of HA via IP injection
Week 4	Monday & Thursday top up treatment of PBS via IP injection	Monday & Thursday top up treatment of HAi via IP injection	Monday & Thursday top up treatment of HA via IP injection

5.2.7. Subcutaneous injection

A further five million cells were split and injected sub-dermally to each mouse, at day zero, to facilitate the ability to visibly monitor tumour growth, as the experiment progressed. The HT115 suspension was injected on the dorsum of the mice in the subcutaneous space using a 12-gauge needle.

5.2.8. Cohort monitoring and care

Mice were carefully monitored daily for general health and condition. They were each formally weighed on a weekly basis and underwent subcutaneous tumour nodule measurements on a twice weekly basis, to facilitate objective assessment of tumour growth. Subcutaneous tumours were not allowed to exceed 1cm in diameter. If larger the experiment would be terminated on grounds of animal welfare.

5.2.9. Tumour assessment

At five weeks following initiation of treatment the mice were culled. Exploratory laparotomies were performed. One millilitre PBS solution was used to irrigate the peritoneal cavity of each mouse and fluid was collected, spun down and cells preserved in 1ml ethanol. Dissection to completely excise all peritoneal tumour deposits was undertaken. All metastatic peritoneal nodules were harvested, counted and photographed using a stereomicroscope (Olympus, Japan). Tumours were measured with a scaled ruler and image pixel scaling. Tumour volume was calculated by using the following formula:

Tumour Volume (mm^3) = 0.5 x tumour nodule width $(mm)^2$ x tumour nodule length (mm)

The collected free-floating cells from the peritoneal fluid were again spun down, rehydrated and counted.

Tumour nodules following resection were frozen at -80°C to facilitate future examination.

5.2.10. Sample size

Sample size estimation for this pilot study was calculated for quantitative data using the following formula (Charan & Kantharia, 2013) and based on limited data on previous in-house animal studies, which have been carried out within the lab research group and calculated using G-power statistical software 3.1 :

Sample size = $2SD^2(Z^{\alpha/2} + Zß)^2/d^2$

Where:

SD= Standard Deviation

$Z^{\alpha/2} = Z_{0.05/2} = Z_{0.025} = 1.96$ *(from Z table) at type 1 error of 5%*

$Z^{ß} = Z_{0.20} = 0.842$ *(from Z table) at 80% power.*

*d= effect size = difference between mean values**

*(*Where effect size is estimated to be between 1.22-9.95, where partial ETA ($n^{2)}$ ranges 0.6-0.99)*

As a result:

Sample size = $2SD^2 (1.96+ 0.842)^2/d^2$

$= 2 \times 2.99^2 (1.96 + 0.842)^2/d^2$

$= (17.88 \times 7.85)/d^2$

= 6-12 mice per group.

5.2.11. *Statistical analysis*

Results were initially tabulated using Microsoft excel spreadsheet and processed accordingly. Further statistical analysis was processed using GraphPad Prism statistical software package.

5.3. Results

5.3.1. Results summary

There was a significant reduction in the number of peritoneal tumour nodules seen in both the HAi and HA treated groups when compared to the control group (p=0.0009). There was also a significant reduction in tumour burden (p=0.0123) and total tumour volume (p=0.0105) between both treated groups when compared to the control.

Important negative findings demonstrated no significant difference between the average body weight of the mice across the three groups, throughout the experiment. Specifically, there was no difference in weight between the three groups at the start (p=0.5646) or at end of the experiment (p=0.2064). Finally, the average tumour nodule volume between cohorts also demonstrated no significant difference between the groups (p=0.1962). Summarised in table 5.3.

All mice remained healthy throughout the experiment, and none required terminating before the planned end of the experiment. Subcutaneous tumour nodule measurements did not exceed 10mm in any of the mice.

Table 5.3: Summary analysis of peritoneal CRC metastatic tumours in mice treated with either HAi or HA compared to a control.

	Control treated group (Mean ± SD)	**HAi Treated Group** (Mean ± SD)	**HA treated Group** (Mean ± SD)	**P-Value Summary**
Average Body Weight at experiment end (g)	27.22 ± 2.51	28.02 ± 2.23	28.08 ± 3.00	0.2064
Number of nodules (n)	11.17 ± 2.99 (Median: 11.5)	6.83 ± 1.60 (Median: 7)	5.33 ± 1.63 (Median: 5.5)	0.0009***
Total tumour volume (mm^3/mouse)	37.83 ± 18.24	24.52 ± 6.25	14.07 ± 5.91	0.0105*
Average tumour volume (mm^3/mouse)	3.37 ± 1.10	3.80 ± 0.211	2.56 ± 0.57	0.1962
Tumour burden (mm^3/g)	1.40 ± 0.70	0.88 ± 0.21	0.51 ± 0.25	0.0123*

Note: Ordinary One-way ANOVA analysis and Tukey's multiple comparisons test was used to assess between the three groups. Tumour burden was calculated using the total tumour volume for each mouse and dividing by the final weight of the corresponding mouse.

5.3.2. Cohort monitoring

None of the mice within the cohort exhibited any signs of adverse effects throughout the experiment. All mice were healthy, active and exhibited normal behaviour. All mice were able to grow subcutaneous tumour nodules bilaterally at the injection sites. There were no concerns raised regarding mice welfare or general health from the independent dedicated mouse laboratory team throughout the experiment duration and no concerns were identified by our team. None of the subcutaneous tumour nodules on the mice grew beyond 10mm in size at termination of experiment. Throughout the experiment there was no significant difference between the mice cohorts in terms of weight at each weekly formal weighing when compared to controls (Table 5.4 and Figure 5.2a). There was no significant difference between the cohort weights at the end of the experiment when the mice were culled (Figure 5.2b). All mice trended to gain weight over the time period at the expected rate related to their age.

Table 5.4: One-way ANOVA analysis with mean and SD comparing mouse weight at each weekly interval. There was no significant difference demonstrated between mice weight between the two treated cohorts throughout the experiment when compared to the control at each weekly check.

	Group A Control treated mice group weight (g)						Group B HAi treated mice group weight (g)						Group C HA treated mice group weight (g)						P-Value
	M1	M2	M3	M4	M5	M6	M1	M2	M3	M4	M5	M6	M1	M2	M3	M4	M5	M6	
Week 0	22.6	25.1	26.5	28.1	26.0	23.7	27.6	26.0	28.1	22.9	28.5	26.8	32.3	25.0	27.2	23.0	25.7	26.9	**0.59**
Week 1	22.8	24.6	26.3	28.7	28.2	24.1	27.8	26.7	27.6	23.6	28.4	28.6	31.6	25.0	26.6	23.6	25.5	28.8	**0.61**
Week 2	23.6	25.9	25.9	29.9	27.7	24.3	27.3	27.1	27.0	23.3	27.9	28.3	31.9	25.2	29.0	23.7	25.7	27.6	**0.78**
Week 3	23.8	26.0	28.6	30.1	27.0	24.6	27.5	28.2	28.4	23.9	27.7	28.1	34.7	26.9	28.0	24.4	26.4	28.4	**0.64**
Week 4	23.8	26.0	28.3	30.6	29.0	25.6	28.7	29.0	28.2	23.7	28.3	30.2	33.0	26.5	27.6	25.2	25.9	30.3	**0.82**

	Group A		Group B		Group C	
	Mean weight (g)	SD	Mean weight (g)	SD	Mean weight (g)	SD
Week 0	23.3	1.98	26.7	2.05	26.7	3.14
Week 1	25.7	2.36	27.1	1.85	26.9	2.91
Week 2	26.2	2.30	26.8	1.79	27.2	2.97
Week 3	26.7	2.39	27.3	1.70	28.1	3.51
Week 4	27.2	2.51	28.0	2.23	28.1	3.00

a.

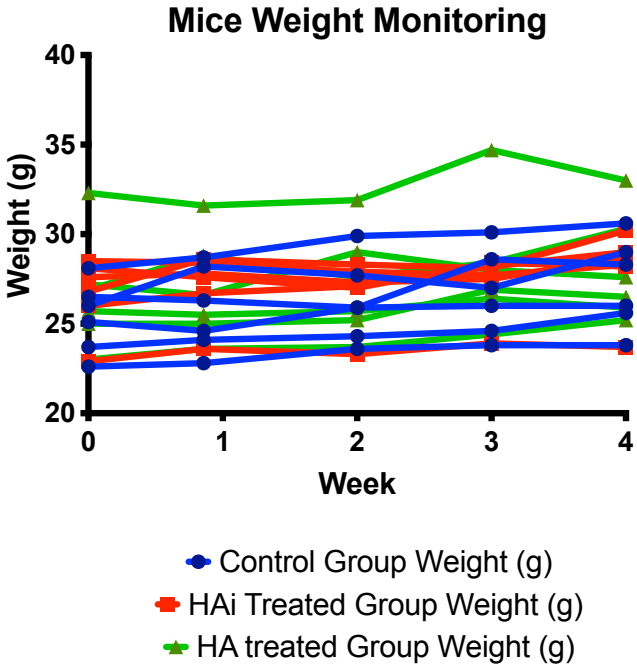

b.

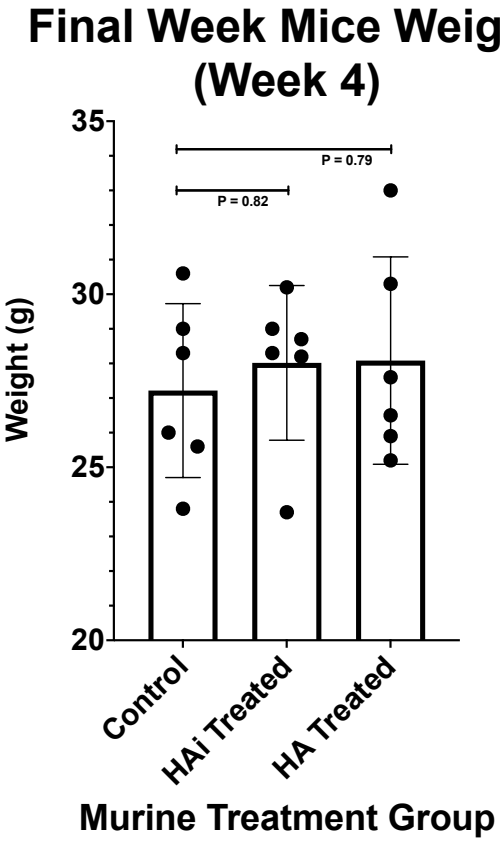

Figure 5.2: 5.2a. Mice weights within each cohort over time. There was no significant difference found at each weekly assessment. One-Way ANOVA. 5.2b. One-ANOVA Dunnett's multiple comparisons test. There was no significant difference found between cohorts at experiment end. See Appendix 3.1.

5.3.3. Peritoneal metastatic dissemination

The mean peritoneal tumour nodule count is shown in **Table 5.5**.

There was a significant reduction in the number of peritoneal tumour nodules in both the HAi (p=0.0094) treated group and the HA treated group (p=0.0009) when compared to the PBS control treated group (Figure 5.3). There was no significant difference demonstrated in the number of tumour nodules between the HAi treated cohort or the HA treated cohort (p=0.4745) (Figure 5.3). Interestingly, within this current study all metastatic nodules were located on the visceral peritoneum of the serosal surfaces small bowel and colon. The parietal peritoneum appeared unaffected. There was no evidence of metastatic spread to the liver or other solid organs. The reasons for these findings are unknown. One possibility could be down to the thickness of the visceral peritoneum being thinner than the parietal peritoneum, which may lead to adhesion to the serosal surfaces, in the timeframe of the experiment, being more amenable.

Table 5.5: Mean peritoneal total tumour count per mouse of each murine treatment cohort with standard deviation.

Cohort	Mean Peritoneal Tumour Nodules (n)	Standard Deviation
Control	11.17	2.99
HAi Treated	6.83	1.60
HA treated	5.33	1.63

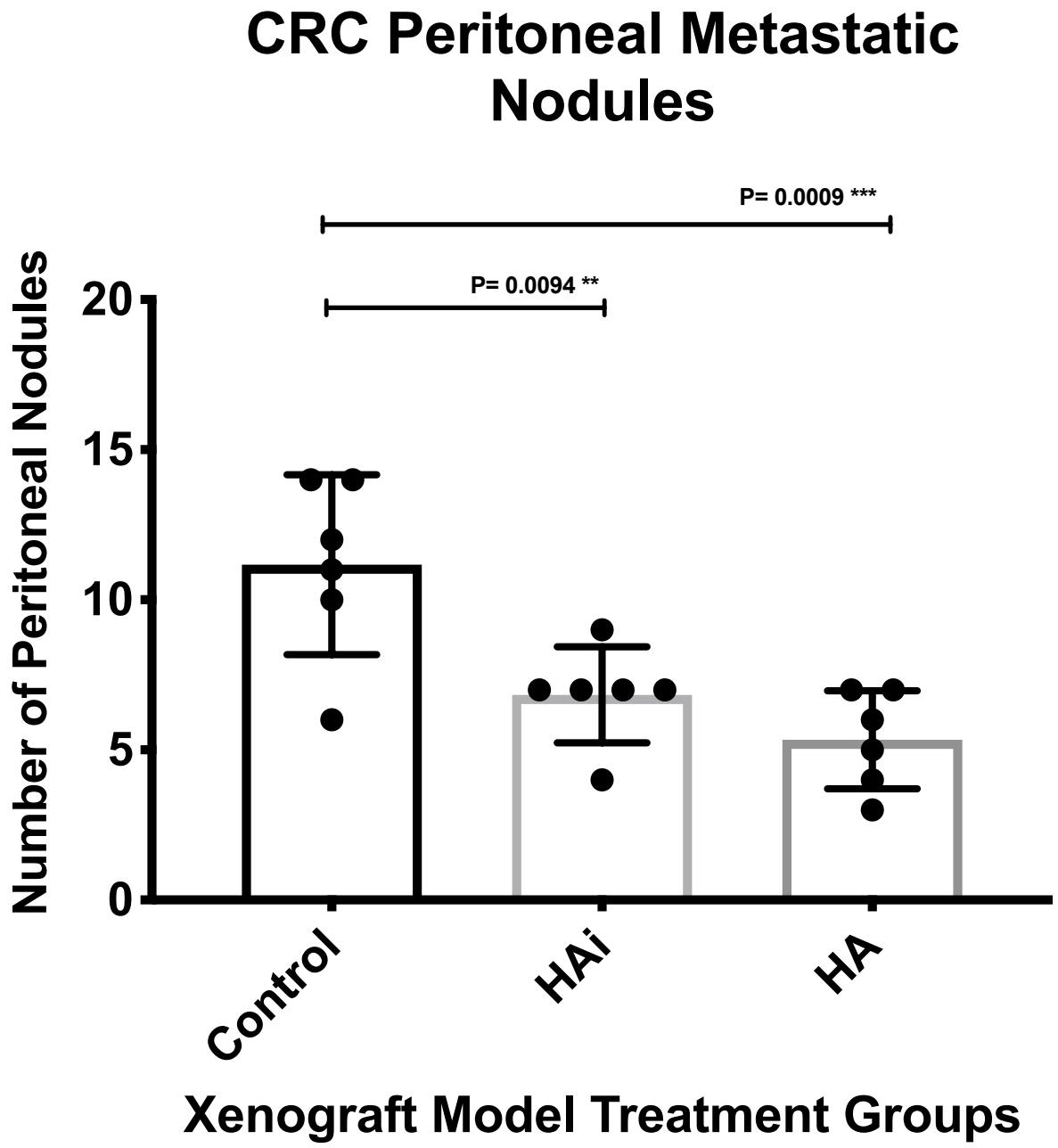

Figure 5.3: Total peritoneal metastatic tumour deposits compared to each cohort. There was found to be both a significant reduction in tumour deposits in the HAi treated group (p=0.0094) and the HA treated group (p=0.0009) when compared to the control group. See Appendix 3.2.

5.3.4. Individual peritoneal metastatic tumour nodule volume

All individual tumour nodules were measured and photographed from each mouse and there was found to be no significant difference in tumour nodule size between any of the cohorts. The mean individual tumour nodule volume was 3.37 mm^3 (SD 1.10 mm^3) for the untreated cohort, 3.80 mm^3 (SD 1.56 mm^3) for the HAi treated cohort and 2.56 mm^3 (SD 0.57 mm^3) for the HA treated cohort.

A one-way ANOVA and Tukey's multiple comparisons test was undertaken which demonstrated no significant difference in average tumour nodule volume between either the treated groups or the control group. (Control vs HAi p=0.7976; control vs HA p= 0.4536; HAi Vs HA p=0.1795) (Figure 5.4).

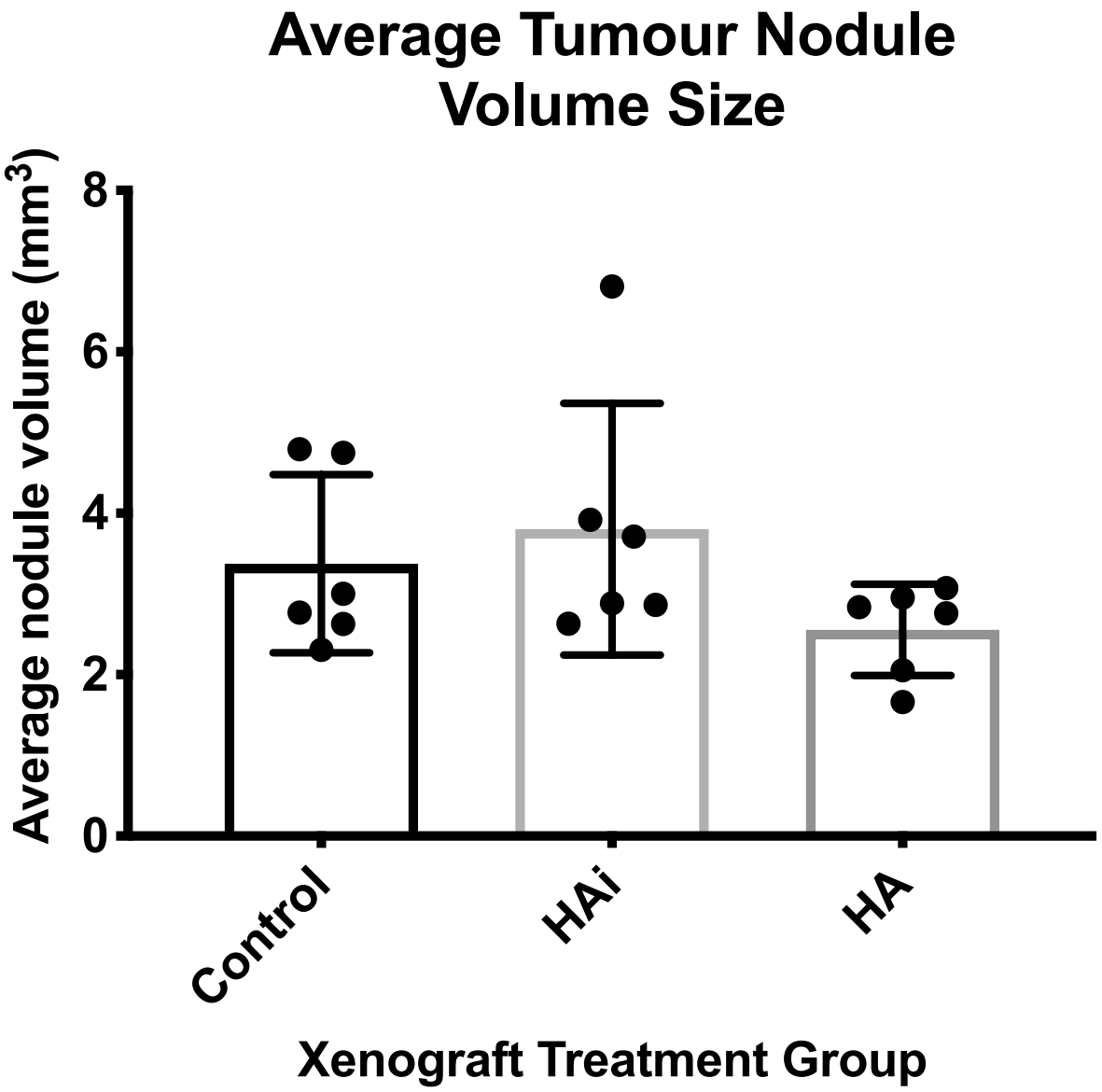

Figure 5.4: The average size of peritoneal nodules for each mouse within each cohort was compared and found to demonstrate no significant difference between metastatic tumour size between the cohorts. See Appendix 3.3.

5.3.5. Tumour burden

Overall total tumour volume per mouse can be calculated with the sum of the individual tumour volumes from the individual tumour nodules (mm^3). However, to put this into context so that it is translatable, the tumour burden is calculated, as it is a calculation relative to the weight of the individual host. Therefore, the tumour burden was calculated based on the total tumour volume measured for each mouse (mm^3) and dividing by the final weight of the mouse within the experiment.

The mean total tumour volume per mouse for the untreated control per mouse was $37.83mm^3$ (SD $\pm 18.23mm^3$), for the HAi treated cohort the mean overall tumour volume per mouse was 24.52 mm^3 (SD ± 6.25 mm^3) and for the HA treated cohort mean overall tumour volume was $14/07mm^3$ (SD $\pm$ 5.91 mm^3). There was a trend seen toward a reduced total tumour volume for both the HAi and HA treated murine cohorts, when compared to the control cohort. However, for the HAi treated group this was not seen to be statistically significant ($p=0.1519$), whereas, for the HA treated group this was found to be statistically significant ($p=0.0080$). (Figure 5.5a)

When total tumour volume was standardised to calculate tumour burden, based on mouse weight, the same observation was still demonstrated. There was a decrease in the standardised tumour burden for both the treated groups when compared to the control group. However, this was only found to be statistically significant in the HA treated group (HAi $p=0.1364$ and HA $p=0.0096$). Mean standardised tumour burden is shown in Table 5.5.

There was no significant difference between total tumour volume (p=0.2957) and standardised tumour burden (p=0.3668) between either of the treated groups. (Figure 5.5b).

Table 5.5: Mean standardised tumour burden of each murine cohort with standard deviation.

Cohort	Standardised tumour burden (mm^3/g)	Standard Deviation (mm^3/g)
Control	1.40	0.70
HAi Treated	0.88	0.21
HA treated	0.51	0.25

a.

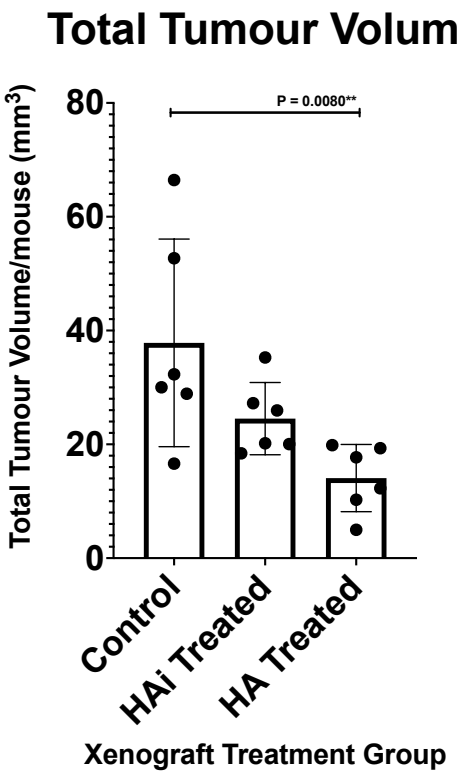

b.

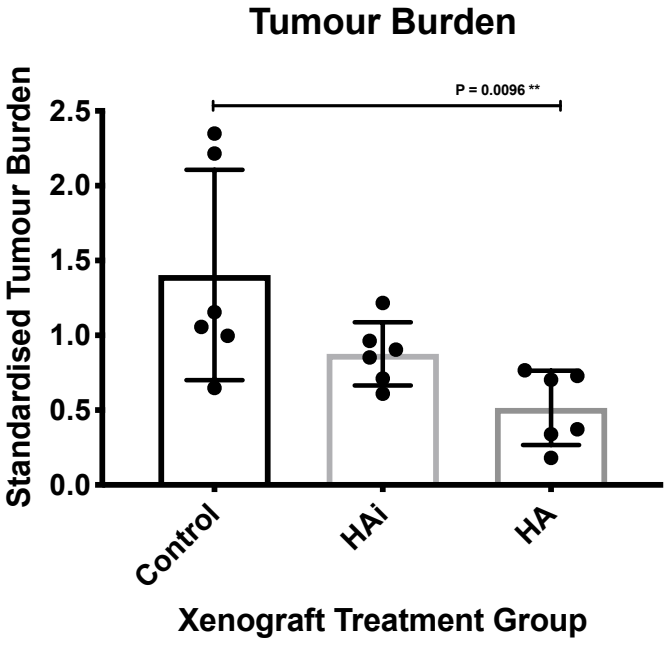

Figure 5.5: 5.5a. Total tumour volume between mice (mm^3) demonstrated a trend towards reduced total tumour volume in the treated groups compared to the control but was only found to be statistically significant in the HA treated group (p=0.0080). 5.5b. The standardised tumour burden demonstrating a trend towards decreased tumour burden in the treated groups, compared to the control. This was found to be statistically significant in the HA treated murine cohort (p=0.0096).

5.3.6. Peritoneal fluid cell assessment

Peritoneal fluid samples were counted using a haemocytometer and a light microscope taking three separate counts of samples from each mouse and mean results were taken. Although was a general trend to a reduction in overall free-floating cell numbers this was not found to be statistically significant in the treated cohorts when compared to the control (control Vs Hai p=0.4145; control vs HA p=0.0695) (Figure 5.6).

This cell count method unfortunately did not and was not able to differentiate between CRC cells and free-floating peritoneal cells from the mice themselves. A more robust method to assess this further would be to tag the colon cancer cells with a fluorescent marker to facilitate a more accurate method of specifically counting cancer cells. However, it is important to note that the treatment groups overall trend for free-floating cells was reduced for all cells in the peritoneal environment, possibly suggesting that treatment with HAi or HA creates a more hostile peritoneal environment for detached free-floating cells. This is a potential area to explore further and specifically identify the colorectal cancer cells in the peritoneal fluid suspension for future work.

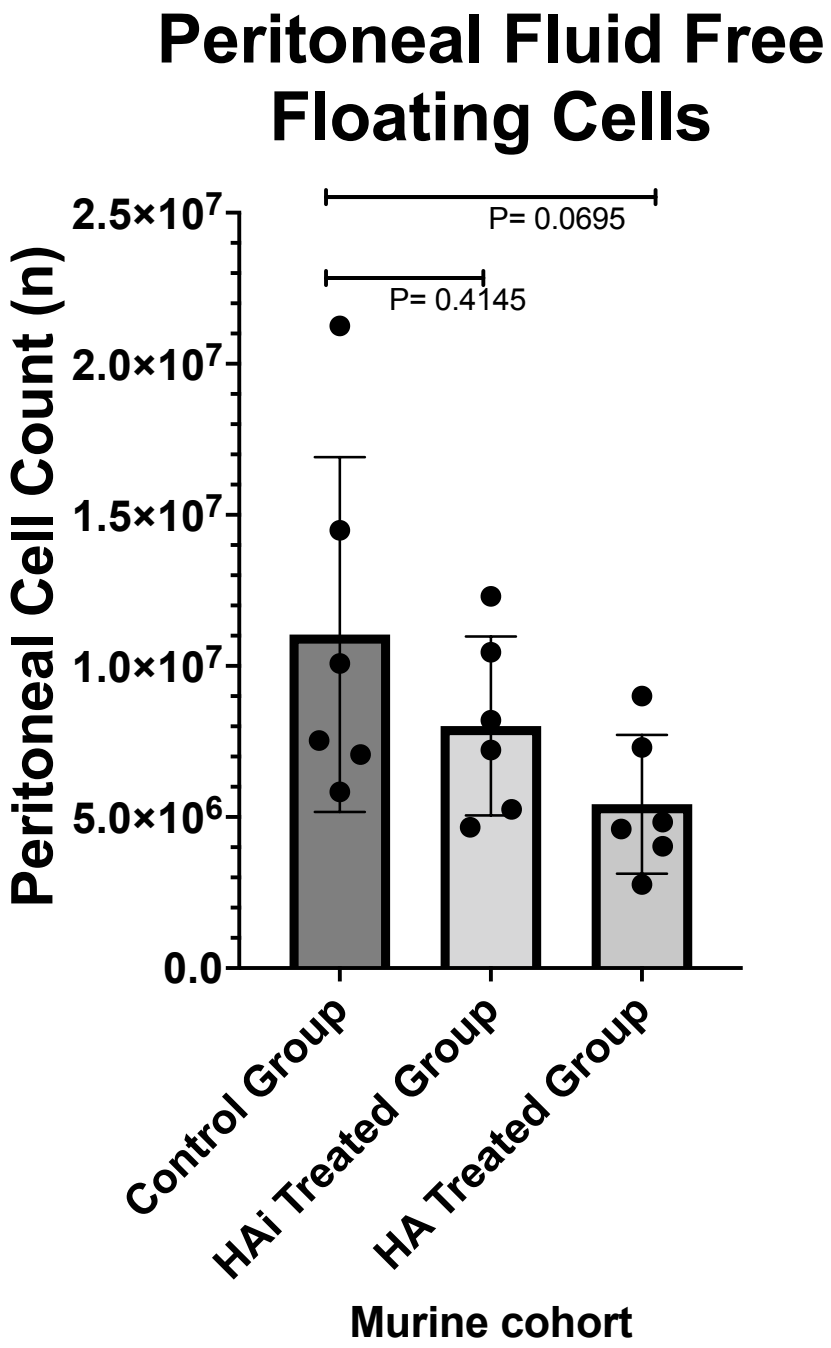

Figure 5.6 One-way ANOVA and Tukey's multiple comparisons analysis assessing free-floating cells from peritoneal fluid. There was a trend towards decreased free-floating peritoneal cell counts in the HAi treated and HA treated groups, compared to controls. However, this was not proven to be statistically significant (control Vs HAi P=0.4145, control vs HA P= 0.0695). See Appendix 3.4.

5.3.7. Histology

All peritoneal tumour nodules were removed, inspected macroscopically and photographed using a stereomicroscope (Figure 5.8). From each cohort, half of the tumour nodules were frozen down at -80°C in dry conditions to preserve the tumours, before being prepared for wax paraffin fixation and then haematoxylin and eosin (H&E) staining for and assessment under light microscopy. The remaining tumour nodules from each cohort were stored preserved in formalin solution for future use. (Figure 5.7).

Frozen specimens were set in wax paraffin fixation and sections taken and placed on glass slides and underwent H&E staining (Figure 5.7 and 5.8). Remaining embedded specimens were placed on sides unstained would be able to be further evaluated with immunostaining for future work.

a.

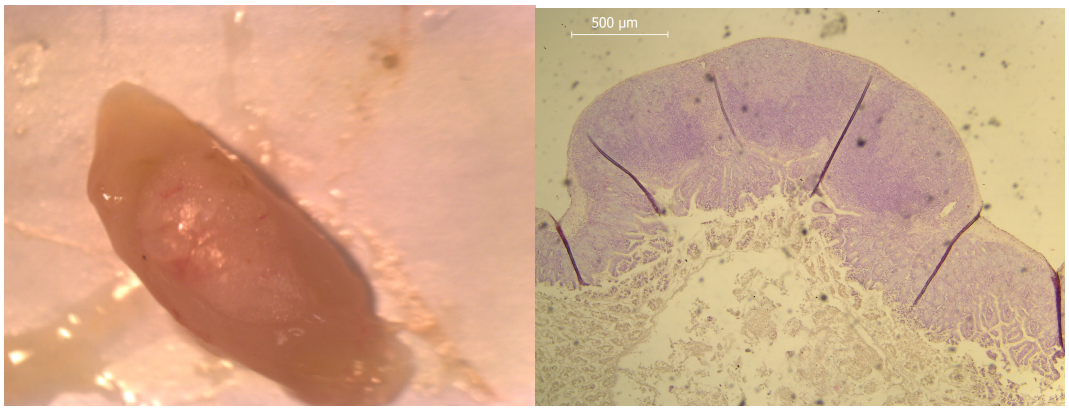

b.

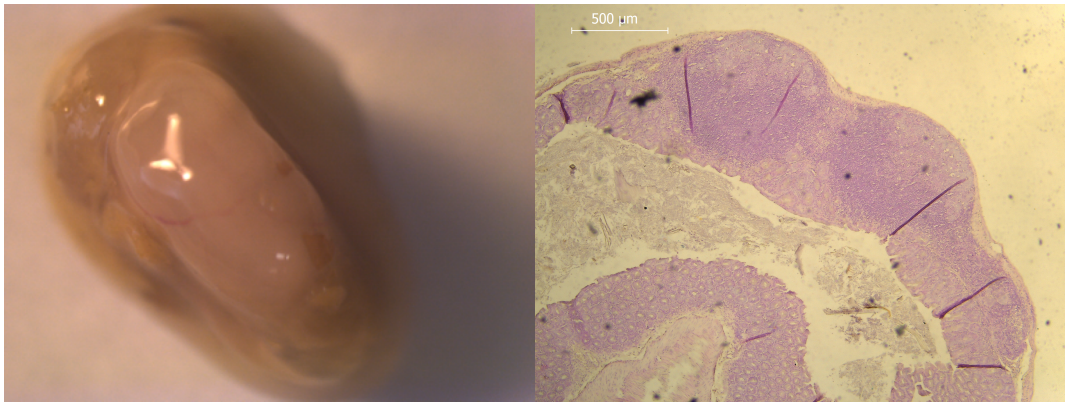

c.

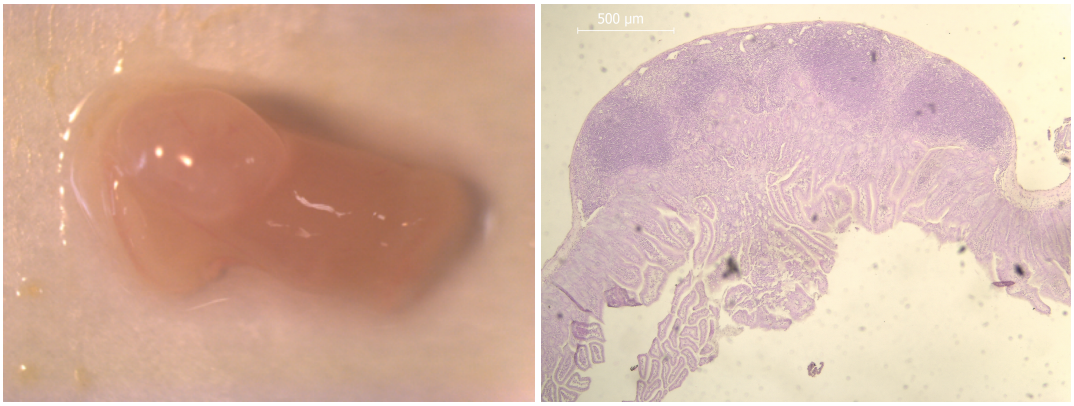

Figure 5.7: Example illustration of the macroscopic imaging of tumour nodules attached to the peritoneum of the small bowel from the three mouse cohorts: a. From the Control group; b. From the HAi Treated group, c. From the HA treated group. Corresponding microscopic images (x4 magnification) H&E-stained tumour nodules. Images are representative of all other tumour nodules obtained from each cohort. Scale of microscopic images is also shown in the top left of the microscope images

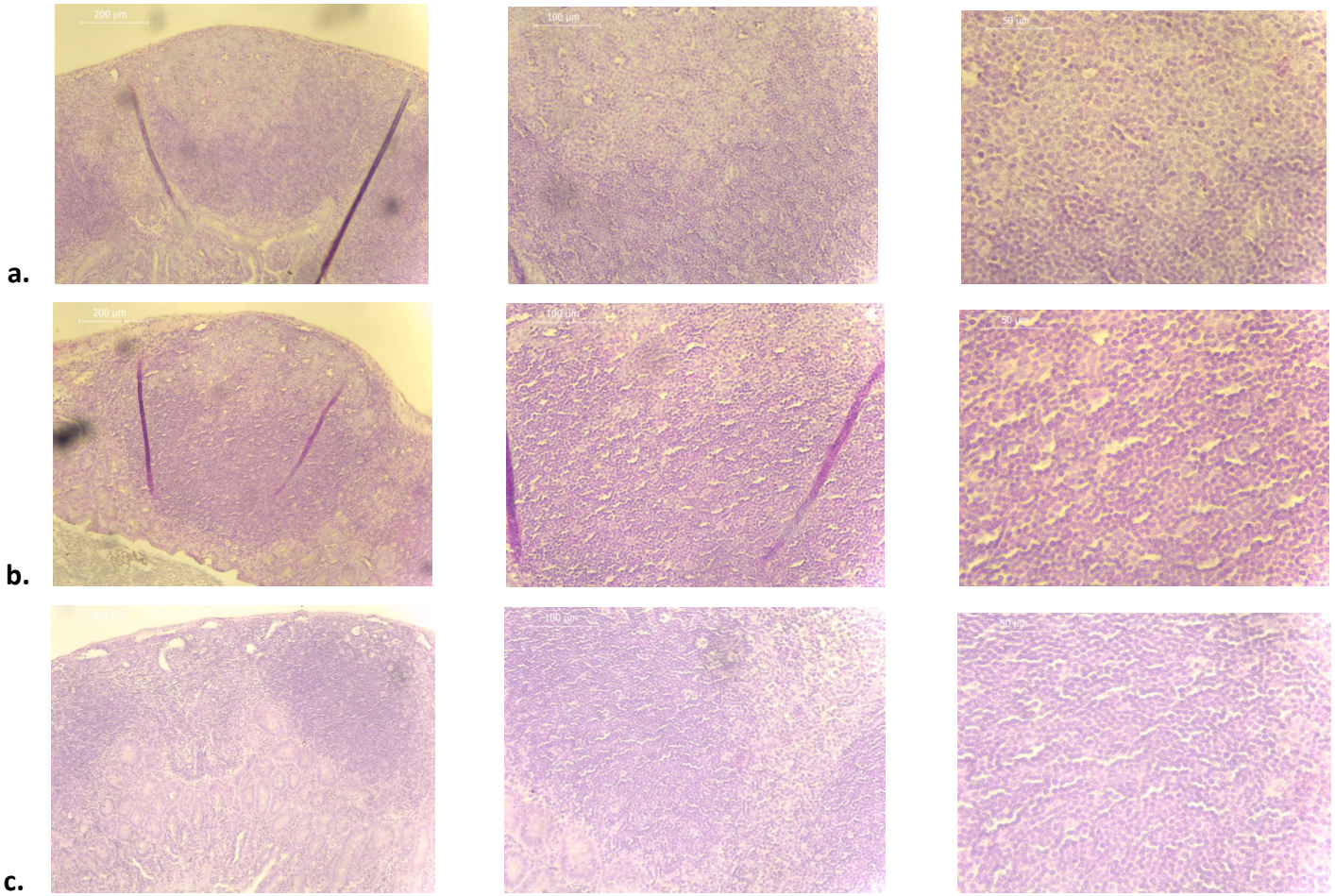

Figure 5.8. Example illustration of the microscopic H&E-stained tumour nodule images taken at x10, x20 and x40 magnification corresponding to Figure 5.7. Tumour nodules attached to the peritoneum of the small bowel from the three mouse cohorts: a. From the Control group; b. From the HAi Treated group, c. From the HA treated group.

5.4. Discussion

5.4.1. General discussion

This chapter builds on preliminary work conducted *in vitro* assessing CRC cell adhesion and disruption using a competitive inhibitor targeting HA receptor molecules (Chapter 4). This initial pilot study has demonstrated both reduced number of established tumour nodules *in vivo* and total tumour burden in cohorts treated with either HAi or excessive exogenous HA when compared to untreated controls.

However, once tumour nodules have become established the rate of growth does not appear to be affected since there was no significant difference in average tumour nodule size between groups. This suggests that HA is involved in the initial process of adhesion of CRC cells to the peritoneum, rather than tumour growth *per se*.

Whilst there is a trend towards decreased free-floating cells in the peritoneal fluid, it is not possible to draw definitive conclusions from this. Further detailed work would be required to assess this further, for example gene tagging the human CRC cells with a fluorescent tracer protein to facilitate the ability to differentiate human cells from free-floating mice cells as well as assess tumour growth (Ashmore-Harris, Iafrate, Saleem *et al.*, 2020; M. Yang, Baranov, Moossa *et al.*, 2000).

The ability of tumour cells to detach from the primary CRC tumour and spread throughout the peritoneal cavity to form PM as described in the peritoneal metastatic model (Sluiter *et al.*, 2016) is undoubtedly a major problem when treating advanced CRC. The ability to target specific points of the metastatic model to prevent tumour dissemination after surgical

resection would be an important addition to treatment options. If cells are indeed unable to survive for prolonged periods in suspension as demonstrated in Chapter 4, then the ability to delay adhesion of CRC cells at distant sites for as long as possible might be an important mechanism to prevent metastases.

For this pilot study it was appropriate to use an orthotopic human tumour xenograft model, particularly as this model has been shown to be useful in assessing drug response in human tumours.

5.4.2. Limitations and further work

There are several limitations identified. Firstly, the xenograft mouse model used, as summarised in Table 5.1**,** carries the inherent drawback of a less realistic tumour microenvironment, particularly stromal interactions, which could potentially affect response to treatment. Secondly the use of single tumour cell lines carries limitations since they do not represent cancer heterogeneity.

Monitoring of intraperitoneal tumour growth was not possible during this experiment. Whilst general health, weight and subcutaneous tumour growth could be monitored, this experiment does not allow any real-time assessment of intraperitoneal effects of treatment or whether the duration of treatment would need to be either longer or shorter for optimum assessment.

This pilot *in vivo* study could be further refined to validate the results demonstrated. Firstly, staining CRC cells with a luciferase to facilitate imaging tracking through bioluminescence

(Taibi, Albouys, Jacques *et al.*, 2019) would be one possible way to facilitate the tracking tumour growth of the xenografts more accurately over the course of the experiment. It would also allow further understanding of the response within the peritoneal cavity to the CRC cells and compare the treated and control cohorts to provide validation of the results. Another alternative is the use of Halo Tag® protein tagging system which provides specific labelling of xenograft tumours in living animals. This system facilitates assessment via fluorescence tagging which can be imaged, rather than bioluminescent (Tseng, Benink, McDougall *et al.*, 2012). This systemic administration intravenously provides irreversible binding of the protein tag and can be both utilised for live imaging. However, HALO Tag is short acting and suitable for real-time imaging assessment. By modifying HT115 cells to emit fluorescence would also facilitate more accurate assessment of free-floating peritoneal cells to differentiate between cancer cells and murine host cells within the peritoneal fluid.

Blinding of xenograft cohorts, to those providing treatment to the mice and those assessing tumour growth at laparotomy and dissection of tumour nodules would be a further way to eliminate any potential bias in scaled up experimentation. Standardisation of tumour nodule recognition and also measurements could again reduce any intra- or inter-observer variation when assessing tumour nodules and tumour burden.

Subcutaneous tumour nodules were unfortunately not retrieved nor stored at the time of terminating the mice and on reflection would have been useful to compare histologically as a verification of the peritoneal tumour morphology. Another way to verify that tumour cells are of human origin would be immunohistochemical staining for cytokeratins (CK) of human colorectal origin such as CK7 or CK20 (Painter, Clayton, & Herbert, 2010).

It has been shown that trauma to the peritoneum at surgery enhances successful seeding of cancer cells and hence peritoneal recurrence (Eggermont, Steller, & Sugarbaker, 1987; Oosterling, van der Bij, van Egmond *et al.*, 2005; M. P. van den Tol, Haverlag, van Rossen *et al.*, 2001; P. M. van den Tol, van Rossen, van Eijck *et al.*, 1998). A model involving peritoneal scratching (Taibi *et al.*, 2019) is available. This would be useful to study the role of peritoneal trauma on CRC PM together with treatment targeting the HA receptor, since the risk of peritoneal recurrence appears to increase following surgery. It may further enhance the results already seen with targeting HA-dependent adhesion.

After further validation of these initial results, consideration should be given to further dosing optimisation *in vivo*.

Tumour nodules from the peritoneal cavity have been stored and can be studied further regarding examining cell function. Comparison of adhesion receptor molecule expression between groups would be interesting. For example, IL-8, in the AKT pathway, has been identified as decreasing apoptosis and promoting proliferation in various cancers, including colorectal cancer (J. Li, Huang, Zhao *et al.*, 2020). Would IL-8 in the AKT pathway be seen to be supressed in the two treatment groups (Pasquier *et al.*, 2018)?

Further *in vivo* experimentation, could examine the effect on free-floating CRC cells to examine anoikis and cell survival, as discussed in chapter 4. Alternatively, or would there be any difference in expression of adhesion molecules in free-floating cell when compared to

established metastatic tumour nodules (Hofmann, Obermeier, Artinger *et al.*, 2007; Taddei, Giannoni, Fiaschi *et al.*, 2012)?

5.4.3. Conclusions

Targeting the HA receptor molecules on CRC cells with a competitive inhibitor is a potential method to reduce the risk of local peritoneal recurrence. Whilst further evaluation is required preliminary results show potential towards a role within treatment either through use with a specific competitive inhibitor or providing excess HA to the tumour environment.

General Discussion

Chapter 6

6.1. Hyaluronic acid in colorectal cancer peritoneal metastases

Peritoneal metastasis (PM) from colorectal cancer (CRC) carries a significant mortality rate for patients, and treatment is challenging. The development of PM is a multistep process involving detachment, adhesion, invasion, and colonisation of the peritoneal cavity. Cytoreductive surgery and HIPEC (hyperthermic intraperitoneal chemotherapy) for PM from CRC has some benefit but overall survival is poor and recurrence rates are high. Treatments to prevent the development or recurrence of peritoneal metastasis could have the potential to improve CRC survival and disease-free outcomes.

The ability of CRC cells to invade the peritoneum and become established metastatic tumours is influenced by a multifactorial and multimolecular process. Hyaluronic acid (HA) coats the mesothelial cells of the peritoneum and has been demonstrated to be potentially utilised in various malignancies as part of the adhesion phase of the peritoneal metastatic model in peritoneal dissemination. CD44, RHAMM (CD168) and ICAM-1 have all been shown to be binding partners for HA, as well as having upregulated expression in CRC. Targeting HA-mediated binding may prevent adhesion at distant sites within the peritoneum through suppression of interaction of these molecules.

HA is a molecule not only involved with the peritoneum but found throughout the body playing a role in many different cellular interactions. It could be considered that current radical surgical and chemotherapeutic regimens, such as CRS, HIPEC or even PIPAC (Pressurised intraperitoneal aerosolised chemotherapy) regimens affect cell-cell interaction, and also influence both peritoneal tumour microenvironment and native host tissues. It has

been shown that the extent of parietal peritonectomy in CRS does not influence or change the pharmacokinetics of chemotherapy drug concentration required, as it does not directly influence plasma absorption of chemotherapeutic drugs (de Lima Vazquez, Stuart, Mohamed *et al.*, 2003). Therefore, non-mesothelial cells are likely to interact with both chemotherapeutic drugs, as well as free-floating cancer cells, in a similar way to that of the mesothelial cells, due to cross-over of cell surface receptor molecules. Cell plasticity, which facilitates the ability to adapt to changing environments, through upregulation or down regulation of cell surface receptors, may also influence this process.

Targeting HA-dependent adhesion may have potential as a prevention therapy for peritoneal metastatic disease in CRC. Targeting CRC-HA interaction at the time of index surgery, where macroscopic disease has been resected but where there is a high risk of detached free-floating CRC cells, may reduce the risk of local recurrence. For example, locally advanced or perforated colorectal tumours are highly likely to shed malignant cells into the peritoneal cavity. Prevention of adhesion and CRC-HA interaction could lead to reduced ability of cells to attach to distant tissues (such as the peritoneum). Disruption of adhesion-dependent CRC cells could promote tumour cell anoikis and is a potential mechanism to exploit for adjuvant treatment modalities. By augmenting the environment for vulnerable free-floating tumour cells, anoikis of these cells by effective multimodal therapy could be enhanced. A more complete understanding of how HA influences cellular interaction with CRC tumour cells may be a key influence in preventing or reducing the burden of peritoneal metastatic disease.

6.2. Main conclusions of this study

6.2.1. Expression of CD44 in colorectal cancer

The tissue microarray data, of mRNA expression of CD44, demonstrated that CD44 has increased expression in colorectal tumours. The expression of CD44 was not related to cancer stage, TNM staging, gender or tumour location. However, CD44 expression was seen to be associated and upregulated in mutated KRAS tumours. Within primary CRC cell lines expression is variable but present on most cell lines. Expression of CD44 was verified on the cell lines HT115, HRT-18, Caco-2 and the mesothelial LP9 cell lines.

6.2.2. Expression of RHAMM in colorectal cancer

The tissue microarray data, of mRNA expression of RHAMM, demonstrated that RHAMM has increased expression in colorectal tumours. The expression of RHAMM was not related to cancer stage, TNM staging, gender, tumour location. However, RHAMM expression was seen to be associated and upregulated in TP53 mutated tumours. Finally, expression of RHAMM was verified on HT115, HRT-18 and Caco-2 cell lines.

6.2.3. Expression of ICAM-1 in colorectal cancer

ICAM-1 mRNA expression, from the tissue microarray, was again increased in colorectal tumours. Expression was not related to bowel cancer stage, gender, or tumour location. In terms of TNM stage there was no difference in N-stage or M-stage, however, T4 tumour expression was increased in comparison to T2 and T3 tumours, but not T1 tumours. ICAM 1 expression appeared to be upregulated in BRAF mutated tumours when compared to wild type.

6.2.4. Influence of targeting hyaluronic acid on colorectal cancer adhesion *in vitro*

Targeting HA with the use of either the peptide inhibitor HAi or excess hyaluronic acid has shown both a reduced ability for anchorage-dependent colorectal cancer cells to adhere to either the peritoneum or other CRC cells.

6.2.5. Disrupting colorectal cancer adhesion and influence on anoikis

Where CRC cells are unable to attach to the extracellular matrix (ECM) and in particular are found in a free-floating single cell state, they are vulnerable to anoikis. Cancer cells are able to exploit several mechanisms to attempt to evade anoikis including:

- Integrin switch to the local ‘soil’ site and utilising integrins to supress anoikis
- EMT change
- Pro-survival signalling
- Deregulating or adapting cellular metabolism

During these transformative processes, cells are vulnerable and are in a state of fine balance of initiating anoikis pathways. By disrupting cellular adhesion, chemotoxic therapies may be enhanced in their effect on tackling potentially otherwise chemo resistant cancer cells, which again may serve to promote anoikis pathways.

6.2.6. Influence of targeting HA receptor binding *in vivo*

Both the use of a specific hyaluronic acid peptide inhibitor and also the use of excess hyaluronic acid was able to achieve a reduction in the total tumour nodules when compared to a control group. The preliminary *in vivo* examination CRC cells through a peritoneal metastatic model demonstrated a reduction in peritoneal cancer nodules and total tumour burden. Conversely it was shown that once tumour nodules had established, at a distant site, there was no difference to the individual tumour nodule size. This potentially implies that growth and/or invasion may not be affected. It also suggests that there is a limited chemotoxic effect to the cells that are already anchored.

6.2.7. Summary of thesis findings

Overall, the results suggest that hyaluronic acid-dependent adhesion is a potential mechanism to target in colorectal cancer treatment. All three hyaluronic acid-binding receptor molecules, which are identified in the literature, are all upregulated in colorectal cancer. It is important to bear in mind the peritoneal metastatic model and the application of exploiting this mechanism should be tailored toward preventing adhesion. Therefore, the timing and delivery of such treatment is important to yield results.

6.2.8. Clinical application

Traditionally the principle of peritoneal lavage with water is thought to be the optimal washout method as a preventative method for local recurrence due to the osmotic gradients causing cell lysis, however the robust evidence for this is limited (Youssef, Beddingham, Soliman *et al.*, 2021). The principle of targeting hyaluronic acid-mediated cellular adhesion in CRC, as a primary preventative strategy to prevent seeding of free-floating peritoneal metastases following macroscopic surgical resection, is a novel approach to consider. Seprafilm™ is an antiadhesion barrier to reduce adhesion scar tissue formation. One of the key components of Seprafilm™ is hyaluronic acid. It is recognised that the use of antiadhesion barriers, such as Seprafilm™, may cause a significant increased rate of both anastomotic leak or enterocutaneous fistula formation in patients where bowel has been anastomosed. However, in the context of non-restorative surgery, where there is evidence or high risk of cell spillage of tumour such as with a perforated tumour, then application of a hyaluronic acid inhibitor or the addition of an excess of hyaluronic acid solution may reduce local or peritoneal recurrence following complete resection of macroscopic tumour.

The principle of preventing or delaying the ability of anchorage-dependent cancer cells to settle and attach to other cells increases the likelihood of the cell failing to thrive and the chance of cell anoikis.

6.3. Limitations

There are a number of limitations regarding the data discussed in this thesis. Firstly, the use of a freely available tissue microarray is not necessarily tailored or specific to the question being asked. Whilst a select range of non-HA-dependent adhesion molecules were able to be studied as a screening process for expression in CRC, not all adhesion molecules identified within the literature were available to be studied in the microarrays used in this study.

Secondly, tissue microarrays for RNA expression do not definitively relate with the cell surface protein expression of molecules. Further work would be important to assess that RNA expression translated to protein cell surface expression of adhesion molecules, in order to further correlate if protein expression was upregulated, supressed, or unchanged in CRC.

Third, primers for CD44 can be non-specific due to the many possible variants of CD44 and it is important to consider this in the context of the colorectal cancer cell lines being studies. Whilst CD44 is present on all the cells as shown in the gene data, it would be prudent to check that HA receptors are present on the CD44 variants present on the particular CRC cell line. It is assumed that HA receptor molecules are present on all CD44 variants, but correlation would be needed. If this is confirmed, further confirmation that the conformational state of each CD44 variant allowed the HA receptor molecule to be able to interact with HA.

The xenograft CD1 peritoneal model in some ways is simplistic in its nature. There is potential for a single immortalised cell line to exclude the complexities of the tumour microenvironment, which is known to be present in many cancers including CRC. It may be argued that the peritoneal model lacks a primary tumour in which cells are able to shed and metastasise, however in the context of a primary tumour resection in real-world practice remaining cells would be free-floating cells within the peritoneal environment,

Funding constraints are a realistic part of cancer research and limit the ability to either fully explore or indeed completely examine an area or question until a positive or significant finding is demonstrated with new work. Reliance on previous published research work helps build on knowledge and directs areas to examine further. To mitigate funding constraints, sometimes the use of older, more laborious, or inefficient laboratory techniques can be used to reduce cost, but still be relevant to attempt to answer the question at hand. Pertinent further questions stemming from initial examination often require significant funding to scale up the investigative process to arrive at conclusions more expediently.

6.4. Future perspectives

This study has, firstly, demonstrated that molecules with a hyaluronic acid receptor (CD44, RHAMM and ICAM-1) are all upregulated in colorectal cancer. Secondly, by targeting the hyaluronic acid receptor with a competitive inhibitor the ability of anchorage-dependent colorectal cancer cells to adhere both *in vitro* and *in vivo* is reduced. Finally, as a result of preventing adhesion of CRC cells the ability for the cells to survive in suspension is diminished.

6.4.1. Correlation of findings

The theory that CRC cells, which have not had time to undergo EMT change to adapt to a free-floating environment, in suspension go into stasis to avoid anoikis has not been demonstrated in this study. Further correlation on EMT expression and change to see if cells do undergo change is required to verify this further. The treatment with a competitive inhibitor to HA-dependent adhesion is seen both to disrupt cell anchorage and cell-cell adhesive properties of cells. This effect is seen to potentiate the effects of anoikis cellular mechanisms. Further verification of apoptotic cell pathways is required to confirm the preliminary results seen in this work.

Downregulation or upregulation of HA-dependent adhesion molecules on CRC cancer cell lines would be an appropriate further step for *in vitro* study. The disruption of the receptor protein itself to affect adhesion would be systematic way to verify the findings seen in this study. GEM cell modelling to further examine this as another route to look into further.

6.4.2. Cell signalling pathways

Anoikis evasion is a hallmark of cancer enabled tumour cells (Paoli *et al.*, 2013). The effect on oxidative stress and hypoxia on CRC cells and their ability to survive within the peritoneal environment can alter cell signalling.

After demonstrating that targeting HA-dependent adhesion in CRC PM appears to be a relevant mechanism to target, one of the next stages of further examination would be to investigate if there is any effect on downstream cell signalling on CRC with treatment application on the tumour microenvironment. Specifically, if there is any negative effect of treatment that causes a rebound effect on CRC proliferation. Replicating the stromal environment, with, for example, with 3D *in vitro* models would potentially provide a more realistic examination of the interactions of CRC cells with the peritoneum and HA.

6.4.3. Additional cell models

Due to time constraints of a MD study, work was focused on demonstrating proof of principle of adhesion inhibition with three cell lines *in vitro* and a single cell line *in vivo*. With additional time, exploration with further colorectal cancer cell lines and other malignancies which are complicated by peritoneal metastases would be explored.

6.4.4. Additional *In vivo* models

Further peritoneal mouse modelling through bioluminescent imaging could provide a more accurate method to track peritoneal dissemination during an experimental time course. Targeting the HA adhesion protein molecules by downregulating or overexpressing CD44, RHAMM and ICAM-1 in CRC cell lines, and then assessing the extent of peritoneal dissemination would further serve to assess whether the mechanism of adhesion is significantly affected.

Chapter 7

Appendices

Appendix 1 – Chapter 3

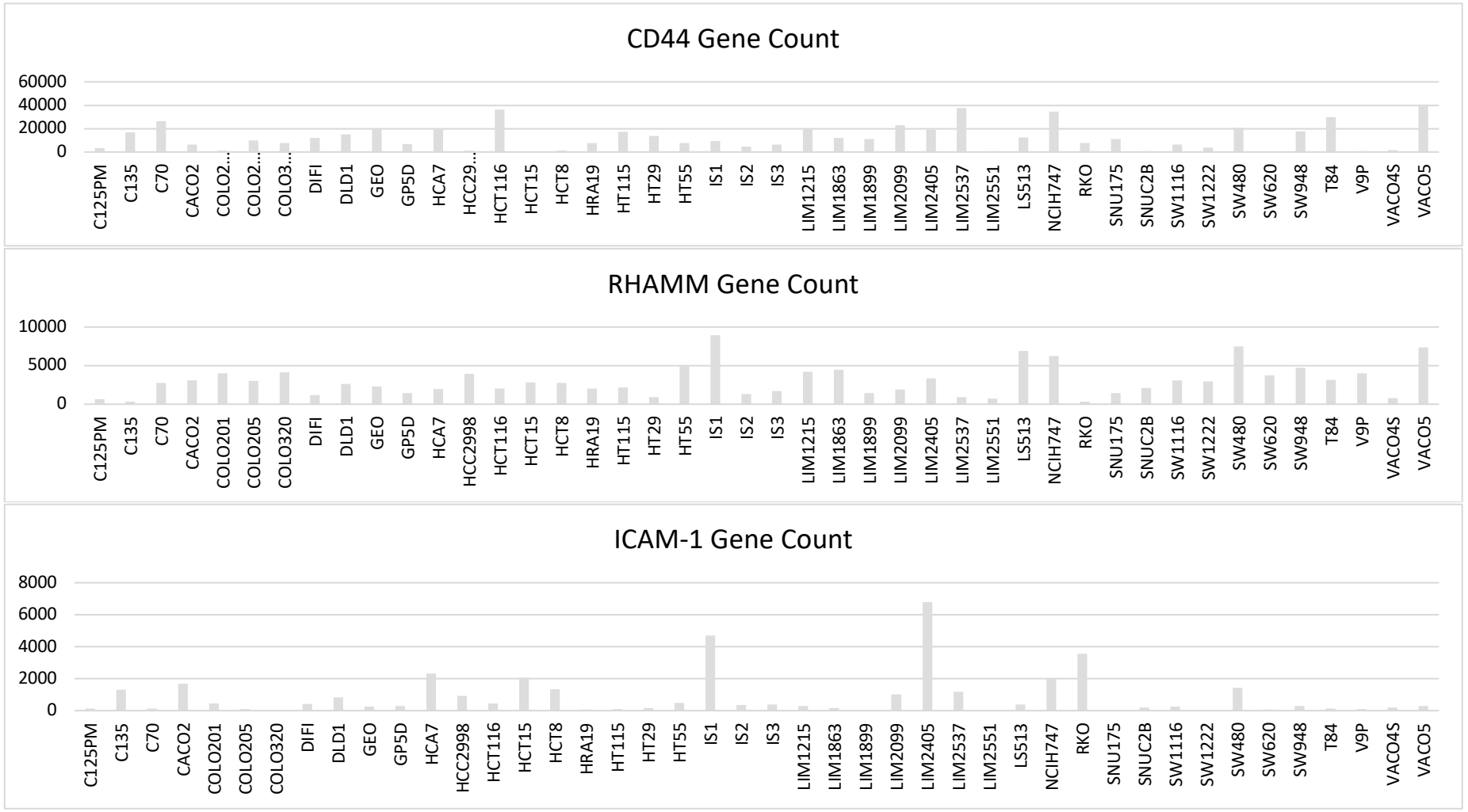

Appendix 1.1 Colorectal Cancer Cell lines and gene expression count for CD44, RHAMM and ICAM-1. Individual data charts. Data extracted from GSE GSE90830.

Cell Line	CD44 Gene Count	RHAMM Gene Count	ICAM-1 Gene Count
C125PM	3548	644	137
C135	16754	353	1319
C70	26452	2779	130
Caco-2	6407	3097	1688
COLO201	1002	3971	436
COLO205	10035	3046	90
COLO320	7770	4161	9
DIFI	11903	1183	429
DLD1	15172	2632	814
GEO	19778	2316	252
GP5D	6824	1423	284
HCA7	20096	1955	2325
HCC2998	1378	3927	911
HCT116	36230	2016	442
HCT15	266	2791	2062
HCT8/HT118	1290	2745	1322
HRA19	7727	2043	55
HT115	17084	2163	101
HT29	13682	937	167
HT55	7841	4901	490
IS1	9449	8963	4708
IS2	4687	1286	351
IS3	6249	1732	386
LIM215	19236	4213	285
LIM1863	12131	4459	165
LIM1899	11107	1427	6
LIM2099	23007	1932	1013
LIM2405	18807	3346	6805
LIM2537	37592	932	1179
LIM2551	660	697	5
LS513	12349	6896	381
NCIH747	34695	6240	1993
RKO	7725	307	3554
SNU175	10956	1409	5
SNUC2B	573	2075	187
SW1116	6205	3084	253
SW1222	3638	2958	43
SW480	20562	7464	1416
SW620	58	3715	54
SW948	17512	4703	274
T84	29631	3123	118
V9P	597	3988	82
VACO4S	1667	778	205
VACO5	40660	7324	283

Appendix 1.2. Colorectal cancer cell lines and gene expression counts of CD44, RHAMM and ICAM-1.

Appendix 2 – Chapter 4

Dunnett's multiple comparisons test	Mean Diff.	95.00% CI of diff.	Below threshold?	Summary	Adjusted P Value	A-?		
No inhibitor vs. 0.02uM	1.000	-5.122 to 7.122	No	ns	0.9683	B	0.02uM	
No inhibitor vs. 0.2uM	3.633	-2.489 to 9.755	No	ns	0.3107	C	0.2uM	
No inhibitor vs. 2uM	2.100	-4.022 to 8.222	No	ns	0.7243	D	2uM	
No inhibitor vs. 20uM	3.900	-2.222 to 10.02	No	ns	0.2598	E	20uM	
Test details	**Mean 1**	**Mean 2**	**Mean Diff.**	**SE of diff.**	**n1**	**n2**	**q**	**DF**
No inhibitor vs. 0.02uM	7.533	6.533	1.000	2.118	3	3	0.4722	10
No inhibitor vs. 0.2uM	7.533	3.900	3.633	2.118	3	3	1.715	10
No inhibitor vs. 2uM	7.533	5.433	2.100	2.118	3	3	0.9915	10
No inhibitor vs. 20uM	7.533	3.633	3.900	2.118	3	3	1.841	10

Appendix 2.1. One-way ANOVA of uncoated plate and HT115 colorectal cancer adhesion treated with a HAi inhibitor. Dunnett's multiple comparisons test.

Dunnett's multiple comparisons test	Mean Diff.	95.00% CI of diff.	Below threshold?	Summary	Adjusted P Value	A-?		
No inhibitor vs. 0.02uM	10.10	-17.18 to 37.38	No	ns	0.6739	B	0.02uM	
No inhibitor vs. 0.2uM	6.900	-20.38 to 34.18	No	ns	0.8736	C	0.2uM	
No inhibitor vs. 2uM	8.667	-18.61 to 35.94	No	ns	0.7694	D	2uM	
No inhibitor vs. 20uM	-5.433	-32.71 to 21.84	No	ns	0.9387	E	20uM	
Test details	**Mean 1**	**Mean 2**	**Mean Diff.**	**SE of diff.**	**n1**	**n2**	**q**	**DF**
No inhibitor vs. 0.02uM	39.67	29.57	10.10	9.436	3	3	1.070	10
No inhibitor vs. 0.2uM	39.67	32.77	6.900	9.436	3	3	0.7312	10
No inhibitor vs. 2uM	39.67	31.00	8.667	9.436	3	3	0.9184	10
No inhibitor vs. 20uM	39.67	45.10	-5.433	9.436	3	3	0.5758	10

Appendix 2.2. One-way ANOVA of Matrigel coated plate and HT115 colorectal cancer adhesion treated with a HAi inhibitor. Dunnett's multiple comparisons test.

Dunnett's multiple comparisons test	Mean Diff.	95.00% CI of diff.	Below threshold?	Summary	Adjusted P Value	A-?		
No inhibitor vs. 0.02uM	8.367	-0.9377 to 17.67	No	ns	0.0803	B	0.02uM	
No inhibitor vs. 0.2uM	12.60	3.296 to 21.90	Yes	**	0.0095	C	0.2uM	
No inhibitor vs. 2uM	18.23	8.929 to 27.54	Yes	***	0.0007	D	2uM	
No inhibitor vs. 20uM	17.47	8.162 to 26.77	Yes	**	0.0010	E	20uM	
Test details	**Mean 1**	**Mean 2**	**Mean Diff.**	**SE of diff.**	**n1**	**n2**	**q**	**DF**
No inhibitor vs. 0.02uM	28.80	20.43	8.367	3.219	3	3	2.599	10
No inhibitor vs. 0.2uM	28.80	16.20	12.60	3.219	3	3	3.914	10
No inhibitor vs. 2uM	28.80	10.57	18.23	3.219	3	3	5.664	10
No inhibitor vs. 20uM	28.80	11.33	17.47	3.219	3	3	5.426	10

Appendix 2.3. One-way ANOVA of LP9 plate and HT115 colorectal cancer adhesion treated with a HAi inhibitor. Dunnett's multiple comparisons test.

Dunnett's multiple comparisons test	Mean Diff.	95.00% CI of diff.	Below threshold?	Summary	Adjusted P Value	A-?		
No inhibitor vs. 0.02uM	3.800	1.257 to 6.343	Yes	**	0.0051	B	0.02uM	
No inhibitor vs. 0.2uM	5.567	3.024 to 8.109	Yes	***	0.0003	C	0.2uM	
No inhibitor vs. 2uM	5.133	2.591 to 7.676	Yes	***	0.0006	D	2uM	
No inhibitor vs. 20uM	5.367	2.824 to 7.909	Yes	***	0.0004	E	20uM	
Test details	**Mean 1**	**Mean 2**	**Mean Diff.**	**SE of diff.**	**n1**	**n2**	**q**	**DF**
No inhibitor vs. 0.02uM	8.133	4.333	3.800	0.8796	3	3	4.320	10
No inhibitor vs. 0.2uM	8.133	2.567	5.567	0.8796	3	3	6.328	10
No inhibitor vs. 2uM	8.133	3.000	5.133	0.8796	3	3	5.836	10
No inhibitor vs. 20uM	8.133	2.767	5.367	0.8796	3	3	6.101	10

Appendix 2.4. One-way ANOVA of HA coated plate and HT115 colorectal cancer adhesion treated with a HAi inhibitor. Dunnett's multiple comparisons test.

HA coated concentration (ug/ml)	Adjusted P Value
0 vs. 1.22	0.9550
0 vs. 2.44	0.9996
0 vs. 4.88	0.9820
0 vs. 9.77	0.2358
0 vs. 19.53	0.1762
0 vs. 39.06	0.0002*
0 vs. 78.125	<0.0001****
0 vs. 156.25	0.0481***
0 vs. 312.5	0.9897
0 vs. 625	0.9990
0 vs. 1250	0.9626
0 vs. 2500	0.9550
0 vs. 5000	0.9998

Appendix 2.5. One way ANOVA multiple comparisons test assessing Hyaluronic acid coated plate and cellular adhesion of HTT115 cells when compared to an uncoated plate. Cell counting method

HA coated concentration (ug/ml)	Adjusted P Value
0 vs. 1.22	0.9994
0 vs. 2.44	0.9990
0 vs. 4.88	0.5715
0 vs. 9.77	0.9991
0 vs. 19.53	0.0005***
0 vs. 39.06	<0.0001****
0 vs. 78.125	<0.0001****
0 vs. 156.25	<0.0001****
0 vs. 312.5	0.0047**
0 vs. 625	0.8814
0 vs. 1250	0.1340
0 vs. 2500	0.9991
0 vs. 5000	0.9994

Appendix 2.6. One way ANOVA multiple comparisons test assessing Hyaluronic acid coated plate and cellular adhesion of HTT115 cells when compared to an uncoated plate. Cell absorbance method.

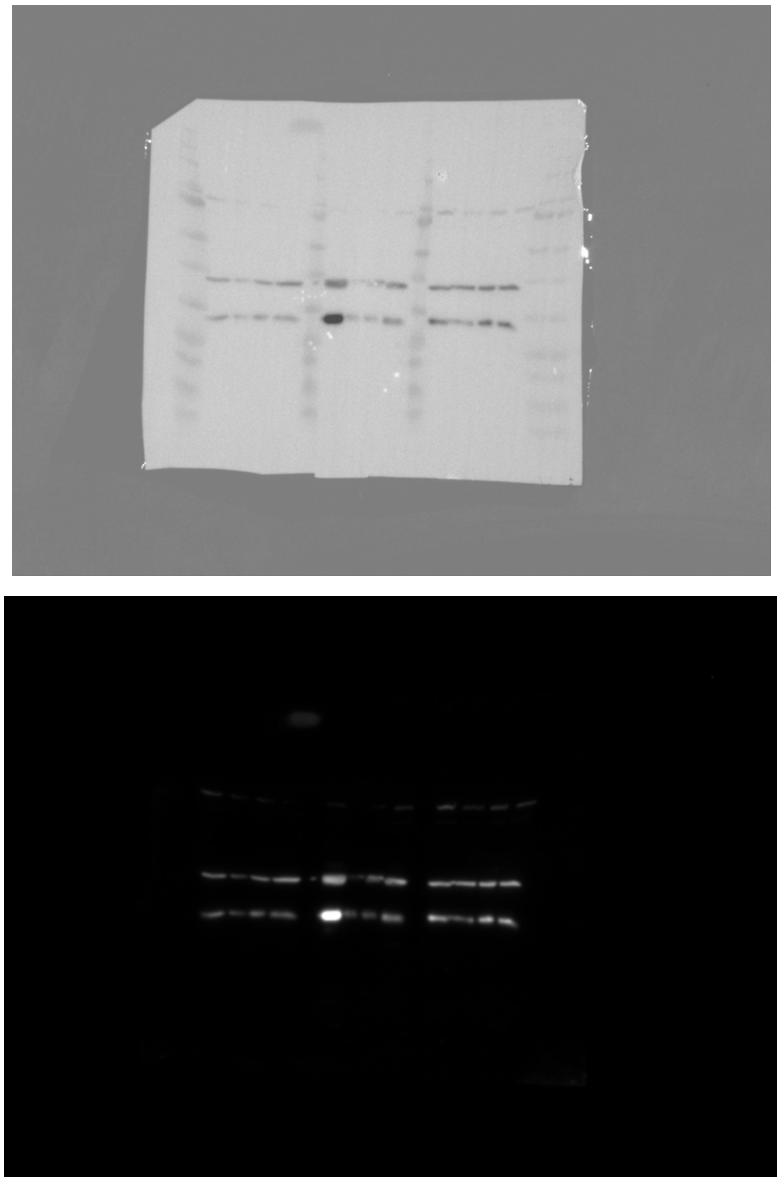

Appendix 2.7 Caspase 3 protein expression. Time course 4hrs cells in suspension. Original images

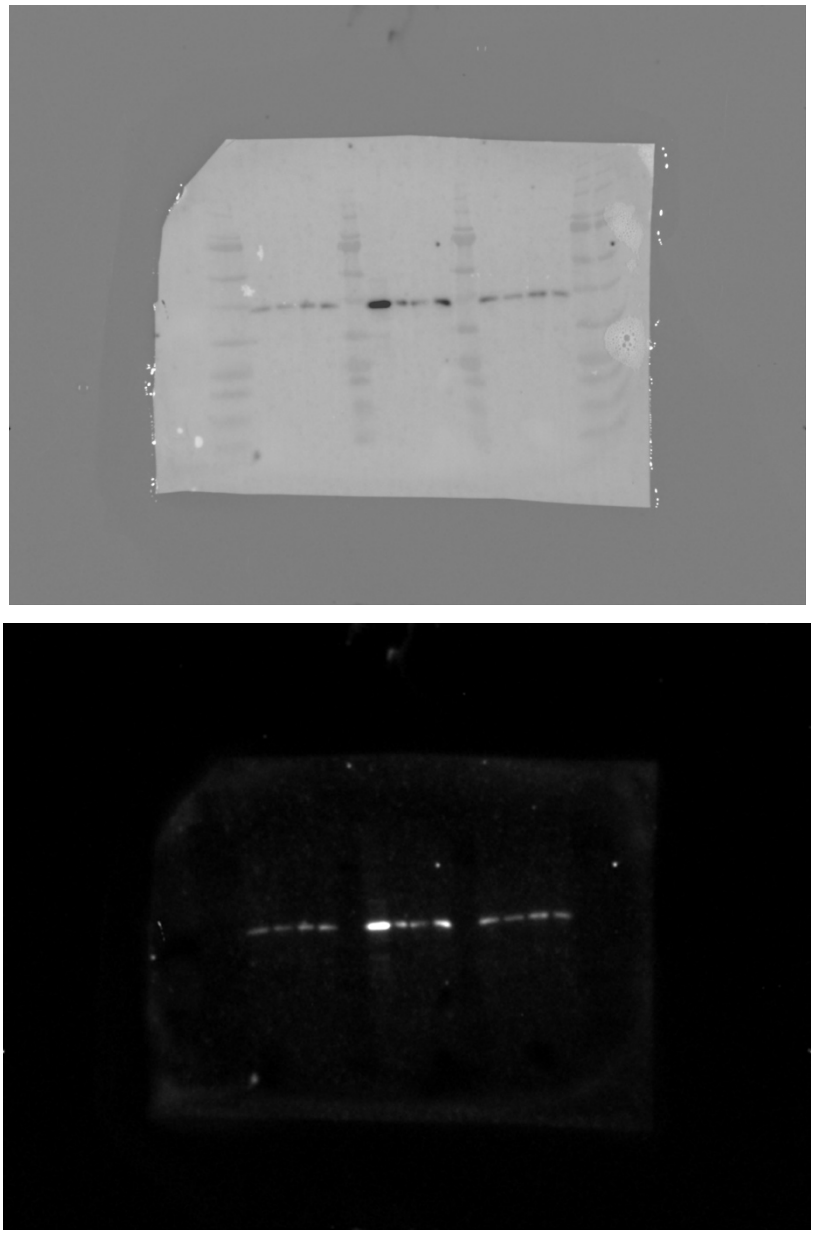

Appendix 2.8 Caspase 8 protein expression. Time course 4hrs cells in suspension. Original images

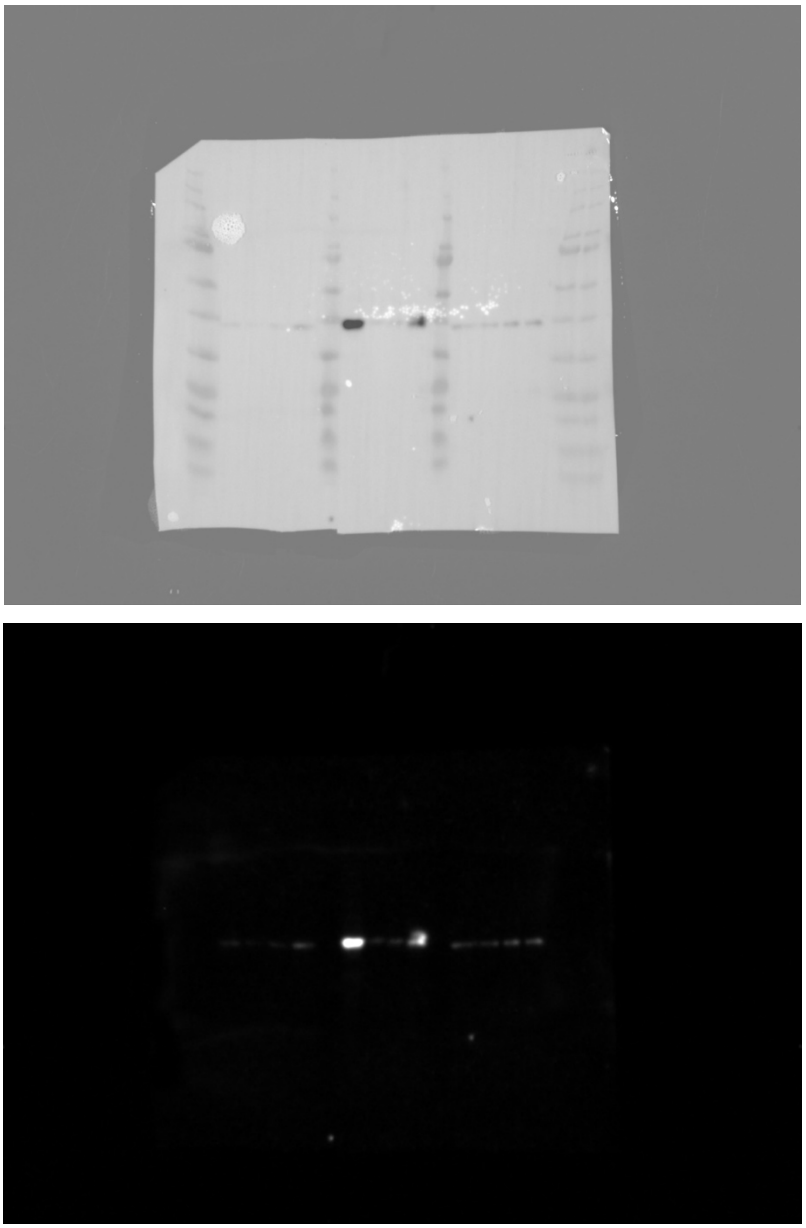

Appendix 2.9 Caspase 9 protein expression. Time course 4hrs cells in suspension. Original images

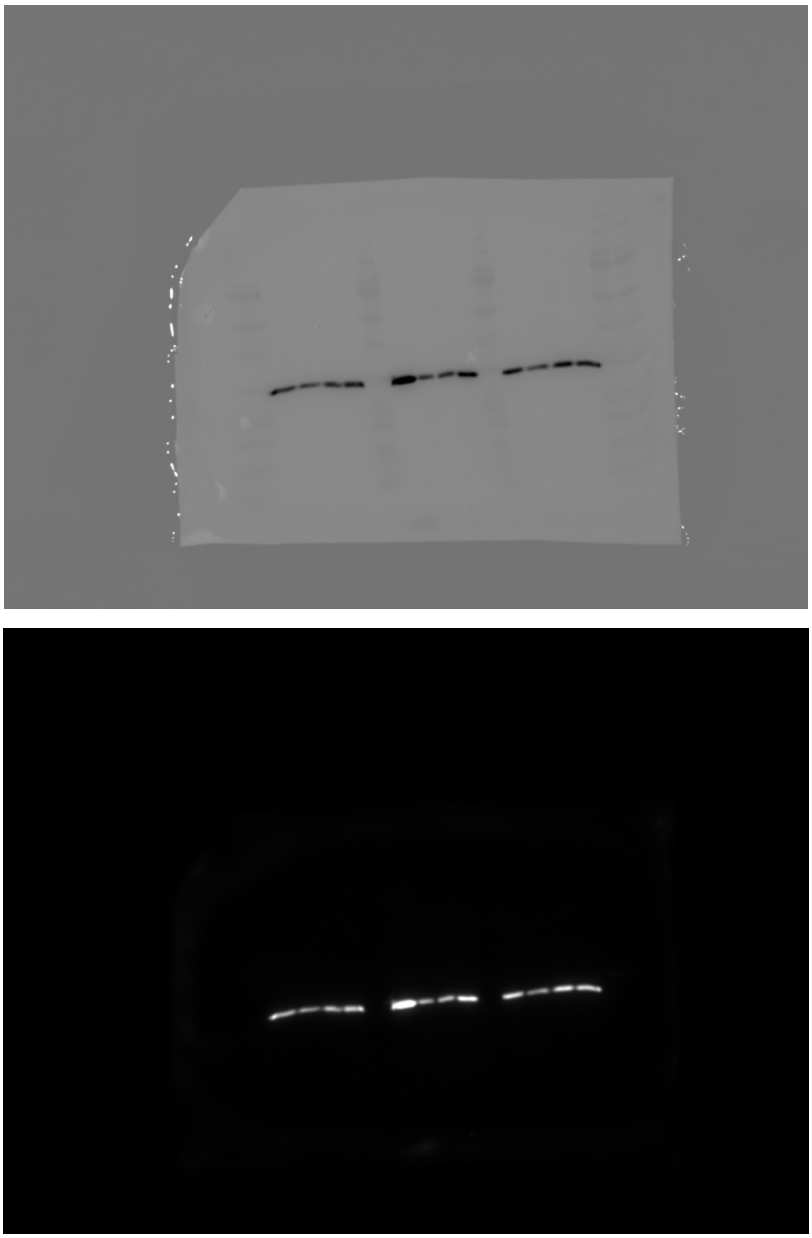

Appendix 2.10 GAPDH protein expression. Time course 4hrs cells in suspension. Original images

Well number (left to right)	Protein
1	Ladder
2	Untreated 1
3	HAi Treated 1
4	HA 312 – run 1
5	HA 624 – run 1
6	Ladder
7	Untreated 2
8	HAi treated 2
9	HA 312 – run 2
10	HA 624 – run 2
11	Ladder
12	Untreated 3
13	HAi Treated 3
14	HA 312 – run 3
15	HA 624 – run 3
16	Ladder
17	Ladder

Appendix 2.11. Western Blot ladder table order for time course 4hours cells in suspension

Appendix 3 – Chapter 5

Compare column means (main column effect)									
Number of parametric families	1								
Number of comparisons per family	3								
Alpha	0.05								
Tukey's multiple comparisons test	Mean Diff.	95.00% CI of diff.	Significant?	Summary	Adjusted P Value				
Control Group Weight (g) vs. HAi treated Group Weight (g)	-0.9333	-2.478 to 0.6114	No	ns	**0.3235**				
Control Group Weight (g) vs. HA treated Group Weight (g)	-1.140	-2.685 to 0.4048	No	ns	**0.1885**				
HAi Treated Group Weight (g) vs. HA treated Group Weight (g)	-0.2067	-1.751 to 1.338	No	ns	**0.9452**				
Test details	Mean 1	Mean 2	Mean Diff.	SE of diff.	N1	N2	q	DF	
Control Group Weight (g) vs. HAi Treated Group Weight (g)	26.25	27.18	-0.9333	0.6460	30	30	2.043	75.00	
Control Group Weight (g) vs. HA treated Group Weight (g)	26.25	27.39	-1.140	0.6460	30	30	2.496	75.00	
HAi Treated Group Weight (g) vs. HA treated Group Weight (g)	27.18	27.39	-0.2067	0.6460	30	30	0.4524	75.00	

Appendix 3.1 Two-way ANOVA multiple comparisons test - comparing the mean (average) weight between the three groups of mice over the study period. There was found to be no significant difference in mice weight between either of the groups.

Number of parametric families	1							
Number of comparisons per family	3							
Alpha	0.05							
Tukey's multiple comparisons test	Mean Diff.	95.00% CI of diff.	Significant?	Summary	Adjusted P Value			
Control vs. HAi	4.333	1.071 to 7.596	Yes	**	**0.0094**	A-B		
Control vs. HA	5.833	2.571 to 9.096	Yes	***	**0.0009**	A-C		
HAi vs. HA	1.500	-1.763 to 4.763	No	ns	**0.4745**	B-C		
Test details	Mean 1	Mean 2	Mean Diff.	SE of diff.	n1	n2	q	DF
Control vs. HAi	11.17	6.833	4.333	1.256	6	6	4.879	15
Control vs. HA	11.17	5.333	5.833	1.256	6	6	6.568	15
HAi vs. HA	6.833	5.333	1.500	1.256	6	6	1.689	15

Appendix 3.2: Ordinary one-way ANOVA multiple comparisons test: Comparing tumour nodule count between mice cohort groups. There was a significant reduction in tumour nodule count in both HAi and HA treated groups when compared to the control group (HAi P= 0.0094, HA P=0.0009).

Number of parametric families	1							
Number of comparisons per family	3							
Alpha	0.05							
Tukey's multiple comparisons test	Mean Diff.	95.00% CI of diff.	Significant?	Summary	Adjusted P Value			
Control vs. HAi	-0.4288	-2.154 to 1.297	No	ns	**0.7976**	A-B		
Control vs. HA	0.8182	-0.9073 to 2.544	No	ns	**0.4536**	A-C		
HAi vs. HA	1.247	-0.4785 to 2.973	No	ns	**0.1795**	B-C		
Test details	Mean 1	Mean 2	Mean Diff.	SE of diff.	n1	n2	q	DF
Control vs. HAi	3.374	3.803	-0.4288	0.6643	6	6	0.9129	15
Control vs. HA	3.374	2.555	0.8182	0.6643	6	6	1.742	15
HAi vs. HA	3.803	2.555	1.247	0.6643	6	6	2.655	15

Appendix 3.3: Ordinary one-way ANOVA multiple comparisons test: Comparing average individual tumour nodule size between murine cohort groups. There was no significant difference in individual tumour nodule size

Number of families	1							
Number of comparisons per family	3							
Alpha	0.05							
Tukey's multiple comparisons test	Mean Diff.	95.00% CI of diff.	Significant?	Summary	Adjusted P Value			
Control Group vs. HAi Treated Group	3027417	-3002134 to 9056967	No	ns	**0.4145**	A-B		
Control Group vs. HA Treated Group	5619500	-410050 to 11649050	No	ns	**0.0695**	A-C		
HAi Treated Group vs. HA Treated Group	2592083	-3437467 to 8621634	No	ns	**0.5189**	B-C		
Test details	Mean 1	Mean 2	Mean Diff.	SE of diff.	n1	n2	q	DF
Control Group vs. HAi Treated Group	11041167	8013750	3027417	2321316	6	6	1.844	15
Control Group vs. HA Treated Group	11041167	5421667	5619500	2321316	6	6	3.424	15
HAi Treated Group vs. HA Treated Group	8013750	5421667	2592083	2321316	6	6	1.579	15

Appendix 3.4: One-way ANOVA analysis of free-floating cells from peritoneal fluid. There was a trend towards decreased free-floating cells found in the peritoneal fluid of the mice in the HAi and HA treated cohort, but no significant difference was able to be demonstrated.

Appendix 4 - Publications

Appendix 4.1.


This image has been omitted for digital publication within
the Cardiff University ORCA repository

Appendix 4.1. Soliman F, Ye L, Jiang W, Hargest R. 2021. Targeting Hyaluronic Acid and Peritoneal Dissemination in Colorectal Cancer. Clinical Colorectal Cancer. https:///doi.org/10.1016/j/clcc.2021/11/008. Impact factor 4.481.

Appendix 4.2

Appendix 4.2: Soliman F, Ye L, Jiang W, Hargest R. 2021. Hyaluronic Acid Dependent Adhesion in Colorectal Cancer Peritoneal Metastases. British Journal of Surgery. 108(S1)i7-i48. doi.org/10.1093/bjs/znab117.017.

Appendix 4.3.

Appendix 4.3: Soliman F, Ye L, Jiang W, Hargest R. 2021. Peritoneal Metastasis in Colorectal Cancer: hyaluronic acid dependent adhesion. European Journal of Surgical Oncology. 47(1): e6. doi.org/10/1016/j.ejso/2020/11/028.

Chapter 8

References

Aaltonen, L. A., Peltomaki, P., Mecklin, J. P., et al. (1994). Replication errors in benign and malignant tumors from hereditary nonpolyposis colorectal cancer patients. *Cancer Res, 54*(7), 1645-1648.

Abou-Zeid, A. A., Khafagy, W., Marzouk, D. M., et al. (2002). Colorectal cancer in Egypt. *Dis Colon Rectum, 45*(9), 1255-1260. doi:10.1097/01.DCR.0000027122.04363.74

Akhurst, R. J., & Derynck, R. (2001). TGF-beta signaling in cancer--a double-edged sword. *Trends Cell Biol, 11*(11), S44-51.

Akita, K., Tanaka, M., Tanida, S., et al. (2013). CA125/MUC16 interacts with Src family kinases, and over-expression of its C-terminal fragment in human epithelial cancer cells reduces cell-cell adhesion. *Eur J Cell Biol, 92*(8-9), 257-263. doi:10.1016/j.ejcb.2013.10.005

Albanese, A. M., Albanese, E. F., Mino, J. H., et al. (2009). Peritoneal surface area: measurements of 40 structures covered by peritoneum: correlation between total peritoneal surface area and the surface calculated by formulas. *Surg Radiol Anat, 31*(5), 369-377. doi:10.1007/s00276-008-0456-9

Alexiou, D., Karayiannakis, A. J., Syrigos, K. N., et al. (2001). Serum levels of E-selectin, ICAM-1 and VCAM-1 in colorectal cancer patients: correlations with clinicopathological features, patient survival and tumour surgery. *Eur J Cancer, 37*(18), 2392-2397. doi:10.1016/s0959-8049(01)00318-5

Alkhamesi, N. A., Roberts, G., Ziprin, P., et al. (2007). Induction of Proteases in Peritoneal Carcinomatosis, the Role of ICAM-1/CD43 Interaction. *Biomark Insights, 2*, 377-384.

Alkhamesi, N. A., Ziprin, P., Pfistermuller, K., et al. (2005). ICAM-1 mediated peritoneal carcinomatosis, a target for therapeutic intervention. *Clin Exp Metastasis, 22*(6), 449-459. doi:10.1007/s10585-005-2893-8

Andreyev, H. J., Norman, A. R., Cunningham, D., et al. (1998). Kirsten ras mutations in patients with colorectal cancer: the multicenter "RASCAL" study. *J Natl Cancer Inst, 90*(9), 675-684.

Arabzadeh, A., & Beauchemin, N. (2012). Stromal CEACAM1 expression regulates colorectal cancer metastasis. *Oncoimmunology, 1*(7), 1205-1207. doi:10.4161/onci.20735

Arlt, M. J., Novak-Hofer, I., Gast, D., et al. (2006). Efficient inhibition of intra-peritoneal tumor growth and dissemination of human ovarian carcinoma cells in nude mice by anti-L1-cell adhesion molecule monoclonal antibody treatment. *Cancer Res, 66*(2), 936-943. doi:10.1158/0008-5472.CAN-05-1818

Aruffo, A., Stamenkovic, I., Melnick, M., et al. (1990). CD44 is the principal cell surface receptor for hyaluronate. *Cell, 61*(7), 1303-1313.

Arur, S., Uche, U. E., Rezaul, K., et al. (2003). Annexin I is an endogenous ligand that mediates apoptotic cell engulfment. *Dev Cell, 4*(4), 587-598. doi:10.1016/s1534-5807(03)00090-x

Ashmore-Harris, C., Iafrate, M., Saleem, A., et al. (2020). Non-invasive Reporter Gene Imaging of Cell Therapies, including T Cells and Stem Cells. *Mol Ther, 28*(6), 1392-1416. doi:10.1016/j.ymthe.2020.03.016

Baldus, S. E., Monig, S. P., Huxel, S., et al. (2004). MUC1 and nuclear beta-catenin are coexpressed at the invasion front of colorectal carcinomas and are both correlated with tumor prognosis. *Clin Cancer Res, 10*(8), 2790-2796. doi:10.1158/1078-0432.ccr-03-0163

Bartakova, A., Michalova, K., Presl, J., et al. (2017). CD44 as a cancer stem cell marker and its prognostic value in patients with ovarian carcinoma. *J Obstet Gynaecol*, 1-5. doi:10.1080/01443615.2017.1336753

Beauchemin, N., & Arabzadeh, A. (2013). Carcinoembryonic antigen-related cell adhesion molecules (CEACAMs) in cancer progression and metastasis. *Cancer Metastasis Rev, 32*(3-4), 643-671. doi:10.1007/s10555-013-9444-6

Behrenbruch, C., Shembrey, C., Paquet-Fifield, S., et al. (2018). Surgical stress response and promotion of metastasis in colorectal cancer: a complex and heterogeneous process. *Clin Exp Metastasis, 35*(4), 333-345. doi:10.1007/s10585-018-9873-2

Behrens, J. (2005). The role of the Wnt signalling pathway in colorectal tumorigenesis. *Biochem Soc Trans, 33*(Pt 4), 672-675. doi:10.1042/BST0330672

Ben, Q., An, W., Fei, J., et al. (2014). Downregulation of L1CAM inhibits proliferation, invasion and arrests cell cycle progression in pancreatic cancer cells in vitro. *Exp Ther Med, 7*(4), 785-790. doi:10.3892/etm.2014.1519

Bendardaf, R., Algars, A., Elzagheid, A., et al. (2006). Comparison of CD44 expression in primary tumours and metastases of colorectal cancer. *Oncol Rep, 16*(4), 741-746.

Bird, N. C., Mangnall, D., & Majeed, A. W. (2006). Biology of colorectal liver metastases: A review. *J Surg Oncol, 94*(1), 68-80. doi:10.1002/jso.20558

Blackburn, S. C., & Stanton, M. P. (2014). Anatomy and physiology of the peritoneum. *Semin Pediatr Surg, 23*(6), 326-330. doi:10.1053/j.sempedsurg.2014.06.002

Boeckel, D. G., Shinkai, R. S., Grossi, M. L., et al. (2014). In vitro evaluation of cytotoxicity of hyaluronic acid as an extracellular matrix on OFCOL II cells by the MTT assay. *Oral Surg Oral Med Oral Pathol Oral Radiol, 117*(6), e423-428. doi:10.1016/j.oooo.2012.07.486

Bogaert, J., & Prenen, H. (2014). Molecular genetics of colorectal cancer. *Ann Gastroenterol, 27*(1), 9-14.

Boparai, K. S., Mathus-Vliegen, E. M., Koornstra, J. J., et al. (2010). Increased colorectal cancer risk during follow-up in patients with hyperplastic polyposis syndrome: a multicentre cohort study. *Gut, 59*(8), 1094-1100. doi:10.1136/gut.2009.185884

Brosens, L. A., Offerhaus, G. J., & Giardiello, F. M. (2015). Hereditary Colorectal Cancer: Genetics and Screening. *Surg Clin North Am, 95*(5), 1067-1080. doi:10.1016/j.suc.2015.05.004

Brosens, L. A., van Hattem, A., Hylind, L. M., et al. (2007). Risk of colorectal cancer in juvenile polyposis. *Gut, 56*(7), 965-967. doi:10.1136/gut.2006.116913

Brown, T. J., Laurent, U. B. G., & Fraser, J. R. E. (1991). Turnover of Hyaluronan in Synovial Joints - Elimination of Labeled Hyaluronan from the Knee-Joint of the Rabbit. *Experimental Physiology, 76*(1), 125-134.

Byers, T. E., Wolf, H. J., Bauer, K. R., et al. (2008). The impact of socioeconomic status on survival after cancer in the United States : findings from the National Program of Cancer Registries Patterns of Care Study. *Cancer, 113*(3), 582-591. doi:10.1002/cncr.23567

CancerResearchUK. (2014). Bowel Cancer Statistics, UK [online] , http://www.cancerresearchuk.org/health-professional/cancer-statistics/statistics-by-cancer-type/bowel-cancer#heading-Zero.

Cao, L., Hu, X., Zhang, J., et al. (2014). CD44(+) CD324(-) expression and prognosis in gastric cancer patients. *J Surg Oncol, 110*(6), 727-733. doi:10.1002/jso.23690

Cao, R., Zhang, S., Ma, D., et al. (2015). A multi-center randomized phase II clinical study of bevacizumab plus irinotecan, 5-fluorouracil, and leucovorin (FOLFIRI) compared with FOLFIRI alone as second-line treatment for Chinese patients with metastatic colorectal cancer. *Med Oncol, 32*(1), 325. doi:10.1007/s12032-014-0325-9

Carmignani, C. P., Sugarbaker, T. A., Bromley, C. M., et al. (2003). Intraperitoneal cancer dissemination: mechanisms of the patterns of spread. *Cancer Metastasis Rev, 22*(4), 465-472.

Carnero, A. (2010). The PKB/AKT pathway in cancer. *Curr Pharm Des, 16*(1), 34-44.

Catterall, J. B., Gardner, M. J., Jones, L. M., et al. (1997). Binding of ovarian cancer cells to immobilized hyaluronic acid. *Glycoconjugate Journal, 14*(5), 647-649.

Ceelen, W., Van Nieuwenhove, Y., Putte, D. V., et al. (2014). Neoadjuvant chemotherapy with bevacizumab may improve outcome after cytoreduction and hyperthermic intraperitoneal chemoperfusion (HIPEC) for colorectal carcinomatosis. *Ann Surg Oncol, 21*(9), 3023-3028. doi:10.1245/s10434-014-3713-7

Celeste, A. J., Iannazzi, J. A., Taylor, R. C., et al. (1990). Identification of transforming growth factor beta family members present in bone-inductive protein purified from bovine bone. *Proc Natl Acad Sci U S A, 87*(24), 9843-9847.

Center, M. M., Jemal, A., Smith, R. A., et al. (2009). Worldwide variations in colorectal cancer. *CA Cancer J Clin, 59*(6), 366-378. doi:10.3322/caac.20038

Chan, A. O., Issa, J. P., Morris, J. S., et al. (2002). Concordant CpG island methylation in hyperplastic polyposis. *Am J Pathol, 160*(2), 529-536. doi:10.1016/S0002-9440(10)64872-9

Charan, J., & Kantharia, N. D. (2013). How to calculate sample size in animal studies? *J Pharmacol Pharmacother, 4*(4), 303-306. doi:10.4103/0976-500X.119726

Chen, C., Zhao, S., Karnad, A., et al. (2018). The biology and role of CD44 in cancer progression: therapeutic implications. *J Hematol Oncol, 11*(1), 64. doi:10.1186/s13045-018-0605-5

Chen, D., Yu, Z., Zhu, Z., et al. (2006). The p53 pathway promotes efficient mitochondrial DNA base excision repair in colorectal cancer cells. *Cancer Res, 66*(7), 3485-3494. doi:10.1158/0008-5472.CAN-05-4103

Chen, H., Feng, J., Zhang, Y., et al. (2015). Pien Tze Huang Inhibits Hypoxia-Induced Angiogenesis via HIF-1 alpha /VEGF-A Pathway in Colorectal Cancer. *Evid Based Complement Alternat Med, 2015*, 454279. doi:10.1155/2015/454279

Chen, Y., Fu, Z., Xu, S., et al. (2014). The prognostic value of CD44 expression in gastric cancer: a meta-analysis. *Biomed Pharmacother, 68*(6), 693-697. doi:10.1016/j.biopha.2014.08.001

Choti, M. (2004). Bevacizumab in combination with irinotecan plus fluorouracil plus leucovorin chemotherapy prolongs survival but increases adverse events in people with metastatic colorectal cancer. *Cancer Treat Rev, 30*(8), 715-717. doi:10.1016/j.ctrv.2004.09.003

Choy, Y. Y., Fraga, M., Mackenzie, G. G., et al. (2016). The PI3K/Akt pathway is involved in procyanidin-mediated suppression of human colorectal cancer cell growth. *Mol Carcinog, 55*(12), 2196-2209. doi:10.1002/mc.22461

Chu, L. Y., Guo, D. M., Chen, J. T., et al. (2020). The Diagnostic Value of Serum L1CAM in Patients With Colorectal Cancer. *Technol Cancer Res Treat, 19*, 1533033820920971. doi:10.1177/1533033820920971

Chu, Z. P., Dai, J., Jia, L. G., et al. (2018). Increased expression of long noncoding RNA HMMR-AS1 in epithelial ovarian cancer: an independent prognostic factor. *Eur Rev Med Pharmacol Sci, 22*(23), 8145-8150. doi:10.26355/eurrev_201812_16506

Clarke, C. N., & Kopetz, E. S. (2015). BRAF mutant colorectal cancer as a distinct subset of colorectal cancer: clinical characteristics, clinical behavior, and response to targeted therapies. *J Gastrointest Oncol, 6*(6), 660-667. doi:10.3978/j.issn.2078-6891.2015.077

Clinicaltrials.gov. (2014). Trial of FOLF(HA)Iri With Cetuximab in mCRC (Chime). ClinicalTrials.gov Identifier: NCT02216487. Retrieved from https://clinicaltrials.gov/ct2/show/NCT02216487?id=NCT01290783+OR+NCT02216487&rank=1&load=cart

Clinicaltrials.gov. (2015). Trial of FOLF(HA)Iri Versus FOLFIRI in mCRC (FOLF(HA)iri). ClinicalTrials.gov Identifier: NCT01290783. Retrieved from https://clinicaltrials.gov/ct2/show/NCT01290783?id=NCT01290783+OR+NCT02216487&rank=2&load=cart

Colussi, D., Brandi, G., Bazzoli, F., et al. (2013). Molecular pathways involved in colorectal cancer: implications for disease behavior and prevention. *Int J Mol Sci, 14*(8), 16365-16385. doi:10.3390/ijms140816365

Cooper, D. L., Dougherty, G., Harn, H. J., et al. (1992). The complex CD44 transcriptional unit; alternative splicing of three internal exons generates the epithelial form of CD44. *Biochem Biophys Res Commun, 182*(2), 569-578.

Cooper, J., & Giancotti, F. G. (2019). Integrin Signaling in Cancer: Mechanotransduction, Stemness, Epithelial Plasticity, and Therapeutic Resistance. *Cancer Cell, 35*(3), 347-367. doi:10.1016/j.ccell.2019.01.007

Cortes-Guiral, D., Hubner, M., Alyami, M., et al. (2021). Primary and metastatic peritoneal surface malignancies. *Nat Rev Dis Primers, 7*(1), 91. doi:10.1038/s41572-021-00326-6

Cowden Dahl, K. D., Symowicz, J., Ning, Y., et al. (2008). Matrix metalloproteinase 9 is a mediator of epidermal growth factor-dependent e-cadherin loss in ovarian carcinoma cells. *Cancer Res, 68*(12), 4606-4613. doi:10.1158/0008-5472.CAN-07-5046

Crowley, L. C., & Waterhouse, N. J. (2016). Detecting Cleaved Caspase-3 in Apoptotic Cells by Flow Cytometry. *Cold Spring Harb Protoc, 2016*(11). doi:10.1101/pdb.prot087312

Damen, M. P. F., van Rheenen, J., & Scheele, C. (2021). Targeting dormant tumor cells to prevent cancer recurrence. *FEBS J, 288*(21), 6286-6303. doi:10.1111/febs.15626

Danielsen, S. A., Eide, P. W., Nesbakken, A., et al. (2015). Portrait of the PI3K/AKT pathway in colorectal cancer. *Biochim Biophys Acta, 1855*(1), 104-121. doi:10.1016/j.bbcan.2014.09.008

Das, V., Bhattacharya, S., Chikkaputtaiah, C., et al. (2019). The basics of epithelial-mesenchymal transition (EMT): A study from a structure, dynamics, and functional perspective. *J Cell Physiol*. doi:10.1002/jcp.28160

Davies, D. E., Farmer, S., White, J., et al. (1994). Contribution of host-derived growth factors to in vivo growth of a transplantable murine mammary carcinoma. *Br J Cancer, 70*(2), 263-269.

Day, T. D. (1950). Connective tissue permeability and the mode of action of hyaluronidase. *Nature, 166*(4227), 785-786.

de Cuba, E. M., Kwakman, R., van Egmond, M., et al. (2012). Understanding molecular mechanisms in peritoneal dissemination of colorectal cancer : future possibilities for personalised treatment by use of biomarkers. *Virchows Arch, 461*(3), 231-243. doi:10.1007/s00428-012-1287-y

de Klerk, C. M., Gupta, S., Dekker, E., et al. (2017). Socioeconomic and ethnic inequities within organised colorectal cancer screening programmes worldwide. *Gut*. doi:10.1136/gutjnl-2016-313311

de Lima Vazquez, V., Stuart, O. A., Mohamed, F., et al. (2003). Extent of parietal peritonectomy does not change intraperitoneal chemotherapy pharmacokinetics. *Cancer Chemother Pharmacol, 52*(2), 108-112. doi:10.1007/s00280-003-0626-8

Dechaud, H., Witz, C. A., Montoya-Rodriguez, I. A., et al. (2001). Mesothelial cell-associated hyaluronic acid promotes adhesion of endometrial cells to mesothelium. *Fertil Steril, 76*(5), 1012-1018. doi:10.1016/s0015-0282(01)02839-4

Deng, L., Li, Q., Lin, G., et al. (2016). P-glycoprotein Mediates Postoperative Peritoneal Adhesion Formation by Enhancing Phosphorylation of the Chloride Channel-3. *Theranostics, 6*(2), 204-218. doi:10.7150/thno.13907

Deng, Z., Wang, H., Liu, J., et al. (2021). Comprehensive understanding of anchorage-independent survival and its implication in cancer metastasis. *Cell Death Dis, 12*(7), 629. doi:10.1038/s41419-021-03890-7

Diamond, M. P. (1996). Reduction of adhesions after uterine myomectomy by Seprafilm membrane (HAL-F): a blinded, prospective, randomized, multicenter clinical study. Seprafilm Adhesion Study Group. *Fertil Steril, 66*(6), 904-910.

Diez-Alonso, M., Mendoza-Moreno, F., Gomez-Sanz, R., et al. (2021). Prognostic Value of KRAS Gene Mutation on Survival of Patients with Peritoneal Metastases of Colorectal Adenocarcinoma. *Int J Surg Oncol, 2021*, 3946875. doi:10.1155/2021/3946875

Dong, Y., Tan, O. L., Loessner, D., et al. (2010). Kallikrein-related peptidase 7 promotes multicellular aggregation via the alpha(5)beta(1) integrin pathway and paclitaxel chemoresistance in serous epithelial ovarian carcinoma. *Cancer Res, 70*(7), 2624-2633. doi:10.1158/0008-5472.CAN-09-3415

Durko, L., Wlodarski, W., Stasikowska-Kanicka, O., et al. (2017). Expression and Clinical Significance of Cancer Stem Cell Markers CD24, CD44, and CD133 in Pancreatic Ductal Adenocarcinoma and Chronic Pancreatitis. *Dis Markers, 2017*, 3276806. doi:10.1155/2017/3276806

Eggermont, A. M., Steller, E. P., & Sugarbaker, P. H. (1987). Laparotomy enhances intraperitoneal tumor growth and abrogates the antitumor effects of interleukin-2 and lymphokine-activated killer cells. *Surgery, 102*(1), 71-78.

El-Nakeep, S., Rashad, N., Oweira, H., et al. (2017). Intraperitoneal chemotherapy and cytoreductive surgery for peritoneal metastases coupled with curative treatment of colorectal liver metastases: an updated systematic review. *Expert Rev Gastroenterol Hepatol, 11*(3), 249-258. doi:10.1080/17474124.2017.1284586

Elliott, V. A., Rychahou, P., Zaytseva, Y. Y., et al. (2014). Activation of c-Met and upregulation of CD44 expression are associated with the metastatic phenotype in the colorectal cancer liver metastasis model. *PLoS ONE [Electronic Resource], 9*(5), e97432.

Ellis, H. (1962). The aetiology of post-operative abdominal adhesions. An experimental study. *Br J Surg, 50*, 10-16. doi:10.1002/bjs.18005021904

Elmore, S. (2007). Apoptosis: a review of programmed cell death. *Toxicol Pathol, 35*(4), 495-516. doi:10.1080/01926230701320337

Entwistle, J., Zhang, S., Yang, B., et al. (1995). Characterization of the murine gene encoding the hyaluronan receptor RHAMM. *Gene, 163*(2), 233-238.

Evanko, S. P., Tammi, M. I., Tammi, R. H., et al. (2007). Hyaluronan-dependent pericellular matrix. *Adv Drug Deliv Rev, 59*(13), 1351-1365. doi:10.1016/j.addr.2007.08.008

Eveno, C., Passot, G., Goere, D., et al. (2014). Bevacizumab doubles the early postoperative complication rate after cytoreductive surgery with hyperthermic intraperitoneal chemotherapy (HIPEC) for peritoneal carcinomatosis of colorectal origin. *Ann Surg Oncol, 21*(6), 1792-1800. doi:10.1245/s10434-013-3442-3

Fang, J. Y., & Richardson, B. C. (2005). The MAPK signalling pathways and colorectal cancer. *Lancet Oncol, 6*(5), 322-327. doi:10.1016/S1470-2045(05)70168-6

Faron, M., Macovei, R., Goere, D., et al. (2016). Linear Relationship of Peritoneal Cancer Index and Survival in Patients with Peritoneal Metastases from Colorectal Cancer. *Ann Surg Oncol, 23*(1), 114-119. doi:10.1245/s10434-015-4627-8

Favoriti, P., Carbone, G., Greco, M., et al. (2016). Worldwide burden of colorectal cancer: a review. *Updates Surg, 68*(1), 7-11. doi:10.1007/s13304-016-0359-y

Fearon, E. R., & Vogelstein, B. (1990). A genetic model for colorectal tumorigenesis. *Cell, 61*(5), 759-767.

Foley-Comer, A. J., Herrick, S. E., Al-Mishlab, T., et al. (2002). Evidence for incorporation of free-floating mesothelial cells as a mechanism of serosal healing. *J Cell Sci, 115*(Pt 7), 1383-1389.

Folkman, J., & Greenspan, H. P. (1975). Influence of geometry on control of cell growth. *Biochim Biophys Acta, 417*(3-4), 211-236. doi:10.1016/0304-419x(75)90011-6

Franko, J., Shi, Q., Meyers, J. P., et al. (2016). Prognosis of patients with peritoneal metastatic colorectal cancer given systemic therapy: an analysis of individual patient data from prospective randomised trials from the Analysis and Research in Cancers of the Digestive System (ARCAD) database. *Lancet Oncol, 17*(12), 1709-1719. doi:10.1016/S1470-2045(16)30500-9

Frisch, S. M., & Francis, H. (1994). Disruption of epithelial cell-matrix interactions induces apoptosis. *J Cell Biol, 124*(4), 619-626. doi:10.1083/jcb.124.4.619

Fujii, T., Shimizu, T., Katoh, M., et al. (2021). Survival of detached cancer cells is regulated by movement of intracellular Na(+),K(+)-ATPase. *iScience, 24*(5), 102412. doi:10.1016/j.isci.2021.102412

Fujisaki, T., Tanaka, Y., Fujii, K., et al. (1999). CD44 stimulation induces integrin-mediated adhesion of colon cancer cell lines to endothelial cells by up-regulation of integrins and c-Met and activation of integrins. *Cancer Res, 59*(17), 4427-4434.

Furuta, K., Zahurak, M., Goodman, S. N., et al. (1998). CD44 expression in the stromal matrix of colorectal cancer: association with prognosis. *Clin Cancer Res, 4*(1), 21-29.

Gaiser, T., Meinhardt, S., Hirsch, D., et al. (2013). Molecular patterns in the evolution of serrated lesion of the colorectum. *International Journal of Cancer, 132*(8), 1800-1810. doi:10.1002/ijc.27869

Ganesh, K., Basnet, H., Kaygusuz, Y., et al. (2020). L1CAM defines the regenerative origin of metastasis-initiating cells in colorectal cancer. *Nat Cancer, 1*(1), 28-45. doi:10.1038/s43018-019-0006-x

Gao, A. C., Lou, W., Dong, J. T., et al. (1997). CD44 is a metastasis suppressor gene for prostatic cancer located on human chromosome 11p13. *Cancer Res, 57*(5), 846-849.

Gardner, M. J., Catterall, J. B., Jones, L. M., et al. (1996). Human ovarian tumour cells can bind hyaluronic acid via membrane CD44: a possible step in peritoneal metastasis. *Clin Exp Metastasis, 14*(4), 325-334.

Gardner, M. J., Jones, L. M., Catterall, J. B., et al. (1995). Expression of cell adhesion molecules on ovarian tumour cell lines and mesothelial cells, in relation to ovarian cancer metastasis. *Cancer Lett, 91*(2), 229-234. doi:10.1016/0304-3835(95)03743-g

Gebauer, F., Wicklein, D., Horst, J., et al. (2014). Carcinoembryonic antigen-related cell adhesion molecules (CEACAM) 1, 5 and 6 as biomarkers in pancreatic cancer. *PLoS ONE, 9*(11), e113023. doi:10.1371/journal.pone.0113023

Gerber, S. A., Rybalko, V. Y., Bigelow, C. E., et al. (2006). Preferential attachment of peritoneal tumor metastases to omental immune aggregates and possible role of a unique vascular microenvironment in metastatic survival and growth. *Am J Pathol, 169*(5), 1739-1752. doi:10.2353/ajpath.2006.051222

Giannoulis, K., Angouridaki, C., Fountzilas, G., et al. (2004). Serum concentrations of soluble ICAM-1 and VCAM-1 in patients with colorectal cancer. Clinical implications. *Tech Coloproctol, 8 Suppl 1*, s65-67. doi:10.1007/s10151-004-0115-z

Giardiello, F. M., Allen, J. I., Axilbund, J. E., et al. (2014). Guidelines on genetic evaluation and management of Lynch syndrome: a consensus statement by the US Multi-society Task Force on colorectal cancer. *Am J Gastroenterol, 109*(8), 1159-1179. doi:10.1038/ajg.2014.186

Gibbs, P., Clingan, P. R., Ganju, V., et al. (2011). Hyaluronan-Irinotecan improves progression-free survival in 5-fluorouracil refractory patients with metastatic colorectal cancer: a randomized phase II trial. *Cancer Chemother Pharmacol, 67*(1), 153-163. doi:10.1007/s00280-010-1303-3

Gille, J., Heidenreich, R., Pinter, A., et al. (2007). Simultaneous blockade of VEGFR-1 and VEGFR-2 activation is necessary to efficiently inhibit experimental melanoma growth and metastasis formation. *Int J Cancer, 120*(9), 1899-1908. doi:10.1002/ijc.22531

Gillern, S. M., Chua, T. C., Stojadinovic, A., et al. (2010). KRAS status in patients with colorectal cancer peritoneal carcinomatosis and its impact on outcome. *Am J Clin Oncol, 33*(5), 456-460. doi:10.1097/COC.0b013e3181b4b160

Glentis, A., Oertle, P., Mariani, P., et al. (2017). Cancer-associated fibroblasts induce metalloprotease-independent cancer cell invasion of the basement membrane. *Nat Commun, 8*(1), 924. doi:10.1038/s41467-017-00985-8

Globocan.iarc.fr. (2012). Fact Sheets by Cancer. [online]. http://globocan.iarc.fr/Pages/fact_sheets_cancer.aspx.

Go, S. I., Ko, G. H., Lee, W. S., et al. (2016). CD44 Variant 9 Serves as a Poor Prognostic Marker in Early Gastric Cancer, But Not in Advanced Gastric Cancer. *Cancer Res Treat, 48*(1), 142-152. doi:10.4143/crt.2014.227

Gonsalves, W. I., Mahoney, M. R., Sargent, D. J., et al. (2014). Patient and tumor characteristics and BRAF and KRAS mutations in colon cancer, NCCTG/Alliance N0147. *J Natl Cancer Inst, 106*(7). doi:10.1093/jnci/dju106

Govindarajan, R., Posey, J., Chao, C. Y., et al. (2016). A comparison of 12-gene colon cancer assay gene expression in African American and Caucasian patients with stage II colon cancer. *BMC Cancer, 16*, 368. doi:10.1186/s12885-016-2365-3

Govindarajan, R., Shah, R. V., Erkman, L. G., et al. (2003). Racial differences in the outcome of patients with colorectal carcinoma. *Cancer, 97*(2), 493-498. doi:10.1002/cncr.11067

Graversen, M., Detlefsen, S., Fristrup, C., et al. (2018). Adjuvant Pressurized IntraPeritoneal Aerosol Chemotherapy (PIPAC) in resected high-risk colon cancer patients - study protocol for the PIPAC-OPC3 Trial. A prospective, controlled phase 2 Study. *Pleura Peritoneum, 3*(2), 20180107. doi:10.1515/pp-2018-0107

Gremonprez, F., Willaert, W., & Ceelen, W. (2016). Animal models of colorectal peritoneal metastasis. *Pleura Peritoneum, 1*(1), 23-43. doi:10.1515/pp-2016-0006

Grothey, A., & Marshall, J. L. (2007). Optimizing palliative treatment of metastatic colorectal cancer in the era of biologic therapy. *Oncology (Williston Park), 21*(5), 553-564, 566; discussion 566-558, 577-558.

Guha, D., Saha, T., Bose, S., et al. (2019). Integrin-EGFR interaction regulates anoikis resistance in colon cancer cells. *Apoptosis, 24*(11-12), 958-971. doi:10.1007/s10495-019-01573-5

Gulmann, C., Sheehan, K. M., Conroy, R. M., et al. (2009). Quantitative cell signalling analysis reveals down-regulation of MAPK pathway activation in colorectal cancer. *J Pathol, 218*(4), 514-519. doi:10.1002/path.2561

Gunthert, U., Hofmann, M., Rudy, W., et al. (1991). A new variant of glycoprotein CD44 confers metastatic potential to rat carcinoma cells. *Cell, 65*(1), 13-24.

Half, E., Bercovich, D., & Rozen, P. (2009). Familial adenomatous polyposis. *Orphanet J Rare Dis, 4*, 22. doi:10.1186/1750-1172-4-22

Hall, C. L., & Turley, E. A. (1995). Hyaluronan: RHAMM mediated cell locomotion and signaling in tumorigenesis. *J Neurooncol, 26*(3), 221-229.

Hall, C. L., Wang, C., Lange, L. A., et al. (1994). Hyaluronan and the hyaluronan receptor RHAMM promote focal adhesion turnover and transient tyrosine kinase activity. *J Cell Biol, 126*(2), 575-588.

Han, S., Zong, S., Shi, Q., et al. (2017). Is Ep-CAM Expression a Diagnostic and Prognostic Biomarker for Colorectal Cancer? A Systematic Meta-Analysis. *EBioMedicine, 20*, 61-69. doi:10.1016/j.ebiom.2017.05.025

Hanahan, D., & Weinberg, R. A. (2011). Hallmarks of cancer: the next generation. *Cell, 144*(5), 646-674. doi:10.1016/j.cell.2011.02.013

Harada, H., Nakata, T., Hirota-Takahata, Y., et al. (2006). F-16438s, novel binding inhibitors of CD44 and hyaluronic acid. I. Establishment of an assay method and biological activity. *Journal of Antibiotics, 59*(12), 770-776.

Hayashi, T., Takahashi, T., Motoya, S., et al. (2001). MUC1 mucin core protein binds to the domain 1 of ICAM-1. *Digestion, 63 Suppl 1*, 87-92. doi:10.1159/000051917

Heath, R. M., Jayne, D. G., O'Leary, R., et al. (2004). Tumour-induced apoptosis in human mesothelial cells: a mechanism of peritoneal invasion by Fas Ligand/Fas interaction. *Br J Cancer, 90*(7), 1437-1442. doi:10.1038/sj.bjc.6601635

Hehlgans, S., Haase, M., & Cordes, N. (2007). Signalling via integrins: implications for cell survival and anticancer strategies. *Biochim Biophys Acta, 1775*(1), 163-180. doi:10.1016/j.bbcan.2006.09.001

Hermanek, P., & Wittekind, C. (1994). The pathologist and the residual tumor (R) classification. *Pathol Res Pract, 190*(2), 115-123. doi:10.1016/S0344-0338(11)80700-4

Hiltunen, E. L., Anttila, M., Kultti, A., et al. (2002). Elevated hyaluronan concentration without hyaluronidase activation in malignant epithelial ovarian tumors. *Cancer Research, 62*(22), 6410-6413.

Hirota-Takahata, Y., Harada, H., Tanaka, I., et al. (2007). F-19848 A, a novel inhibitor of hyaluronic acid binding to cellular receptor CD44. *Journal of Antibiotics, 60*(10), 633-639.

Hofmann, C., Lippert, E., Falk, W., et al. (2009). Primary human colonic epithelial cells are transiently protected from anoikis by a Src-dependent mechanism. *Biochem Biophys Res Commun, 390*(3), 908-914. doi:10.1016/j.bbrc.2009.10.075

Hofmann, C., Obermeier, F., Artinger, M., et al. (2007). Cell-cell contacts prevent anoikis in primary human colonic epithelial cells. *Gastroenterology, 132*(2), 587-600. doi:10.1053/j.gastro.2006.11.017

Holloway, S. E., Beck, A. W., Girard, L., et al. (2005). Increased expression of Cyr61 (CCN1) identified in peritoneal metastases from human pancreatic cancer. *J Am Coll Surg, 200*(3), 371-377. doi:10.1016/j.jamcollsurg.2004.10.005

Hu, Q., Peng, J., Liu, W., et al. (2014). Elevated cleaved caspase-3 is associated with shortened overall survival in several cancer types. *Int J Clin Exp Pathol, 7*(8), 5057-5070.

Hubbard, S. C., & Burns, J. W. (2002). Effects of a hyaluronan-based membrane (Seprafilm) on intraperitoneally disseminated human colon cancer cell growth in a nude mouse model. *Dis Colon Rectum, 45*(3), 334-341; discussion 341-334. doi:10.1007/s10350-004-6178-0

Hugen, N., van de Velde, C. J. H., de Wilt, J. H. W., et al. (2014). Metastatic pattern in colorectal cancer is strongly influenced by histological subtype. *Ann Oncol, 25*(3), 651-657. doi:10.1093/annonc/mdt591

Hurwitz, H., Fehrenbacher, L., Novotny, W., et al. (2004). Bevacizumab plus irinotecan, fluorouracil, and leucovorin for metastatic colorectal cancer. *N Engl J Med, 350*(23), 2335-2342. doi:10.1056/NEJMoa032691

Imano, M., Itoh, T., Satou, T., et al. (2013). High expression of epithelial cellular adhesion molecule in peritoneal metastasis of gastric cancer. *Target Oncol, 8*(4), 231-235. doi:10.1007/s11523-012-0239-4

Irby, K., Anderson, W. F., Henson, D. E., et al. (2006). Emerging and widening colorectal carcinoma disparities between Blacks and Whites in the United States (1975-2002). *Cancer Epidemiol Biomarkers Prev, 15*(4), 792-797. doi:10.1158/1055-9965.EPI-05-0879

Iseki, Y., Shibutani, M., Maeda, K., et al. (2017). Significance of E-cadherin and CD44 expression in patients with unresectable metastatic colorectal cancer. *Oncol Lett, 14*(1), 1025-1034. doi:10.3892/ol.2017.6269

Ishigami, S., Ueno, S., Nishizono, Y., et al. (2011). Prognostic impact of CD168 expression in gastric cancer. *BMC Cancer, 11*, 106. doi:10.1186/1471-2407-11-106

Jacquet, P., & Sugarbaker, P. H. (1996). Clinical research methodologies in diagnosis and staging of patients with peritoneal carcinomatosis. *Cancer Treat Res, 82*, 359-374. doi:10.1007/978-1-4613-1247-5_23

Jansen, M., Menko, F. H., Brosens, L. A., et al. (2014). Establishing a clinical and molecular diagnosis for hereditary colorectal cancer syndromes: Present tense, future perfect? *Gastrointest Endosc, 80*(6), 1145-1155. doi:10.1016/j.gie.2014.07.049

Jayne, D. G., Fook, S., Loi, C., et al. (2002). Peritoneal carcinomatosis from colorectal cancer. *Br J Surg, 89*(12), 1545-1550. doi:10.1046/j.1365-2168.2002.02274.x

Jayne, D. G., O'Leary, R., Gill, A., et al. (1999). A three-dimensional in-vitro model for the study of peritoneal tumour metastasis. *Clin Exp Metastasis, 17*(6), 515-523.

Jelinek, M., Balusikova, K., Schmiedlova, M., et al. (2015). The role of individual caspases in cell death induction by taxanes in breast cancer cells. *Cancer Cell Int, 15*(1), 8. doi:10.1186/s12935-015-0155-7

Jiang, W., Zhang, Y., Kane, K. T., et al. (2015). CD44 regulates pancreatic cancer invasion through MT1-MMP. *Mol Cancer Res, 13*(1), 9-15. doi:10.1158/1541-7786.MCR-14-0076

Jie, D., Zhongmin, Z., Guoqing, L., et al. (2013). Positive expression of LSD1 and negative expression of E-cadherin correlate with metastasis and poor prognosis of colon cancer. *Dig Dis Sci, 58*(6), 1581-1589. doi:10.1007/s10620-012-2552-2

Johns, D. B., Rodgers, K. E., Donahue, W. D., et al. (1997). Reduction of adhesion formation by postoperative administration of ionically cross-linked hyaluronic acid. *Fertil Steril, 68*(1), 37-42. doi:10.1016/s0015-0282(97)81472-0

Johnson, P., & Ruffell, B. (2009). CD44 and its role in inflammation and inflammatory diseases. *Inflamm Allergy Drug Targets, 8*(3), 208-220.

Jojovic, M., Delpech, B., Prehm, P., et al. (2002). Expression of hyaluronate and hyaluronate synthase in human primary tumours and their metastases in scid mice. *Cancer Letters, 188*(1-2), 181-189.

Jones, N., Vogt, S., Nielsen, M., et al. (2009). Increased colorectal cancer incidence in obligate carriers of heterozygous mutations in MUTYH. *Gastroenterology, 137*(2), 489-494, 494 e481; quiz 725-486. doi:10.1053/j.gastro.2009.04.047

Jordan, A. R., Racine, R. R., Hennig, M. J., et al. (2015). The Role of CD44 in Disease Pathophysiology and Targeted Treatment. *Front Immunol, 6*, 182. doi:10.3389/fimmu.2015.00182

Kaidi, A., Qualtrough, D., Williams, A. C., et al. (2006). Direct transcriptional up-regulation of cyclooxygenase-2 by hypoxia-inducible factor (HIF)-1 promotes colorectal tumor cell survival and enhances HIF-1 transcriptional activity during hypoxia. *Cancer Res, 66*(13), 6683-6691. doi:10.1158/0008-5472.CAN-06-0425

Kajiwara, Y., Ueno, H., Hashiguchi, Y., et al. (2011). Expression of l1 cell adhesion molecule and morphologic features at the invasive front of colorectal cancer. *Am J Clin Pathol, 136*(1), 138-144. doi:10.1309/AJCP63NRBNGCTXVF

Kalluri, R., & Weinberg, R. A. (2009). The basics of epithelial-mesenchymal transition. *J Clin Invest, 119*(6), 1420-1428. doi:10.1172/JCI39104

Kang, B. W., Kim, T. W., Lee, J. L., et al. (2009). Bevacizumab plus FOLFIRI or FOLFOX as third-line or later treatment in patients with metastatic colorectal cancer after failure of 5-fluorouracil, irinotecan, and oxaliplatin: a retrospective analysis. *Med Oncol, 26*(1), 32-37. doi:10.1007/s12032-008-9077-8

Karanikiotis, C., Skiadas, I., Karina, M., et al. (2005). A novel chromatographic method for Ep-CAM mRNA detection in peripheral blood and bone marrow of patients with metastatic colorectal cancer. *Anticancer Res, 25*(1A), 319-323.

Katoh, S., Goi, T., Naruse, T., et al. (2015). Cancer stem cell marker in circulating tumor cells: expression of CD44 variant exon 9 is strongly correlated to treatment refractoriness, recurrence and prognosis of human colorectal cancer. *Anticancer Research, 35*(1), 239-244.

Kaw, L. L., Jr., Punzalan, C. K., Crisostomo, A. C., et al. (2002). Surgical pathology of colorectal cancer in Filipinos: implications for clinical practice. *J Am Coll Surg, 195*(2), 188-195.

Kaya, M., Basak, F., Sisik, A., et al. (2017). Validation of microsatellite instability histology scores with Bethesda guidelines in hereditary nonpolyposis colorectal cancer. *J Cancer Res Ther, 13*(2), 356-361. doi:10.4103/0973-1482.174558

Kazemzadeh, M., Safaralizadeh, R., Feizi, M. A., et al. (2017). Misregulation of the dependence receptor DCC and its upstream lincRNA, LOC100287225, in colorectal cancer. *Tumori, 103*(1), 40-43. doi:10.5301/tj.5000426

Ke, T. W., Wei, P. L., Yeh, K. T., et al. (2015). MiR-92a Promotes Cell Metastasis of Colorectal Cancer Through PTEN-Mediated PI3K/AKT Pathway. *Ann Surg Oncol, 22*(8), 2649-2655. doi:10.1245/s10434-014-4305-2

Kellett-Clarke, H., Stegmann, M., Barclay, A. N., et al. (2015). CD44 Binding to Hyaluronic Acid Is Redox Regulated by a Labile Disulfide Bond in the Hyaluronic Acid Binding Site. *PLoS ONE [Electronic Resource], 10*(9), e0138137.

Kim, J. H., Bae, J. M., Kim, K. J., et al. (2014). Differential Features of Microsatellite-Unstable Colorectal Carcinomas Depending on EPCAM Expression Status. *Korean J Pathol, 48*(4), 276-282. doi:10.4132/KoreanJPathol.2014.48.4.276

Kim, J. H., Bae, J. M., Song, Y. S., et al. (2016). Clinicopathologic, molecular, and prognostic implications of the loss of EPCAM expression in colorectal carcinoma. *Oncotarget, 7*(12), 13372-13387. doi:10.18632/oncotarget.5618

Klaver, C. E., Groenen, H., Morton, D. G., et al. (2017). Recommendations and consensus on the treatment of peritoneal metastases of colorectal origin: a systematic review of national and international guidelines. *Colorectal Dis, 19*(3), 224-236. doi:10.1111/codi.13593

Klein, C. L., Bittinger, F., Skarke, C. C., et al. (1995). Effects of cytokines on the expression of cell adhesion molecules by cultured human omental mesothelial cells. *Pathobiology, 63*(4), 204-212.

Knudson, C. B., Munaim, S. I., & Toole, B. P. (1995). Ectodermal stimulation of the production of hyaluronan-dependent pericellular matrix by embryonic limb mesodermal cells. *Dev Dyn, 204*(2), 186-191. doi:10.1002/aja.1002040209

Kocak, I., Unlu, C., Akcan, Y., et al. (1999). Reduction of adhesion formation with cross-linked hyaluronic acid after peritoneal surgery in rats. *Fertil Steril, 72*(5), 873-878. doi:10.1016/s0015-0282(99)00368-4

Koelzer, V. H., Huber, B., Mele, V., et al. (2015). Expression of the hyaluronan-mediated motility receptor RHAMM in tumor budding cells identifies aggressive colorectal cancers. *Hum Pathol, 46*(11), 1573-1581. doi:10.1016/j.humpath.2015.07.010

Koh, C. E., Ansari, N., Morris, D., et al. (2019). Beware mis-representation of PRODIGE 7: danger of throwing out the cytoreductive surgery baby with the hyperthermic intraperitoneal chemotherapy bathwater. *ANZ J Surg, 89*(9), 992-994. doi:10.1111/ans.15424

Kong, D. H., Kim, Y. K., Kim, M. R., et al. (2018). Emerging Roles of Vascular Cell Adhesion Molecule-1 (VCAM-1) in Immunological Disorders and Cancer. *Int J Mol Sci, 19*(4). doi:10.3390/ijms19041057

Konishi, S., Wheeler, M. E., Donaldson, D. I., et al. (2000). Neural correlates of episodic retrieval success. *Neuroimage, 12*(3), 276-286. doi:10.1006/nimg.2000.0614

Koppe, M. J., Boerman, O. C., Oyen, W. J., et al. (2006). Peritoneal carcinomatosis of colorectal origin: incidence and current treatment strategies. *Ann Surg, 243*(2), 212-222. doi:10.1097/01.sla.0000197702.46394.16

Korchynskyi, O., Landstrom, M., Stoika, R., et al. (1999). Expression of Smad proteins in human colorectal cancer. *Int J Cancer, 82*(2), 197-202.

Ksiazek, K., Mikula-Pietrasik, J., Catar, R., et al. (2010). Oxidative stress-dependent increase in ICAM-1 expression promotes adhesion of colorectal and pancreatic cancers to the senescent peritoneal mesothelium. *Int J Cancer, 127*(2), 293-303. doi:10.1002/ijc.25036

Lampropoulos, P., Zizi-Sermpetzoglou, A., Rizos, S., et al. (2012). TGF-beta signalling in colon carcinogenesis. *Cancer Lett, 314*(1), 1-7. doi:10.1016/j.canlet.2011.09.041

Lan, T., Pang, J., Wu, Y., et al. (2016). Cross-linked hyaluronic acid gel inhibits metastasis and growth of gastric and hepatic cancer cells: in vitro and in vivo studies. *Oncotarget, 7*(40), 65418-65428. doi:10.18632/oncotarget.11739

Lascorz, J., Forsti, A., Chen, B., et al. (2010). Genome-wide association study for colorectal cancer identifies risk polymorphisms in German familial cases and implicates MAPK signalling pathways in disease susceptibility. *Carcinogenesis, 31*(9), 1612-1619. doi:10.1093/carcin/bgq146

Laurent, T. C., & Fraser, J. R. (1992). Hyaluronan. *Faseb j, 6*(7), 2397-2404.

Laurent, T. C., Laurent, U. B., & Fraser, J. R. (1996). The structure and function of hyaluronan: An overview. *Immunol Cell Biol, 74*(2), A1-7. doi:10.1038/icb.1996.32

Lawson, C., & Wolf, S. (2009). ICAM-1 signaling in endothelial cells. *Pharmacol Rep, 61*(1), 22-32. doi:10.1016/s1734-1140(09)70004-0

Lee, G. H., Malietzis, G., Askari, A., et al. (2015). Is right-sided colon cancer different to left-sided colorectal cancer? - a systematic review. *Eur J Surg Oncol, 41*(3), 300-308. doi:10.1016/j.ejso.2014.11.001

Lee, J. G., Ahn, J. H., Jin Kim, T., et al. (2015). Mutant p53 promotes ovarian cancer cell adhesion to mesothelial cells via integrin beta4 and Akt signals. *Sci Rep, 5*, 12642. doi:10.1038/srep12642

Lee, J. W., Shahzad, M. M., Lin, Y. G., et al. (2009). Surgical stress promotes tumor growth in ovarian carcinoma. *Clin Cancer Res, 15*(8), 2695-2702. doi:10.1158/1078-0432.CCR-08-2966

Lemoine, L., Sugarbaker, P., & Van der Speeten, K. (2016). Pathophysiology of colorectal peritoneal carcinomatosis: Role of the peritoneum. *World J Gastroenterol, 22*(34), 7692-7707. doi:10.3748/wjg.v22.i34.7692

Lemoine, L., Sugarbaker, P., & Van der Speeten, K. (2017). Drugs, doses, and durations of intraperitoneal chemotherapy: standardising HIPEC and EPIC for colorectal, appendiceal, gastric, ovarian peritoneal surface malignancies and peritoneal mesothelioma. *Int J Hyperthermia, 33*(5), 582-592. doi:10.1080/02656736.2017.1291999

Lesley, J., & Hyman, R. (1998). CD44 structure and function. *Front Biosci, 3*, d616-630.

Levy, A. D., Shaw, J. C., & Sobin, L. H. (2009). Secondary tumors and tumorlike lesions of the peritoneal cavity: imaging features with pathologic correlation. *Radiographics, 29*(2), 347-373. doi:10.1148/rg.292085189

Li, J., Huang, L., Zhao, H., et al. (2020). The Role of Interleukins in Colorectal Cancer. *Int J Biol Sci, 16*(13), 2323-2339. doi:10.7150/ijbs.46651

Li, J., Ye, L., Owen, S., et al. (2015). Emerging role of CCN family proteins in tumorigenesis and cancer metastasis (Review). *Int J Mol Med, 36*(6), 1451-1463. doi:10.3892/ijmm.2015.2390

Li, X. P., Zhang, X. W., Zheng, L. Z., et al. (2015). Expression of CD44 in pancreatic cancer and its significance. *Int J Clin Exp Pathol, 8*(6), 6724-6731.

Liang, G., Li, S., Du, W., et al. (2017). Hypoxia regulates CD44 expression via hypoxia-inducible factor-1alpha in human gastric cancer cells. *Oncol Lett, 13*(2), 967-972. doi:10.3892/ol.2016.5473

Liang, Y., & Sasaki, K. (2000). Expression of adhesion molecules relevant to leukocyte migration on the microvilli of liver peritoneal mesothelial cells. *Anat Rec, 258*(1), 39-46.

Lin, B. R., Chang, C. C., Che, T. F., et al. (2005). Connective tissue growth factor inhibits metastasis and acts as an independent prognostic marker in colorectal cancer. *Gastroenterology, 128*(1), 9-23. doi:10.1053/j.gastro.2004.10.007

Lin, B. R., Chang, C. C., Chen, R. J., et al. (2011). Connective tissue growth factor acts as a therapeutic agent and predictor for peritoneal carcinomatosis of colorectal cancer. *Clin Cancer Res, 17*(10), 3077-3088. doi:10.1158/1078-0432.CCR-09-3256

Lin, J., & Ding, D. (2017). The prognostic role of the cancer stem cell marker CD44 in ovarian cancer: a meta-analysis. *Cancer Cell Int, 17*, 8. doi:10.1186/s12935-016-0376-4

Liu, D., & Sy, M. S. (1996). A cysteine residue located in the transmembrane domain of CD44 is important in binding of CD44 to hyaluronic acid. *Journal of Experimental Medicine, 183*(5), 1987-1994.

Liu, J., Geng, X., & Li, Y. (2016). Milky spots: omental functional units and hotbeds for peritoneal cancer metastasis. *Tumour Biol, 37*(5), 5715-5726. doi:10.1007/s13277-016-4887-3

Liu, Y., Bunston, C., Hodson, N., et al. (2017). Psoriasin promotes invasion, aggregation and survival of pancreatic cancer cells; association with disease progression. *Int J Oncol, 50*(5), 1491-1500. doi:10.3892/ijo.2017.3953

Liu, Y., Luan, L., & Wang, X. (2015). A randomized Phase II clinical study of combining panitumumab and bevacizumab, plus irinotecan, 5-fluorouracil, and leucovorin (FOLFIRI) compared with FOLFIRI alone as second-line treatment for patients with metastatic colorectal cancer and KRAS mutation. *Onco Targets Ther, 8*, 1061-1068. doi:10.2147/OTT.S81442

Lokeshwar, V. B., Mirza, S., & Jordan, A. (2014). Targeting hyaluronic acid family for cancer chemoprevention and therapy. *Adv Cancer Res, 123*, 35-65. doi:10.1016/B978-0-12-800092-2.00002-2

Lu, L., Wu, M., Sun, L., et al. (2016). Clinicopathological and prognostic significance of cancer stem cell markers CD44 and CD133 in patients with gastric cancer: A comprehensive meta-analysis with 4729 patients involved. *Medicine (Baltimore), 95*(42), e5163. doi:10.1097/MD.0000000000005163

Lugli, A., Zlobec, I., Gunthert, U., et al. (2006). Overexpression of the receptor for hyaluronic acid mediated motility is an independent adverse prognostic factor in colorectal cancer. *Mod Pathol, 19*(10), 1302-1309. doi:10.1038/modpathol.3800648

Lurvink, R. J., Rovers, K. P., Wassenaar, E. C. E., et al. (2021). Patient-reported outcomes during repetitive oxaliplatin-based pressurized intraperitoneal aerosol chemotherapy for isolated unresectable colorectal peritoneal metastases in a multicenter, single-arm, phase 2 trial (CRC-PIPAC). *Surg Endosc*. doi:10.1007/s00464-021-08802-6

Lurvink, R. J., Tajzai, R., Rovers, K. P., et al. (2021). Systemic Pharmacokinetics of Oxaliplatin After Intraperitoneal Administration by Electrostatic Pressurized Intraperitoneal

Aerosol Chemotherapy (ePIPAC) in Patients with Unresectable Colorectal Peritoneal Metastases in the CRC-PIPAC Trial. *Ann Surg Oncol, 28*(1), 265-272. doi:10.1245/s10434-020-08743-9

Lynch, H. T., & Shaw, T. G. (2013). Practical genetics of colorectal cancer. *Chin Clin Oncol, 2*(2), 12. doi:10.3978/j.issn.2304-3865.2013.03.04

Ma, J., Shen, H., Kapesa, L., et al. (2016). Lauren classification and individualized chemotherapy in gastric cancer. *Oncol Lett, 11*(5), 2959-2964. doi:10.3892/ol.2016.4337

MacCarthy-Morrogh, L., & Martin, P. (2020). The hallmarks of cancer are also the hallmarks of wound healing. *Sci Signal, 13*(648). doi:10.1126/scisignal.aay8690

Maciver, A. H., McCall, M., & James Shapiro, A. M. (2011). Intra-abdominal adhesions: cellular mechanisms and strategies for prevention. *Int J Surg, 9*(8), 589-594. doi:10.1016/j.ijsu.2011.08.008

Maeda, K., Kang, S. M., Sawada, T., et al. (2002). Expression of intercellular adhesion molecule-1 and prognosis in colorectal cancer. *Oncol Rep, 9*(3), 511-514.

Makiguchi, Y., Hinoda, Y., & Imai, K. (1996). Effect of MUC1 mucin, an anti-adhesion molecule, on tumor cell growth. *Jpn J Cancer Res, 87*(5), 505-511. doi:10.1111/j.1349-7006.1996.tb00252.x

Marley, A. R., & Nan, H. (2016). Epidemiology of colorectal cancer. *Int J Mol Epidemiol Genet, 7*(3), 105-114.

Martin, M., Pujuguet, P., & Martin, F. (1996). Role of stromal myofibroblasts infiltrating colon cancer in tumor invasion. *Pathol Res Pract, 192*(7), 712-717. doi:10.1016/S0344-0338(96)80093-8

Massague, J. (1990). The transforming growth factor-beta family. *Annu Rev Cell Biol, 6*, 597-641. doi:10.1146/annurev.cb.06.110190.003121

Maurer, C. A., Friess, H., Kretschmann, B., et al. (1998). Over-expression of ICAM-1, VCAM-1 and ELAM-1 might influence tumor progression in colorectal cancer. *Int J Cancer, 79*(1), 76-81. doi:10.1002/(sici)1097-0215(19980220)79:1<76::aid-ijc15>3.0.co;2-f

Mayer, B., Jauch, K. W., Gunthert, U., et al. (1993). De-novo expression of CD44 and survival in gastric cancer. *Lancet, 342*(8878), 1019-1022.

McCourt, P. A., Ek, B., Forsberg, N., et al. (1994). Intercellular adhesion molecule-1 is a cell surface receptor for hyaluronan. *J Biol Chem, 269*(48), 30081-30084.

Mele, V., Sokol, L., Kolzer, V. H., et al. (2017). The hyaluronan-mediated motility receptor RHAMM promotes growth, invasiveness and dissemination of colorectal cancer. *Oncotarget, 8*(41), 70617-70629. doi:10.18632/oncotarget.19904

Menke-van der Houven van Oordt, C. W., Gomez-Roca, C., van Herpen, C., et al. (2016). First-in-human phase I clinical trial of RG7356, an anti-CD44 humanized antibody, in patients with advanced, CD44-expressing solid tumors. *Oncotarget, 7*(48), 80046-80058. doi:10.18632/oncotarget.11098

Mi, Y., Mu, L., Huang, K., et al. (2020). Hypoxic colorectal cancer cells promote metastasis of normoxic cancer cells depending on IL-8/p65 signaling pathway. *Cell Death Dis, 11*(7), 610. doi:10.1038/s41419-020-02797-z

Mikelsaar, R. H., & Scott, J. E. (1994). Molecular modelling of secondary and tertiary structures of hyaluronan, compared with electron microscopy and NMR data. Possible sheets and tubular structures in aqueous solution. *Glycoconjugate Journal, 11*(2), 65-71.

Mikula-Pietrasik, J., Uruski, P., Kucinska, M., et al. (2017). The protective activity of mesothelial cells against peritoneal growth of gastrointestinal tumors: The role of soluble ICAM-1. *Int J Biochem Cell Biol, 86*, 26-31. doi:10.1016/j.biocel.2017.03.013

Mikula-Pietrasik, J., Uruski, P., Tykarski, A., et al. (2018). The peritoneal "soil" for a cancerous "seed": a comprehensive review of the pathogenesis of intraperitoneal cancer metastases. *Cell Mol Life Sci, 75*(3), 509-525. doi:10.1007/s00018-017-2663-1

Mironov, V. A., Gusev, S. A., & Baradi, A. F. (1979). Mesothelial stomata overlying omental milky spots: scanning electron microscopic study. *Cell Tissue Res, 201*(2), 327-330.

Misra, S., Hascall, V. C., Markwald, R. R., et al. (2015). Interactions between Hyaluronan and Its Receptors (CD44, RHAMM) Regulate the Activities of Inflammation and Cancer. *Front Immunol, 6*, 201. doi:10.3389/fimmu.2015.00201

Mizoguchi, T., Yamada, K., Furukawa, T., et al. (1990). Expression of the MDR1 gene in human gastric and colorectal carcinomas. *J Natl Cancer Inst, 82*(21), 1679-1683. doi:10.1093/jnci/82.21.1679

Mizutani, K., Kofuji, K., & Shirouzu, K. (2000). The significance of MMP-1 and MMP-2 in peritoneal disseminated metastasis of gastric cancer. *Surg Today, 30*(7), 614-621. doi:10.1007/s005950070101

Mody, K., Baldeo, C., & Bekaii-Saab, T. (2018). Antiangiogenic Therapy in Colorectal Cancer. *Cancer J, 24*(4), 165-170. doi:10.1097/PPO.0000000000000328

Mokhtari, M., & Zakerzade, Z. (2017). EPCAM Expression in Colon Adenocarcinoma and its Relationship with TNM Staging. *Adv Biomed Res, 6*, 56. doi:10.4103/2277-9175.205529

Motohara, T., Fujimoto, K., Tayama, S., et al. (2016). CD44 Variant 6 as a Predictive Biomarker for Distant Metastasis in Patients With Epithelial Ovarian Cancer. *Obstet Gynecol, 127*(6), 1003-1011. doi:10.1097/AOG.0000000000001420

Mulder, J. W., Kruyt, P. M., Sewnath, M., et al. (1994). Colorectal cancer prognosis and expression of exon-v6-containing CD44 proteins. *Lancet, 344*(8935), 1470-1472.

Mummert, M. E., Mohamadzadeh, M., Mummert, D. I., et al. (2000). Development of a peptide inhibitor of hyaluronan-mediated leukocyte trafficking. *J Exp Med, 192*(6), 769-779. doi:10.1084/jem.192.6.769

Muniyan, S., Haridas, D., Chugh, S., et al. (2016). MUC16 contributes to the metastasis of pancreatic ductal adenocarcinoma through focal adhesion mediated signaling mechanism. *Genes Cancer, 7*(3-4), 110-124. doi:10.18632/genesandcancer.104

Murphy, K. M., Zhang, S., Geiger, T., et al. (2006). Comparison of the microsatellite instability analysis system and the Bethesda panel for the determination of microsatellite instability in colorectal cancers. *J Mol Diagn, 8*(3), 305-311. doi:10.2353/jmoldx.2006.050092

Mutsaers, S. E. (2002). Mesothelial cells: their structure, function and role in serosal repair. *Respirology, 7*(3), 171-191.

Mutsaers, S. E., Prele, C. M., Pengelly, S., et al. (2016). Mesothelial cells and peritoneal homeostasis. *Fertil Steril, 106*(5), 1018-1024. doi:10.1016/j.fertnstert.2016.09.005

Nakamura, K., Sawada, K., Kinose, Y., et al. (2017). Exosomes Promote Ovarian Cancer Cell Invasion through Transfer of CD44 to Peritoneal Mesothelial Cells. *Mol Cancer Res, 15*(1), 78-92. doi:10.1158/1541-7786.MCR-16-0191

Nakamura, T., Matsumoto, K., Kiritoshi, A., et al. (1997). Induction of hepatocyte growth factor in fibroblasts by tumor-derived factors affects invasive growth of tumor cells: in vitro analysis of tumor-stromal interactions. *Cancer Res, 57*(15), 3305-3313.

Nazemalhosseini Mojarad, E., Kuppen, P. J., Aghdaei, H. A., et al. (2013). The CpG island methylator phenotype (CIMP) in colorectal cancer. *Gastroenterol Hepatol Bed Bench, 6*(3), 120-128.

Nittka, S., Gunther, J., Ebisch, C., et al. (2004). The human tumor suppressor CEACAM1 modulates apoptosis and is implicated in early colorectal tumorigenesis. *Oncogene, 23*(58), 9306-9313. doi:10.1038/sj.onc.1208259

Niv, Y. (2008). MUC1 and colorectal cancer pathophysiology considerations. *World J Gastroenterol, 14*(14), 2139-2141. doi:10.3748/wjg.14.2139

O'Sullivan, G. C., & Shanahan, F. (1999). Escape from the Smad world by colon cancer. *Gastroenterology, 116*(6), 1496-1497.

Oosterling, S. J., van der Bij, G. J., Bogels, M., et al. (2008). Anti-beta1 integrin antibody reduces surgery-induced adhesion of colon carcinoma cells to traumatized peritoneal surfaces. *Ann Surg, 247*(1), 85-94. doi:10.1097/SLA.0b013e3181588583

Oosterling, S. J., van der Bij, G. J., van Egmond, M., et al. (2005). Surgical trauma and peritoneal recurrence of colorectal carcinoma. *Eur J Surg Oncol, 31*(1), 29-37. doi:10.1016/j.ejso.2004.10.005

Orian-Rousseau, V., Chen, L., Sleeman, J. P., et al. (2002). CD44 is required for two consecutive steps in HGF/c-Met signaling. *Genes Dev, 16*(23), 3074-3086. doi:10.1101/gad.242602

Osada, S., Matsui, S., Komori, S., et al. (2010). Effect of hepatocyte growth factor on progression of liver metastasis in colorectal cancer. *Hepatogastroenterology, 57*(97), 76-80.

Painter, J. T., Clayton, N. P., & Herbert, R. A. (2010). Useful immunohistochemical markers of tumor differentiation. *Toxicol Pathol, 38*(1), 131-141. doi:10.1177/0192623309356449

Paoli, P., Giannoni, E., & Chiarugi, P. (2013). Anoikis molecular pathways and its role in cancer progression. *Biochim Biophys Acta, 1833*(12), 3481-3498. doi:10.1016/j.bbamcr.2013.06.026

Papachristos, A., Kemos, P., Katsila, T., et al. (2019). VEGF-A and ICAM-1 Gene Polymorphisms as Predictors of Clinical Outcome to First-Line Bevacizumab-Based Treatment in Metastatic Colorectal Cancer. *Int J Mol Sci, 20*(22). doi:10.3390/ijms20225791

Park, D. Y., Sakamoto, H., Kirley, S. D., et al. (2007). The Cables gene on chromosome 18q is silenced by promoter hypermethylation and allelic loss in human colorectal cancer. *Am J Pathol, 171*(5), 1509-1519. doi:10.2353/ajpath.2007.070331

Park, S. Y., Lee, S. J., Cho, H. J., et al. (2016). Dehydropeptidase 1 promotes metastasis through regulation of E-cadherin expression in colon cancer. *Oncotarget, 7*(8), 9501-9512. doi:10.18632/oncotarget.7033

Parker, D. (1995). Colorectal cancer prognosis and expression of exon-v6-containing CD44 proteins. *Lancet, 345*(8949), 583-584.

Pasquier, J., Vidal, F., Hoarau-Vechot, J., et al. (2018). Surgical peritoneal stress creates a pro-metastatic niche promoting resistance to apoptosis via IL-8. *J Transl Med, 16*(1), 271. doi:10.1186/s12967-018-1643-z

Patriarca, C., Macchi, R. M., Marschner, A. K., et al. (2012). Epithelial cell adhesion molecule expression (CD326) in cancer: a short review. *Cancer Treat Rev, 38*(1), 68-75. doi:10.1016/j.ctrv.2011.04.002

Peach, R. J., Hollenbaugh, D., Stamenkovic, I., et al. (1993). Identification of hyaluronic acid binding sites in the extracellular domain of CD44. *Journal of Cell Biology, 122*(1), 257-264.

Pino, M. S., & Chung, D. C. (2010). The chromosomal instability pathway in colon cancer. *Gastroenterology, 138*(6), 2059-2072. doi:10.1053/j.gastro.2009.12.065

Pirker, R., Wallner, J., Gsur, A., et al. (1993). MDR1 gene expression in primary colorectal carcinomas. *Br J Cancer, 68*(4), 691-694. doi:10.1038/bjc.1993.411

Pocard, M., Debruyne, P., Bras-Goncalves, R., et al. (2001). Single alteration of p53 or E-cadherin genes can alter the surgical resection benefit in an experimental model of colon cancer. *Dis Colon Rectum, 44*(8), 1106-1112.

Poerwosusanta, H., Gunadi, Oktaviyanti, I. K., et al. (2020). Laparoscopic procedures impact on mast cell mediators, extracellular matrix and adhesion scoring system in rats. *Ann Med Surg (Lond), 58*, 102-106. doi:10.1016/j.amsu.2020.08.043

Ponta, H., Sherman, L., & Herrlich, P. A. (2003). CD44: from adhesion molecules to signalling regulators. *Nat Rev Mol Cell Biol, 4*(1), 33-45. doi:10.1038/nrm1004

Popat, S., & Houlston, R. S. (2005). A systematic review and meta-analysis of the relationship between chromosome 18q genotype, DCC status and colorectal cancer prognosis. *Eur J Cancer, 41*(14), 2060-2070. doi:10.1016/j.ejca.2005.04.039

Pretzsch, E., Bosch, F., Neumann, J., et al. (2019). Mechanisms of Metastasis in Colorectal Cancer and Metastatic Organotropism: Hematogenous versus Peritoneal Spread. *J Oncol, 2019*, 7407190. doi:10.1155/2019/7407190

Qi, Y., Zhou, F., Zhang, L., et al. (2015). Construction of interference vector targeting Ep-CAM gene and its effects on colorectal cancer cell proliferation. *Drug Des Devel Ther, 9*, 2647-2652. doi:10.2147/DDDT.S82917

Quenet, F., Elias, D., Roca, L., et al. (2021). Cytoreductive surgery plus hyperthermic intraperitoneal chemotherapy versus cytoreductive surgery alone for colorectal peritoneal metastases (PRODIGE 7): a multicentre, randomised, open-label, phase 3 trial. *Lancet Oncol, 22*(2), 256-266. doi:10.1016/S1470-2045(20)30599-4

Raftery, A. T. (1973). Regeneration of parietal and visceral peritoneum: an electron microscopical study. *Journal of Anatomy, 115*(Pt 3), 375-392.

Rahmani, F., Avan, A., Hashemy, S. I., et al. (2017). Role of Wnt/beta-catenin signaling regulatory microRNAs in the pathogenesis of colorectal cancer. *J Cell Physiol*. doi:10.1002/jcp.25897

Rankin, E. B., & Giaccia, A. J. (2016). Hypoxic control of metastasis. *Science, 352*(6282), 175-180. doi:10.1126/science.aaf4405

Re, F., Zanetti, A., Sironi, M., et al. (1994). Inhibition of anchorage-dependent cell spreading triggers apoptosis in cultured human endothelial cells. *J Cell Biol, 127*(2), 537-546. doi:10.1083/jcb.127.2.537

Rein, D. T., Roehrig, K., Schondorf, T., et al. (2003). Expression of the hyaluronan receptor RHAMM in endometrial carcinomas suggests a role in tumour progression and metastasis. *J Cancer Res Clin Oncol, 129*(3), 161-164. doi:10.1007/s00432-003-0415-0

Reinartz, S., Failer, S., Schuell, T., et al. (2012). CA125 (MUC16) gene silencing suppresses growth properties of ovarian and breast cancer cells. *Eur J Cancer, 48*(10), 1558-1569. doi:10.1016/j.ejca.2011.07.004

Rex, D. K., Ahnen, D. J., Baron, J. A., et al. (2012). Serrated Lesions of the Colorectum: Review and Recommendations From an Expert Panel. *American Journal of Gastroenterology, 107*(9), 1315-1330. doi:10.1038/ajg.2012.161

Ribeiro, K. B., da Silva Zanetti, J., Ribeiro-Silva, A., et al. (2016). KRAS mutation associated with CD44/CD166 immunoexpression as predictors of worse outcome in metastatic colon cancer. *Cancer Biomark, 16*(4), 513-521. doi:10.3233/CBM-160592

Richmond, A., & Su, Y. (2008). Mouse xenograft models vs GEM models for human cancer therapeutics. *Dis Model Mech, 1*(2-3), 78-82. doi:10.1242/dmm.000976

Riss, T. L., Moravec, R. A., Niles, A. L., et al. (2004). Cell Viability Assays. In S. Markossian, A. Grossman, K. Brimacombe, M. Arkin, D. Auld, C. P. Austin, . . . X. Xu (Eds.), *Assay Guidance Manual*. Bethesda (MD).

Rodgers, K. E., Johns, D. B., Girgis, W., et al. (1997). Reduction of adhesion formation with hyaluronic acid after peritoneal surgery in rabbits. *Fertil Steril, 67*(3), 553-558. doi:10.1016/s0015-0282(97)80085-4

Rodriguez-Bigas, M. A., Boland, C. R., Hamilton, S. R., et al. (1997). A National Cancer Institute Workshop on Hereditary Nonpolyposis Colorectal Cancer Syndrome: meeting highlights and Bethesda guidelines. *J Natl Cancer Inst, 89*(23), 1758-1762.

Roux, P. P., & Blenis, J. (2004). ERK and p38 MAPK-activated protein kinases: a family of protein kinases with diverse biological functions. *Microbiol Mol Biol Rev, 68*(2), 320-344. doi:10.1128/MMBR.68.2.320-344.2004

Rovers, K. P., Lurvink, R. J., Wassenaar, E. C., et al. (2019). Repetitive electrostatic pressurised intraperitoneal aerosol chemotherapy (ePIPAC) with oxaliplatin as a palliative monotherapy for isolated unresectable colorectal peritoneal metastases: protocol of a Dutch, multicentre, open-label, single-arm, phase II study (CRC-PIPAC). *Bmj Open, 9*(7), e030408. doi:10.1136/bmjopen-2019-030408

Rovers, K. P., Wassenaar, E. C. E., Lurvink, R. J., et al. (2021). Pressurized Intraperitoneal Aerosol Chemotherapy (Oxaliplatin) for Unresectable Colorectal Peritoneal Metastases: A Multicenter, Single-Arm, Phase II Trial (CRC-PIPAC). *Ann Surg Oncol, 28*(9), 5311-5326. doi:10.1245/s10434-020-09558-4

Rozen, P., Liphshitz, I., & Barchana, M. (2011). The changing epidemiology of colorectal cancer and its relevance for adapting screening guidelines and methods. *Eur J Cancer Prev, 20*(1), 46-53. doi:10.1097/CEJ.0b013e328341e309

Rubin, J., Clawson, M., Planch, A., et al. (1988). Measurements of peritoneal surface area in man and rat. *Am J Med Sci, 295*(5), 453-458.

Rump, A., Morikawa, Y., Tanaka, M., et al. (2004). Binding of ovarian cancer antigen CA125/MUC16 to mesothelin mediates cell adhesion. *J Biol Chem, 279*(10), 9190-9198. doi:10.1074/jbc.M312372200

Sadler, T. W. a. L., J. (2012). *Langman's Medical Embryology*: Wolters Kluwer Health/Lippincott Williams & Wilkins Philadelphia.

Sakamoto, M., Takamura, M., Ino, Y., et al. (2001). Involvement of c-Src in carcinoma cell motility and metastasis. *Jpn J Cancer Res, 92*(9), 941-946.

Salomon, D. S., Brandt, R., Ciardiello, F., et al. (1995). Epidermal growth factor-related peptides and their receptors in human malignancies. *Crit Rev Oncol Hematol, 19*(3), 183-232.

Sanchez, I., Xu, C. J., Juo, P., et al. (1999). Caspase-8 is required for cell death induced by expanded polyglutamine repeats. *Neuron, 22*(3), 623-633. doi:10.1016/s0896-6273(00)80716-3

Sanchez-Hidalgo, J. M., Rodriguez-Ortiz, L., Arjona-Sanchez, A., et al. (2019). Colorectal peritoneal metastases: Optimal management review. *World J Gastroenterol, 25*(27), 3484-3502. doi:10.3748/wjg.v25.i27.3484

Santini, D., Loupakis, F., Vincenzi, B., et al. (2008). High concordance of KRAS status between primary colorectal tumors and related metastatic sites: implications for clinical practice. *Oncologist, 13*(12), 1270-1275. doi:10.1634/theoncologist.2008-0181

Sato, H., Kotake, K., Sugihara, K., et al. (2016). Clinicopathological Factors Associated with Recurrence and Prognosis after R0 Resection for Stage IV Colorectal Cancer with Peritoneal Metastasis. *Dig Surg, 33*(5), 382-391. doi:10.1159/000444097

Sausville, E. A., & Burger, A. M. (2006). Contributions of human tumor xenografts to anticancer drug development. *Cancer Res, 66*(7), 3351-3354, discussion 3354. doi:10.1158/0008-5472.CAN-05-3627

Sawada, K., Radjabi, A. R., Shinomiya, N., et al. (2007). c-Met overexpression is a prognostic factor in ovarian cancer and an effective target for inhibition of peritoneal dissemination and invasion. *Cancer Res, 67*(4), 1670-1679. doi:10.1158/0008-5472.CAN-06-1147

Sawada, T., Hasegawa, K., Tsukada, K., et al. (1999). Adhesion preventive effect of hyaluronic acid after intraperitoneal surgery in mice. *Hum Reprod, 14*(6), 1470-1472. doi:10.1093/humrep/14.6.1470

Schellerer, V. S., Langheinrich, M., Hohenberger, W., et al. (2014). Tumor-associated fibroblasts isolated from colorectal cancer tissues exhibit increased ICAM-1 expression and affinity for monocytes. *Oncol Rep, 31*(1), 255-261. doi:10.3892/or.2013.2860

Schutze, A., Vogeley, C., Gorges, T., et al. (2016). RHAMM splice variants confer radiosensitivity in human breast cancer cell lines. *Oncotarget, 7*(16), 21428-21440. doi:10.18632/oncotarget.7258

Scott, J. E., Cummings, C., Brass, A., et al. (1991). Secondary and tertiary structures of hyaluronan in aqueous solution, investigated by rotary shadowing-electron microscopy and computer simulation. Hyaluronan is a very efficient network-forming polymer. *Biochemical Journal, 274*(Pt 3), 699-705.

Serafino, A., Zonfrillo, M., Andreola, F., et al. (2011). CD44-targeting for antitumor drug delivery: a new SN-38-hyaluronan bioconjugate for locoregional treatment of peritoneal carcinomatosis. *Curr Cancer Drug Targets, 11*(5), 572-585. doi:10.2174/156800911795655976

Shariati, M., Lollo, G., Matha, K., et al. (2020). Synergy between Intraperitoneal Aerosolization (PIPAC) and Cancer Nanomedicine: Cisplatin-Loaded Polyarginine-Hyaluronic Acid Nanocarriers Efficiently Eradicate Peritoneal Metastasis of Advanced Human Ovarian Cancer. *ACS Appl Mater Interfaces, 12*(26), 29024-29036. doi:10.1021/acsami.0c05554

Sherman, L. S., Rizvi, T. A., Karyala, S., et al. (2000). CD44 enhances neuregulin signaling by Schwann cells. *J Cell Biol, 150*(5), 1071-1084.

Shida, D., Kanemitsu, Y., Hamaguchi, T., et al. (2019). Introducing the eighth edition of the tumor-node-metastasis classification as relevant to colorectal cancer, anal cancer and appendiceal cancer: a comparison study with the seventh edition of the tumor-node-metastasis and the Japanese Classification of Colorectal, Appendiceal, and Anal Carcinoma. *Jpn J Clin Oncol, 49*(4), 321-328. doi:10.1093/jjco/hyy198

Shimao, Y., Nabeshima, K., Inoue, T., et al. (1999). Role of fibroblasts in HGF/SF-induced cohort migration of human colorectal carcinoma cells: fibroblasts stimulate migration associated with increased fibronectin production via upregulated TGF-beta1. *Int J Cancer, 82*(3), 449-458.

Siegel, R., Desantis, C., & Jemal, A. (2014). Colorectal cancer statistics, 2014. *CA Cancer J Clin, 64*(2), 104-117. doi:10.3322/caac.21220

Siegel, R. L., Miller, K. D., Fedewa, S. A., et al. (2017). Colorectal cancer statistics, 2017. *CA Cancer J Clin, 67*(3), 177-193. doi:10.3322/caac.21395

Siegel, R. L., Miller, K. D., & Jemal, A. (2015). Cancer statistics, 2015. *CA Cancer J Clin, 65*(1), 5-29. doi:10.3322/caac.21254

Siegelman, M. H., DeGrendele, H. C., & Estess, P. (1999). Activation and interaction of CD44 and hyaluronan in immunological systems. *J Leukoc Biol, 66*(2), 315-321.

Sluiter, N., de Cuba, E., Kwakman, R., et al. (2016). Adhesion molecules in peritoneal dissemination: function, prognostic relevance and therapeutic options. *Clin Exp Metastasis, 33*(5), 401-416. doi:10.1007/s10585-016-9791-0

Sneath, R. J., & Mangham, D. C. (1998). The normal structure and function of CD44 and its role in neoplasia. *Mol Pathol, 51*(4), 191-200.

Sohr, S., & Engeland, K. (2008). RHAMM is differentially expressed in the cell cycle and downregulated by the tumor suppressor p53. *Cell Cycle, 7*(21), 3448-3460. doi:10.4161/cc.7.21.7014

Soliman, F., Ye, L., Jiang, W., et al. (2021). Targeting Hyaluronic Acid and Peritoneal Dissemination in Colorectal Cancer. *Clin Colorectal Cancer*. doi:10.1016/j.clcc.2021.11.008

Song, J. H., Cao, Z., Yoon, J. H., et al. (2011). Genetic alterations and expression pattern of CEACAM1 in colorectal adenomas and cancers. *Pathol Oncol Res, 17*(1), 67-74. doi:10.1007/s12253-010-9282-6

Steinkamp, M. P., Winner, K. K., Davies, S., et al. (2013). Ovarian tumor attachment, invasion, and vascularization reflect unique microenvironments in the peritoneum: insights from xenograft and mathematical models. *Front Oncol, 3*, 97. doi:10.3389/fonc.2013.00097

Stoker, M., Gherardi, E., Perryman, M., et al. (1987). Scatter factor is a fibroblast-derived modulator of epithelial cell mobility. *Nature, 327*(6119), 239-242. doi:10.1038/327239a0

Stotz, M., Herzog, S. A., Pichler, M., et al. (2017). Cancer Stem Cell Gene Variants in CD44 Predict Outcome in Stage II and Stage III Colon Cancer Patients. *Anticancer Res, 37*(4), 2011-2018. doi:10.21873/anticanres.11545

Streppel, M. M., Vincent, A., Mukherjee, R., et al. (2012). Mucin 16 (cancer antigen 125) expression in human tissues and cell lines and correlation with clinical outcome in adenocarcinomas of the pancreas, esophagus, stomach, and colon. *Hum Pathol, 43*(10), 1755-1763. doi:10.1016/j.humpath.2012.01.005

Strobel, T., Swanson, L., & Cannistra, S. A. (1997). In vivo inhibition of CD44 limits intra-abdominal spread of a human ovarian cancer xenograft in nude mice: a novel role for CD44 in the process of peritoneal implantation. *Cancer Res, 57*(7), 1228-1232.

Sugarbaker, P. H. (1995). Patient selection and treatment of peritoneal carcinomatosis from colorectal and appendiceal cancer. *World J Surg, 19*(2), 235-240. doi:10.1007/BF00308632

Sugarbaker, P. H. (2005a). Colorectal carcinomatosis: a new oncologic frontier. *Curr Opin Oncol, 17*(4), 397-399.

Sugarbaker, P. H. (2005b). Peritoneal surface oncology: review of a personal experience with colorectal and appendiceal malignancy. *Tech Coloproctol, 9*(2), 95-103. doi:10.1007/s10151-005-0205-6

Sun, F., Feng, M., & Guan, W. (2017). Mechanisms of peritoneal dissemination in gastric cancer. *Oncol Lett, 14*(6), 6991-6998. doi:10.3892/ol.2017.7149

Sun, J., Sun, B., Zhu, D., et al. (2017). HMGA2 regulates CD44 expression to promote gastric cancer cell motility and sphere formation. *Am J Cancer Res, 7*(2), 260-274.

Suthananthan, A. E., Bhandari, M., & Platell, C. (2017). Influence of primary site on metastatic distribution and survival in stage IV colorectal cancer. *ANZ J Surg*. doi:10.1111/ans.13969

Tachimori, A., Yamada, N., Sakate, Y., et al. (2005). Up regulation of ICAM-1 gene expression inhibits tumour growth and liver metastasis in colorectal carcinoma. *Eur J Cancer, 41*(12), 1802-1810. doi:10.1016/j.ejca.2005.04.036

Taddei, M. L., Giannoni, E., Fiaschi, T., et al. (2012). Anoikis: an emerging hallmark in health and diseases. *J Pathol, 226*(2), 380-393. doi:10.1002/path.3000

Taibi, A., Albouys, J., Jacques, J., et al. (2019). Comparison of implantation sites for the development of peritoneal metastasis in a colorectal cancer mouse model using non-invasive bioluminescence imaging. *PLoS ONE, 14*(7), e0220360. doi:10.1371/journal.pone.0220360

Takeuchi, A., Yokoyama, S., Nakamori, M., et al. (2019). Loss of CEACAM1 is associated with poor prognosis and peritoneal dissemination of patients with gastric cancer. *Sci Rep, 9*(1), 12702. doi:10.1038/s41598-019-49230-w

Talmadge, J. E., Singh, R. K., Fidler, I. J., et al. (2007). Murine models to evaluate novel and conventional therapeutic strategies for cancer. *Am J Pathol, 170*(3), 793-804. doi:10.2353/ajpath.2007.060929

Tampakis, A., Tampaki, E. C., Nonni, A., et al. (2020). L1CAM expression in colorectal cancer identifies a high-risk group of patients with dismal prognosis already in early-stage disease. *Acta Oncol, 59*(1), 55-59. doi:10.1080/0284186X.2019.1667022

ten Raa, S., van Grevenstein, H. M., ten Kate, M., et al. (2007). The influence of reactive oxygen species on the adhesion of pancreatic carcinoma cells to the peritoneum. *Cell Adh Migr, 1*(2), 77-83. doi:10.4161/cam.1.2.4283

Thibodeau, S. N., Bren, G., & Schaid, D. (1993). Microsatellite instability in cancer of the proximal colon. *Science, 260*(5109), 816-819.

Thorne, R. F., Legg, J. W., & Isacke, C. M. (2004). The role of the CD44 transmembrane and cytoplasmic domains in co-ordinating adhesive and signalling events. *J Cell Sci, 117*(Pt 3), 373-380. doi:10.1242/jcs.00954

Thornton, M. H., Johns, D. B., Campeau, J. D., et al. (1998). Clinical evaluation of 0.5% ferric hyaluronate adhesion prevention gel for the reduction of adhesions following peritoneal cavity surgery: open-label pilot study. *Hum Reprod, 13*(6), 1480-1485. doi:10.1093/humrep/13.6.1480

Tjhay, F., Motohara, T., Tayama, S., et al. (2015). CD44 variant 6 is correlated with peritoneal dissemination and poor prognosis in patients with advanced epithelial ovarian cancer. *Cancer Sci, 106*(10), 1421-1428. doi:10.1111/cas.12765

Tolg, C., McCarthy, J. B., Yazdani, A., et al. (2014). Hyaluronan and RHAMM in wound repair and the "cancerization" of stromal tissues. *Biomed Res Int, 2014*, 103923. doi:10.1155/2014/103923

Torre, L. A., Bray, F., Siegel, R. L., et al. (2015). Global cancer statistics, 2012. *CA Cancer J Clin, 65*(2), 87-108. doi:10.3322/caac.21262

Toyota, M., Ahuja, N., Ohe-Toyota, M., et al. (1999). CpG island methylator phenotype in colorectal cancer. *Proc Natl Acad Sci U S A, 96*(15), 8681-8686.

Trimbath, J. D., & Giardiello, F. M. (2002). Review article: genetic testing and counselling for hereditary colorectal cancer. *Aliment Pharmacol Ther, 16*(11), 1843-1857.

Trzpis, M., McLaughlin, P. M., de Leij, L. M., et al. (2007). Epithelial cell adhesion molecule: more than a carcinoma marker and adhesion molecule. *Am J Pathol, 171*(2), 386-395. doi:10.2353/ajpath.2007.070152

Tseng, J. C., Benink, H. A., McDougall, M. G., et al. (2012). In Vivo Fluorescent Labeling of Tumor Cells with the HaloTag(R) Technology. *Curr Chem Genomics, 6*, 48-54. doi:10.2174/1875397301206010048

Turley, E. A. (1982). Purification of a hyaluronate-binding protein fraction that modifies cell social behavior. *Biochem Biophys Res Commun, 108*(3), 1016-1024.

Turley, E. A. (1989). The role of a cell-associated hyaluronan-binding protein in fibroblast behaviour. *Ciba Found Symp, 143*, 121-133; discussion 133-127, 281-125.

Turley, E. A. (1992). Hyaluronan and cell locomotion. *Cancer Metastasis Rev, 11*(1), 21-30.

Turley, E. A., Moore, D., & Hayden, L. J. (1987). Characterization of hyaluronate binding proteins isolated from 3T3 and murine sarcoma virus transformed 3T3 cells. *Biochemistry, 26*(11), 2997-3005.

Turley, E. A., & Torrance, J. (1985). Localization of hyaluronate and hyaluronate-binding protein on motile and non-motile fibroblasts. *Exp Cell Res, 161*(1), 17-28.

van Baal, J., van Noorden, C. J. F., Nieuwland, R., et al. (2018). Development of Peritoneal Carcinomatosis in Epithelial Ovarian Cancer: A Review. *J Histochem Cytochem, 66*(2), 67-83. doi:10.1369/0022155417742897

van Baal, J. O., Van de Vijver, K. K., Nieuwland, R., et al. (2017). The histophysiology and pathophysiology of the peritoneum. *Tissue Cell, 49*(1), 95-105. doi:10.1016/j.tice.2016.11.004

van de Stolpe, A., & van der Saag, P. T. (1996). Intercellular adhesion molecule-1. *J Mol Med (Berl), 74*(1), 13-33. doi:10.1007/BF00202069

van den Tol, M. P., Haverlag, R., van Rossen, M. E., et al. (2001). Glove powder promotes adhesion formation and facilitates tumour cell adhesion and growth. *Br J Surg, 88*(9), 1258-1263. doi:10.1046/j.0007-1323.2001.01846.x

van den Tol, P. M., van Rossen, E. E., van Eijck, C. H., et al. (1998). Reduction of peritoneal trauma by using nonsurgical gauze leads to less implantation metastasis of spilled tumor cells. *Ann Surg, 227*(2), 242-248. doi:10.1097/00000658-199802000-00014

van Grevenstein, W. M., Hofland, L. J., van Rossen, M. E., et al. (2007). Inflammatory cytokines stimulate the adhesion of colon carcinoma cells to mesothelial monolayers. *Dig Dis Sci, 52*(10), 2775-2783. doi:10.1007/s10620-007-9778-4

Wagner, B. J., Lob, S., Lindau, D., et al. (2011). Simvastatin reduces tumor cell adhesion to human peritoneal mesothelial cells by decreased expression of VCAM-1 and beta1 integrin. *Int J Oncol, 39*(6), 1593-1600. doi:10.3892/ijo.2011.1167

Waite, K., & Youssef, H. (2017). The Role of Neoadjuvant and Adjuvant Systemic Chemotherapy with Cytoreductive Surgery and Heated Intraperitoneal

Chemotherapy for Colorectal Peritoneal Metastases: A Systematic Review. *Ann Surg Oncol, 24*(3), 705-720. doi:10.1245/s10434-016-5712-3

Wang, C., Thor, A. D., Moore, D. H., 2nd, et al. (1998). The overexpression of RHAMM, a hyaluronan-binding protein that regulates ras signaling, correlates with overexpression of mitogen-activated protein kinase and is a significant parameter in breast cancer progression. *Clin Cancer Res, 4*(3), 567-576.

Wang, D., Narula, N., Azzopardi, S., et al. (2016). Expression of the receptor for hyaluronic acid mediated motility (RHAMM) is associated with poor prognosis and metastasis in non-small cell lung carcinoma. *Oncotarget, 7*(26), 39957-39969. doi:10.18632/oncotarget.9554

Wang, H. S., & Wang, L. H. (2015). The expression and significance of Gal-3 and MUC1 in colorectal cancer and colon cancer. *Onco Targets Ther, 8*, 1893-1898. doi:10.2147/OTT.S83502

Wang, K., & Zhang, T. (2016). Prognostic significance of CD168 overexpression in colorectal cancer. *Oncol Lett, 12*(4), 2555-2559. doi:10.3892/ol.2016.4974

Wang, Q. L., Li, B. H., Liu, B., et al. (2009). Polymorphisms of the ICAM-1 exon 6 (E469K) are associated with differentiation of colorectal cancer. *J Exp Clin Cancer Res, 28*, 139. doi:10.1186/1756-9966-28-139

Wang, R., Song, S., Harada, K., et al. (2020). Multiplex profiling of peritoneal metastases from gastric adenocarcinoma identified novel targets and molecular subtypes that predict treatment response. *Gut, 69*(1), 18-31. doi:10.1136/gutjnl-2018-318070

Wang, Y., Wu, N., Pang, B., et al. (2017). TRIB1 promotes colorectal cancer cell migration and invasion through activation MMP-2 via FAK/Src and ERK pathways. *Oncotarget, 8*(29), 47931-47942. doi:10.18632/oncotarget.18201

Wang, Y., Xu, R. C., Zhang, X. L., et al. (2012). Interleukin-8 secretion by ovarian cancer cells increases anchorage-independent growth, proliferation, angiogenic potential, adhesion and invasion. *Cytokine, 59*(1), 145-155. doi:10.1016/j.cyto.2012.04.013

Wangpu, X., Yang, X., Zhao, J., et al. (2015). The metastasis suppressor, NDRG1, inhibits "stemness" of colorectal cancer via down-regulation of nuclear beta-catenin and CD44. *Oncotarget, 6*(32), 33893-33911.

Waniewski, J. (2013). Peritoneal fluid transport: mechanisms, pathways, methods of assessment. *Arch Med Res, 44*(8), 576-583. doi:10.1016/j.arcmed.2013.10.010

Weg-Remers, S., Hildebrandt, U., Feifel, G., et al. (1998). Soluble CD44 and CD44v6 serum levels in patients with colorectal cancer are independent of tumor stage and tissue expression of CD44v6. *Am J Gastroenterol, 93*(5), 790-794. doi:10.1111/j.1572-0241.1998.226_a.x

Weg-Remers, S., Schuder, G., Zeitz, M., et al. (1998). CD44 expression in colorectal cancer. *Ann N Y Acad Sci, 859*, 304-306. doi:10.1111/j.1749-6632.1998.tb11151.x

Wielenga, V. J., Heider, K. H., Offerhaus, G. J., et al. (1993). Expression of CD44 variant proteins in human colorectal cancer is related to tumor progression. *Cancer Res, 53*(20), 4754-4756.

Wielenga, V. J., van der Voort, R., Mulder, J. W., et al. (1998). CD44 splice variants as prognostic markers in colorectal cancer. *Scand J Gastroenterol, 33*(1), 82-87.

Wimmenauer, S., Keller, H., Ruckauer, K. D., et al. (1997). Expression of CD44, ICAM-1 and N-CAM in colorectal cancer. Correlation with the tumor stage and the phenotypical characteristics of tumor-infiltrating lymphocytes. *Anticancer Res, 17*(4A), 2395-2400.

Witek, M. A., & Fung, L. W. (2013). Quantitative studies of caspase-3 catalyzed alphaII-spectrin breakdown. *Brain Res, 1533*, 1-15. doi:10.1016/j.brainres.2013.08.010

Wu, Y., Li, Z., Zhang, C., et al. (2015). CD44 family proteins in gastric cancer: a meta-analysis and narrative review. *Int J Clin Exp Med, 8*(3), 3595-3606.

Xie, J. W., Huang, C. M., Zheng, C. H., et al. (2013). [Expression tumor stem cell surface marker CD44 in gastric cancer and its significance]. *Zhonghua Wei Chang Wai Ke Za Zhi, 16*(11), 1107-1112.

Xie, W., Rimm, D. L., Lin, Y., et al. (2003). Loss of Smad signaling in human colorectal cancer is associated with advanced disease and poor prognosis. *Cancer J, 9*(4), 302-312.

Yaeger, R., Cercek, A., Chou, J. F., et al. (2014). BRAF mutation predicts for poor outcomes after metastasectomy in patients with metastatic colorectal cancer. *Cancer, 120*(15), 2316-2324. doi:10.1002/cncr.28729

Yamada, Y., Arao, T., Matsumoto, K., et al. (2010). Plasma concentrations of VCAM-1 and PAI-1: a predictive biomarker for post-operative recurrence in colorectal cancer. *Cancer Sci, 101*(8), 1886-1890. doi:10.1111/j.1349-7006.2010.01595.x

Yamaguchi, A., Goi, T., Taguchi, S., et al. (1998). Clinical significance of serum levels of CD44 variant exons 8-10 protein in colorectal cancer. *J Gastroenterol, 33*(3), 349-353.

Yamaguchi, K., Hirabayashi, Y., Suematsu, T., et al. (2001). Hyaluronic acid secretion during carbon dioxide pneumoperitoneum and its association with port-site metastasis in a murine model. *Surg Endosc, 15*(1), 59-62. doi:10.1007/s004640000238

Yamamoto, N., Oshima, T., Yoshihara, K., et al. (2017). Clinicopathological significance and impact on outcomes of the gene expression levels of IGF-1, IGF-2 and IGF-1R, IGFBP-3 in patients with colorectal cancer: Overexpression of the IGFBP-3 gene is an effective predictor of outcomes in patients with colorectal cancer. *Oncol Lett, 13*(5), 3958-3966. doi:10.3892/ol.2017.5936

Yamane, N., Tsujitani, S., Makino, M., et al. (1999). Soluble CD44 variant 6 as a prognostic indicator in patients with colorectal cancer. *Oncology, 56*(3), 232-238. doi:11970

Yang, B., Yang, B. L., Savani, R. C., et al. (1994). Identification of a common hyaluronan binding motif in the hyaluronan binding proteins RHAMM, CD44 and link protein. *EMBO J, 13*(2), 286-296.

Yang, M., Baranov, E., Moossa, A. R., et al. (2000). Visualizing gene expression by whole-body fluorescence imaging. *Proc Natl Acad Sci U S A, 97*(22), 12278-12282. doi:10.1073/pnas.97.22.12278

Yeh, Y. S., Tsai, H. L., Huang, C. W., et al. (2016). Prospective analysis of UGT1A1 promoter polymorphism for irinotecan dose escalation in metastatic colorectal cancer patients treated with bevacizumab plus FOLFIRI as the first-line setting: study protocol for a randomized controlled trial. *Trials, 17*, 46. doi:10.1186/s13063-016-1153-3

Yeo, T. K., Nagy, J. A., Yeo, K. T., et al. (1996). Increased hyaluronan at sites of attachment to mesentery by CD44-positive mouse ovarian and breast tumor cells. *American Journal of Pathology, 148*(6), 1733-1740.

Yonemura, Y., & Endou, Y. (2000). [Molecular mechanisms of peritoneal dissemination]. *Nihon Shokakibyo Gakkai Zasshi, 97*(6), 680-690.

Yonemura, Y., Endou, Y., Nojima, M., et al. (1997). A possible role of cytokines in the formation of peritoneal dissemination. *Int J Oncol, 11*(2), 349-358.

Yoo, C. H., & Noh, S. H. (2003). The Serum Assay of Soluble CD44 Standard, CD44 Variant 5, and CD44 Variant 6 in Patients with Gastric Cancer. *Cancer Res Treat, 35*(1), 3-8. doi:10.4143/crt.2003.35.1.3

Youssef, N., Beddingham, J., Soliman, F., et al. (2021). EP.TH.299Is peritoneal lavage with water the optimal washout as a preventative method for peritoneal disease following colorectal cancer resection? A systematic review. *British Journal of Surgery, 108*(Supplement_7). doi:10.1093/bjs/znab309.038

Yu, G., Tang, B., Yu, P. W., et al. (2010). Systemic and peritoneal inflammatory response after laparoscopic-assisted gastrectomy and the effect of inflammatory cytokines on adhesion of gastric cancer cells to peritoneal mesothelial cells. *Surg Endosc, 24*(11), 2860-2870. doi:10.1007/s00464-010-1067-1

Yuan, X., Zhang, X., Zhang, W., et al. (2016). SALL4 promotes gastric cancer progression through activating CD44 expression. *Oncogenesis, 5*(11), e268. doi:10.1038/oncsis.2016.69

Zeilstra, J., Joosten, S. P., Vermeulen, L., et al. (2013). CD44 expression in intestinal epithelium and colorectal cancer is independent of p53 status. *PLoS ONE [Electronic Resource], 8*(8), e72849. doi:10.1371/journal.pone.0072849

Zhang, D., Bi, J., Liang, Q., et al. (2020). VCAM1 Promotes Tumor Cell Invasion and Metastasis by Inducing EMT and Transendothelial Migration in Colorectal Cancer. *Front Oncol, 10*, 1066. doi:10.3389/fonc.2020.01066

Zhang, L., Hu, Y., Xi, N., et al. (2016). Partial Oxygen Pressure Affects the Expression of Prognostic Biomarkers HIF-1 Alpha, Ki67, and CK20 in the Microenvironment of Colorectal Cancer Tissue. *Oxid Med Cell Longev, 2016*, 1204715. doi:10.1155/2016/1204715

Zhang, S., Chang, M. C., Zylka, D., et al. (1998). The hyaluronan receptor RHAMM regulates extracellular-regulated kinase. *J Biol Chem, 273*(18), 11342-11348.

Zhang, Y., Xia, M., Jin, K., et al. (2018). Function of the c-Met receptor tyrosine kinase in carcinogenesis and associated therapeutic opportunities. *Mol Cancer, 17*(1), 45. doi:10.1186/s12943-018-0796-y

Zhao, L. H., Lin, Q. L., Wei, J., et al. (2015). CD44v6 expression in patients with stage II or stage III sporadic colorectal cancer is superior to CD44 expression for predicting progression. *Int J Clin Exp Pathol, 8*(1), 692-701.

Zhao, Q., Xu, L., Sun, X., et al. (2017). MFG-E8 overexpression promotes colorectal cancer progression via AKT/MMPs signalling. *Tumour Biol, 39*(6), 1010428317707881. doi:10.1177/1010428317707881

Zhou, W., He, M. R., Jiao, H. L., et al. (2015). The tumor-suppressor gene LZTS1 suppresses colorectal cancer proliferation through inhibition of the AKT-mTOR signaling pathway. *Cancer Lett, 360*(1), 68-75. doi:10.1016/j.canlet.2015.02.004

Zhu, W. (2016). p < 0.05, < 0.01, < 0.001, < 0.0001, < 0.00001, < 0.000001, or < 0.0000001. *J Sport Health Sci, 5*(1), 77-79. doi:10.1016/j.jshs.2016.01.019

Zlobec, I., Terracciano, L., Tornillo, L., et al. (2008). Role of RHAMM within the hierarchy of well-established prognostic factors in colorectal cancer. *Gut, 57*(10), 1413-1419. doi:10.1136/gut.2007.141192